Department of the Built Environment
Building Physics and Services

Multi-story residential buildings in the event of fire: relief of the fire-induced overpressure without causing smoke spread via the ventilation system

Master Thesis

N.H. (Nora) Kuiper

0955443

45 ECTS

Supervisors:

dr. ir. T.A.J. (Twan) van Hooff
ir. R.A.P. (Ruud) van Herpen
dr. ir. R.P. (Rick) Kramer

Eindhoven, 6th of October, 2023

This master's thesis has been carried out in accordance with the rules of the TU/e Code of Scientific Integrity.

Abstract

Today, more and more attention is paid to decreasing the energy demand of buildings. To reduce the energy demand for heating and cooling, buildings are increasingly airtight and heat recovery ventilation (HRV) units are implemented in the mechanical ventilation systems. Two challenges, with regards to the fire safety in buildings, arise from this modern way of building: (1) in case of fire an overpressure occurs in the fire compartment, which might potentially hinders safe evacuation of occupants; (2) smoke spread to other compartments is observed consecutive to the overpressure in the fire compartment. This is of relevance for all buildings, but particularly for residential complexes as they consist of relatively small fire compartments.

In this graduation project, the essence was to explore the potential solutions to relax the fire-induced pressure via the ventilation system, without increasing smoke spread to other apartments. Two studies were performed, developing a decoupled modeling approach with the zone model CFAST and the multizone model CONTAM. This link was made to overcome the limitations of both modeling software. The potential of this modeling approach was tested in a calibration study based on a reference case, and proven as the pressure development was adequately predicted, especially during the growth phase of the fire, and smoke spread to other apartments was revealed.

The methodology and the findings of the calibration study were used as a reference for the case study, to predict the pressure development and the smoke spread for the case study building. The case study showed that implementing a bypass would not significantly reduce the overpressure in the fire apartment. Smoke spread was found primarily via the inlet system, and therefore, additional simulations on implementing fire dampers were performed. The fire dampers limited smoke spread to apartments connected via the collective ducts, but as expected, led to an increase in overpressure in the fire apartment. Consequently, this enhanced smoke spread to other apartments via the interior separation structure. The case study showed that evacuation would be necessary to ensure personal safety of occupants of the apartments connected via the collective ducts if no fire dampers were implemented, and to ensure personal safety of occupants of the apartments directly adjacent to the fire apartments if fire dampers were applied.

Based on the two studies and multiple tests of different variants, it is concluded that there is no solution found in the ventilation configuration that would satisfy the two problem statements. Therefore, it is recommended to explore solutions in the building structure instead.

Preface

In your hands, you find the report on my final project, marking the end of my time as a student at the Eindhoven University of Technology (TU/e). I started my bachelor's degree here at the Faculty of the Built Environment, inspired by how I could express my creativity in the design of buildings. Little did I know, that this creativity would be used in the process of creating solutions for the safety of buildings, particularly, the fire safety of buildings. A topic that, in my opinion, is still underexposed these days.

During my master's degree at the TU/e, I got in touch with Ruud van Herpen. He always seemed to have a project ready in which I could combine my interests. This included thinking about fire safe façade design using thermally thin facades, the topic on which I did an earlier research project. And for this graduation project, where I could combine my interest in fire safety engineering with my interest in building services. I am very grateful for these opportunities to work on something that I really like and find highly relevant.

I would like to start by thanking Ruud van Herpen for these opportunities, for the support, help and feedback throughout this graduation project, and for helping me get an internship at Peutz B.V.. At Peutz B.V., I gained valuable knowledge, not only on the topic, but also on the relationship between theory and practice in our work field as a (consulting) engineer. Therefore, I should also say a huge thank you to my colleagues at Peutz Eindhoven and Mook, for welcoming me, helping me out by sharing their knowledge and supporting me with the experiments performed in the laboratory for Building Physics.

Apart from the employees of Peutz B.V., I would like to thank Rolf Franssen from Wijnen Bouw and Eric Vogels from Wijnen Installaties, who helped me to understand ventilations systems even better and to gain insight and understanding in the active challenges that companies face in the building- and services sector. I also want to thank Welmoed Siebesma and Job Hanssen from K+ Adviesgroep for making it possible to join for blower door tests on the building site of one of their projects.

As for the defense of my thesis, I would like to thank Ruud van Herpen, Twan van Hooff and Rick Kramer for being flexible in their guidance, participating in my supervising committee and most importantly, their trust in me.

Lastly, I would like to thank my family and my friends, who stood by me and put their confidence in me throughout this graduation project, but more importantly, throughout my studies and any hard times that I or we had to endure. You helped me stay motivated and keep the eye on the finish line.

I hope you will enjoy reading as much as I enjoyed working on this project and this report!

Kind regards,
Nora Kuiper

Eindhoven, 6th October 2023

Contents

Abstract iii
Preface iv
Contents v
List of Figures vi
List of Tables vii
List of Symbols viii
1. Introduction 1
1.1 Problem statements 1
1.2 Performance based approach 2
1.3 Research questions 3
2. Methodology 5
3. Starting points, boundary conditions and assessment criteria 6
3.1 Starting points and boundary conditions 6
3.2 Assessment criteria 8
4. Overview simulation software 9
5. Calibration study 12
5.1 Introduction calibration case 12
5.2 Methodology 14
5.3 Results 22
5.4 Discussion 28
6. Case study 30
6.1 Introduction 30
6.2 Methodology 32
6.3 Results 40
6.4 Discussion 47
7. Evaluation 49
8. Conclusion 50
Bibliography 51
List of Appendices 56

List of Figures

Figure 4-1. Schematic view of the level of detail of different simulation software 9
Figure 5-1. Plan view of the hypothetical residential building [10] 12
Figure 5-2. Predicted pressure development [10] 13
Figure 5-3. Simulations peak pressures bar plots [10] 14
Figure 5-4. Visualization of smoke concentration 170 s after ignition [10] 14
Figure 5-5. Plan view as created in CONTAM 17
Figure 5-6. Comparison of the computed T_{av} versus the curve of the trapezoidal day schedule 19
Figure 5-7. Expected and actual heat release rate curves for fire scenario 3.1.1 where t_g = 300 s (left) and 3.2.1 where t_g = 150 s (right) 23
Figure 5-8. Weighted average temperature for fire scenario 3.1.1 where t_g = 300 s (left) and 3.2.1 where t_g = 150 s (right) 23
Figure 5-9. Weighted average temperature for all fire scenarios with a medium fire growth rate 24
Figure 5-10. Weighted average temperature for all fire scenarios with a fast fire growth rate 24
Figure 5-11. Predicted pressure development for fire scenario 3.1.1 where t_g = 300 s and 3.2.1 where t_g = 150 s 26
Figure 5-12. Predicted pressure development for fire scenario 3.1.3 where t_g = 300 s (left) and 3.2.3 where t_g = 150 s (right) 26
Figure 5-13. Calculated visibility in the non-fire apartments 27
Figure 6-1. Impression of De Cavaliere, Helmond 30
Figure 6-2. Floor plans of the first two floors of De Cavaliere [65] 30
Figure 6-3. Floor plans with apartments 3.04, 3.06 and 4.05 highlighted 31
Figure 6-4. Heat recovery ventilation (HRV) unit schematically explained 31
Figure 6-5. Schematic overview of the test set-up 33
Figure 6-6. Model geometry of apartments 3.04 (left), 3.06 (middle), and 4.05 (right), visualized in SmokeView 34
Figure 6-7. Floor plan of floor 4 (left) and floor 5 (right) 35
Figure 6-8. CONTAM geometry of apartment 4/A2 without (left) and with (right) modelled bypass.. 37
Figure 6-9. Indication of duct segments 34, 39 and 42, and junctions 34, 39 and 41 on the floor plan of apartment 4/A2 40
Figure 6-10. Expected and actual HRR of the fire scenarios where t_g = 300 s 42
Figure 6-11. Expected and actual HRR HRR of the fire scenarios where t_g = 150 s 42
Figure 6-12. T_{av} curve of the fire scenarios where t_g = 300 s 43
Figure 6-13. T_{av} curve of the fire scenarios where t_g = 150 s 43
Figure 6-14. Mass flow rates for ducts 34, 39 and 42 when t_g = 300 s 44
Figure 6-15. Mass flow rates for ducts 34, 39 and 42 when t_g = 150 s 44
Figure 6-16. Pressure development over air flow path 120 when t_g = 300 s 45
Figure 6-17. Pressure development over air flow path 120 when t_g = 150 s 45
Figure 6-18. Minimum visibility in zones when t_g = 300 s 46
Figure 6-19. Minimum visibility in zones when t_g = 150 s 46

List of Tables

Table 5-1. Specifications of the exterior structure [10] 12
Table 5-2. All fire scenarios 15
Table 5-3. Time schedule for the different ventilation configurations (Open/Close Criterion: Time).. 15
Table 5-4. Fire characteristics..... 16
Table 5-5. Temperature schedule of the fire apartment for fire scenario 3.1.1..... 18
Table 5-6. Temperature schedule of the fire apartment for fire scenario 3.2.1..... 18
Table 5-7. Schedule for the generation rate for 3.1.1 (medium fire growth rate, near zero façade, Damper=Off)..... 20
Table 5-8. Schedule for the generation rate for 3.2.1 (fast fire growth rate, near zero façade, Damper=Off)..... 20
Table 5-9. Fan operation schedule of the additional fan for fire scenario 3.1.1..... 22
Table 5-10. Fan operation schedule of the additional fan for fire scenario 3.2.1..... 22
Table 5-11. Pressure peaks found in the calibration study for all scenarios with a medium fire growth rate 25
Table 5-12. Pressure peaks found in the calibration study for all scenarios with a fast fire growth rate 25
Table 5-13. Comparison peak mass flow rates resulting from the CFAST- and CONTAM simulations. 27
Table 6-1. Results blower door tests Cavaliere 31
Table 6-2. List of ventilation requirements 32
Table 6-3. Comparison actual and tested HRV unit 33
Table 6-4. Measurement configurations..... 33
Table 6-5. Input characteristics for the CFAST models 34
Table 6-6. Leakage input for CONTAM simulations 36
Table 6-7. Day schedules for duct 34 and duct 38, t_g = 300 s 38
Table 6-8. Day schedules for duct 34 and duct 38, t_g = 150 s 38
Table 6-9. Day schedules for duct 34 and duct 38, t_g = 300 s, dampers close after 150 s 39
Table 6-10. Day schedules for duct 34 and duct 38, t_g = 150 s, dampers close after 90..... 39
Table 6-11. Day schedules for duct 34 and duct 38, t_g = 300 s, dampers close after 200 s 39
Table 6-12. Day schedules for duct 34 and duct 38, t_g = 150 s, dampers close after 120 s 39
Table 6-13. List of valves per space..... 41
Table 6-14. Summary of the results of the regression analysis 41
Table 6-15. Peak overpressure over air flow path 120 for all scenarios 45

List of Symbols

Symbol	*Definition*	*Unit*
A	Area	m^2
A_L	Equivalent leakage area	m^2
C	Capacity of the air flow resistances	Pa^n*dm^3/s
c	Specific heat capacity	J/kg*K
D	Smoke particles density	g/m^3
ELA	Equivalent leakage area	m^2
f	Fraction	-
G	Pyrolysis rate	kg/s
H_c	Heat of combustion	kJ/kg
HRR	Heat release rate	kW or MW
m	Mass	kg
m_{soot}	Mass of soot particles in smoke	kg
$\dot{m}$	Mass flow rate	kg/s
n	Flow factor	-
n^{-1}	Flow coefficient	-
n_{50}	Air change rate per hour at Δp = 50 Pa	h^{-1}
OD	Optical density	m^{-1}
p	Pressure	Pa
p_{st}	Static pressure	Pa
$Q(t)$	Heat release rate	kW or MW
$q_{v;10}$	Air flow rate at Δp = 10 Pa	$m^3/h*m^2$
$q_{v;50}$	Air flow rate at Δp = 50 Pa	$m^3/h*m^2$
R_e	Mass optical density	$m^{-1}*m^3/g$
RD_e	Light extinction coefficient: optical smoke density per light path traveled	m^{-1}
S	Visibility	m
T	Temperature	°C or K
T_{av}	Weighted average temperature	°C or K
t	Time	s
t_g	Fire growth time	s
V	Volume	m^3
$\dot{V}$	Volume flow rate	m^3/s
V_{50}	Volume flow rate at Δp = 50 Pa	m^3/s
v	Flow velocity	m/s
Y_{CO}	CO yield	kg/kg
Y_{soot}	Soot yield	kg/kg
z	Layer height	m
α	Coefficient for a t^2 curve	kW/s^2
Δp	Pressure difference	Pa
ρ	Density	kg/m^3

1. Introduction

1.1 Problem statements

To house the growing population in the Netherlands, cities are building more and more medium- to high-rise apartment buildings which are subjected to strict regulations regarding their energy performance. Common strategies to reduce the energy demand for heating are applying thermal insulation, creating an airtight building envelope, and implementing balanced ventilation with heat recovery. Regarding these strategies, the Passive House requirements [1] describe various values related to the building characteristics: the heat transfer coefficient (U-value) through the building envelope must be 0.15 W/m²K at most and the infiltration rate should not exceed 0.6 of the total volume per hour, tested for an overpressure of 50 Pa. In such buildings, mechanical ventilation is needed for the supply of fresh air and with the use of a heat recovery ventilation (HRV) unit, up to 90% of the heat from the exhaust air is transferred to the fresh air [1], [2]. Conforming to the insulation requirements of the Passive House requirements results in a reduction of the heating demand by 15%; the implementation of an HRV unit further reduces the heating demand by 50-65% [3].

These medium- to high-rise buildings come with challenges regarding the fire safety. In the event of fire, the main goals are safety of the occupants and limitation of uncontrolled fire spread to adjacent fire compartments and/or neighboring plots. Focusing on the prevention of casualties, two strategies can be used as a starting point for fire safe design, namely 1) design for safe evacuation (according to the Dutch building code) or 2) design for a stay-in-place, or stay-put, policy [4]. Important for buildings with a stay-in-place policy, is that the building itself forms a protective barrier against the fire and smoke and keeps the residents safe in their own apartments. Structurally, this is achieved by the design of very reliable load bearing structures, fire compartmentation and smoke compartmentation. Proper ventilation design plays an important role too, as smoke propagation via ventilation ducts may form a potential hazard for residents that conform to the stay-in-place policy.

Currently, many medium- to high-rise buildings are designed and built for a stay-in-place policy. In the Netherlands, to the knowledge of the author, the stay-in-place policy has only been discussed for healthcare institutions [5]–[7]. However, in the United Kingdom, the strategy has been put into practice for a while now and for a broader variety of buildings. Yet, a survey conducted during the Fire Safety Week showed that 72% of the apartment building residents indicated to ignore the stay-in-place policy if a fire broke out in their building [4], [8]. This implies that the natural instinct of people is still to leave their apartment in the case of fire in one of the apartments, highlighting the need for implementing safe evacuation design also in medium- to high-rise apartment buildings.

While the Dutch Building Code has well defined regulations regarding safe evacuation in the event of fire, new problems arise due to new building standards optimized for energy efficiency, especially regarding insulation and airtightness. Experimental and numerical research have shown that fire in an airtight compartment may lead to overpressures well over 2000 Pa in situations without any mechanical ventilation [9], [10], and overpressures up until ~ 700 Pa with mechanical ventilation and natural vents fully open [9]–[11]. To put this into perspective, an overpressure of 100 Pa is already hindering evacuation as it becomes impossible to open an inward opening door [10], [12], [13]. Another consequence of overpressures in airtight apartments is increased spread of smoke and toxic gases to other apartments via collective ventilation ducts [10], [14]. The overpressure pushes the smoke and gases into the ventilation ducts, both outlet and inlet, distributing the smoke and gases to the other apartments. This puts the health and safety of the occupants at risk when a stay-in-place policy is imposed, as inhalation of smoke and gases may be damaging the respiration system [15], [16]. Smoke may also spread towards escape routes, resulting in not only increased health and safety risks for the occupants but significantly hinder evacuation by a decrease in visibility [10].

Implementing existing solutions to limit smoke spread, such as fire dampers and fire damper cartridges offers a method of limiting smoke spread in apartment buildings, but simultaneously generate new challenges. When the temperature exceeds 72 °C, the fusing link will melt, and the cartridge will close. However, 'cold' smoke does not trigger these cartridges, allowing smoke to spread via the ventilation system in the early stages after ignition. To solve this problem, check valves can be included in the ventilation system, blocking the reverse flow in the admission duct caused by the fire-induced overpressure. These check valves are sensitive to pressure changes, and may cause noise hindrance in a non-fire situation when they start to clatter due to a change in pressure. Another solution would be using dampers that are smoke detector controlled. These are best suited for compliance to the building code (BBL: Besluit bouwwerken leefomgeving) and NEN 6075. Both documents prescribe that fire dampers should respond to cold smoke as well as to high temperatures. Yet, the design of these combined dampers is highly impractical for apartment buildings as the dampers require a laminated flow through the duct, thus call for a longer horizontal duct to create such a flow. For most apartments buildings, this causes problems in the design of the ventilation system and the technical spaces. From a financial point of view, the use of these combined dampers with smoke detector included is also undesirable, as the costs of these dampers is much higher. Lastly, the use of these systems will negatively affect the fire-induced overpressure in the apartment where the fire started, as the closed dampers do not allow for pressure relief.

Currently, there is not yet a general solution for limiting the fire-induced pressure buildup in airtight apartments sufficiently for occupants of apartment buildings to allow safe evacuation. The mechanical ventilation systems applied in airtight apartment buildings may offer a solution, but also impose a new risk of increased propagation of smoke and toxic gases into other apartments. Consequently, even if occupants are willing to abide by a stay-in-place policy, their health and safety would be at risk. It is therefore of vital importance to gain understanding on how fire-induced pressure can be restrained to a certain (safe) limit, possibly via the mechanical ventilation system and without endangering other apartments.

1.2 Performance based approach

In fire safety engineering, the main objective is ensuring personal safety for building occupants, and thus preventing injuries and deaths as a result of a building fire. The secondary objective is the prevention of damage to third parties (i.e. neighboring plots). These two objectives, as also set in the Dutch Building Code, are divided in six different subobjectives [17]:
1) the safety of the environment (i.e. neighboring plots);
2) the safety of the building (i.e. its loadbearing structure);
3) the safety of the fire compartmentation (i.e. spread of fire);
4) the safety of the smoke compartmentation (i.e. internal smoke propagation);
5) the safety of evacuation routes (i.e. the building occupants); and
6) the safety of attack routes (i.e. the fire fighters and other aid workers).

Nowadays, buildings are often designed with the fire safety regulations in mind, leading up to a so-called prescriptive design. This may not be satisfactory at all times. It was therefore that the Fire Safety Committee of the NKB (Nordic Committee on Building Regulations) published a proposed model for a performance-based code rather than a prescriptive design [18]. This shift took place in 1994, and the main idea behind this code was to formulate performance requirements which secured the stipulated safety level without dictating detailed design and selection of materials [19]. Again, the two main aims are distinguished: sufficient safety for the building occupants (including facilities for rescue of persons and for firefighting), and prevention of fire spread to buildings and activities both on the same and adjoining plots. Five functional requirements were set in the model by the NKB, that are similar to those that are used in the Netherlands:

- The load-bearing capacity can be assumed for a specific period of time (safety of the building);
- The generation and spread of fire and smoke within the building is limited (safety of the compartment);
- The spread of fire to neighboring construction works is limited (safety of the environment);
- People in the building on fire can leave it or be rescued by other means (safety of evacuation routes); and
- The safety of fire and rescue service personnel is taken into consideration (safety of attack routes) [18], [19].

Overall, utilizing performance-based design goes beyond code application [20]. In the SFPE Engineering Guide to Performance Based Fire Protection [21], performance-based design was defined as "an engineering approach to fire protection design based on (1) agreed upon fire safety goals and objectives, (2) deterministic and/or probabilistic analysis of fire scenarios, and (3) quantitative assessment of design alternatives against the fire safety goals and objectives using accepted engineering tools, methodologies, and performance criteria." [21].

For this project, the main research objective is to identify approaches to ensure personal safety of occupants of modern, airtight medium- to high-rise residential buildings, in the event of fire. Two functional requirements are thus especially significant for this graduation project: enabling safe evacuation from the apartment where the fire occurs (thus the safety of evacuation routes), and ensuring the safety and health of occupants in other apartments when a stay-in-place policy is in effect (thus the safety of the compartment).

The aforementioned functional requirements are translated into project-specific performance requirements. The first aspect, enabling safe evacuation from the apartment where the fire occurs, has to do with the previously mentioned restraint on the fire-induced pressure buildup in airtight apartment buildings. Simulation models have been proven to accurately predict these overpressures, based on validation done with experimental research [22]–[26]. Care should be taken to correctly model the building characteristics into the simulation program to generate reliable results. The largest challenge is expected to be in the modeling of the leakage paths and the modeling of the ventilation system, especially when one or multiple heat recovery ventilation unit(s) (HRVs) is/are incorporated in the system. Different fire sources may be considered as the fire load, as long as they are an accurate representation of a real fire source [27]. The second aspect, ensuring the safety and health of occupants in other apartments when a stay-in-place concept is in effect, is based on the findings that overpressures lead to reverse flow in the (collective) inlet duct of a ventilation system, consequently causing spread of smoke and toxic gases into other apartments. Numerical research has shown that the spread of smoke and toxic gases can be prevented based on ventilation configuration [10], [14]. However, modern ventilation strategies (i.e. individual HRV-units) are yet to be implemented into these models.

1.3 Research questions

Based on the problem statements and on the performance requirements, with the emphasis on ensuring safe evacuation from the fire apartment and the protection of the safety and health of occupants in other apartments, the following research question is formulated:

How can the fire-induced pressure build-up in an airtight apartment be sufficiently limited, without compromising the safety of the escape route and other apartments due to potential spread of smoke and toxic gases via the ventilation system?

To approach the main research question, the following sub questions have been formulated:

1. Which are the relevant building- and fire characteristics for (numerically) predicting the pressure buildup during the initial stage of an apartment fire, as well as smoke spread to other apartments?
2. What is the air resistance of different elements of the ventilation system?
3. What types of modeling software are available?
4. What is the potential of using a coupled modeling approach to predict the smoke propagation to other apartments, based on a calibration study?
5. What is the effect of these resistances on the pressure relief in the fire apartment and on the internal propagation of smoke and toxic gases?
6. What recommendations can be made to improve the ventilation system to ensure safety?

2. Methodology

To address the main research question and sub questions, different phases were undertaken within this project. Firstly, an inventory was made of the relevant starting points, boundary conditions and assessment criteria, as found in previously conducted research. The starting points and boundary conditions were split under three categories: building characteristics, ventilation characteristics and fire characteristics. The assessment criteria were linked to the problem statements. The inventory on starting points, boundary conditions and assessment criteria is found in the corresponding chapter "Starting points, boundary conditions and assessment criteria".

While going through literature, the different research methods were evaluated, with a focus on the simulation methods. An overview of the findings can be found in the chapter "Simulation models". Here, the different simulation programs found are discussed, including the validity and shortcomings of the different modeling programs.

The third phase of this research was the calibration study, discussed in chapter "Calibration study". The calibration study was performed to explore the potential of coupling a zone model with a multizone model in a fire scenario regarding this method's ability to adequately predict the pressure development in a fire apartment and smoke spread to non-fire apartments, a method originally presented by Klote in 2012 [30]. The calibration study was based on a case study on a hypothetical residential building, conducted by Hostikka et al. [10] The chapter focusing on the calibration study includes an introduction to the case study, a methodology for the CFAST simulations, a methodology for the CONTAM simulations, the results of the calibration study, a discussion on the results and the conclusions drawn.

The last phase of this research consisted of a case study on the newly built residential complex De Cavaliere, located in Helmond [31]. The method of coupling the zone model CFAST with the multizone model CONTAM was implemented to predict the pressure buildup in the fire apartment and the smoke spread to the other apartments. Research on the case study included not only the simulations, but also a site visit to measure the airtightness of several apartments and measurements on the resistance of a HRV-unit typically used for residential buildings. The results of the measurements formed the basis for the simulations. In total, eight scenarios were examined, with the attempt to reduce the smoke spread with a bypass and prevent smoke spread using fire dampers. The chapter "Case study" goes further into depth on the case study, including an elaborate introduction of the case study building; the methodology of the measurements, the CFAST simulations and the CONTAM simulations; the results of the study; a discussion and conclusions drawn.

3. Starting points, boundary conditions and assessment criteria

This chapter shortly introduces the starting points, the boundary conditions and the assessment criteria. The starting points and boundary conditions are categorized under 'building characteristics', 'ventilation characteristics' and 'fire characteristics'. The starting points and boundary conditions are assessed for the cases found in literature, and will be treated for the validation study and the case study of this project in their respective chapters. The assessment criteria describe the desired outcome from the CFAST and CONTAM simulations.

3.1 Starting points and boundary conditions

3.1.1 Building characteristics

The starting points regarding the building characteristics include the amount of floors, the amount of apartments per floor and the dimensions of an apartment. These characteristics are defined in the architectural drawings, i.e. the floor plans and sections. Also the airtightness of the exterior structure and the interior structure are a starting point, as these influence the pressure development within the fire apartment [10], [32].

Simultaneously, the airtightness of the exterior structure and the interior structure form a boundary condition. In studies, the airtightness of the exterior structure is often based on the requirements as set in building codes or for specific certifications, such as Passive House. However, for actual constructed buildings, the airtightness of the exterior structure is largely dependent on the quality of the construction process. It is therefore that pressurization tests (i.e. blower door tests) are done to establish the actual airtightness. These tests can be done for the building as a whole or per apartment. Usually, buildings are tested for an under- and/or overpressure of 50 Pa. Internationally, the results are expressed as infiltration rates at 50 Pa, or as airtightness level in cfm/ft² of the building envelop at 50 Pa, corresponding to the unit dm³/s*m² of the building envelop [33]. In the Netherlands, the airtightness is expressed as a value for $Q_{v;10}$, which indicates the volume flow rate at an under- and/or overpressure of 10 Pa. The $Q_{v;10}$ value is in dm³/s*m² floor area. [34].

In some studies, the airtightness of the interior structure is neglected (thus considered fully airtight) [10], [14]. In the report "Smoke propagation and personal safety", the NIPV offered a method of calculating interior leakages of floors, walls and ceilings, assuming the leakage via these elements to be a fraction of the leakage via the exterior structure and shafts:

- Floors/ceilings: half the leakage through the exterior structure;
- Walls between apartments: half the leakage through the exterior structure;
- Walls towards a hallway: equal to the leakage through the exterior structure [27].

Using these ratios, the leakage per construction element can be estimated as a fraction of the total leakage found during pressurization tests.

3.1.2 Ventilation characteristics

The first starting point for the ventilation characteristics is the ventilation strategy, thus whether apartments are ventilated naturally, mechanically or hybrid. This goes for both problem statements. For mechanically ventilated apartments, part of the strategy is also whether a HRV-unit is applied, collectively for multiple apartments or separately for all apartments. The specifications of the HRV-unit are also included as a starting point; most importantly the maximum air flow, the stalling or drop-off pressure, the surge pressure and the resistance the HRV-unit exerts on the air flow. Most of these properties are tested by an independent party and publicly available via the manufacturer.

For the other elements, i.e. ducts, joints, bents, valves and dampers, air leakages of the ventilation system and the resistance exerted on the air flow form a starting point. Similar to the resistance that

a HRV-unit exerts on the air flow rate, all other elements of the ventilation system exert a certain resistance on the air flow rate as well. This resistance is dependent on the design and dimensions of the individual elements, the air flow velocity, the resistance factor and the roughness of ducts [35], [36]. Leakages may occur at connections between elements, or an element itself may not be completely airtight. In previous research, it was often chosen to neglect leakages of the system [14], [35].

Lastly, the flow rate and the configuration of the ventilation system are conveyed as starting points. The maximum flow rate is either described as a volumetric flow rate or a mass flow rate and can be calculated from the number of rooms and their functions. Generally, fresh air is supplied in living rooms, bed rooms and laundry rooms, and air is extracted from the bathroom, toilet and kitchen. For a majority of time, HRV units are capable of providing apartments with sufficient fresh air, while functioning on a low setting. This implies that the system would operate on 25% or 33% of its maximum capacity, depending on the specific unit installed. Adjustments in settings may be done by the building occupant or automatically set by unit itself, controlled by sensors. Therefore, a wide range of settings can be found throughout a residential complex. Using the low setting of the HRV unit as a starting point is considered a boundary condition.

Previous research compared different configurations to explore how the ventilation configuration would affect the pressure development in the fire apartment and potential of smoke spread to other apartments [9], [10], [14], [24], [35]. Most of these studies tested the effect of fan configuration (on/off), ventilation flow rate and fire dampers on the pressure development [9], [10], [14], [24], [35], some also the smoke spread [10], [14] Wahlqvist and van Hees also explored the effect of flow direction and alternative duct placement (i.e. inlet at floor level). They found that conversion of flow direction could offer some pressure relief, as well as placing the inlet at floor level, but not significantly [14].

3.1.3 Fire characteristics

The fire characteristics that are relevant for the prediction of the fire-induced pressure in the fire apartment are the fire source, the heat release rate (HRR), the heat of combustion, CO yield, soot yield and the fire growth rate. All are properties of the material used as starting point for the design fire.

Experiments performed in experimental facilities were conducted with different fire sources. As these experimental facilities were often performed in facilities with the size of a shipping container (12 m in length, 2.38 m in width and 2.44 m in height [9]). The fire sources found in literature are stacks of pallets [9], wooden cribs [9], [37] and pool fires [11], [24], [25]. The HRR for these fire sources had a peak between 250 and 650 kW; this peak occurred within minutes after ignition.

The NIPV (Nederlands Instituut van Publieke Veiligheid) used a couch as fire load for the simulations in their report about the feasibility of a stay-in-place concept [27]. One could consider a couch as an accurate representation of a fire load found in apartments. The HRR of this specific couch (filled with polyurethane foam) follows a parabolic curve and reaches up to approximately 3250 kW; this peak occurs 7 minutes after ignition. This peak HRR is significantly higher than peak HRRs found in other references.

For simulations, these fire characteristics retrieved from the experiments were used as input in order to validate the models. In some research, a comparison of the used fire loads was made to the t^2-curves was found in articles by Li et al. [25] and by the NIPV [27]. In a t^2 fire, the HRR is assumed to be proportional to the square of the elapsed time [38], [39]. The following equation displays this:

$$Q(t) = \alpha t^2 \qquad \text{Eq. 1}$$

With:

Q(t) heat release rate in [kW];

t time in [s];

α coefficient for a t^2 fire in [kW/s^2].

This formula applies up to a maximum HRR as specified by the user or by the Eurocode (NEN-EN 1991-1-2+C3:2019) [40]. Four different growth rates considered: slow, medium, fast and ultra-fast. These fire growth rates help illustrate how the pressure evolution links to the temporal evolution of the HRR, especially for simulations [25] and are loosely based on HRR curves of different elements, e.g. furniture [39].

Following the maximum HRR considered by Hostikka et al. (4000 kW [10]), the NIPV (3250 kW [27]), the NFPA (4000 – 8000 kW [39]) and Blomqvist et al. (3500 – 5500 kW [41]), a HRR value of this order of magnitude should be used as a starting point to correctly represent an apartment fire.

3.2 Assessment criteria

The first assessment criterium is the overpressure development in the fire apartment. As mentioned, the overpressure should not exceed 100 Pa to guarantee safe evacuation from the fire apartment [10], [12], [13]. Opening of the front drop will temporarily relax the overpressure, but Van Herpen found that after the door was closed, the pressure will further its development based on the initial fire scenario (thus without the opening of a door) [42].

It was also shown in previously conducted research that overpressure in the fire apartment may lead to smoke spread via collective ventilation systems [9], [10], [14], [24], [35]. Indicators of smoke spread include visibility in other apartments [10], soot accumulation in kg [14] or reverse flow in the ventilation ducts [9], [14], [24], [35]. Reverse flow is shown when negative flow velocities occur. The visibility in other apartments can be calculated from the optical density and smoke concentration [10], [43]. The method of calculating the visibility will be discussed in depth in the methodology for the calibration study (Section 5.2).

Following the requirements for a stay-in-place concept, also the temperature and concentrations of asphyxiant gases could be considered as an assessment criteria for safe stay in non-fire apartments [27]. The temperature should not exceed 45 °C; the concentration of toxic and asphyxiant gases should stay below a certain dose depending on the particular type (e.g. CO, NOx). However, short term exposure to toxic and asphyxiant gases is not relevant if the visibility in an apartment is above 10 m. Short term exposure refers to an exposure time of 15 minutes or less. The exposure to toxic and asphyxiant gases is not relevant for longer duration if the visibility in an apartment is above 30 m. Therefore, these values will be used as assessment criteria.

4. Overview simulation software

Three different types of modeling software are distinguished for the execution of this project: modeling software based on computational fluid dynamics (CFD), zone models and multizone models. The principle of each model and their respective level of detail is schematically explained by Figure 4-1, with the zone model on the left, the multizone model in the middle and the CFD model on the right.

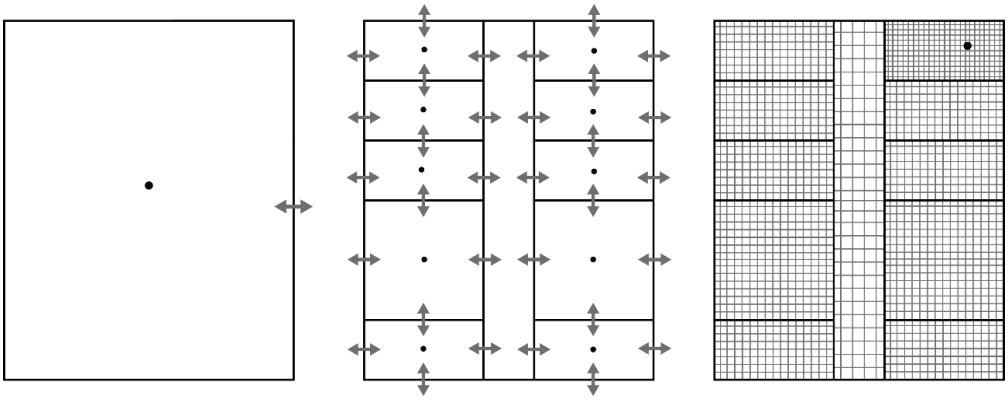

Figure 4-1. Schematic view of the level of detail of different simulation software

The name zone model comes from its level of detail: it usually solves equations for conservation of mass and energy for one zone or compartment (i.e. one control volume), to represent the processes encountered in fire by interrelated mathematical expressions based on physics and chemistry. The outcome in many fire models consider two control volumes: one upper (hot) layer and one lower (cool) layer. Heat transfer focuses primarily on buoyancy-driven flows: hot gases produced by the fire are assumed to be instantaneously transported into the hot layer. For both layers, the result is an output for averaged temperatures, concentrations and mass flow rates [44].

Zone models are developed for a wide variety of uses, so the use of every zone model may differ from the use of other zone models. The advantage of using zone models is that running them requires limited amounts of computational power and they provide results relatively quickly. Despite their limited level of detailing, zone models have proved to be a practical and effective method for providing estimates of fire effects in enclosures [44].

An example of a zone model used for predicting overpressures in airtight compartments is CFAST, developed by the National Institute of Standards and Technology (NIST). Brohez & Caravita performed both experimental research and examined the predictive capability of CFAST for quantifying the fire-induced overpressure [9], for one situation with and one situation without mechanical ventilation. The outcome parameters considered were pressure, temperature, gas concentrations and the volumetric flow rate in the ducts. Two shortcomings were observed regarding the calculation capability of CFAST:

1. Using a fixed leakage area resulted in an overestimation of the fire-induced pressure by a factor of 4, when the mechanical was off. This comes from the governing equations in CFAST: only large openings with a turbulent flow (flow coefficient $n^{-1} = 0.5$) can be simulated. CFAST cannot calculate well with small openings where the flow is laminar rather than turbulent, with a corresponding flow coefficient between 0.5 and 1.0. The leakages in the building structure are the most important example of such small leakages. The solution provided by Brohez & Caravita to overcome this shortage was to create a table of leakage area varying in function of time to take into account the evolution of pressure during fire.
2. When overpressure occurs, CFAST neither takes into account reverse flow in the supply system nor the extra flow rate in the exhaust system. An extra opening towards the exhaust system was added to overcome these limitations. Thanks to this methodology, the sum of the fan flow rate and the volume flow rate through this additional opening resembled the experimental results for the volume flow rate in the duct.

The estimation of fumes temperature and the prediction of CO_2 and O_2 concentrations corresponded to the experimental results. With the aforementioned adjustments to the CFAST model, also the predictions for the pressure evolution and the flow rates were similar to the measured ones [9].

Similar adjustments were made by Tenbült, who examined the pressure buildup in a real residential unit based on performed leakage measurements. As a result, the simulated volume flow rates aligned better with the calculated volume flow rates, for all compartments and pressures up to 1300-1350 Pa [45].

Most widely used to predict both fire-induced overpressures and smoke propagation to other apartments is Fire Dynamics Simulator (FDS) [10], [24], [25], [37], [46]. FDS, like CFAST, is a simulation software developed by NIST. This simulation software is an example of a computational fluid dynamics (CFD) modelling program, specifically developed to model fire-induced smoke and heat transport in a space and between different compartments [47]. CFD offers the highest level of detail as it solves the Navier-Stokes equations for many separate control volumes.

Janardhan & Hostikka [24] compared experiments with numerical simulations in FDS to validate FDS as a means to predict the pressure development in apartment fires, with a pool fire as fire source. Apart from the pressure development, temperatures at different heights were measured, as well as gas concentrations and flow velocity in the ventilation ducts. The results showed an underestimation in temperatures in higher regions in the apartment, and an overestimation in the lower regions of the apartment. One possible reason could be that mixing of the hot and cold layer is overestimated by FDS. With ducts fully open, the overpressure is overestimated in all three modeling methods (localized leakage, bulk leakage – 5 cm mesh, and bulk leakage – 10 cm mesh). For the other two ventilation configurations (normal valves installed and ducts closed), the pressure development was predicted more accurately. The flow velocity in the (exhaust) ducts was estimated accurately up to and including the fully-developed phase of the fire. When reverse flow occurred during the decay-phase, its corresponding flow velocity was underestimated [24].

Li et al. also compared results from FDS simulations with experimental results [25]. Overall, the pressure development found by simulating in FDS resembled the pressure development found in the experiments for both the small and the large pool fire. The overpressure peak for the small pool fire was overestimated by just 6.5%; the overpressure peak for the large pool fire was slightly underestimated, namely 1.6%. The underpressure peak for both the small pool fire and the large pool fire were overestimated by 40% and 22%, respectively [25].

Apart from their research in CFAST [9], Brohez & Caravita also examined the use of FDS for predicting fire-induced overpressures [46]. With a constant leakage area applied in both FDS and CFAST, similar results were obtained. As mentioned before, the overpressure in this case was largely overestimated. Therefore, a localized leakage set up was integrated in the FDS model, similarly to the localized leakage as implemented in CFAST. This led to satisfactory results, with only an error of about 9%. Also, tests were performed using the pressure zone leakage model as developed in FDS version 6.5.0, leading to even better results: the overpressure peaks were overestimated by just 2-3% [46].

FDS was also used to perform to predict smoke spread to other apartments, by both Hostikka et al. [10] and Wahlqvist & Van Hees [14]. Both tested multiple ventilation configurations and strategies to find out what effect each would have on the smoke spread. However, these FDS simulations have not yet been validated with experimental data.

Overall, it can be said that using FDS yields reliable results for the fire-induced pressure development. Previous research highlighted the importance of taking into consideration the increase in leakage as a

result of the rising pressure inside the compartment. FDS has also appeared to be useful in predicting smoke spread, but the results are yet to be validated.

One major drawback of using FDS to model multiple compartments, the ventilation system and all interconnections between these elements, is the computational power required. One simulation may take multiple hours, days or even weeks, depending on the mesh refinement.

Multizone models are the third category of models considered for this project. Multizone models are interesting as they often offer a means to model more complex building systems, where zone models and fire models using CFD are lacking. For multizone models, detailed descriptions can be put into the modeling software for different rooms, the building structure, the elements of the ventilation system and any air handling units (AHUs). An example of a multizone model is CONTAM, another simulation program developed by NIST. CONTAM has the ability to calculate steady and transient building air flow rates and pressure differences between different zones within the building, taking into account the pressure difference exponent of an air flow path [48]. CONTAM also includes a rich set of contaminant transport analysis capabilities, making it interesting to explore its potential for use in fire safety engineering. A guide for using CONTAM to predict the spread of smoke was written by J. Klote et al. [30], [49], published in the Handbook of Smoke Control Engineering [50].

One disadvantage of CONTAM is that it does not perform heat transfer calculations. Therefore, the sofware is often coupled to multizone heat transfer models attain a complete overview of all building aspects. For its “regular” use, so non-fire scenarios, CONTAM has been coupled with EnergyPlus [51], [52] and TRNSYS [53]. These software provide the data on indoor temperatures and system air flows [52]. When modeling a fire scenario in CONTAM, the temperature development and soot generation can be manually entered as a time-dependent schedule. This data is retrieved from a fire (zone) model, e.g. CFAST [30].

The last simulation software evaluated is SYLVIA. SYLVIA is a software system developed by the IRSN (Institut de Radioprotection et de Sûreté Nucléaire) and is used for analyzing ventilation and aero contamination in fire situations [54]. The fire is modelled with a zone-based approach, thus similarly to CFAST. The ventilation system is modelled by creating a network of elements, conduits, filters, valves, fans, etc. This is comparable to the multi-zone modelling as in CONTAM.

SYLVIA is less widely used for academic research: searching via the TU/e online library environment gave so much as 12 results, using the search term “SYLVIA IRSN”, thus not even specifically focused on fire scenarios yet. Searching the same term in Google Scholar resulted in a list of 153 hits. Adding “fire” in the search term, reduced the results to 65.

Barely any documents were found on the validation of SYLVIA, primarily just a statement on the website of IRSN saying that “constant attention is paid to the system validation, particularly on the basis of the numerous full-scale tests performed by the IRSN” [54]. Validated is the ability of SYLVIA to model transient flows [55], [56]. Also, the concentrations of O_2 and CO_2 may be predicted accurately for mechanically-ventilated compartments. This was shown in research by Melis & Audouin (2006) [57]. However, from the same research, it was shown that in the first few minutes, the peak pyrolysis rate of the fuel was largely underestimated and also expected earlier than experiments showed [57]. This puts its functionality for this project into debate, since especially the first few minutes after ignition are of interest.

SYLVIA may be coupled to the CFD-program ISIS, also by IRSN. Looking up “ISIS IRSN” resulted in more hits in both the TU/e online library environment (14 hits) and in Google Scholar (446 hits), with respect to “SYLVIA IRSN”. Literature was found on validation and verification studies [26], [58]–[60]. However, this is still very limited with respect to using FDS as a CFD model for fire scenarios.

5. Calibration study

This chapter discusses the course of the calibration study, based on a case study performed by Hostikka et al. [10]. The objectives of the case study of Hostikka et al. were to predict and compare the (over-) pressure development for different fire scenarios in a fire apartment, and to evaluate the ability of Fire Dynamics Simulator (FDS) to predict smoke propagation to the non-fire apartments.

This chapter begins with summarizing the conducted research by Hostikka et al., introducing the building-, ventilation- and fire characteristics, assessment criteria, results and conclusions. Following this, the chapter delves into the methodology of the calibration study, including the reproduction of the case study building in the simulation software CFAST and CONTAM. Subsequently, the results from the simulation programs are presented, along with the conclusions drawn from them.

5.1 Introduction calibration case

As prior mentioned, the calibration study is based on the research by Hostikka et al. [10]. Hostikka and colleagues used FDS to simulate an apartment fire in a hypothetical residential building. This residential building consisted of ten apartments, all located on a single floor. The floor plan of the hypothetical residential building is retrieved from the paper on this study and can be found in Figure 5-1.

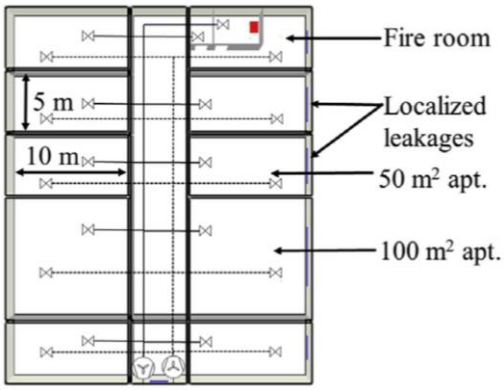

Figure 5-1. Plan view of the hypothetical residential building [10]

5.1.1 Building characteristics

The building of the calibration study consists of a single story containing ten apartments, each measuring either 50 m² or 100 m². The ceiling height is 2.5 m. Both the building envelope and the interior separation structure consist of normal weight concrete walls with a thickness of 0.15 m. Similarly, the floor and ceiling are made of 0.15 m thick concrete. It is assumed that the interior structure is adiabatic and fully airtight.

Whereas all other apartments are simplified into a single zone, the fire apartment consists of a separate living space, bedroom and bathroom. Like the other structural components, these separation walls are modelled as concrete walls with a thickness of 0.15 m. The doors within the apartment are open during the fire situation. Any door towards the corridor was left out of consideration.

For the exterior structure, three levels of airtightness are simulated: “traditional”, “modern” and “near-zero”. The specifications regarding the airtightness levels of the exterior structure are listed in Table 5-1. The interior structure is assumed fully airtight.

Table 5-1. Specifications of the exterior structure [10]

	q_{50} [m³/h*m²]	V_{50} [m³/s]	n_{50} [h⁻¹]	A_L [m²]
Traditional	3	0.146	4.2	0.02690
Modern	1.5	0.073	2.1	0.01345
Near-zero	0.75	0.036	1.05	0.006725

5.1.2 Ventilation characteristics

As the floorplan shows, all apartments are modelled with one supply vent and one exhaust vent. The fire apartment is the exception: it is equipped with one supply vent in the living room and with two exhaust vents, located in a bedroom and a bathroom. The ducts leading to the individual apartments have a diameter of 0.125 m; the collective ducts have a diameter of 0.25 m. The ventilation rate for all apartments in the non-fire situation is 40 L/s, with a slightly negative pressure in the apartment. Both collective fans have a stalling pressure of P_{max} = 550 Pa and a zero-pressure flow rate of $\dot{V}_{max}$ = 650 L/s. The pressure loss over the fan unit was tuned to 150 Pa.

Hostikka et al. investigated three damper configurations:

- Damper=Off Both inlet and outlet remain open during the fire;
- Damper=Inlet The inlet duct of the fire apartment is closed by a damper 10 s after ignition;
- Damper=Both Both inlet and outlet are closed by dampers 10 s from the ignition.

5.1.3 Fire characteristics

Three different fire scenarios were used in the simulations, corresponding to the profiles of three of the typical t^2-curves. The fire scenarios had a fire growth rate t_g of 300 s (medium), 150 s (fast) and 70 s (ultra-fast). The maximum heat release rate (HRR) for the medium and fast growing fire was set to 4 MW; for the ultra-fast growing fire the maximum HRR was set on 1 MW.

4 MW is considered a realistic value for apartment fires [10], [61] and is likely to consume the available oxygen, resulting in an accurate duration of fire and yield of combustion products.

5.1.4 Research objectives

The research by Hostikka et al. had two main objectives: namely to predict the pressure development in the fire apartment, as well as smoke propagation to other apartments. The pressure development over time were visualized in a line graph; the peak results for the different simulations were presented in a bar graph. Smoke spread was assessed both quantitively and qualitively. The smoke spread was assessed quantitively by taking the visibility, as reduced visibility is an indicator of smoke spread. The results were presented in a box plot. Qualitively, the smoke concentrations, at a point in time, were presented in plan views of the residential complex.

5.1.5 Results and conclusions

The research by Hostikka et al. showed that the pressure development was strongly dependent on the fire growth rate, as can be observed for the scenarios with the highest airtightness and wcventilation configuration “Damper=Both” (Figure 5-2).

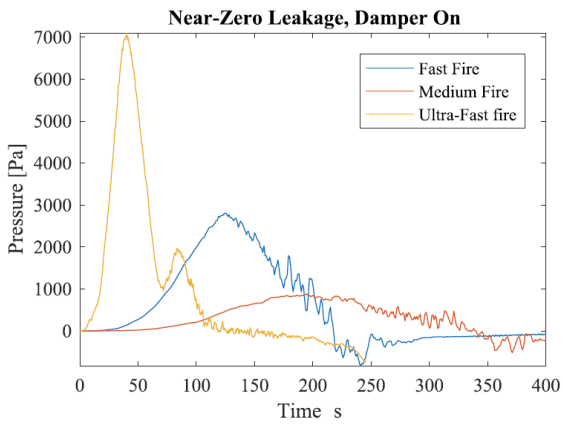

Figure 5-2. Predicted pressure development [10]

Not only did the pressure peak earlier for the fast and ultra-fast growing fires, compared to the fire scenario with a medium fire growth rate, the peak itself was also significantly higher. All peak values as retreived from the study by Hostikka et al. are presented in Figure 5-3. These peak values for overpressure also show the dependency on airtightness and damper configuration.

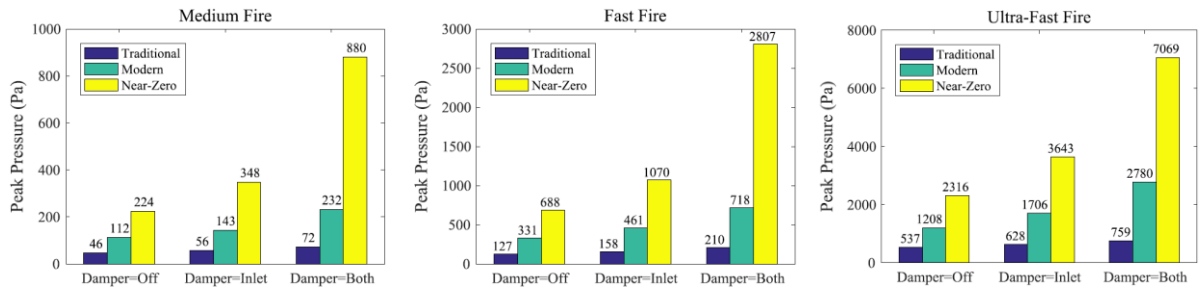

Figure 5-3. Simulations peak pressures bar plots [10]

From the predicted peak values, it is concluded that when fires occur in traditional buildings with a medium fire growth rate, it would be possible to evacuate the fire apartment. For apartments with a higher airtightness and/or a faster fire growth rate, opening the door would be more challenging. A side note to this conclusion is that these peak values do not reveal the duration of the pressure peaks.

The pressure results indicate that open ventilation ducts could be used as a potential path for pressure relief. However, open ventilation ducts showed an important route for smoke propagation, undermining the (smoke) compartmentation between the different apartments. The study of Hostikka et al. showed smoke spread to all other apartments in the cases with no dampers implemented in the ventilation ducts, and regardless of the fan operation (on or off). The inlet duct appeared to cause the smoke spread, as when a damper was used solely within the inlet duct, no smoke spread was observed. Figure 5-4 shows the retrieved visualization of the smoke spread, at 170 s after ignition.

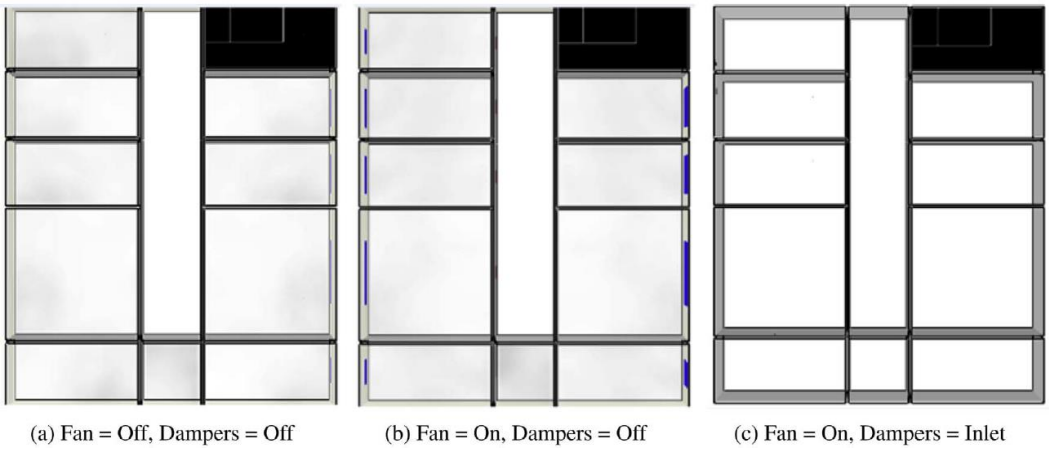

Figure 5-4. Visualization of smoke concentration 170 s after ignition [10]

5.2 Methodology

This section elaborates on the methodology of the calibration study, which entails a decoupled modeling approach using the zone-modeling software CFAST and the multizone-modeling software CONTAM. The methods specific to CFAST and CONTAM are discussed in their respective sections.

In total, 18 scenarios were evaluated, presented in Table 5-2. The input and output for fire scenarios 3.1.1 and 3.2.1 will be highlighted throughout this chapter. Other input and output will be found in the appendices, indicated throughout the chapter.

Table 5-2. All fire scenarios

	Ventilation configuration	*t^2 = 300 s (medium)*	*t^2 = 150 s (fast)*
Traditional facade	Damper=Off	1.1.1	1.2.1
	Damper=Inlet	1.1.2	1.2.2
	Damper=Both	1.1.3	1.2.3
Modern facade	Damper=Off	2.1.1	2.2.1
	Damper=Inlet	2.1.2	2.2.2
	Damper=Both	2.1.3	2.2.3
Near-zero facade	Damper=Off	3.1.1	3.2.1
	Damper=Inlet	3.1.2	3.2.2
	Damper=Both	3.1.3	3.2.3

5.2.1 Modeling in CFAST

The fire apartment is created as a single zone in CFAST. This, as according to the ASTM E779-10, an apartment can be considered as single-zone if the pressure difference between the rooms is no more than 5% of the inside to outside pressure difference [62]. As the doors of the fire apartment were open throughout the simulations [10], it is assumed that the conditions in the fire apartment in non-fire conditions meet this requirement. The building characteristics, ventilation characteristics and fire characteristics can be found in the subsections below, as well as the output and assessment criteria.

The simulation time for the CFAST simulations was set to 400 s. The output from CFAST was retrieved for intervals of 5 seconds.

Building characteristics

The fire apartment is modeled with an occupant area of 50 m² (width 5 m; length 10 m) and a ceiling height of 2.5 m. The material for all structural components is "Concrete, normal weight", with a thickness of 0.15 m.

The airtightness is modeled as a Wall Vent, with a height of 2.5 m and a width of 0.01076 m, 0.00538 m and 0.00269 m for the traditional-, modern- and near-zero facades, respectively. This, to create a leakage area that corresponds to the A_L calculated by Hostikka et al. (Table 5-1).

Ventilation characteristics

The mechanical ventilation is simplified to only one opening for inlet and exhaust, each with a surface area of 0.01227 m² and an air flow rate of 0.04 m³/s (equivalent to 40 L/s). Both ventilation openings are configurated with a drop off pressure of 200 Pa and a zero flow pressure of 550 Pa.

The three different ventilation configurations are simulated by creating a time schedule for the mechanical vents, as can be found in Table 5-3. A fraction of 1 implies that the ventilation duct is fully open; a fraction of 0 implies that the ventilation duct is fully closed.

Table 5-3. Time schedule for the different ventilation configurations (Open/Close Criterion: Time)

Time	*Damper=Open*		*Damper=Inlet*		*Damper=Both*	
	Inlet	Outlet	Inlet	Outlet	Inlet	Outlet
0 s	1	1	1	1	1	1
10 s	1	1	0	1	0	0
400 s	1	1	0	1	0	0

Fire characteristics

The simulated fire for the scenarios is a standard t^2-curve fire, with a medium- and fast fire growth rate. These fire growth rate corresponds to the Eurocode EN 1991-1-2 for residential buildings [40].

The HRR_{max} is 4 MW or 4000 kW. Since Hostikka et al. did not provide other fire characteristics, the parameters as presented in Table 5-4 are used as CFAST input. The full CFAST input for scenarios 3.1.1 and 3.2.1 can be found in Appendix A.

Table 5-4. Fire characteristics

Fuel type	Cellulose ($C_4H_6O_3$)
Maximum heat release rate (HRR_{max})	4000 kW
Heat of combustion (H_c)	17,500 kJ/kg
CO yield (Y_{CO})	0.04
Soot yield (Y_{soot})	0.01
Medium fire growth rate (t_g)	300 s
Fast fire growth rate (t_g)	150 s

Output and assessment criteria

As prior mentioned, the assessment criteria of the study by Hostikka et al. included exclusively pressure and visibility, both retrieved from the FDS results. For the calibration study, other output parameters were of importance: some are required as inputs for the CONTAM simulations, while others aid understanding the development of the fire.

The first output parameter considered was the actual heat release rate (HRR). The actual HRR was compared to the calculated HRR to give an indication of the course of the fire, i.e. whether the simulated fire was fuel- or ventilation controlled. The actual HRR was also used to obtain the generation rate of the contaminant, which needed to be used as input for the CONTAM simulations.

Secondly, the layer temperatures were obtained from the CFAST output. Together with the layer height, the layer temperatures were used to calculate the weighted average temperature. This value was required as input for the CONTAM model. The following formula was used to calculate the weighted average temperature T_{av}, by the example of Klote [30]:

$$T_{av} = \frac{T_U * (H - z) + T_L * z}{H} \qquad \text{Eq. 2}$$

With:

T_{av}	Weighted average temperature [°C]
T_U	Upper layer temperature [°C]
T_L	Lower layer temperature [°C]
H	Compartment height [m]
z	Zone layer height [m]

Additionally, the peak values for the overpressure for all scenarios, and the mass flow rates for scenarios 3.1.1 and 3.2.1 were retrieved from the CFAST results.

Lastly, as only the fire apartment was modeled and the focus was on smoke spread rather than smoke development in the fire apartment, the visibility as calculated by CFAST was not assessed. The results from Hostikka et al. only showed qualitive smoke development for the fire apartment, i.e. the fire apartment was completely filled by the smoke.

5.2.2 Modeling in CONTAM

As prior mentioned, CONTAM is a multizone model. In the model space of the software, different zones are drawn to resemble the apartments and the hallway as found in the hypothetical residential building used in the study by Hostikka et al. The CONTAM User Guide recommends to maintain the general topology of the actual floor plan of the building as a starting point [48]. Figure 5-5 illustrates the floor plan as created in CONTAM. The ceiling height is adjusted in the settings to 2.5 m.

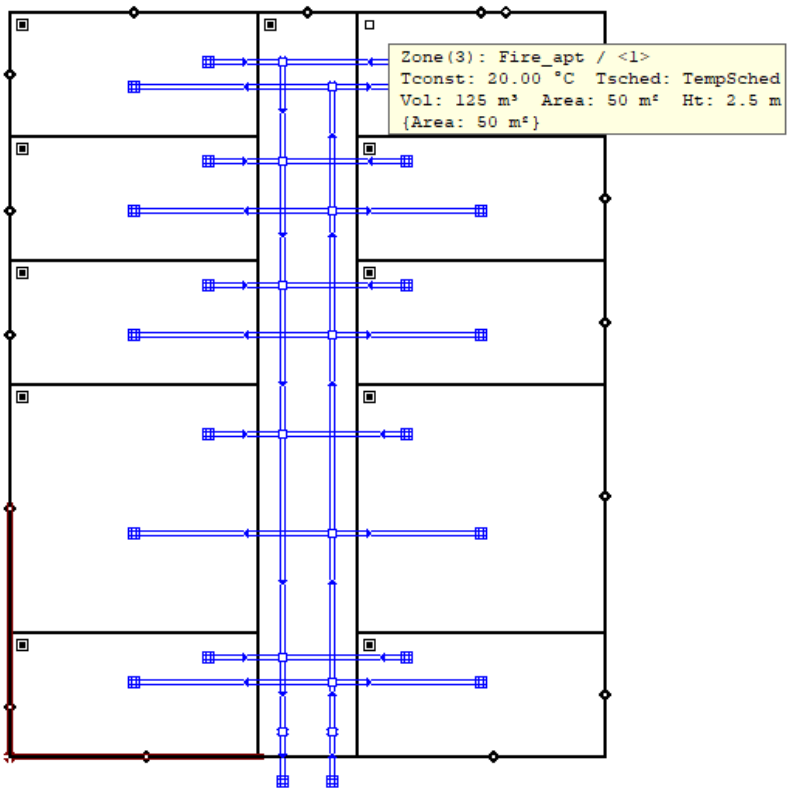

Figure 5-5. Plan view as created in CONTAM

All input data is available in Appendix B, but this section goes more into depth on the modeling of the building characteristics, ventilation characteristics and fire characteristics.

Building characteristics

For each zone, a zone name is required and zone properties are specified. These include the dimensions (expressed in volume and floor area) and the indoor air temperature. The temperature is set as either stable temperature for the duration of the simulation, or set to change over time according to a manually entered schedule. The temperature of the ambient and the temperature of all zones is set to 20 °C. The fire apartment has a manually defined schedule, further discussed under fire characteristics.

The airtightness is set as air flow path per facade element. In the plan view as presented in Figure 5-5, these air flow paths are indicated as a tiny dot along the exterior walls. A new air flow element is created, using the Power Law Model 'Leakage Area Data'. From Table 5-1, the equivalent leakage area is taken. For the parts of the façade that are 10 m in length, 2/3 of the total equivalent leakage area is put in. For the parts of 5 m, this is 1/3 of the total equivalent leakage area. The reference pressure is set to 50 Pa, the discharge coefficient to 0.6 and the flow exponent to 0.65. The height of the leakages is set to 1.25 m.

Ventilation characteristics

As mentioned in the introduction of the calibration case, all apartments are connected to a collective duct system. Ducts can be drawn in the model space of CONTAM, again creating a similar topology as the duct system of the case study by Hostikka et al. The duct systems are indicated by the blue lines, such as visible in Figure 5-5. Terminals and junctions are created automatically.

The flow element model chosen for the duct segments was the Darcy-Colebrook model, which combines the Darcy-Weisbach relation that relates the pressure loss due to friction along the duct, and Colebrook's natural roughness function [48]. The default value for roughness is 0.09 mm. This value is kept for the calibration study. Other parameters assigned to the ducts are the shape, dimensions and leakage rate. The assigned shape and dimensions are as in the calibration study, so circular with a diameter of 0.125 m for the ducts leading to the individual apartments and circular with a diameter of 0.25 m for the collective ducts. The leakage rate is assumed to be 0 L/s/m². The flow direction is indicated with the blue arrow, located on every duct segment.

The duct air flow elements in the fire apartment is changed for the scenarios with "Damper=Inlet" and "Damper=Both", then simulating the ducts in the fire apartment using the Backdraft Damper Flow Model. This is done to be able to close the duct at 10 s to recreate the configurations with closed ducts. As the resistance for the backdraft damper differentiates from the resistance of a "Darcy-Colebrook"-duct element, resulting in a different pressure in the fire apartment, it is chosen to only use this element when the duct should be closed.

Also, the two duct segments and terminals at the bottom are different. A "Constant volume flow" model was picked, under "Fan and Forced-flow models". These represent the admission and exhaust fans, with a maximum flow rate of 650 L/s. The parameters under Shape, Size and Leakage are kept the same as for the other collective ducts. The two terminals that are connected to the ambient, have a free face area of 0.049 m² and a design flow rate of 400 L/s, so sufficient air is available and exhausted for all 10 apartments.

For every terminal, a design flow rate is set. The design flow rate for all terminals located in the apartments corresponds to the 40 L/s as used in the calibration study. The free face area is set to 0.0123 m², which is equal to the round up from the calculated area of the duct segment.

For the junctions, the default settings are kept. For this case study building, the option "Horizontal connection only" satisfies. If the ventilation system were to connect multiple floors, this is indicated here.

Fire characteristics

As mentioned, the fire apartment has a manually defined temperature schedule to simulate the course of the weighted average temperature during 400. The amount of time steps for the schedule is reduced in such a way, that the trapezoidal curve still represents the curve of the course of the weighted average temperature. All time schedules are found in Appendix C. The temperature day schedules for scenario 3.1.1 and 3.2.1 are given in Table 5-5 and Table 5-6, respectively. For illustration, the comparison between the weighted average temperature curve from the CFAST simulation and the trapezoidal curve from the temperature schedule is shown in Figure 5-6 for scenarios 3.1.1 (left) and 3.2.1 (right).

Table 5-5. Temperature schedule of the fire apartment for fire scenario 3.1.1

Time [s]	*0*	*30*	*60*	*80*	*105*	*135*	*185*	*195*	*210*	*280*	*360*	*400*
Time [mm:ss]	00:00	00:30	01:00	01:20	01:45	02:15	03:05	03:15	03:30	04:40	06:00	06:40
Temp. [°C]	20	21.4	29	40.7	66	115.8	242.4	222.2	197.3	154	113	98.1

Table 5-6. Temperature schedule of the fire apartment for fire scenario 3.2.1

Time [s]	*0*	*30*	*45*	*60*	*80*	*100*	*115*	*155*	*200*	*245*	*290*	*330*	*400*
Time [mm:ss]	00:00	00:30	00:45	01:00	01:20	01:40	01:55	02:35	03:20	04:05	04:50	05:30	06:40
Temp. [°C]	20	24.7	35.5	57.1	108.3	188.7	286.2	196.3	141.1	102.5	76.9	62.6	49.2

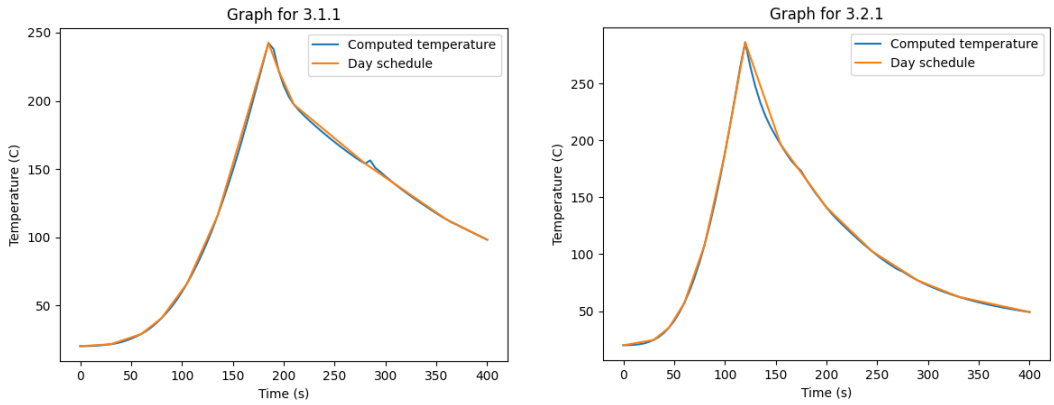

Figure 5-6. Comparison of the computed T_{av} versus the curve of the trapezoidal day schedule

To complete the day schedule for the weighted average temperature, a temperature is added at time 24:00:00 (hh:mm:ss). The value equals the same temperature as at 400 s or 06:40 (mm:ss).

Then, under Contaminants in CONTAM, contaminant species can be defined. For this calibration study, a contaminant is created with the name $C_4H_6O_3$. A Source is then added to the fire apartment, defined with a constant coefficient element. The pyrolysis rate of this element is obtained by using the formula as presented by Klote et al. [30]:

$$G_{max} = \frac{HRR_{max}}{H_c} \qquad \textit{Eq. 3}$$

With:

G_{max}	Pyrolysis rate [kg/s]
HRR_{max}	Maximum heat release rate [kW]
H_c	Heat of combustion [kJ/kg]

As HRR_{max} is defined as 4000 kW and H_c is defined as 17,500 kW, G_{max} is calculated to be 0.23 kg/s. For all fire scenarios, a day schedule is created based on the actual HRR curves of the fire scenarios. These day schedules are defined with the fraction of the generation rate, based on the actual HRR curve and the HRR_{max} of 4000 kW:

$$f_g = \frac{HRR_i}{HRR_{max}} \qquad \textit{Eq. 4}$$

With:

f_g	Fraction of the generation rate [-]
HRR_i	Actual HRR at time i [kW]
HRR_{max}	Maximum heat release rate [kW]

The day schedule of the fire scenario 3.1.1 is given in Table 5-7; the day schedule of the fire scenario of 3.2.1 is given in Table 5-8. All other day schedules can be found in Appendix C. Similar as for the day schedules for the temperature profile, the day schedule in CONTAM is to be completed with a value for the time 24:00:00 (hh:mm:ss). This value is the same value as for t = 400 s.

Table 5-7. Schedule for the generation rate for 3.1.1 (medium fire growth rate, near zero façade, Damper=Off)

Time [s]	*0*	*30*	*60*	*90*	*120*	*150*	*185*	*195*	*200*	*215*	*260*
Time [mm:ss]	00:00	00:30	01:00	01:30	02:00	02:30	03:05	03:15	03:20	03:35	04:20
Actual HRR [kW]	0	40	160	360	640	1000	1526.7	384.1	350.8	418.8	250.7
Fraction [-]	0	0.01	0.04	0.09	0.16	0.25	0.382	0.096	0.088	0.105	0.063

Time [s]	*265*	*270*	*275*	*280*	*345*	*350*	*355*	*400*
Time [mm:ss]	04:25	04:30	04:35	04:40	05:45	05:50	05:55	06:40
Actual HRR [kW]	441.9	144.7	173.7	123.8	14.7	19.2	3.9	0.00
Fraction [-]	0.110	0.036	0.043	0.031	0.004	0.005	0.001	0.00

Table 5-8. Schedule for the generation rate for 3.2.1 (fast fire growth rate, near zero façade, Damper=Off)

Time [s]	*0*	*15*	*45*	*75*	*90*	*115*	*125*	*135*	*165*	*170*	*175*
Time [mm:ss]	00:00	00:15	00:45	01:15	01:30	01:55	02:05	02:15	02:45	02:50	02:55
Actual HRR [kW]	0	40	360	1000	1440	2360	836.4	614.7	331.7	430.3	121.9
Fraction [-]	0	0.01	0.09	0.25	0.36	0.59	0.21	0.15	0.08	0.11	0.03

Time [s]	*180*	*205*	*210*	*215*	*240*	*275*	*400*
Time [mm:ss]	03:00	03:15	03:30	03:45	04:00	04:35	06:40
Actual HRR [kW]	212	124.4	136.5	111	36.2	16.1	0.00
Fraction [-]	0.053	0.031	0.034	0.028	0.01	0.00	0.00

Output and assessment criteria

The output from the CONTAM simulations includes the pressure in the different apartments and the contaminant concentrations in the other apartments. Both can be retrieved from the CONTAM simulations.

The pressure development is now based on the temperature increase in the apartment, rather than on the course of the fire as found with CFAST. The pressure peaks and the course of the pressure development from the CONTAM simulation will be compared to the pressure peaks and development resulting from the research by Hostikka et al.

The output for the contaminant concentrations was exported from CONTAM for all apartments, default in [kg/kg]. The following formula was used to convert the concentration to [g/m³] [48]:

$$D\left[\frac{g}{m^3}\right] = D\left[\frac{kg}{kg}\right] * 1000 * \rho_{air} \qquad \textit{Eq. 5}$$

This concentration value was then used to calculate visibility. This was done using the following formulae, offered in a report on smoke density and visibility by Van Herpen [43]:

$$RD_e = R_e * D \qquad \textit{Eq. 6}$$

$$S = \frac{1.3}{RD_e} \qquad \textit{Eq. 7}$$

With:

RD_e	Light extinction coefficient: optical smoke density per light path traveled [m^{-1}]
D	Smoke particles density [g/m³]
R_e	Mass optical density [m^{-1}*m³/g]
S	Visibility in black smoke [m]

The R_e value for alfa-Cellulose was retrieved from Husted's report on optical smoke units and smoke potential, where it was specified as 0.22 m^{-1}*m³/g [63].

Correction of the CONTAM model

Doing with exploratory simulations in CONTAM on the calibration study, it was found that a higher interior temperature did not result in a significantly higher pressure in the fire apartment (< 7 Pa), regardless the airtightness level and ventilation configuration. This can be explained through two of the model assumptions presented in the Technical Notes [48], under *well-mixed zones* and *thermal effects*. Every zone is treated as a single node, wherein the air has well-mixed conditions throughout regarding temperature, pressure and contaminant concentrations. Equilibria, such as a change in air density, are reached within a single time step. The thermal effect, i.e. the temperature difference between the fire apartment and the ambient, causes air flows through the openings. The pressures shown at the openings, are due to the stack effect inside the fire apartment, caused by the defiltration via the openings.

To overcome the conflicting results, it was decided to model a fan as additional air flow path through the facade to create a pressure development more comparable to the pressure development as found by Hostikka et al. Ideally, this would be a fan based on the mass flow rate $\dot{m}$ calculated from the HRR in [W], using the following equation:

$$\mathrm{Q(t)} = \rho_{air} * c_{air} * V(t) * \Delta T \qquad \textit{Eq. 8}$$

With:

ρ_{air}	Density of air at 20 °C [kg/m³]
c_{air}	Specific heat capacity of air [J/kgK]
V(t)	Volumetric flow rate [m³/s]

The mass flow rate could then be retrieved from $\rho_{air} * \dot{V}$. However, this method turned out unattainable as CONTAM only includes temperature differences between zones. In addition, the input for the fan is limited to a constant mass flow rate in kg/s and a dimensionless day schedule.

Ultimately, it was decided to base the additional fan on a mass flow rate calculated from the weighted average temperature from the CFAST results, using the ideal gas law and conservation of mass as starting point.

Firstly, the ρ_{air} per time step was calculated with the following equation [64]:

$$\rho_{air,T} = \frac{353}{(273 + T_{av})} \qquad \textit{Eq. 9}$$

With:

$\rho_{air,T}$	Density of air at a temperature T [kg/m³]
T_{av}	Calculated weighted average temperature [°C]

The mass of air (m_{air}) in the fire apartment could then be calculated using:

$$m_{air} = \rho_{air,T} * V \qquad \textit{Eq. 10}$$

The difference in mass between every two consecutive time steps was divided by 5 to get a mass flow rate $\dot{m}_{air}$ in [kg/s]. The absolute value was used to prevent calculating with a negative flow rate through the fan. The maximum mass flow rate retrieved for the fire scenarios with a medium fire growth rate was 0.61 kg/s, and for the fire scenarios modeled with a fast fire growth rate 1.1 kg/s. A day schedule was created for each fire scenario, based on the fraction of $\dot{m}_{air}$ relative to the maximum $\dot{m}_{air}$. The schedules for fire scenarios 3.1.1 and 3.2.1 are presented in Table 5-9 and Table 5-10. All other schedules are found in Appendix C.

Table 5-9. Fan operation schedule of the additional fan for fire scenario 3.1.1

Time [s]	*0*	*15*	*45*	*60*	*95*	*130*	*160*	*180*	*185*	*220*	*285*	*290*	*295*	*400*
Time [mm:ss]	00:00	00:15	00:45	01:00	01:35	02:10	02:40	03:00	03:05	03:40	04:45	04:50	04:55	06:40
$\dot{m}_{air}$ *[kg/s]*	0	0.02	0.11	0.18	0.42	0.58	0.58	0.5	0.48	0.16	0.11	0.26	0.15	0.11
Fraction of max. $\dot{m}_{air}$ *[-]*	0.00	0.03	0.18	0.30	0.69	0.95	0.95	0.82	0.79	0.26	0.18	0.43	0.25	0.18

Table 5-10. Fan operation schedule of the additional fan for fire scenario 3.2.1

Time [s]	*0*	*30*	*45*	*60*	*80*	*100*	*115*	*150*	*170*	*175*	*180*	*235*	*270*
Time [mm:ss]	00:00	00:30	00:45	01:00	01:20	01:40	01:55	02:30	02:50	02:55	03:00	03:55	04:30
$\dot{m}_{air}$ *[kg/s]*	0	0.19	0.43	0.71	0.98	0.99	0.84	0.31	0.22	0.19	0.34	0.23	0.19
Fraction of max. $\dot{m}_{air}$ *[-]*	0.00	0.17	0.39	0.65	0.89	0.90	0.76	0.28	0.20	0.17	0.31	0.21	0.17

Time [s]	*280*	*330*	*400*
Time [mm:ss]	04:40	05:30	06:40
$\dot{m}_{air}$ *[kg/s]*	0.2	0.1	0.06
Fraction of max. $\dot{m}_{air}$ *[-]*	0.18	0.09	0.05

The peak pressures were compared to the peak pressures found by Hostikka et al. Using the calculated maximum $\dot{m}_{air}$, resulted in a strong overestimation of the overpressures for most scenarios. Therefore, different values for the maximum $\dot{m}_{air}$ were explored for the different façade types and different fire growth rates. The fits are discussed in the result sections.

5.3 Results

In this section, the results for the CFAST and CONTAM simulations are presented and discussed.

5.3.1 CFAST simulations

Heat release rate

Figure 5-7 shows the results for the computed heat release rate (HRR) and the actual HRR curves for fire scenario 3.1.1 (left) and 3.2.1 (right). It is observed that during the growth phase of the fire, the actual HRR curves follow the course of the computed HRR curve up until 185 s for fire scenario 3.1.1 and until 115 s for fire scenario 3.2.1. The early decay indicates that the simulated fire is ventilation controlled for both scenarios; the fire decays as result of oxygen depletion in the fire apartment. The difference in time and HRR peak is related to the fire growth rate of the fire.

Compared to the other curves, the actual HRR curve of fire scenario 3.1.1 followed a similar curve as of the other cases with a medium fire growth rate. Likewise, the actual HRR curve of fire scenario 3.2.1 followed a similar curve as of the other cases with a fast fire growth rate. During the decay phase of the fire, only slight dependency on airtightness and ventilation configuration was observed

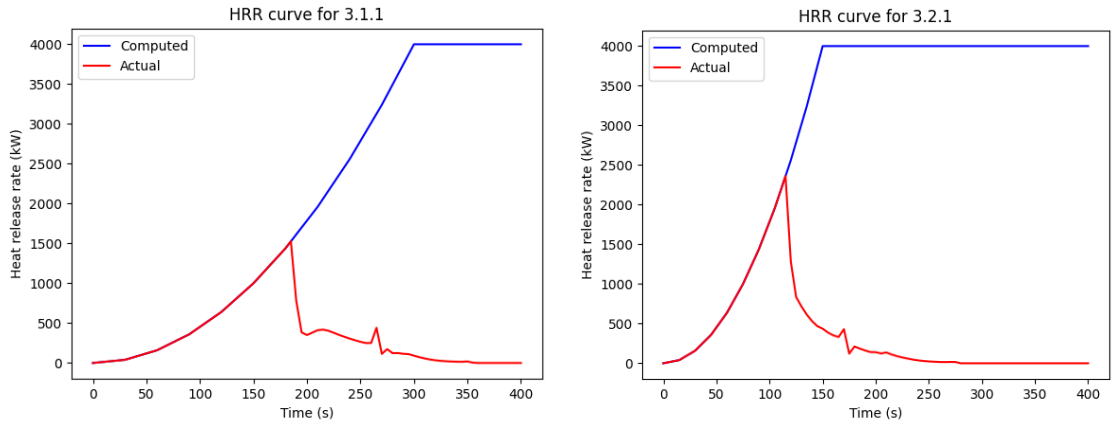

Figure 5-7. Expected and actual heat release rate curves for fire scenario 3.1.1 where t_g = 300 s (left) and 3.2.1 where t_g = 150 s (right)

Weighted average temperature

The calculated weighted average temperature for scenarios 3.1.1 and 3.2.1 are shown in Figure 5-8. It is observed that the temperature development is related to the fire growth rate: a higher t_g results in a faster temperature development as well as a higher peak in T_{av}.

Only slight dependency was observed for ventilation configuration and level of airtightness: all graphs followed similar curves. Comparison of the different configurations showed that the temperature peak is highest for the "near-zero" configurations, and that during the decay phase of the fire, the temperatures were highest for the configurations with "Damper=Inlet" and lowest for the configurations with "Damper=Off". Figure 5-9 and Figure 5-10, showing the comparison of all weighted average temperatures, support this statement.

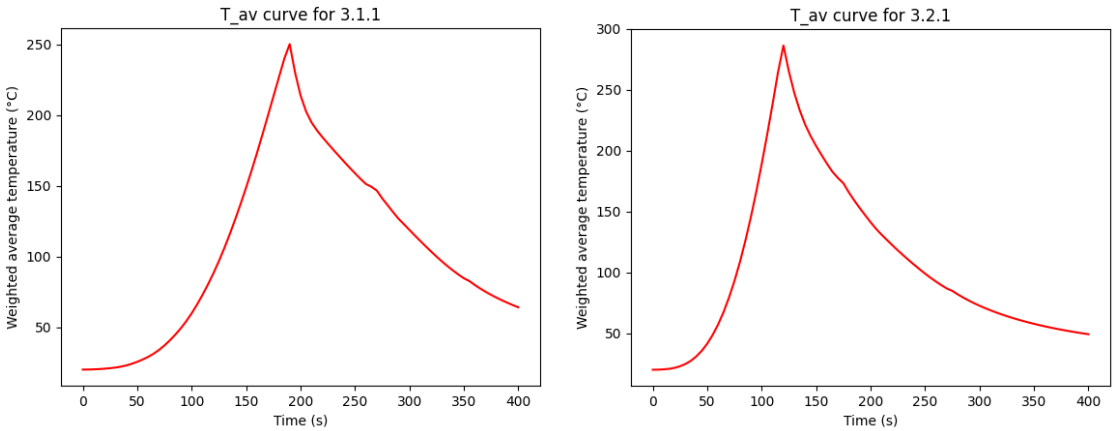

Figure 5-8. Weighted average temperature for fire scenario 3.1.1 where t_g = 300 s (left) and 3.2.1 where t_g = 150 s (right)

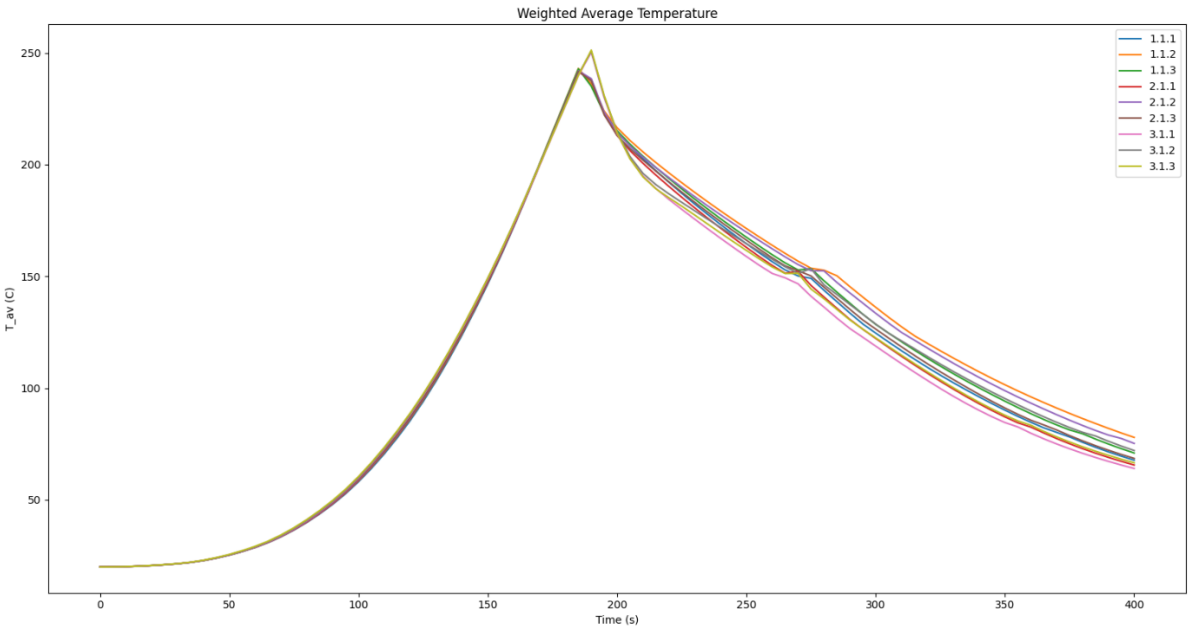

Figure 5-9. Weighted average temperature for all fire scenarios with a medium fire growth rate

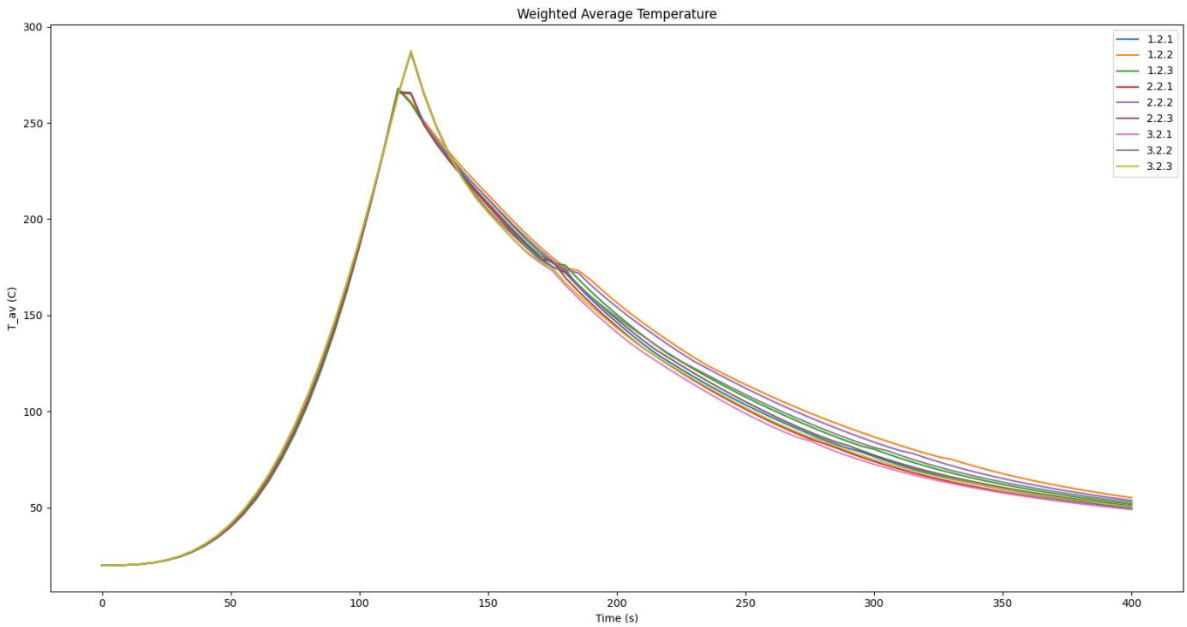

Figure 5-10. Weighted average temperature for all fire scenarios with a fast fire growth rate

Peak pressures

The peak pressures resulting from the CFAST simulations are put in Table 5-11 and Table 5-12, next to the peak pressures as found by Hostikka et al. The results from the CFAST simulations were largely overestimated. This was in line with the expectations based on literature [9], [45] and showed the substantiation for combining CFAST with another simulation software.

Tables 5-11 and 5-12 also show the results from the CONTAM simulations, but these will be evaluated in the next section.

Peak mass flow rate

The mass flow rates through the wall vents and the mechanical vents, resulted from the CFAST simulations, were retrieved from the "vents"-output files. The peak value of the sum of the mass flow rates for scenario 3.1.1 was found to be 0.51 kg/s; for scenario 3.2.1 the maximum mass flow rate was 0.91 kg/s. The mass flow rate was observed preliminary via the wall vent. The mass flow rate through the mechanical inlet vent was reduced to 0 kg/s, the mass flow rate through the mechanical outlet vent was limited to 0.05 kg/s. The output files are found in Appendix D.

5.3.2 CONTAM simulations

Pressure development

Regarding the pressure development in the fire apartment, the pressure peaks (for all fire scenarios) and the pressure development (only 3.1.1 and 3.2.1) were compared to the results as found by Hostikka et al.

First, all simulations were run with one maximum air flow rate: i.e. 0.61 kg/s for the fire scenarios with a medium fire growth rate and 1.1 kg/s for the fire scenarios with a fast fire growth rate. The results are presented in Table 5-11 for the scenarios with a medium fire growth rate and in Table 5-12 for the scenarios with a fast fire growth rate. Observed from the simulation results was the sensitivity of this method to the different airtightness levels and damper configurations. For most scenarios, the peak overpressure was largely overestimated. It was chosen to calibrate the maximum mass flow rate of the fan only to the Damper=Off scenarios, and check for 80% and 60% of the calculated maximum mass flow rate. The results were much more satisfactory for these maximum mass flow rates through the fans, as can be seen in Table 5-11 and Table 5-12.

Table 5-11. Pressure peaks found in the calibration study for all scenarios with a medium fire growth rate

Scenario	*Hostikka et al. Pressure [Pa]*	*CFAST simulations Pressure [Pa]*	*Pressure [Pa]*	*Pressure [Pa]*	*Pressure [Pa]*
Fan operation			*0.61 kg/s*	*0.49 kg/s*	*0.37 kg/s*
Factor [-]			1.0	0.8	0.6
1.1.1	46	733.6	117.3	82.9	54
1.1.2	56	732.2	188.5	130.8	81.8
1.1.3	72	798.5	476.5	340.2	220.8
2.1.1	112	2833.7	183.3	128.5	-
2.1.2	143	2839.5	347.1	238.4	-
2.1.3	232	3095.8	1296.5	909.7	-
3.1.1	224	9680.6	297.3	208.9	-
3.1.2	348	9702.5	548.3	374.8	-
3.1.3	880	10598.3	3646.5	2603.3	-

Table 5-12. Pressure peaks found in the calibration study for all scenarios with a fast fire growth rate

Scenario	*Hostikka et al. Pressure [Pa]*	*CFAST simulations Pressure [Pa]*	*Pressure [Pa]*	*Pressure [Pa]*	*Pressure [Pa]*
Fan operation			*1.1 kg/s*	*0.88 kg/s*	*0.66 kg/s*
Factor [-]			1.0	0.8	0.6
1.2.1	127	2428.1	286.5	197.7	123.6
1.2.2	158	2434.0	484.9	333.8	206.4
1.2.3	210	2539.6	1083.7	768.8	493.9
2.2.1	331	8768.0	465.8	319.4	-
2.2.2	461	8793.2	878.5	598.4	-
2.2.3	718	9185.7	3051.2	2164.6	-
3.2.1	688	23552.7	725.1	-	-
3.2.2	1070	23625.3	1440.4	-	-
3.2.3	2807	25069.5	8448.5	-	-

The pressure development is presented in Figure 5-11 for fire scenarios 3.1.1 and 3.2.1. For scenario 3.1.1, the peak pressure was reached at 160 s after ignition. CONTAM predicted exceedance of 100 Pa between 90 s and 195 s. For fire scenario 3.2.1, the overpressure in the fire apartment exceeded this value at 40 s after ignition. The peak occurred at 100 s. After 200 s, the overpressure was lower than 100 Pa and remained below the critical value after that.

The results for scenarios 3.1.3 and 3.2.3 are presented in Figure 5-12. The development of these curves was found to be almost identical to the curves of scenarios 3.1.1 and 3.2.1, which could be explained by the similarities of the HRR curves and temperature curves of the fire scenarios. The development of the curves during the growth phase was also similar to the pressure development curves of Hostikka et al., earlier presented in Figure 5-2 for comparison. For the decay phase, the curves retrieved from the CONTAM simulations showed a sharper drop in overpressure than the results by Hostikka et al. In addition, the fluctuations as found by Hostikka et al. were not predicted by CONTAM.

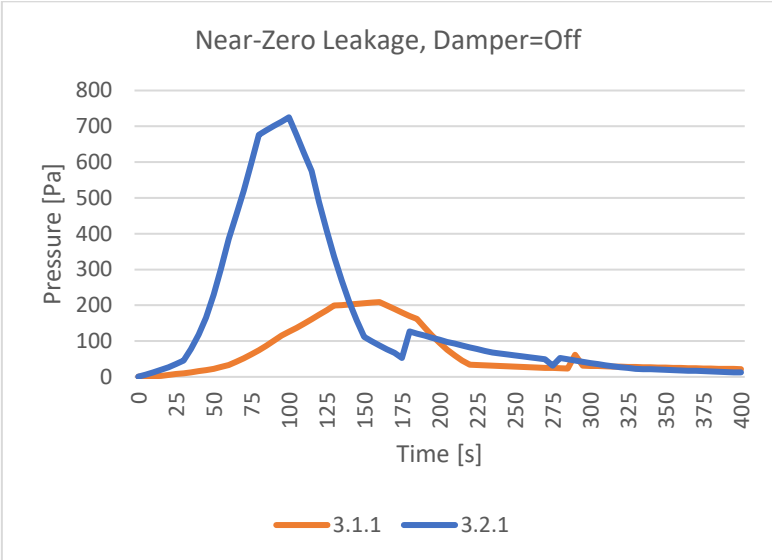

Figure 5-11. Predicted pressure development for fire scenario 3.1.1 where t_g = 300 s and 3.2.1 where t_g = 150 s

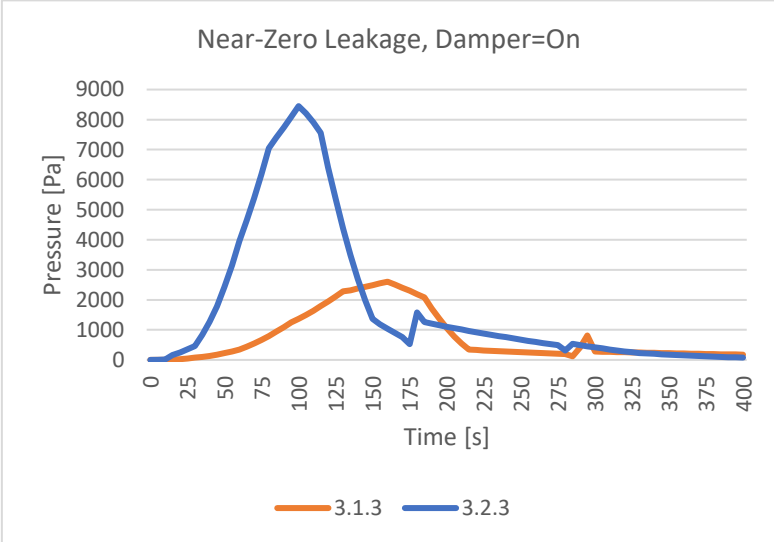

Figure 5-12. Predicted pressure development for fire scenario 3.1.3 where t_g = 300 s (left) and 3.2.3 where t_g = 150 s (right)

Mass flow rate

The mass flow rate through the wall leakages and the ventilation systems were retrieved from the CONTAM simulations for leakage paths #3 and #6, and through duct segments #2 and #4. The peak value of the sum of these mass flow rates are presented in Table 5-13, and compared to the results from the CFAST simulations. It is shown that the leakage through the façade is highly overestimated for the CFAST simulations, compared to the CONTAM simulations. This can be explained by the inability of CFAST regarding predicting of reverse flow in the inlet duct and the maximum value for the mass flow rate via the exhaust; therefore enhancing the flow through the façade. CONTAM was actually able to predict the reverse flow in the inlet duct, an important indicator of possible smoke spread, and an increased mass flow rate through the exhaust duct, caused by the overpressure in the fire apartment.

Table 5-13. Comparison peak mass flow rates resulting from the CFAST- and CONTAM simulations

	Results from CFAST		*Results from CONTAM*	
	Peak of total mass flow rate [kg/s]	Peak mass flow rate through leakages [kg/s]	Peak of total mass flow rate [kg/s]	Peak mass flow rate through leakages [kg/s]
3.1.1	0.61	0.58	0.51	0.10
3.2.1	0.95	0.92	0.97	0.21

The output files from the CONTAM simulations for leakage paths #3 and #6 and duct segments #2 and #4, are found in Appendix E.

Visibility in the non-fire apartments

From the retrieved contaminant concentrations, the visibility was calculated using the method presented in section 0, and presented in Figure 5-13.

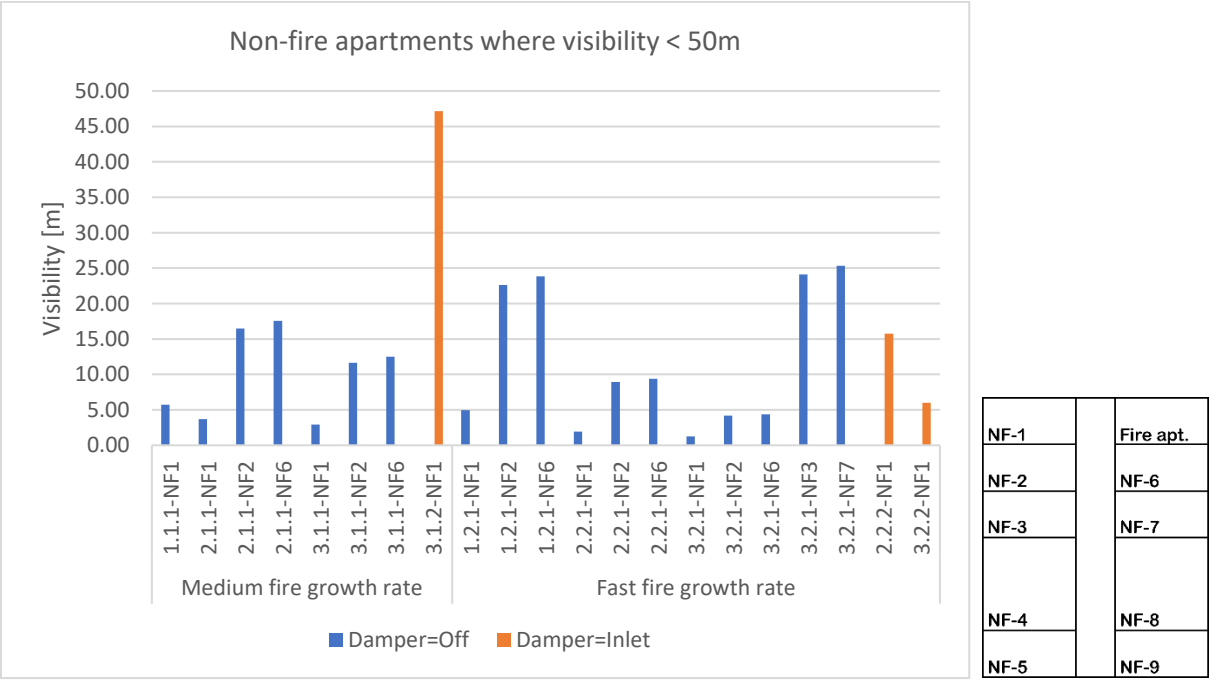

Figure 5-13. Calculated visibility in the non-fire apartments

Smoke spread to at least one other apartment was found for all scenarios with the ventilation configuration Damper=Off. Contrary to the prediction on smoke spread by FDS in the study by Hostikka et al., smoke did not spread to all other apartments. From the simulations in CONTAM, it was retrieved that most smoke spread was to the apartment across the fire apartment (NF1), and secondarily to the two neighboring apartments (NF2 and NF6). The visibility was below 10 m for NF1 for all scenarios, for

NF2 and NF6 only for the scenarios with a fast fire growth rate and a modern or near-zero façade airtightness. For scenario 3.2.1, smoke spread was additionally observed to NF3 and NF7, the non-fire apartments adjacent to NF2 and NF6.

Some smoke spread towards NF1 was also observed for fire scenarios 3.1.2, 2.2.2 and 3.2.2, indicating that smoke spread via the exhaust network would be an actual threat if the overpressure in the fire apartment is above a certain level.

5.4 Discussion

The primary aim of the calibration study was to examine the potential of using a decoupled modeling approach with CFAST and CONTAM to predict overpressure and smoke spread, based on the case study by Hostikka et al. on a hypothetical residential building. For the coupling, the heat release rate, the upper layer temperature, the lower layer temperature and the layer height were retrieved from the CFAST simulations. Unfortunately, these parameters could not be compared to the actual HRR found by Hostikka et al., or the temperatures in the fire apartment as the focus of the study by Hostikka et al. was solely on the pressure development and the smoke spread. However, Fourneau et al., Janardhan & Hostikka and Wahlqvist & Van Hees found temperatures of similar order of magnitude, up to 350 °C [14], [24], [32].

The pressure development was observed from the CFAST simulation results. As expected, they showed a great overestimation of the overpressure. This highlighted the need of coupling CFAST to another modeling software.

The results from the initial CONTAM simulations were significantly different from the results found by Hostikka et al. CONTAM was not developed as a software to model fire scenarios in, which was most obvious in the handling of the relation between increasing temperature, decreasing air density and increase in pressure. The additional fan, based on the ideal gas law and conservation of mass, offered a way method to stimulate overpressure. Using this method resulted in an overestimation of the overpressure, but especially during the growth phase, the method resulted in an accurate estimation of the pressure development. CONTAM did not predict the fluctuations as observed in the research by Hostikka et al. It could be that the input for the day schedule is not detailed enough (user error).

Later was found that the sum of the mass flow rates retrieved from the CFAST vents results, was approximately equal to the mass flow rates calculated by using the ideal gas law and conservation of mass. This also eliminated the necessity of iterating the maximum mass flow rate of the fan to fit the results by Hostikka et al. It can therefore be stated, that using these CFAST results directly would have been a more efficient method of modeling the additional fan.

Significant distinction was found in the results for visibility, as Hostikka et al. predicted a visibility below 10 m for all apartments using FDS. As presented, CONTAM predicted a visibility below 10 m for non-fire apartment NF1 for all scenarios with ventilation configuration “Damper=Off”, as well as for apartments NF2 and NF6 for the scenarios with a fast fire growth rate and a modern or near-zero façade airtightness. This conflicts with the results found by Hostikka et al. Considering the purpose of CONTAM, namely predicting contaminant spread, it does not necessarily mean that the results of the decoupling approach are wrong. One reason for the difference could be that the generation rate of smoke was calculated differently in FDS, and that the method offered by Klote underestimated this generation rate. Another reason could be that the smoke/contaminant propagation via the ventilation system is calculated differently in FDS and CONTAM. For both simulation methods, more research is recommended on smoke spread, preferably substantiated with experimental data.

Overall, it is observed that the decoupled modeling approach leads to acceptable results. Overpressure could be predicted with an additional fan of which the mass flow rate was substantiated with the ideal gas law and conservation of mass. Smoke spread to at least 5 of the non-fire apartments was predicted by the CONTAM simulations.

6. Case study

6.1 Introduction

The case study building is the modern residential complex “De Cavaliere”, in Helmond. An impression of the building can be found in images in Figure 6-1 [31].

Figure 6-1. Impression of De Cavaliere, Helmond

6.1.1 Building characteristics

This residential complex is U-shaped and consists of 70 apartments on five different floors. The floor plans are overall nearly identical. The floor plans of the first two floors are provided in Figure 6-2, all other floor plans can be found in Appendix F [65].

Figure 6-2. Floor plans of the first two floors of De Cavaliere [65]

The apartments vary in size, the floor area ranging between 60 and 135 m². The floor-to-floor height is 3.0 m and the floor-to-ceiling height is estimated on 2.6 m. The apartments are reached via an exterior corridor; the elevators and stairs are located at both ends of the U-shape.

The airtightness of several apartments was measured by doing (de-)pressurization tests in apartments 3.04, 3.06 and 4.05. In the floorplans in Figure 6-3, these apartments are highlighted in pink. The (de-) pressurization tests were performed according to the standards NEN-EN 13829 (method A), NEN 2686, NEN-EN-ISO 9972:2015 and the SKH-Assessment basis 13-01 Airtightness measurements (SKH-beoordelingsgrondslag 13-01 LUCHTDICHTHEIDSMETINGEN), in collaboration with K+ Adviesgroep. The results of these tests are summarized in Table 6-1. The full reports are available in Appendix G.

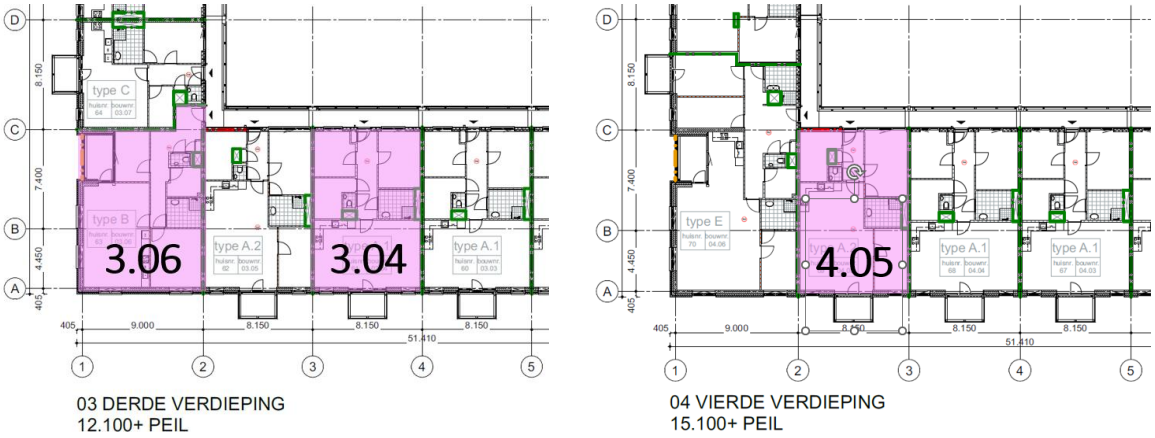

Figure 6-3. Floor plans with apartments 3.04, 3.06 and 4.05 highlighted

Table 6-1. Results blower door tests Cavaliere

	Overpressure			*Underpressure*		
#	Qv;10	ELA	EqLA	Qv;10	ELA	EqLA
	[L/(s*m²)]	cm²	cm²	L/s*m²	cm²	cm²
3.04 (A_F = 96 m²)	0.162	38.07	62.41	0.215	50.72	83.15
3.06 (A_F = 102 m²)	0.235	58.84	96.45	0.295	73.80	121.0
4.05 (A_F = 96 m²)	0.364	85.65	140.4	0.371	87.37	143.2

6.1.2 Ventilation characteristics

All apartments are mechanically ventilated, driven by a heat recovery ventilation (HRV) unit in each apartment. The capacity of the HRV unit is 300 m³/h, tested for pressures (p_{st}) up to 150 Pa. This implies that at its full functioning, the HRV unit supplies the apartment with 300 m³ of fresh air per hour. The HRV unit is equipped with a bypass, which leads the warm extracted air around the heat exchanger during summer in order to prevent the outdoor air from heating up further. The functioning of the HRV unit is schematically illustrated in Figure 6-4. Please note that the appearance of the HRV unit differs per brand and type, and thus that this figure is for illustrative purposes only.

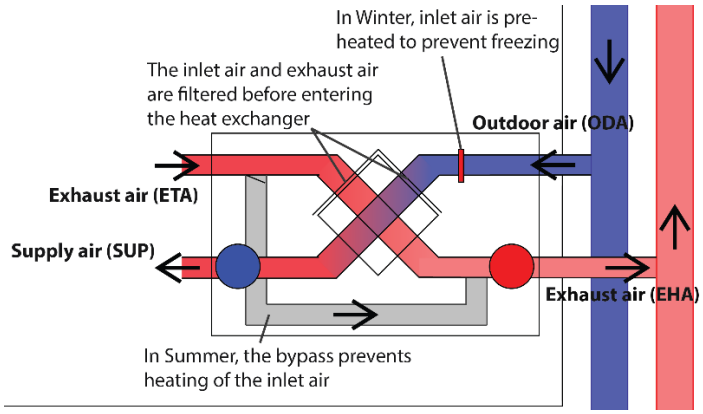

Figure 6-4. Heat recovery ventilation (HRV) unit schematically explained

Via the duct system above the apartment ceiling, the air is distributed to the living room, bedroom and technical space, which also serves as laundry room. Extraction of air is done in the kitchen, bathroom and toilet. The design flow rates, substantiated by the requirements set in the NEN 1087, are listed in Table 6-2, and will be used as starting point for the CONTAM simulations.

Table 6-2. List of ventilation requirements

	Supply [m³/h]	*Return [m³/h]*
Living room	150	
Kitchen		150
Open kitchen		150
Bedroom	25	
Bathroom		50
Toilet		25
Laundry room	50	
Other "dry" rooms	25	

The apartments that are located above each other are all connected to the collective inlet and exhaust ducts, located in shafts. Fire dampers are supplied that should prevent fire and hot smoke from entering the collective ducts and shafts, and have a fusible link that causes the damper to close if the temperature reaches 72 °C.

6.1.3 Fire characteristics

The fire characteristics are kept the same as for the calibration study, presented in section 0.

6.2 Methodology

6.2.1 Inventory of the ventilation system components

An inventory was made for the different apartments and ventilation systems. The starting point was the minimum air flow rate according to the NEN 1087 per apartment type (A, B, C and E) and per space. From the standard, it was also retrieved that the maximum air flow rate in a duct should be lower than 3 m/s to avoid noise hindrance. In the main ducts, the velocity may be up to 5 m/s. These values were used to calculate the duct diameter.

To prevent sensation of draughts, the flow velocity through inlet and extraction valves should not exceed 2 m/s. For inlet valves connected to ducts with a diameter of 125 mm, the volume flow rate should be under 50 m³/h. For extraction valves, the maximum volume flow rate should not exceed 75 m3/ . The free face area of the valves can be calculated by dividing the volume flow rate $\dot{V}$ in [m³/s] by the flow velocity v in [m/s].

For the inlet and exhaust at the roof, the velocities at the roof fan are 3 m/s for the inlet fan, to avoid rain water from entering the ventilation system, and 8 m/s for the exhaust. Again, the free face area can be calculated by dividing the volume flow rate $\dot{V}$ in [m³/s] by the flow velocity v in [m/s].

The results are listed in the results section.

6.2.2 Determining resistance on air flow by the HRV unit

As prior mentioned, the apartments of the Cavaliere are all equipped with an HRV unit with a capacity up to 300 m³/h. At the Peutz B.V. laboratory for building physics, a slightly different unit was tested for its resistance on air flow. Some of the system properties are compared in Table 6-3.

Table 6-3. Comparison actual and tested HRV unit

	Actual	*Tested*
Energy label	Label A/A+ (2017) [66]	Label A/A+ (2020) [67]
Exterior dimensions	W: 725 mm H: 850 mm D: 570 mm (incl. mounting bracket) [68]	W: 740 mm H: 957 mm D: 585 mm (incl. mounting bracket) [69]
Inner diameter for connection with ducts	Ø 160 mm [68]	Ø 160 mm [69]
Control system	3 levels (low 33% of the full set-up capacity, medium 66% of the full set-up capacity, high 100% of the full set-up capacity) [70]	3 levels (low 25% of the full set-up capacity, medium 50% of the full set-up capacity, high 100% of the full set-up capacity) [71]
Maximum air flow rate	300 m³/h [68]	325 m³/h [69]
Minimum air flow rate	100 m³/h with preheater on; 45 m³/h with preheater off [68]	81 m³/h [71]
Other		Two openings for SUP to allow for multizone ventilation strategies [72]

The measurement setup is provided schematically in Figure 6-5, based on the NEN-EN 13141-7 [73]. An image of the setup is added to give a better indication of the connections at the HRV unit. The fan used for the measurements was the Retrotec Ducttester 400 with different plugs as suited for the measurements. The pressures 10 Pa, 30 Pa, 50 Pa, 70 Pa, 100 Pa and 130 Pa were put into the control panel as aimed for overpressures. During the measurements, these would vary and values very close to the aimed for overpressures were noted, as well as the corresponding volume flow rate in m³/h.

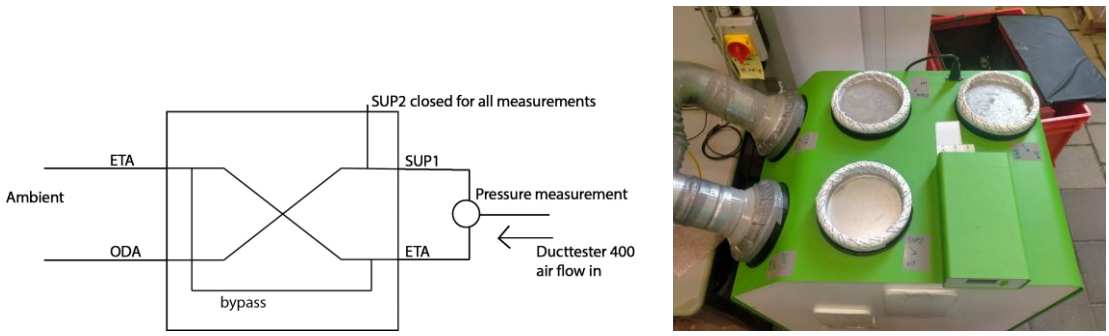

Figure 6-5. Schematic overview of the test set-up

In total, eight configurations were tested, listed in Table 6-4. The second opening for supply air, indicated in Figure 6-5 for completeness, was not included in the configurations and was therefore closed with a lid and secured with duct tape to prevent leakage via this opening. The HRV unit was set to function on its low level.

Table 6-4. Measurement configurations

	HRV unit On/off	*Bypass Open/closed*	*ODA & EHA Open/closed*
i	Off	Closed	Open
ii	Off	Closed	Closed
iii	Off	Open	Open
iv	Off	Open	Closed
v	On	Closed	Open
vi	On	Closed	Closed
vii	On	Open	Open
viii	On	Open	Closed

The results are discussed based on a regression analysis. The results of this regression analysis present a value for C, the capacity of the air flow resistances, and a value for n, the flow coefficient. From n, the resistance coefficient n^{-1} is determined. With these values, the following formula for air flow rate q_v through the HRV unit for different pressure differences can be filled in:

$$q_v = C * (\Delta P)^{n^{-1}} \qquad \text{Eq. 11}$$

With:

q_v	Air flow rate [dm³/s]
C	Capacity of the air flow resistances [Pa^n*dm³/s]
ΔP	Pressure difference [Pa]
n^{-1}	Resistance coefficient [-]
n	Flow coefficient [-]

Additionally, a r^2 value results from the regression analysis. This value indicates how well the regression model fits the measurement results. A value higher than 0.95 indicates a good fit.

The measurements for the system being closed (ODA & EHA closed) are all put together to determine the leakage to the exterior of the HRV unit itself. This, as the interior configuration should not influence the leakage of the exterior of the HRV unit.

The regression analysis on the closed system is used to correct the regression analyses on the open system. This is done by calculating the air flow rate at 5 fixed pressure differences (10, 50, 100, 150 and 200 Pa), based on the regression models. The air flow rate in the closed system is then subtracted from the air flow rate in open system. From the resulting air flow rates, a new regression model is established for the configurations with the openings kept open.

Comparisons of the regression analyses are done on the effect of the HRV unit being on or off and the bypass being open or closed.

6.2.3 Modeling in CFAST

Building characteristics

For the CFAST modeling, the simulation model is a simplified version of the actual apartment. The properties of each model are given in Table 6-5. A visual presentation of the models are added in Figure 6-6. The leakage areas will be treated more in depth for the CONTAM simulations.

Table 6-5. Input characteristics for the CFAST models

		3.04	*3.06*	*4.05*
Compartment width	m	8.15	8.15	8.15
Compartment length	m	11.85	11.85	11.85
Compartment height	m	2.6	2.6	2.6
Wall vent height	m	2.6	2.6	2.6
Wall vent width	m	0.0024	0.0037	0.0024
Ceiling vent area	m²	-	-	0.0078

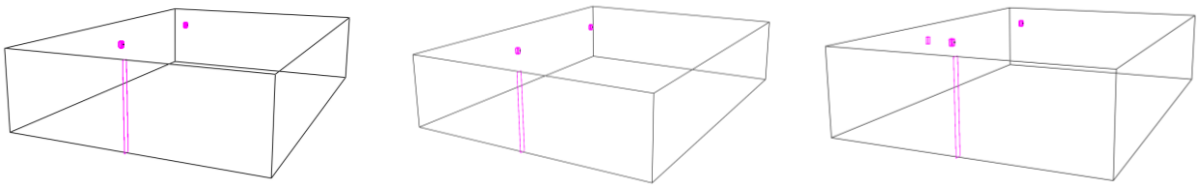

Figure 6-6. Model geometry of apartments 3.04 (left), 3.06 (middle), and 4.05 (right), visualized in SmokeView

Ventilation characteristics

The modeling is performed with the characteristics of the tested HRV unit. The capacity is set to the low level of the system (25% of the full capacity), thus 81 m^3/h. This corresponds to an air flow rate of 0.0225 m^3/s. Similar as for the calibration study, the system is modeled as two separate ventilation openings located in the ceiling: one inlet and one exhaust. From the technical specifications, it was taken that the drop-off pressure is 150 Pa. The surge pressure, where no flow takes place, is set at 550 Pa.

As the possibilities for input mechanical ventilation is limited in CFAST, it is chosen to use the properties of the actual applied HRV-unit, directly onto the ceiling. In Figure 6-6, the placement of these mechanical vents is seen for all three apartment types.

Fire characteristics

As mentioned, the fire characteristics are kept the same as for the calibration study. Again, fires are tested with a medium and a fast fire growth rate.

In Appendix H, all input for the CFAST simulations is provided regarding the building-, ventilation and fire characteristics.

Output parameters and assessment criteria

The first analyzed output parameters of the CFAST model were the computed and actual heat release rate (HRR) curves. As prior mentioned in section 0, these values were used to gain insight on the fire development. By method of Klote, the value for the actual HRR was also used to create a contaminant day schedule in CONTAM, described in section 0.

Secondly, the layer temperatures and layer height were retrieved. These were used to calculate the weighted average temperature, using Eq. 2, which was subsequently used to create a temperature day schedule for the fire apartment and for calculating the additional fan to simulate the pressure development, as described in section 0.

6.2.4 Modeling in CONTAM

Building characteristics

It was chosen to model 5 adjacent apartments on five levels. Amongst these 25 apartments, were apartments 3.04, 3.06 and 4.05, for which the leakage data was known. An overview of the floor plans for the fourth and fifth floor are presented in Figure 6-7, thus the floors on which apartments 3.04, 3.06 and 4.05 were located. The zones have been renamed based on the apartment type. The fire was modeled in apartment 3.04, or apartment 4/A2 from now on. The full input of the CONTAM model for the case study is found in Appendix I.

Figure 6-7. Floor plan of floor 4 (left) and floor 5 (right)

Where the apartments were simplified for the CFAST simulations, it was decided to imitate the geometry of the apartments as much as possible. Every room was therefore modeled as a separate zone, connected via a Two-way Model representing an open door of height 2 m and width 0.8 m. By default, the discharge coefficient was 0.78.

Leakages were modeled based on the performed measurements, combined with the assumption presented in the NIPV report on smoke propagation. The NIPV substantiated that internal leakages are trice the leakages through the envelop, excluding leakage via the door. For the floor and ceiling, the leakage is half the leakage of the envelop. The leakages between different apartments are also half the leakage of the envelop. The NIPV considered the leakage to the interior hallway to equal the leakage through the envelop. Different leakages were assigned to different building elements. An overview is given in Table 6-6. From the (de)pressurizing tests, it appeared that the roof had a large contribution of the overall equivalent leakage area and is therefore taken into account as a separate leakage area on the sixth level. For the rest of the leakage areas, the values are the same as for 3.04, as the apartments have the same outer dimensions.

Table 6-6. Leakage input for CONTAM simulations

			3.04	*3.06*	*4.05*
Total ELA		*[cm²]*	*62.41*	*96.45*	*140.4*
Exterior facade	¼ of total ELA	[cm²]	15.60	24.11	15.60
Interior leakage, of which:	¾ of total ELA				
Leakage to hallway	Equals exterior	[cm²]	15.60	24.11	15.60
Leakage to apartment below	½ of exterior	[cm²]	7.80	12.06	7.80
Leakage to apartment above	½ of exterior	[cm²]	7.80	12.06	-
Leakage to adjacent apartment 1	½ of exterior	[cm²]	7.80	7.80	7.80
Leakage to adjacent apartment 2	½ of exterior	[cm²]	7.80	16.31	7.80
Leakage via the roof		[cm²]	-	-	85.79

Ventilation characteristics

For the case study, two different methods of modeling ventilation systems were used. The difference in systems can be observed in the floorplan in Figure 6-7, when comparing the system of 4/A2 or 5/A2 with the system of other apartments.

For all non-fire apartments, the ventilation systems were modeled with an individual air handling system (AHS). The rooms were ventilated with supply and return points, with the design flow rates in m³/h as presented in the inventory in the results section of this chapter (Table 6-13). These supply and return points were linked to the AHS of the apartment. As the measurements on the HRV unit were performed on the system in its low setting, the supply and return points in the apartments were scheduled in a low setting (25%).

For the fire apartment and the non-fire apartments linked to the fire apartments by the collective ducts, the ventilation system was modeled in detail. The ducts within the apartment were modeled with a diameter of 125 mm. Where all ducts came together, they were given a diameter of 160 mm. The vertical ducts are connected at the terminals in the shaft, which would then function as junctions for downward and upward connections. The downward duct was defined with a diameter of 355 mm and a length of 2.6 m. The resistance for all ducts was calculated by the Darcy-Colebrook equations, with a roughness set to 0.09 mm. For the terminals, the free face area was assigned according to the outcome of the inventory (Table 6-13). The terminal loss coefficient was kept 0.125 by default setting. Lastly, the duct segments were the air would enter the apartment were defined with a constant volume flow. They are not connected, as the air flows do not mix. The volume flow rate assigned corresponds to the low setting of the tested HRV unit, thus 81 m³/h.

In the fire apartment, a similar duct system was drawn. However, in the technical space, the supply and extract air flows were connected where the HRV unit would be. This can be seen in Figure 6-7. The HRV unit was modeled as a backdraft damper with C = 19.796 and n^{-1} = 0.309, as resulted from the regression analysis on the measurements performed with a closed bypass (Table 6-14). A resistance flow model did not suffice here as it could not be described using a varying leakage area (n^{-1} < 0.5).

Fire characteristics

The focus of the CONTAM apartments was on a fire scenario for apartment 3.04. The temperature profile for the fire apartment was based on the calculated weighted average temperature, calculated from the CFAST results. The maximum generation rate was set as 0.23 kg/s, based on the calculation in section 0. The maximum mass flow rate of the additional fan was again calculated according to the method described in section 0, and set to 0.91 kg/s for the scenarios with a medium fire growth rate and to 1.56 kg/s for the scenarios with a fast fire growth rate. All day schedules are found in Appendix J.

Scenarios

In total, eight different scenarios are simulated for an apartment fire in apartment 3.04, for both the fire scenario with a medium fire growth rate and the fire scenario with the fast fire growth rate:

1. ***Base scenario***

The ventilation system was modeled as previously described.

2. ***Bypass HRV***

The ventilation system was modeled as previously presented. The HRV unit (duct 37) is modeled with the “bypass open”-properties, resulting from the measurement data as presented in Table 6-14 (C = 9.117 and n^{-1} = 0.418).

3. ***Bypass extra***

The ventilation system was modeled as previously described, but with an additional duct representing the bypass. The bypass was modeled around the HRV-unit (duct 37), from the extraction ducts to the exhaust duct. It is open during the entire simulation time (06:40 [mm:ss]). This creates a new geometry, as can be seen in Figure 6-8. The bypass, duct 38, was modeled with the Darcy-Colebrook resistance model with roughness 0.09 mm and Ø = 0.16 mm.

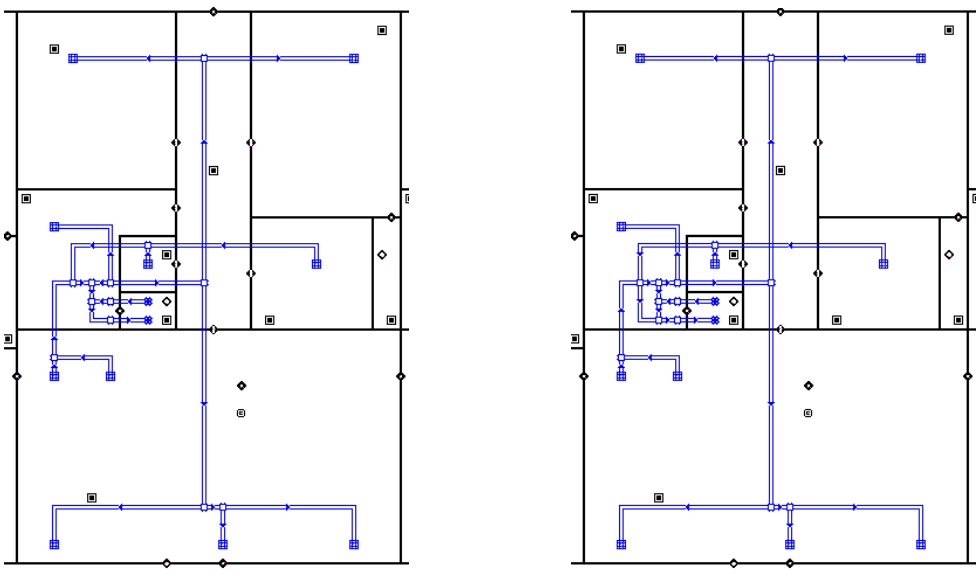

Figure 6-8. CONTAM geometry of apartment 4/A2 without (left) and with (right) modelled bypass

4. *Bypass scheduled*

The ventilation system was modeled with the additional duct representing the bypass. The exhaust duct towards the HRV, duct 34, was modeled as a fan with a constant mass flow rate with a schedule based on the air flow data found in the duct in the base scenario. The activation of a valve cutting off the air flow towards the HRV and opening a bypass, is assumed to happen with a fusible link at 72 °C. As CONTAM does not model heat flow, the activation of the valve was be linked to the contaminant concentration. When the concentration at this junction was the same concentration as in the living room at 72 °C, it is assumed that a valve cuts of the flow towards the HRV (duct 34) and opens the duct (duct 38) that functions as bypass. Duct 38 is modeled with the resistance flow model for volume flow, with Ø = 0.16 mm, C = 0.14 and n^{-1} = 0.5.

The moment at which the interior temperature exceeded 72 °C was retrieved from the CFAST results and the calculation of T_{av}. Figure 6-12 and Figure 6-13 in section 6.3.3 show that the interior temperature exceeds 72 °C at 150 s for the scenario with a medium fire growth rate and at 90 s for the scenario with a fast fire growth rate. For the scenario with the medium fire growth rate, the corresponding contaminant concentration was 0.0199 kg/kg; for the scenario with the fast fire growth rate, the contaminant concentration was 0.0218 kg/kg.

The schedules for the ducts for the fire scenario with a medium fire growth rate and a fast fire growth rate are then as presented in Table 6-7 and Table 6-8, respectively. The schedules are both based on fractions: for duct 34, this is the fraction of a mass flow rate of 1 kg/s; for duct 38, it is the fraction open (1) or closed (0).

Table 6-7. Day schedules for duct 34 and duct 38, t_g = 300 s

Time [s]	*0*	*30*	*60*	*130*	*150*	*185*	*186*	*400*
Time [mm:ss]	00:00	00:30	01:00	02:10	02:30	03:05	03:06	06:40
Duct 34	0	0.02	0.08	0.34	0.40	0.44	0	0
Duct 38	0	0	0	0	0	0	1	1

Table 6-8. Day schedules for duct 34 and duct 38, t_g = 150 s

Time [s]	*0*	*15*	*30*	*45*	*80*	*90*	*105*	*110*	*111*	*400*
Time [mm:ss]	00:00	00:15	00:30	00:45	01:20	01:30	01:45	01:50	01:51	06:40
Duct 34	0	0.02	0.08	0.20	0.56	0.64	0.73	0.75	0	0
Duct 38	0	0	0	0	0	0	0	0	1	1

5. *Fire damper inlet activation at 150 s / 90 s*

The ventilation system was modeled as previously presented for the base scenario. A constant mass flow fan is modeled at the duct segment between the HRV and the collective inlet duct, thus duct segment 39. The mass flow rate is based on the mass flow rate found in duct in the base scenario. This is modeled with a day schedule, presented in Table 6-9 for the scenario with t_g = 300 s and in Table 6-10 for the scenario with t_g = 150 s. In these tables, the mass flow rates are represented as a fraction of a maximum mass flow rate 1 kg/s. The mass flow is set to 0 when the interior temperature reached 72 °C.

6. *Fire damper inlet and exhaust activation at 150 s / 90 s*

Similarly, a constant mass flow rate fan was modeled at the duct segment between the HRV and the collective exhaust duct, thus duct segment 42. Here, both dampers were closed at the time when the interior zone temperature reached 72 °C. Table 6-9 and Table 6-10 show also the mass flow rates in duct 42 as a fraction of the maximum mass flow rate of 1 kg/s.

Table 6-9. Day schedules for duct 34 and duct 38, t_g = 300 s, dampers close after 150 s

Time [s]	*0*	*30*	*60*	*130*	*150*	*151*	*400*
Time [mm:ss]	00:00	00:30	01:00	02:10	02:30	02:31	06:40
Duct 39	0	0.04	0.10	0.36	0.42	0	0
Duct 42	0	0	0.06	0.28	0.33	0	0

Table 6-10. Day schedules for duct 34 and duct 38, t_g = 150 s, dampers close after 90

Time [s]	*0*	*15*	*30*	*45*	*80*	*90*	*91*	*400*
Time [mm:ss]	00:00	00:15	00:30	00:45	01:20	01:30	01:31	06:40
Duct 39	0	0.03	0.09	0.21	0.58	0.67	0	0
Duct 42	0	0	0.06	0.16	0.47	0.54	0	0

7. Fire damper inlet activation at 200 s / 120 s

In reality, a fire damper closes when the temperature at the damper is 72 °C, as the fusible link will melt. Here, the same approach is used to determine when the damper in the inlet would close, as for the valve regulating the bypass in the fourth scenario. The contaminant concentration at junction 39 was retrieved and compared to contaminant concentration in the zones when the temperature in the zones reached 72 °C. From this comparison, the time at which the damper would close was determined at 200 s for the fire scenario with a medium fire growth rate and at 90 s for the fire scenario with a fast fire growth rate. The extended day scheduled are presented in Table 6-11 and Table 6-12.

8. Fire damper inlet and exhaust activation at 200 s / 120 s

Similarly, the time at which the damper would close in the exhaust duct was determined and adjusted in the model according to the determined day schedules as presented in Table 6-11 and Table 6-12.

Table 6-11. Day schedules for duct 34 and duct 38, t_g = 300 s, dampers close after 200 s

Time [s]	*0*	*30*	*60*	*130*	*150*	*190*	*200*	*201*	*400*
Time [mm:ss]	00:00	00:30	01:00	02:10	02:30	03:10	03:20	03:21	06:40
Duct 39	0	0.04	0.10	0.36	0.42	0.47	0.46	0	0
Duct 42	0	0	0.06	0.28	0.33	0.37	0.36	0	0

Table 6-12. Day schedules for duct 34 and duct 38, t_g = 150 s, dampers close after 120 s

Time [s]	*0*	*15*	*30*	*45*	*80*	*90*	*105*	*120*	*121*	*400*
Time [mm:ss]	00:00	00:15	00:30	00:45	01:20	01:30	01:45	02:00	02:21	06:40
Duct 39	0	0.03	0.09	0.21	0.58	0.67	0.76	0.79	0	0
Duct 42	0	0	0.06	0.16	0.47	0.54	0.62	0.64	0	0

Output and assessment criteria

Output parameters included the pressure development and peak pressures and contaminant concentrations in the zones, but also the mass flow rate at duct segments 34 (ETA), 39 (ODA) and 42 (EHA), the contaminant concentration and zone temperature in zone LivingA2 on level 4 and the contaminant concentration at junctions 34, 39 and 41. These output parameters were necessary to model scenarios 4, 5, 6, 7 and 8. The duct segments and junctions are indicated in Figure 6-9.

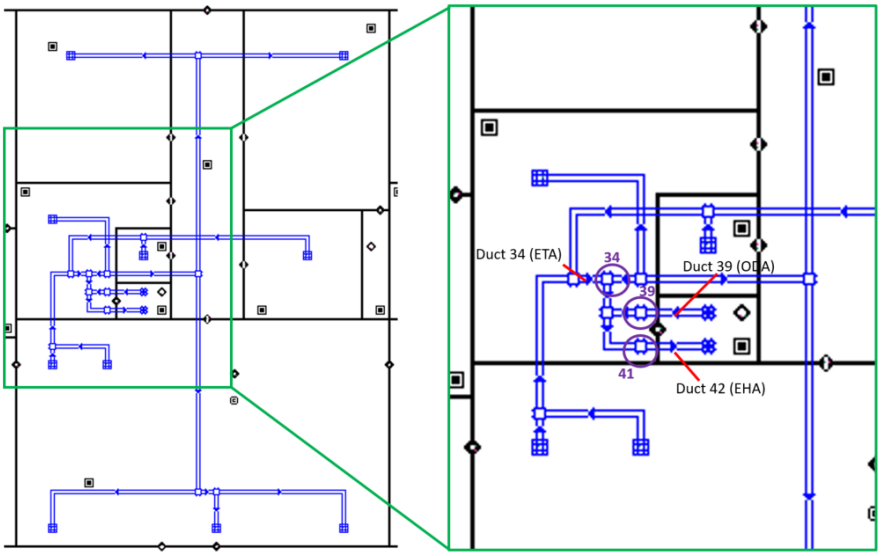

Figure 6-9. Indication of duct segments 34, 39 and 42, and junctions 34, 39 and 41 on the floor plan of apartment 4/A2

The pressure development and peak pressures counted as the first assessment criteria from the CONTAM simulations. The results are exported from the air flow path from the hall to the ambient (air flow path 120). A peak pressure < 100 Pa was taken as indicator for safe evacuation; the pressure development showed the time for which this threshold was potentially exceeded.

For all scenarios, the contaminant concentrations of all zones were exported. With a total of 521 zones, filtering the data was necessary. This was done in Microsoft Excel. The results for all zones at 400 s were filtered for values smaller than $9.81*10^{-5}$ kg/kg, as this was calculated to correspond to a visibility of > 50 m in the zone using the equations presented in section 0. For the zones remaining, thus with a contaminant concentration above than $9.81*10^{-5}$ kg/kg, the visibility was calculated at all time steps and a minimum visibility retrieved. These results were presented in a dot plot, excluding the zones of the fire apartment.

The pressure development over an air flow path, in this case air flow path 120, can directly be exported from CONTAM, as can the contaminant concentrations. This air flow path showed the leakage via the exterior separation structure to the outside on the front side of the apartment. Note that while this air flow path was located at the place of the front door, it does not show the leakage via the front door.

For retrieving the air flow rates in ducts and contaminant concentrations at junctions, the online CONTAM Results Export Tool needed be used [74].

6.3 Results

6.3.1 Inventory of the ventilation system components

Firstly, the ventilation rate was calculated for every apartment type. From the calculation, the ventilation rate was 250 m³/h for most apartments. This implies that ducts of 160 mm would suffice for the total air flow of each individual apartment. Calculating with the maximum ventilation capacity of the HRV unit installed, thus 300 m³/h, this would imply that the flow velocity would not exceed 4.15 m/s. Within the apartments, ventilation ducts with a diameter of 125 mm suffice. No more than 150 m³/h would go via these ducts, corresponding to a flow velocity of 3.40 m/s. Each valve has its branch, in which the air flow rate is at most 75 m³/h, corresponding to a flow velocity of 1.70 m/s.

In the Appendix K, a list is put on the ventilation rate (supply or extraction) per room, the amount of valves, the free face area of these valves, and the diameter per ducts, based on the maximum flow velocity in the duct of 3 m/s. A summary can be found in Table 6-13.

Table 6-13. List of valves per space

	Supply [m³/h]	Return [m³/h]	# valves	$\dot{V}$ per valve [m³/h]	$\dot{V}$ per valve [m³/s]	v [m/s]	Free face area [m²]
Living room	150		3	50	0.0139	2	0.0069
Kitchen		150	2	75	0.0208	2	0.0104
Open kitchen		150	2	75	0.0208	2	0.0104
Bedroom	25		1	25	0.0069	2	0.0034
Bathroom		50	1	75	0.0208	2	0.0069
Toilet		25	1	25	0.0069	2	0.0034
Laundry room	50		1	50	0.0139	2	0.0069
Other "dry" rooms	25		1	25	0.0069	2	0.0034

The collective inlet and exhaust ducts should have a total capacity of 1500 m³/h, determined from the maximum ventilation capacity of five installed HRV units. A collective duct with diameter 355 mm results in a flow velocity of at most 4.21 m/s in the collective ducts.

At the inlet, the flow velocity should not exceed 3 m/s to prevent rain from entering the ventilation system. Again, the maximum volume flow rate is considered 1500 m³/h. The free face area at the inlet is then 0.140 m². As the flow velocity at the exhaust may be up to 8 m/s, the free face area is calculated to be 0.050 m².

6.3.2 Determining resistance on air flow by HRV unit

A summarization of the results of the regression analysis performed on the measurements determining air flow through the tested HRV unit is given in Table 6-14. The measurement data and full regression analysis can be found in Appendix L.

Before the correction was performed, so for the regression analyses done with the raw measurement results, the r^2 value for all analyses was above 0.95. This implies that the generated regression models are a good fit for the measurement results. The values for the capacity of the air flow resistance of the HRV unit with the HRV unit were very similar for both bypass open and closed. Turning the HRV unit on made a difference for both configurations (bypass open and closed), with respect to the configurations tested with the HRV unit off and with respect to the other. This shows the effect of the fans on the resistance of the HRV unit as a whole. Unsurprisingly, the lowest capacity of the resistances was found for the configuration with the HRV unit on and the bypass open. With the bypass closed and the supply fan promoting overpressure, the resistance of the HRV unit is highest.

Doing the correction resulted in a perfect fit (r^2=1.000) as the input data consisted of calculated air flow rates rather than measured data. Overall, the values were very similar due to the low airtightness of the exterior of the HRV unit. The C values were slightly larger, whereas the n^{-1} values were slightly lower. This shows that for higher pressure differences, the air flow through the system is lower.

Table 6-14. Summary of the results of the regression analysis

	Description		r^2	C	n	n^{-1}
i	HRV off, bypass closed,	Before correction	0.991	15.355	2.777	0.360
	ODA & EHA open	After correction	1.000	15.399	2.805	0.356
iii	HRV off, bypass open,	Before correction	0.995	15.622	2.855	0.350
	ODA & EHA open	After correction	1.000	15.671	2.887	0.346
v	HRV on, bypass closed,	Before correction	0.972	19.722	3.200	0.313
	ODA & EHA open	After correction	1.000	19.796	3.232	0.309
vii	HRV on, bypass open,	Before correction	0.998	9.102	2.369	0.422
	ODA & EHA open	After correction	1.000	9.117	2.392	0.418
ii, iv, vi, viii	All, ODA & EHA closed		0.993	0.029	1.291	0.774

6.3.3 CFAST simulations

Figure 6-10 and Figure 6-11 show that the fire scenarios are likely very similar in the three apartments. The fire with a medium growth rate starts its decay phase around 240 s, from which is concluded that the fire is ventilation controlled. The fire with a fast fire growth rate starts its decay phase at 150 s, right after the maximum heat release rate was reached. This indicates that also these fires are ventilation controlled and start to decay due to lack of oxygen.

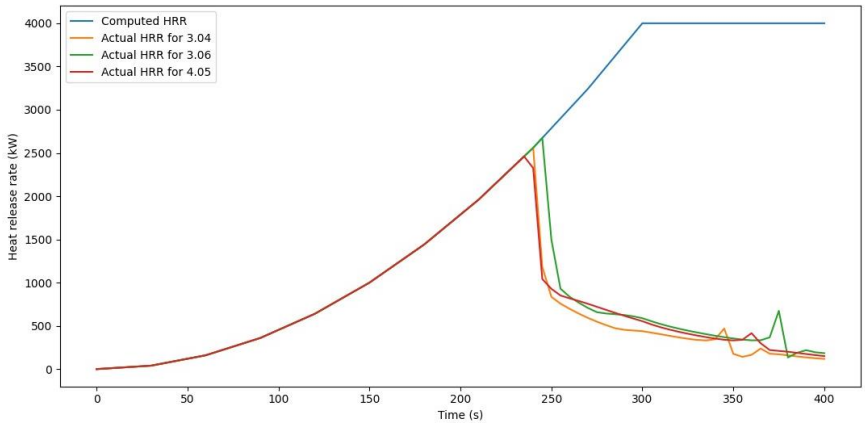

Figure 6-10. Expected and actual HRR of the fire scenarios where t_g = 300 s

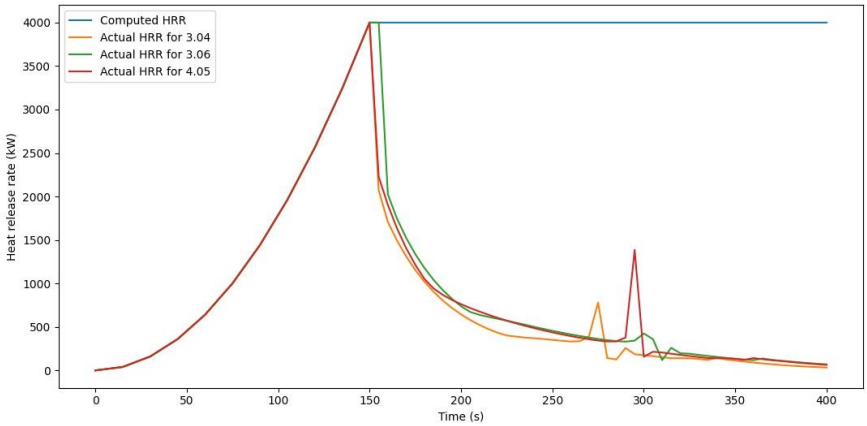

Figure 6-11. Expected and actual HRR HRR of the fire scenarios where t_g = 150 s

The temperature curves for the fire apartments are presented in Figure 6-12 and Figure 6-13. The temperature day schedules defined for CONTAM were based on these results.

For apartment 3.04, it is observed that the temperature exceeds 72 °C around 150 s when t_g = 300 s, and around 90 s when t_g = 150 s. As prior stated, 72 °C is the temperature at which fire dampers would close. These results are subsequently used as input for the CONTAM simulations for the scenarios with fire dampers.

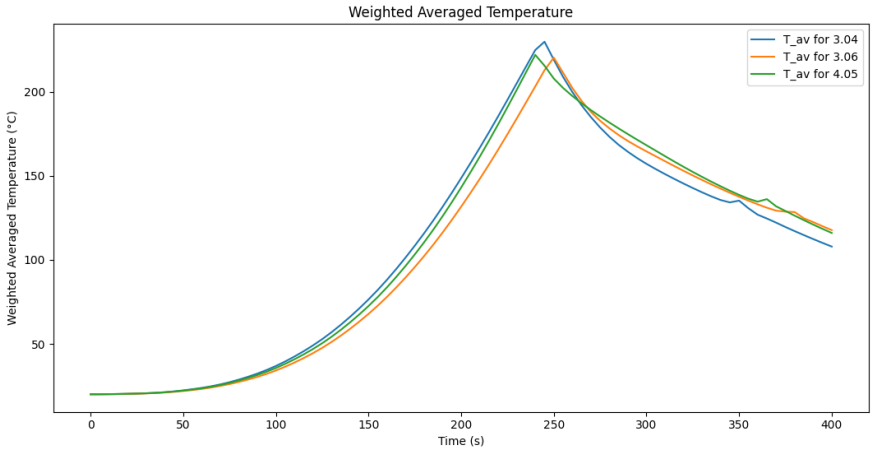

Figure 6-12. T_{av} curve of the fire scenarios where t_g = 300 s

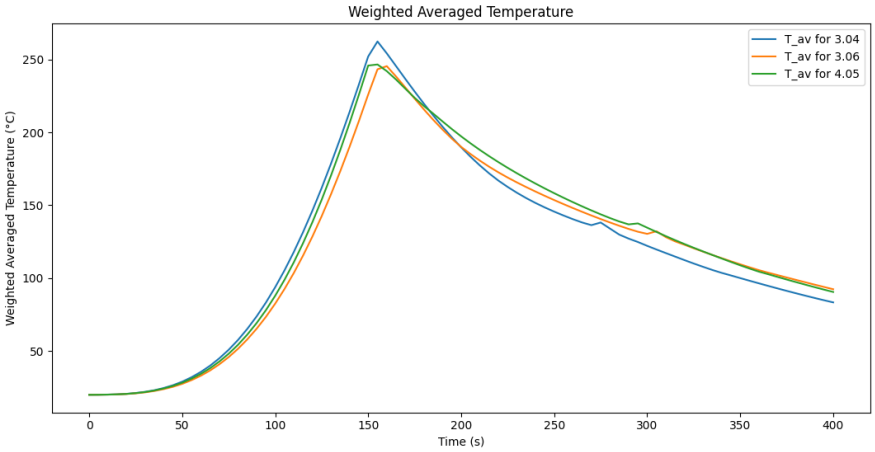

Figure 6-13. T_{av} curve of the fire scenarios where t_g = 150 s

6.3.4 CONTAM simulations

Contaminant concentrations at junctions

Using the CONTAM Results Export Tool, the files were extracted for the mass flow rate through duct segments 34, 39 and 42 and the contaminant concentration at junctions 34, 39 and 41. These files are bundled and available in Appendix M.

For the determination of the moment of activation of the valves, the concentration in zone LivingA2 on level 4 was determined at the time at which the temperature exceeded 72 °C. This temperature was exceeded at 150 s for the scenario with the medium fire growth rate and at 90 s for the scenario with the fast fire growth rate. The contaminant concentrations were then 0.0199 kg/kg and 0.0218 kg/kg, respectively. The concentrations at the junctions were compared to these concentrations. For the base scenario modeled with the medium fire growth rate, the contaminant concentrations for junctions 34, 39 and 41 were equal to or exceeded the concentration at 185 s, 200 s and 200 s, respectively. For the base scenario modeled with the fast fire growth rate, the contaminant concentrations for junctions 34, 39 and 41 were equal to or exceeded the concentration at 110 s, 120 s and 120 s, respectively.

Mass flow rates in the ducts

The schedules for duct segments 34, 39 and 42 were based on the mass flow results of those ducts during the base simulations. The flow rates to these ducts are plotted in Figure 6-14 and Figure 6-15. The negative mass flow rate for duct 39 emphasizes the reverse flow in the inlet duct.

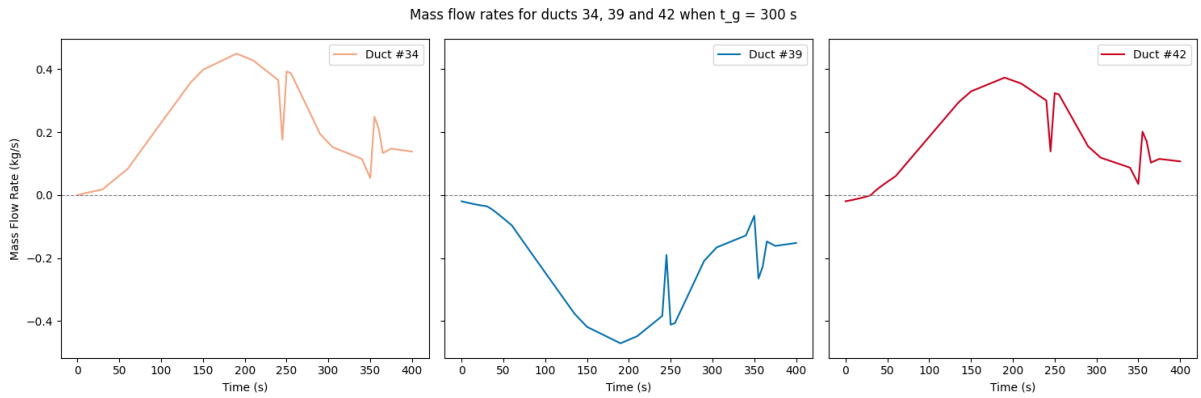

Figure 6-14. Mass flow rates for ducts 34, 39 and 42 when t_g = 300 s

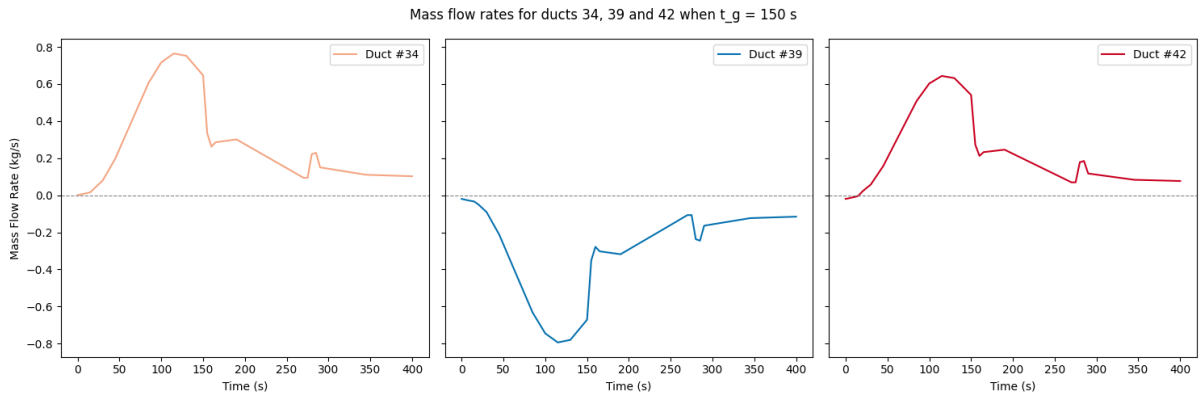

Figure 6-15. Mass flow rates for ducts 34, 39 and 42 when t_g = 150 s

Pressure development over a flow path

The pressure development over air flow path 120 (from Hall to Ambient) is plotted in Figure 6-16 for the fire scenario with a medium fire growth rate and in Figure 6-17 for the fire scenario with a fast fire growth rate.

For the scenarios with a medium fire growth rate and without dampers, the pressure does not exceed 100 Pa for the entire simulation. Introducing fire dampers to prevent smoke spread makes the pressure increase significantly, especially if a damper is applied for both inlet and exhaust duct. For the scenarios with a medium fire growth rate, the introduction of a bypass did not result in a significant decrease in pressure.

For the scenarios with a fast fire growth rate, similar trends are observed. The development is faster as a result of the fast fire growth rate, and as a result of the faster temperature development (Figure 6-16 and Figure 6-17), the resulting pressure is higher. Again, the introduction of a bypass did not result in a significant decrease in pressure.

It is observed that for all scenarios, the overpressure is no longer than 1.5 – 2 minutes above 100 Pa. The decay in overpressure exhibits more gradual decrease for the fire scenarios with a medium fire growth rate, with respect to those with a fast fire growth rate. Here, in Figure 6-17, a sharp drop is observed after 150 s. It is likely that this drop is overestimated, as similar trends were observed in the calibration case study (Figure 5-11) when comparing the CONTAM results to the FDS results from the study by Hostikka et al. [10].

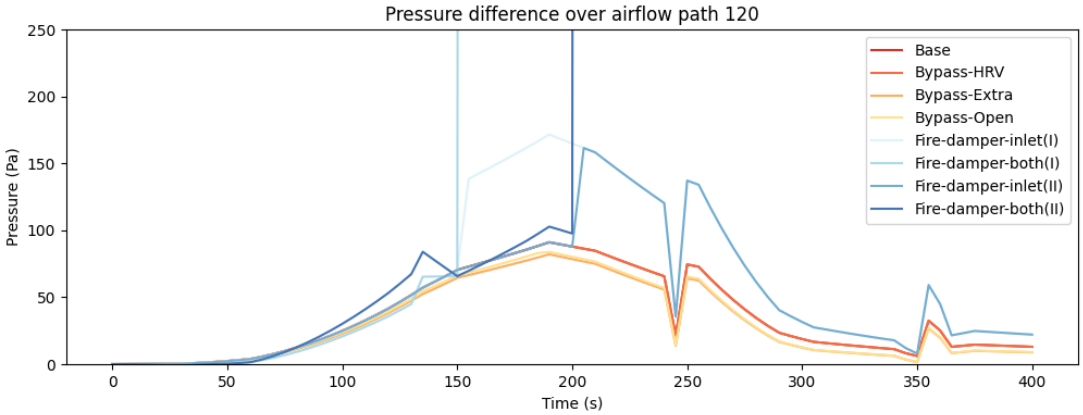

Figure 6-16. Pressure development over air flow path 120 when t_g = 300 s

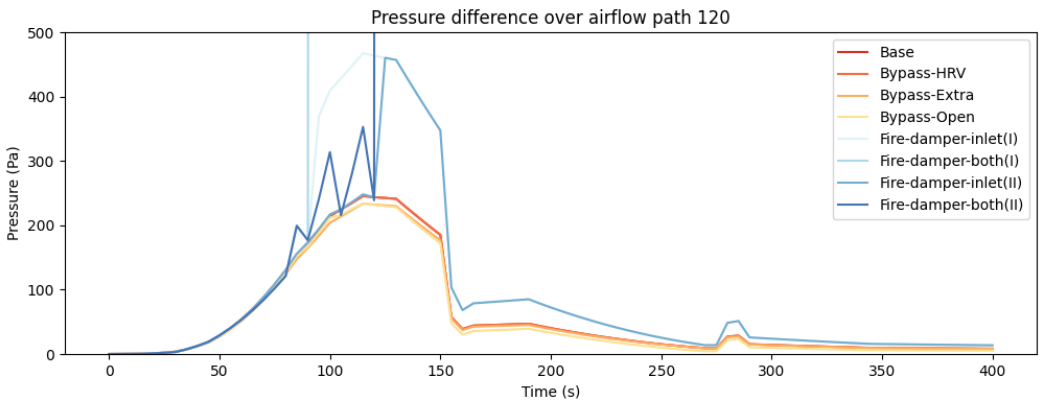

Figure 6-17. Pressure development over air flow path 120 when t_g = 150 s

Overpressure peaks over a flow path

The peak overpressures are presented in Table 6-15. Again, it is shown that introducing a bypass to the ventilation system has no significant effect on the overpressure, and that dampers have a significant negative effect on the overpressure, especially for the cases with a damper on both the inlet and exhaust duct. This was also observed for the cases with a fire damper on both the inlet and exhaust in the calibration study, and it is therefore possible that these values are largely overestimated.

Table 6-15. Peak overpressure over air flow path 120 for all scenarios

	Δp to ambient in [Pa] t_g *= 300 s*	*Δp to ambient in [Pa]* t_g *= 150 s*
Base	91.03	245.46
Bypass HRV	91.03	245.47
Bypass extra	82.03	233.80
Bypass scheduled "Bypass-Open"	83.81	233.72
Damper ODA at 150 s / 90 s	171.49	467.33
Damper ODA and EHA at 150 s / 90 s	8198.11	19747.70
Damper ODA at 200 s / 120 s	161.46	460.14
Damper ODA and EHA at 200 s / 120 s	8099.98	19747.70

Visibility

In Figure 6-18 and Figure 6-19, the results for minimum visibility are plotted with the assessment criteria indicated with the blue and red dotted lines at S = 30 m and S = 10 m, respectively. When the visibility falls below 30 m, long term exposure poses risks to the health and safety of occupants. When the visibility is lower than 10 m, short term exposure is critical and evacuation necessary.

From the plots, it was observed that a high fire growth rate resulted in higher pressures in the rooms and subsequently lead to lower visibility for all zones compared in Figure 6-18 and Figure 6-19. It was also shown that as a result of the higher pressures, more zones were jeopardized.

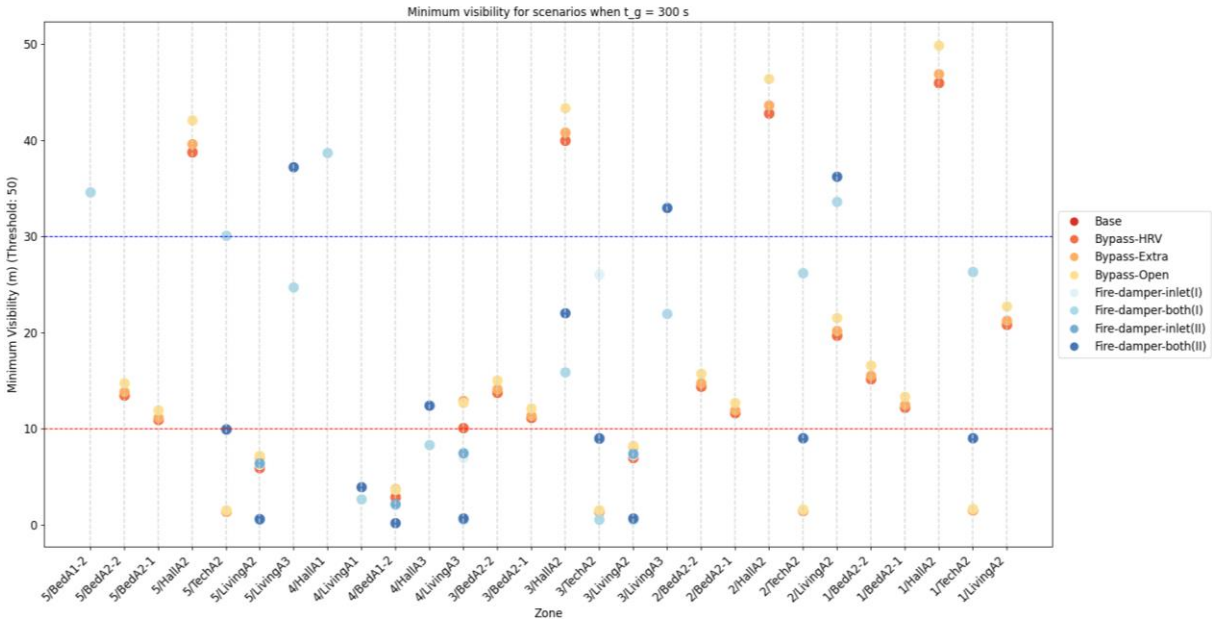

Figure 6-18. Minimum visibility in zones when t_g = 300 s

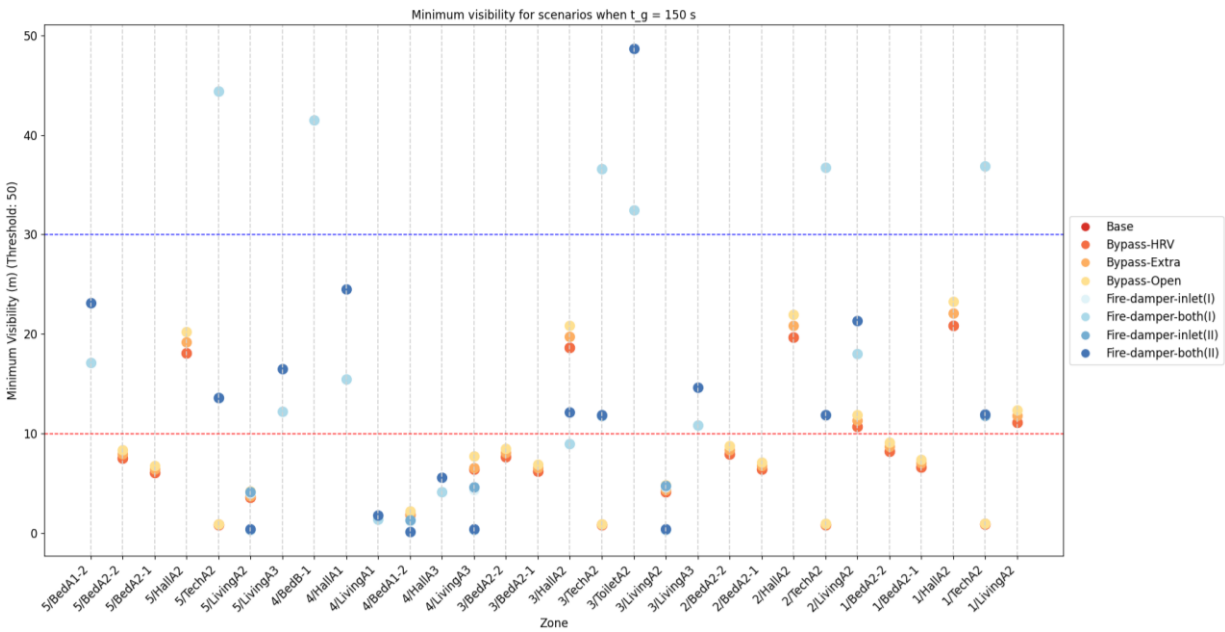

Figure 6-19. Minimum visibility in zones when t_g = 150 s

For the scenarios without dampers, it was observed that all zones connected to the inlet duct are threatened. This meant that obvious smoke spread was primarily observed for the bedrooms, hallways, technical spaces and living rooms of the "A2" apartments. The results showed dependency on the ventilation rate and the route traveled in the system towards a terminal, explained by how the visibility in bedrooms A2-2 and A2-1 was observed to be much better than for the technical spaces. The better visibility in the living rooms could be explained by the longer trajectory via the duct system and the kitchen exhaust removing the soot particles from the zones. As the living rooms on the third and fifth floor were adjacent to the fire zone and connected by a modeled leakage path, the visibility here was worse than for the living rooms on the first and second floor. This was already an indicator

of smoke spread via the interior separation structure. This was also the case for the bedroom of A1 and the living room A3 on the fourth floor. Here, the smoke spread was solely via the interior separation structure, as these apartments were not connected to the fire apartment by the ventilation system.

When dampers were implemented in the system, visibility vastly improved for the apartments connected via the ventilation system. For the living rooms on the third and fifth floor, the visibility was not improved due the aforementioned modeled leakage path. An exception was also found for the technical spaces, where the visibility was somewhat improved but not as well as for the other rooms. This implied that the visibility significantly decreased in these rooms within 200 s for fire scenarios with a medium fire growth rate, and within 120 s for the fire scenarios with a fast fire growth rate. From the difference in visibility for the different scenarios with fire dampers in these rooms, it was derived that smoke spread was also considerably related to the activation time of the fire dampers.

From the assessment criteria, it was extracted that evacuation of the apartments connected to the collective ducts would be necessary for fire scenarios with a fast growth rate, and recommended for fire scenarios with a medium fire growth rate, if no fire dampers were implemented. With fire dampers implemented and taking smoke spread via the interior separation structure into account, it is recommended to evacuate the apartments directly adjacent to the fire apartment.

6.4 Discussion

The aim of the case study was to examine the potential of a bypass as a means of pressure relief, as well as the effect on smoke spread to adjacent apartments. It was also tested how the fire dampers would affect the overpressure in the fire apartment and the smoke spread via the interior separation structure.

Using the same methodology of coupling CFAST and CONTAM as described for the calibration study worked well for the case study and the targeted goals. Some comments could be made on the level of detail of the model. Per floor, five apartments were modelled in detail, including all separate rooms, supply vents and extract vents. For the results regarding the pressure development in the fire apartment, this level of detail in adjacent levels was not necessary. For the apartments connected to the ventilation system, differences were observed per space as result of duct lengths and ventilation strategy, so here the level of detail showed its purpose. Considering the minimal smoke spread observed in apartment B for all scenarios, it could be argued that modeling only the directly adjacent apartments would have been sufficient. This would have been advantageous in terms of reducing the total amount of zones.

The case study showed that a solution for sufficient pressure relief was not found within the existing ventilation system, or with the implementation of a bypass. This underlines a need for searching a solution, possibly within the building characteristics. The potential of measures for pressure relief via the façade, or even to the shafts, were out of the scope of this project as they were deemed undesirable. This, as they would presumably affect the airtightness of the building, and therefore the energetic performance of the building. This was in line with previous performed research, i.e. by Wahlqvist and Van Hees [14]. They found that only self-regulating pressure hatches would significantly reduce the fire-induced overpressure, but also argued the downside of it being influential to environmental conditions such as wind pressure. It would be interesting to explore measures as such in future research, as well as the design of such measures.

Regarding smoke spread, it can be argued that the spread via the ventilation system is overestimated. This would be the result of the modeled configuration for the HRV unit. This configuration was based on the measurement set up, where the SUP and EHA openings were simultaneously put under pressure

but no distinction was made for the flow at the ODA and EHA openings. This was satisfactory for the prediction of overpressure, but possibly resulted in a higher contaminant flow into the collective supply duct. Separation of the ducts could yield different results.

The predicted smoke spread via the ventilation system was successfully reduced by implementing fire dampers, shown by the results of this study. This was further supported by Hostikka et al. [10] and Wahlqvist and Van Hees [14]. However, the increase in pressure as result of the closed fire dampers, resulted in an increase in smoke spread via the interior separation structure.

Not examined was the potential of changing the ventilation strategy of the apartments adjacent to the fire apartment to reduce the smoke spread via the interior separation structure. It could be argued that inducing an overpressure via the ventilation system in these apartments would limit the flow of air containing smoke particles. For the apartments connected to the same collective ventilation system as the fire apartment, this is no solution, as it would result in an increase in smoke spread via the inlet ducts.

7. Evaluation

The research started off with formulating the relevant building-, ventilation- and fire characteristics, forming the starting points for the (numerical) prediction of pressure development and smoke spread to other apartments. Building characteristics included the dimensions of compartments and the level of airtightness. The ventilation characteristics included ventilation strategy, configuration, system elements and the design and actual volumetric or mass flow rates. By using the building regulations as guidelines, detailed properties could be assigned to the different elements in a system. The most important parameters regarding the fire characteristics were the design and actual heat release rate, the fire growth rate and the soot yield corresponding to a cellulose fire.

The modeling software considered were Fire Dynamics Simulator (NIST), CFAST (NIST), CONTAM (NIST) and SYLVIA (IRSN). Every program had its advantages and limitations. It was decided to work with zone model CFAST and multizone model CONTAM, to overcome the limitations of both software and examine their potential for predicting the pressure development in a fire compartment and the smoke spread to other compartments. The calibration study on this decoupled modeling approach showed that CONTAM is capable of estimating the development of the overpressure. However, this overpressure was incited with a fan with a determined mass flow rate, as the software itself neglects thermal effects. The mass flow rate of the fan was based on the ideal gas law and conservation of mass, and calculated using the temperature differences resulting from the CFAST simulations. This yielded a good estimation of the pressure development, especially during the growth phase of the fire. For the decay phase, a pressure drop was observed from the CONTAM simulations where the FDS simulations showed a fluctuating decrease in pressure.

Upon reviewing the CFAST results for the mass flow rate via all vents, thus the wall vent and the mechanical vents, it was brought up that using the found values offered potentially a more efficient way of modeling the additional fan, given the similarity in the results. However, this theory was not further examined.

Smoke spread was observed for 5 out of the 9 non-fire apartments, but with a higher visibility than in the reference study. The difference could not be explained, as the description on the input for the ventilation system was limited in the reference study. However, the results for minimum visibility as found in the decoupled modeling approach could be explained based on the design of the system, as smoke spread fastest to the apartments directly adjacent to the fire apartment.

The decoupled modeling approach using CFAST and CONTAM was also used for the case study in this graduation project, namely De Cavaliere in Helmond. The case study was done to predict the prospect of overpressure development and smoke spread in an actually built building. From the results, it was obtained that for fire scenarios with a medium fire growth rate, the pressure remained below the threshold of 100 Pa when no dampers were applied. This value was exceeded for the fire scenarios with a fast fire growth rate. For both situations, the modeled bypass did not serve as an effective pressure relief. Smoke spread was observed for all scenarios with both a medium fire growth rate and a fast fire growth rate. The implementation of a fire damper in the inlet duct prevented smoke propagation to the apartments connected via the ventilation system. However, the resulting increase in pressure after damper activation caused additional smoke spread to adjacent apartments.

8. Conclusion

The main goal of this project was to establish a method to significantly limit the fire-induced pressure build-up in an airtight apartment, i.e. under 100 Pa, without compromising the safety of the escape route and other apartments due to potential spread of smoke and toxic gases via the ventilation system. Broadly discussed was the methodology of using CFAST and CONTAM. The link between the zone model and the multizone model satisfied for predicting the pressure development and smoke spread to other apartments, taking into account all elements in the ventilation system, the leakages of the exterior separation structure and leakages of the interior separation structure.

The case study offered no solution that would limit the fire-induced overpressure sufficiently to guarantee safe evacuation from the fire apartment. Smoke spread was observed for all scenarios without dampers. Means to prevent smoke spread, i.e. implementation of fire dampers in the inlet and/or exhaust duct, were proven to further increase the overpressure in the fire compartment, as well as increasing smoke spread via the interior separation structure. From the assessment criteria for visibility, it was concluded that evacuation of the apartments connected to the collective ducts would be necessary for fire scenarios with a fast growth rate, and recommended for fire scenarios with a medium fire growth rate, if no fire dampers were implemented. With fire dampers implemented and taking smoke spread via the interior separation structure into account, it is recommended to evacuate the apartments directly adjacent to the fire apartment.

As this graduation project focused on proving the usability of the decoupled modeling approach and means of pressure relief via the ventilation system, potential pressure relief via the exterior separation structure of the building was not explored. As relief cannot be sufficiently realized via the ventilation system, it is recommended to explore the feasibility and design of pressure relief measures using the building structure.

Bibliography

[1] International Passive House Association, “Passive House certification criteria.” https://passivehouse-international.org/index.php?page_id=150 (accessed Jun. 15, 2022).

[2] “Balansventilatie | Vereniging Eigen Huis.” https://www.eigenhuis.nl/verduurzamen/maatregelen/isoleren-en-ventileren/balansventilatie (accessed Jul. 01, 2023).

[3] S. Alavirad, S. Mohammadi, P.-J. Hoes, L. Xu, and J. L. M. Hensen, “Future-Proof Energy-Retrofit strategy for an existing Dutch neighbourhood,” *Energy Build*, vol. 260, 2022, doi: 10.1016/j.enbuild.2022.111914.

[4] “What Is a ‘Stay Put’ Policy? | Fire Risk Assessment Network.” https://fire-risk-assessment-network.com/blog/stay-put-policy/ (accessed Oct. 07, 2022).

[5] “Evacueren bij brand of niet? - Vakblad Veiligheid.” https://vakbladveiligheid.nl/evacueren-bij-brand-of-niet/ (accessed Oct. 07, 2022).

[6] “Het nieuwe ontruimingsconcept bij brand: ‘Stay in Place’ | De Zorg Brandveilig.” https://www.dezorgbrandveilig.nl/nieuws/het-nieuwe-ontruimingsconcept-bij-brand-‘stay-place’ (accessed Oct. 07, 2022).

[7] “Stay-in-place: robuust concept voor de toekomst - Brandveilig.” https://www.brandveilig.com/nieuws/stay-in-place-robuust-concept-voor-de-toekomst-67606 (accessed Oct. 07, 2022).

[8] “Stay Put Advice for Tenants | Fire Door Safety Week.” https://www.firedoorsafetyweek.co.uk/news-events/stay-put-advice/ (accessed Oct. 07, 2022).

[9] S. Brohez and I. Caravita, “Overpressure induced by fires in airtight buildings,” in *Journal of Physics: Conference Series*, Institute of Physics Publishing, Nov. 2018. doi: 10.1088/1742-6596/1107/4/042031.

[10] S. Hostikka, R. K. Janardhan, U. Riaz, and T. Sikanen, “Fire-induced pressure and smoke spreading in mechanically ventilated buildings with air-tight envelopes,” *Fire Saf J*, vol. 91, pp. 380–388, Jul. 2017, doi: 10.1016/J.FIRESAF.2017.04.006.

[11] H. Prétrel, W. Le Saux, and L. Audouin, “Pressure variations induced by a pool fire in a well-confined and force-ventilated compartment,” *Fire Saf J*, vol. 52, pp. 11–24, Aug. 2012, doi: 10.1016/J.FIRESAF.2012.04.005.

[12] D. Vanhaverbeke, “Fire development in passive houses: qualitative description and design on full-scale fire tests,” University of Edinburgh, 2015.

[13] B. Karlsson and J. Quintiere, *Enclosure fire dynamics*. CRC press, 1999.

[14] J. Wahlqvist and P. Van Hees, “Evaluating methods for preventing smoke spread through ventilation systems using fire dynamics simulator,” *Fire Mater*, vol. 41, no. 6, pp. 625–645, 2016, doi: 10.1002/fam.2404.

[15] “Blijf uit de rook - Brandweer.” https://www.brandweer.nl/onderwerpen/blijf-uit-de-rook/ (accessed Nov. 01, 2022).

[16] Milieudefensie, “Roet, de gevaarlijkste luchtvervuiler.” Amsterdam, 2016.

[17] R. A. P. van Herpen, “Consequenties voor een FSE benadering,” Sep. 23, 2013. Accessed: Jan. 05, 2022. [Online]. Available: https://www.nieman.nl/wp-content/uploads/2013/10/BriP_2013-09_Consequenties-FSE-benadering.pdf

[18] Nordic Committee on Building Regulations (NKB), *Performance Requirements for Fire Safety and Technical Guide for Verification by Calculation*, vol. 1994:07 E. 1994.

[19] F. Nystedt, “Verifying Fire Safety Design in Sprinklered Buildings,” Lund, 2011. [Online]. Available: http://www.brand.lth.se/english

[20] M. J. Hurley and E. R. Rosenbaum, “Performance-based design,” in *SFPE Handbook of Fire Protection Engineering, Fifth Edition*, Springer New York, 2016, pp. 1233–1261. doi: 10.1007/978-1-4939-2565-0_37.

[21] National Fire Protection Association, *SFPE Engineering Guide to Performance-Based Fire Protection*. Quincy: SFPE, 2007.

[22] S. Hostikka and R. K. Janardhan, “Pressure management in compartment fires,” Helsinki, 2017. Accessed: Aug. 18, 2023. [Online]. Available: https://aaltodoc.aalto.fi/handle/123456789/24038

[23] J. Li, T. Beji, S. Brohez, and B. Merci, “CFD study of fire-induced pressure variation in a mechanically-ventilated air-tight compartment,” *Fire Saf J*, vol. 115, p. 103012, Jul. 2020, doi: 10.1016/J.FIRESAF.2020.103012.

[24] R. K. Janardhan and S. Hostikka, “Experiments and Numerical Simulations of Pressure Effects in Apartment Fires,” *Fire Technol*, vol. 53, no. 3, pp. 1353–1377, 2017, doi: 10.1007/s10694-016-0641-z.

[25] J. Li, T. Beji, S. Brohez, and B. Merci, “Experimental and numerical study of pool fire dynamics in an air-tight compartment focusing on pressure variation,” *Fire Saf J*, vol. 120, p. 103128, Mar. 2021, doi: 10.1016/J.FIRESAF.2020.103128.

[26] H. Pretrel and S. Vaux, “Experimental and numerical analysis of fire scenarios involving two mechanically ventilated compartments connected together with a horizontal vent,” 2019, doi: 10.1002/fam.2695.

[27] R. van Liempd, L. de Witte, M. Karemaker, R. van Herpen, and V. Jansen, “Rookverspreiding en persoonlijke veiligheid,” 2022, [Online]. Available: https://nipv.nl/wp-content/uploads/2022/07/20220701-NIPV-Rookverspreiding-en-persoonlijke-veiligheid.pdf

[28] T. Yamada and Y. Akizuki, “Visibility and Human Behavior in Fire Smoke,” in *SFPE Handbook of Fire Protection Engineering*, M. J. Hurley, D. Gottuk, J. R. Hall, K. Harada, E. Kuligowski, M. Puchovsky, J. Torero, J. M. Watts, and C. Wieczorek, Eds., New York, NY: Springer New York, 2016, pp. 2181–2206. doi: 10.1007/978-1-4939-2565-0_61.

[29] R. A. P. Herpen and C. Rojas, “Benefits of sprinkler protection for personal safety of building occupants,” Aug. 2020.

[30] J. H. Klote, “Tenability Analysis and CONTAM,” in *Handbook of Smoke Control Engineering*, Atlanta: ASHRAE, 2012, pp. 387–404. [Online]. Available: www.ashrae.org

[31] “De Cavaliere, Helmond - 70 appartementen.” https://www.hurenindecavaliere.nl/ (accessed Aug. 30, 2023).

[32] C. Fourneau, N. Cornil, C. Delvosalle, H. Breulet, S. Desmet, and S. Brohez, “Comparison of Fire Hazards in Passive and Conventional Houses,” *Chem Eng Trans*, vol. 26, pp. 375–380, 2012, doi: 10.3303/CET1226063.

[33] “(PDF) Airtightness requirements for high performance building envelopes.” https://www.researchgate.net/publication/242617281_Airtightness_requirements_for_high_performance_building_envelopes (accessed Aug. 17, 2023).

[34] “Eisen luchtdichtbouwen - Nieman.” https://www.nieman.nl/specialismen/bouwtechniek-en-praktijk/luchtdicht-bouwen/eisen/ (accessed Aug. 18, 2023).

[35] J. Li, H. Prétrel, S. Suard, T. Beji, and B. Merci, “Experimental study on the effect of mechanical ventilation conditions and fire dynamics on the pressure evolution in an air-tight compartment,” *Fire Saf J*, vol. 125, p. 103426, 2021, doi: 10.1016/j.firesaf.2021.103426.

[36] R. van Herpen, “Meerzone luchtstroomodellen,” 2005.

[37] J. Jiang, H. Zhao, J. Li, T. Beji, and B. Merci, “Preliminary Numerical Study of Fire-Induced Pressure Rise in a Passive House Compartment,” p. 42026, 2018, doi: 10.1088/1742-6596/1107/4/042026.

[38] D. Torvi, D. Raboud, G. Hadjisophocleous, and I. Reid, “FIERAsystem t^2 Fire Development Model Report,” Ottawa, Sep. 2000. doi: 10.4224/20331350.

[39] National Fire Protection Association, “NFPA 92B - Standard for Smoke Management Systems in Malls, Atria, and Large Spaces.” Quincy, 2008. [Online]. Available: www.edufire.ir

[40] Normcommissie TGB Basiseisen en belastingen, “National Annex to NEN-EN 1991-1-2+C3: Eurocode 1 - Actions on structures - Part 1-2: General actions - Actions on structures exposed to fire,” in *NEN-EN 1991-1-2+C3: Eurocode 1 - Actions on structures - Part 1-2: General actions - Actions on structures exposed to fire*, Delft: NEN, 2019.

[41] P. Blomqvist, L. Rosell, and M. Simonson, “Emissions from Fires Part II: Simulated Room Fires,” *Fire Technol*, vol. 40, no. 1, pp. 59–73, 2004, doi: 10.1023/B:FIRE.0000003316.63475.16.

[42] R. van Herpen, “Rookbeheersing in woongebouwen met CERA 200 ventilatiesysteem,” 2022.

[43] R. van Herpen, “Rookdichtheid en zichtlengte,” 2007.

[44] W. D. Walton, D. J. Carpenter, and C. B. Wood, “Zone computer fire models for enclosures,” in *SFPE Handbook of Fire Protection Engineering, Fifth Edition*, Springer New York, 2016, pp. 1024–1033. doi: 10.1007/978-1-4939-2565-0_31.

[45] N. Tenbült, “Impact of the balanced mechanical ventilation system on overpressure in airtight houses in case of fire M1 Nick Tenbült,” 2017.

[46] S. Brohez and I. Caravita, “Fire induced pressure in airthigh houses: Experiments and FDS validation,” *Fire Saf J*, vol. 114, 2020, doi: https://doi.org/10.1016/j.firesaf.2020.103008.

[47] K. McGrattan, S. Hostikka, R. McDermott, J. Floyd, C. Weinschenk, and K. Overhold, “Fire Dynamics Simulator User’s Guide,” *NIST Special Publication 1019*, vol. Sixth Edition. 2022. doi: http://dx.doi.org/10.6028/NIST.SP.1019.

[48] W. S. Dols and B. J. Polidoro, “CONTAM User Guide and Program Documentation Version 3.2,” Gaithersburg, MD, Sep. 2015. doi: 10.6028/NIST.TN.1887.

[49] J. H. Klote, “Network Modeling and CONTAM,” in *Handbook of Smoke Control Engineering*, Atlanta: ASHRAE, 2012, pp. 291–314.

[50] J. H. Klote, J. A. Milke, P. G. Turnbull, A. Kashef, and M. J. Ferreira, *Handbook of Smoke Control Engineering*. Atlanta: ASHRAE, 2012.

[51] W. S. Dols, S. J. Emmerich, and B. J. Polidoro, “Coupling the multizone airflow and contaminant transport software CONTAM with EnergyPlus using co-simulation Article History”, doi: 10.1007/s12273-016-0279-2.

[52] M. Justo Alonso, W. S. Dols, and H. M. Mathisen, “Using Co-simulation between EnergyPlus and CONTAM to evaluate recirculation-based, demand-controlled ventilation strategies in an office building,” *Build Environ*, vol. 211, Mar. 2022, doi: 10.1016/J.BUILDENV.2021.108737.

[53] W. S. Dols, S. J. Emmerich, and B. J. Polidoro, “Using coupled energy, airflow and indoor air quality software (TRNSYS/CONTAM) to evaluate building ventilation strategies,” *Building Services Engineering Research and Technology*, vol. 37, no. 2, pp. 163–175, Mar. 2016, doi: 10.1177/0143624415619464/FORMAT/EPUB.

[54] “Calculation software system SYLVIA.” https://www.irsn.fr/EN/Research/Scientific-tools/Computer-codes/Pages/Calculation-software-system-SYLVIA-4577.aspx (accessed Mar. 03, 2023).

[55] N. le Roux, X. Faure, C. Inard, S. Soares, and L. Ricciardi, “Reduced-scale study of transient flows inside mechanically ventilated buildings subjected to wind and internal overpressure effects,” *Build Environ*, vol. 62, pp. 18–32, Apr. 2013, doi: 10.1016/J.BUILDENV.2013.01.011.

[56] S. Vaux and H. Prétrel, “Relative effects of inertia and buoyancy on smoke propagation in confined and forced ventilated enclosure fire scenarios,” 2013, doi: 10.1016/j.firesaf.2013.01.013.

[57] S. Melis and L. Audouin, “Effects of Vitiation on the Heat Release Rate in Mechanically-Ventilated Compartment Fires,” 2008, doi: 10.3801/IAFSS.FSS.9-931.

[58] L. Audouin *et al.*, “Verification and Validation of the ISIS CFD Code for Fire Simulation) View project Verification and Validation of the ISIS CFD Code for Fire Simulation,” 2006, Accessed: Mar. 03, 2023. [Online]. Available: https://www.researchgate.net/publication/266607290

[59] C. Lapuerta, S. Suard, F. Babik, and L. Rigollet, “Validation process of ISIS CFD software for fire simulation,” *Nuclear Engineering and Design*, vol. 253, pp. 367–373, Dec. 2012, doi: 10.1016/J.NUCENGDES.2011.09.068.

[60] F. Babik, C. Lapuerta, J.-C. Latché, S. Suard, and D. Vola, “Modeling and Numerical Studies of Fires in Confined, Ventilated Environments: the ISIS Code,” in *Scientific and Technical Report*, Fontenay-aux-Roses: IRSN, 2007, pp. 173–180.

[61] P. Blomqvist, L. Rosell, and M. Simonson, “Emissions from fires part II: Simulated room fires,” *Fire Technol*, vol. 40, no. 1, pp. 59–73, Jan. 2004, doi: 10.1023/B:FIRE.0000003316.63475.16/METRICS.

[62] ASTM International, “E779-10 Standard Test Method for Determining Air Leakage Rate by Fan Pressurization,” *Book of Standards* , vol. 04.11. 2018. Accessed: May 16, 2023. [Online]. Available: https://www.astm.org/e0779-10.html

[63] B. P. Husted, “Optical smoke units and smoke potential of different products,” Fredericia, 2004.

[64] “Natural Draft - Air Flow Volume and Velocity.” https://www.engineeringtoolbox.com/natural-draught-ventilation-d_122.html (accessed May 29, 2023).

[65] LXarchitecten, “Waterburcht W7 - Uitvoeringgereed Ontwerp.” Helmond, 2021.

[66] Zehnder Group, “Prestatieverklaring voor woonhuisventilatiesystemen volgens EU verordening Nr. 1254/2014. - Ventilatiesysteem met warmteterugwinning Zehnder ComfoAir E 300,” 2017.

[67] Duco, “Installatiehandleiding DucoBox Energy Premium,” 2020. [Online]. Available: www.duco.eu

[68] Zehnder Group Nederland B.V., “ComfoAir E 300 en ComfoAir E 400 - Handleiding voor de installateur,” Zwolle, 2022. [Online]. Available: www.zehnder.nl

[69] DUCO Ventilation and Sun Control, “Technische Fiche - DucoBox Energy Premium 325,” 2022. [Online]. Available: www.duco.eu

[70] Zehnder Group Nederland B.V., “ComfoAir E 300 en ComfoAir E 400 - Handleiding voor de servicemonteur,” Zwolle, 2022. Accessed: Aug. 09, 2023. [Online]. Available: www.zehnder.nl

[71] DUCO Ventilation and Sun Control, “DucoBox Energy Premium 325,” Veurne.

[72] DUCO Ventilation and Sun Control, “DucoBox Energy Premium | Balansventilatie met warmteterugwinning.” https://www.duco.eu/nl/producten/mechanische-ventilatie/ventilatie-units/ducobox-energy (accessed Aug. 09, 2023).

[73] Normcommissie Ventilatie en luchtdoorlatendheid, “NEN-EN 13141-7:2021 en - Ventilatie van gebouwen - Prestatiebeproeving van onderdelen/producten voor woningventilatie - Deel 7: Prestatiebeproeving van mechanische toe- en afvoereenheden (inclusief warmteterugwinning) met luchtkanalen,” Delft, Apr. 2021.

[74] “CONTAM Results Export Tool.” https://pages.nist.gov/CONTAM-apps/webapps/contam_results_exporter/index.htm (accessed Sep. 04, 2023).

List of Appendices

Appendix A Input CFAST for scenarios 3.1.1 and 3.2.1
Appendix B List of elements in CONTAM for the calibration study
Appendix C Schedules for CONTAM for the calibration study
Appendix D Calculation of the mass flow rates for the calibration study (CFAST)
Appendix E Calculation of the mass flow rates for the calibration study (CONTAM)
Appendix F Floor plans of De Cavaliere
Appendix G Reports on (de)pressurization tests by K+ Adviesgroep
Appendix H Input CFAST for a fire scenario in apartment 3.04 (t_g = 300 s) and 4.05 (t_g = 150 s)
Appendix I List of elements in CONTAM for the case study
Appendix J Schedules for CONTAM for the case study
Appendix K Inventory on the ventilation rate
Appendix L Regression analysis on the measurement results of an HRV unit
Appendix M Mass flow rates for ducts 34, 39 and 42

Appendix A – Input CFAST for scenarios 3.1.1 and 3.2.1

CFAST

Release Version : CFAST 7.7.3
Revision   : CFAST7.7.3-4-g0c33733b
Revision Date   : Thu May 12 10:19:24 2022 -0400
Compilation Date : Fri 05/13/2022 01:48 PM

Data file: C:\Users\n.kuiper\OneDrive - Peutz B.V\0. Afstudeerproject Nora\Val_new2\1. Medium\Case_3_1_1.in
Title: CFAST Simulation

OVERVIEW

Compartments	Doors, ...	Ceil. Vents, ...	MV Connects
1	1	0	2

Simulation Time (s)	Output Interval (s)	Smokeview Interval (s)	Spreadsheet Interval (s)
400.00	10.00	5.00	5.00

AMBIENT CONDITIONS

Interior Temperature (C)	Interior Pressure (Pa)	Exterior Temperature (C)	Exterior Pressure (Pa)
20.	101325.	20.	101325.

THERMAL PROPERTIES

Name	Conductivity (kW/(m °C))	Specific Heat (kJ/(m °C))	Density (kg/m^3)	Thickness (m)	Emissivity
CONCRETE	2.00	840.	2.400E+03	0.150	0.940
DEFAULT	0.120	900.	800.	1.200E-02	0.900

COMPARTMENTS

Compartment	Name	Width (m)	Depth (m)	Height (m)	Floor Height (m)	Ceiling Height (m)	Shaft	Hall	Wall Leakage (m^2)	Floor Leakage (m^2)

1	Fire_apt	5.00	10.00	2.50	0.00	2.50	0.0	0.0

COMPARTMENT MATERIALS

Compartment	Name	Surface	Layer	Conductivity (kW/(m °C))	Specific Heat (kJ/(m °C))	Density (kg/m^3)	Thickness (m)	Emissivity	Material
1	Fire_apt	Ceiling	1	2.00	840.	2.400E+03	0.150	0.940	CONCRETE
		Walls	1	2.00	840.	2.400E+03	0.150	0.940	CONCRETE

VENT CONNECTIONS

Wall Vents (Doors, Windows, ...)

From Compartment	To Compartment	Vent Number	Width (m)	Sill Height (m)	Soffit Height (m)	Open/Close Type (m)	Trigger Value (C/W/m^2)	Target	Initial Time (s)	Initial Fraction	Final Time (s)	Final Fraction
Fire_apt	Outside	1	0.00	0.00	2.50	Time			0.00	1.00		

There are no vertical natural flow connections

Mechanical Vents (Fans)

From Compartment	To Compartment	Fan Number	Area (m^2)	Flowrate (m^3/s)	Open/Close Type	Trigger Value (C/W/m^2)	Target	Initial Time (s)	Initial Fraction	Final Time (s)	Final Fraction
Outside	Fire_apt	1	0.04	0.01	RAMP # 1						
Fire_apt	Outside	2	0.04	0.01	RAMP # 2						

VENT RAMPS

Type	From Compartment	To Compartment	Vent Number	(s)	(s)	(s)	(s)	(s)	(s)	(s)	(s)	(s)	(s)

FIRES

Name: New Fire 1 Referenced as object # 1 Normal fire

Compartment	Fire Type	Time to Flaming	Position (x,y,z)	Relative Humidity	Lower O2 Limit	Radiative Fraction

Fire_apt	Constrained	0.0	2.50	5.00	0.00	50.0	15.00	0.35

Chemical formula of the fuel

Carbon	Hydrogen	Oxygen	Nitrogen	Chlorine
4.000	6.000	3.000	0.000	0.000

Time (s)	Mdot (kg/s)	Hcomb (J/kg)	Qdot (W)	Zoffset (m)	Soot (kg/kg)	CO (kg/kg)	HCN (kg/kg)	HCl (kg/kg)	TS (kg/kg)
0.	0.0	1.75E+07	0.0	0.0	1.00E-02	4.00E-02	0.0	0.0	0.0
30.	2.29E-03	1.75E+07	4.00E+04	0.0	1.00E-02	4.00E-02	0.0	0.0	0.0
60.	9.14E-03	1.75E+07	1.60E+05	0.0	1.00E-02	4.00E-02	0.0	0.0	0.0
90.	2.06E-02	1.75E+07	3.60E+05	0.0	1.00E-02	4.00E-02	0.0	0.0	0.0
120.	3.66E-02	1.75E+07	6.40E+05	0.0	1.00E-02	4.00E-02	0.0	0.0	0.0
150.	5.71E-02	1.75E+07	1.00E+06	0.0	1.00E-02	4.00E-02	0.0	0.0	0.0
180.	8.23E-02	1.75E+07	1.44E+06	0.0	1.00E-02	4.00E-02	0.0	0.0	0.0
210.	0.11	1.75E+07	1.96E+06	0.0	1.00E-02	4.00E-02	0.0	0.0	0.0
240.	0.15	1.75E+07	2.56E+06	0.0	1.00E-02	4.00E-02	0.0	0.0	0.0
270.	0.19	1.75E+07	3.24E+06	0.0	1.00E-02	4.00E-02	0.0	0.0	0.0
300.	0.23	1.75E+07	4.00E+06	0.0	1.00E-02	4.00E-02	0.0	0.0	0.0
900.	0.23	1.75E+07	4.00E+06	0.0	1.00E-02	4.00E-02	0.0	0.0	0.0
930.	0.19	1.75E+07	3.24E+06	0.0	1.00E-02	4.00E-02	0.0	0.0	0.0
960.	0.15	1.75E+07	2.56E+06	0.0	1.00E-02	4.00E-02	0.0	0.0	0.0
990.	0.11	1.75E+07	1.96E+06	0.0	1.00E-02	4.00E-02	0.0	0.0	0.0
1020.	8.23E-02	1.75E+07	1.44E+06	0.0	1.00E-02	4.00E-02	0.0	0.0	0.0
1050.	5.71E-02	1.75E+07	1.00E+06	0.0	1.00E-02	4.00E-02	0.0	0.0	0.0
1080.	3.66E-02	1.75E+07	6.40E+05	0.0	1.00E-02	4.00E-02	0.0	0.0	0.0
1110.	2.06E-02	1.75E+07	3.60E+05	0.0	1.00E-02	4.00E-02	0.0	0.0	0.0
1140.	9.14E-03	1.75E+07	1.60E+05	0.0	1.00E-02	4.00E-02	0.0	0.0	0.0
1170.	2.29E-03	1.75E+07	4.00E+04	0.0	1.00E-02	4.00E-02	0.0	0.0	0.0
1200.	0.0	1.75E+07	0.0	0.0	1.00E-02	4.00E-02	0.0	0.0	0.0
1210.	0.0	1.75E+07	0.0	0.0	1.00E-02	1.00E-02	0.0	0.0	0.0

```
****************************
* Time =      0.0 seconds. *
****************************
```

Compartment	Upper Temp. (C)	Lower Temp (C)	Inter. Height (m)	Upper Vol (m^3)	Upper Absor (1/m)	Lower Absorb (1/m)	Pressure (Pa)
Fire_apt	20.00	20.00	2.500	1.25E-02(0%)	72.0	6.741E-02	0.00

FIRES

Compartment	Fire	Ign	Plume Flow	Pyrol Rate	Fire Size	Flame Height	Fire in Upper	Fire in Lower	Vent Fire	Convec.	Radiat.	Pyrolysate	Trace

CFAST

Release Version : CFAST 7.7.3
Revision   : CFAST7.7.3-4-g0c33733b
Revision Date   : Thu May 12 10:19:24 2022 -0400
Compilation Date : Fri 05/13/2022 01:48 PM

Data file: C:\Users\n.kuiper\OneDrive - Peutz B.V\0. Afstudeerproject Nora\Val_new2\2. Fast\Case_3_2_1.in
Title: CFAST Simulation

OVERVIEW

Compartments	Doors, ...	Ceil. Vents, ...	MV Connects
1	1	0	2

Simulation Time (s)	Output Interval (s)	Smokeview Interval (s)	Spreadsheet Interval (s)
400.00	10.00	5.00	5.00

AMBIENT CONDITIONS

Interior Temperature (C)	Interior Pressure (Pa)	Exterior Temperature (C)	Exterior Pressure (Pa)
20.	101325.	20.	101325.

THERMAL PROPERTIES

Name	Conductivity (kW/(m °C))	Specific Heat (kJ/(m °C))	Density (kg/m^3)	Thickness (m)	Emissivity
CONCRETE	2.00	840.	2.400E+03	0.150	0.940
DEFAULT	0.120	900.	800.	1.200E-02	0.900

COMPARTMENTS

Compartment	Name	Width (m)	Depth (m)	Height (m)	Floor Height (m)	Ceiling Height (m)	Shaft	Hall	Wall Leakage (m^2)	Floor Leakage (m^2)
1	Fire_apt	5.00	10.00	2.50	0.00	2.50			0.0	0.0

COMPARTMENT MATERIALS

Compartment	Name	Surface	Layer	Conductivity (kW/(m °C))	Specific Heat (kJ/(m °C))	Density (kg/m^3)	Thickness (m)	Emissivity	Material
1	Fire_apt	Ceiling	1	2.00	840.	2.400E+03	0.150	0.940	CONCRETE
		Walls	1	2.00	840.	2.400E+03	0.150	0.940	CONCRETE

VENT CONNECTIONS

Wall Vents (Doors, Windows, ...)

From Compartment	To Compartment	Vent Number	Width (m)	Sill Height (m)	Soffit Height (m)	Open/Close Type (m)	Trigger Value (C/W/m^2)	Target	Initial Time (s)	Initial Fraction	Final Time (s)	Final Fraction
Fire_apt	Outside	1	0.00	0.00	2.50	Time			0.00	1.00		

There are no vertical natural flow connections

Mechanical Vents (Fans)

From Compartment	To Compartment	Fan Number	Area	Flowrate	Open/Close Type	Trigger Value	Target	Initial Time	Initial Fraction	Final Time

| | | |

90.	8.23E-02	1.75E+07	1.44E+06	0.0	1.00E-02	4.00E-02	0.0	0.0	0.0
105.	0.11	1.75E+07	1.96E+06	0.0	1.00E-02	4.00E-02	0.0	0.0	0.0
120.	0.15	1.75E+07	2.56E+06	0.0	1.00E-02	4.00E-02	0.0	0.0	0.0
135.	0.19	1.75E+07	3.24E+06	0.0	1.00E-02	4.00E-02	0.0	0.0	0.0
150.	0.23	1.75E+07	4.00E+06	0.0	1.00E-02	4.00E-02	0.0	0.0	0.0
450.	0.23	1.75E+07	4.00E+06	0.0	1.00E-02	4.00E-02	0.0	0.0	0.0
465.	0.19	1.75E+07	3.24E+06	0.0	1.00E-02	4.00E-02	0.0	0.0	0.0
480.	0.15	1.75E+07	2.56E+06	0.0	1.00E-02	4.00E-02	0.0	0.0	0.0
495.	0.11	1.75E+07	1.96E+06	0.0	1.00E-02	4.00E-02	0.0	0.0	0.0
510.	8.23E-02	1.75E+07	1.44E+06	0.0	1.00E-02	4.00E-02	0.0	0.0	0.0
525.	5.71E-02	1.75E+07	1.00E+06	0.0	1.00E-02	4.00E-02	0.0	0.0	0.0
540.	3.66E-02	1.75E+07	6.40E+05	0.0	1.00E-02	4.00E-02	0.0	0.0	0.0
555.	2.06E-02	1.75E+07	3.60E+05	0.0	1.00E-02	4.00E-02	0.0	0.0	0.0
570.	9.14E-03	1.75E+07	1.60E+05	0.0	1.00E-02	4.00E-02	0.0	0.0	0.0
585.	2.29E-03	1.75E+07	4.00E+04	0.0	1.00E-02	4.00E-02	0.0	0.0	0.0
600.	0.0	1.75E+07	0.0	0.0	1.00E-02	4.00E-02	0.0	0.0	0.0
610.	0.0	1.75E+07	0.0	0.0	1.00E-02	4.00E-02	0.0	0.0	0.0

```
****************************
* Time =      0.0 seconds. *
****************************
```

Compartment	Upper Temp. (C)	Lower Temp (C)	Inter. Height (m)	Upper Vol (m^3)	Upper Absor (1/m)	Lower Absorb (1/m)	Pressure (Pa)
Fire_apt	20.00	20.00	2.500	1.25E-02(0%)	72.0	6.741E-02	0.00

FIRES

Compartment	Fire	Ign	Plume Flow (kg/s)	Pyrol Rate (kg/s)	Fire Size (W)	Flame Height (m)	Fire in Upper (W)	Fire in Lower (W)	Vent Fire (W)	Convec. (W)	Radiat. (W)	Pyrolysate (kg)	Trace (kg)
	New Fire 2	Y	0.00	0.00	0.00	0.00				0.00	0.00	0.00	0.00

Appendix B – List of elements in CONTAM for the calibration study

Normal mode (scenario 3.1.1)

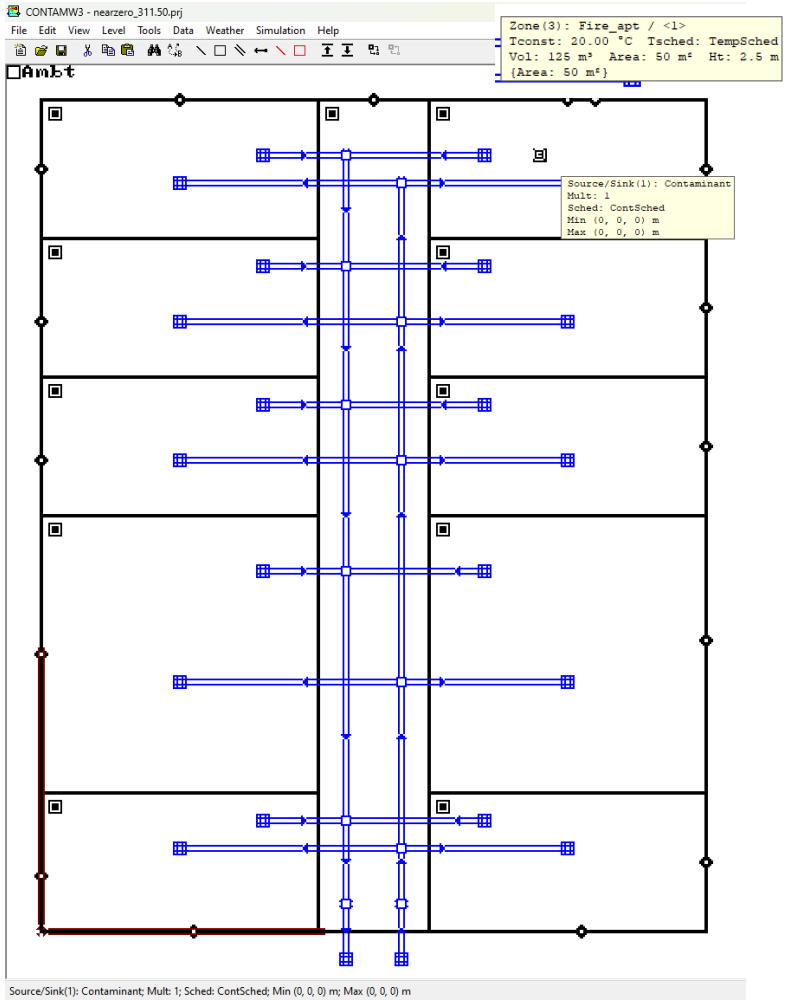

Results mode (scenario 3.1.1 at t=240 s) →

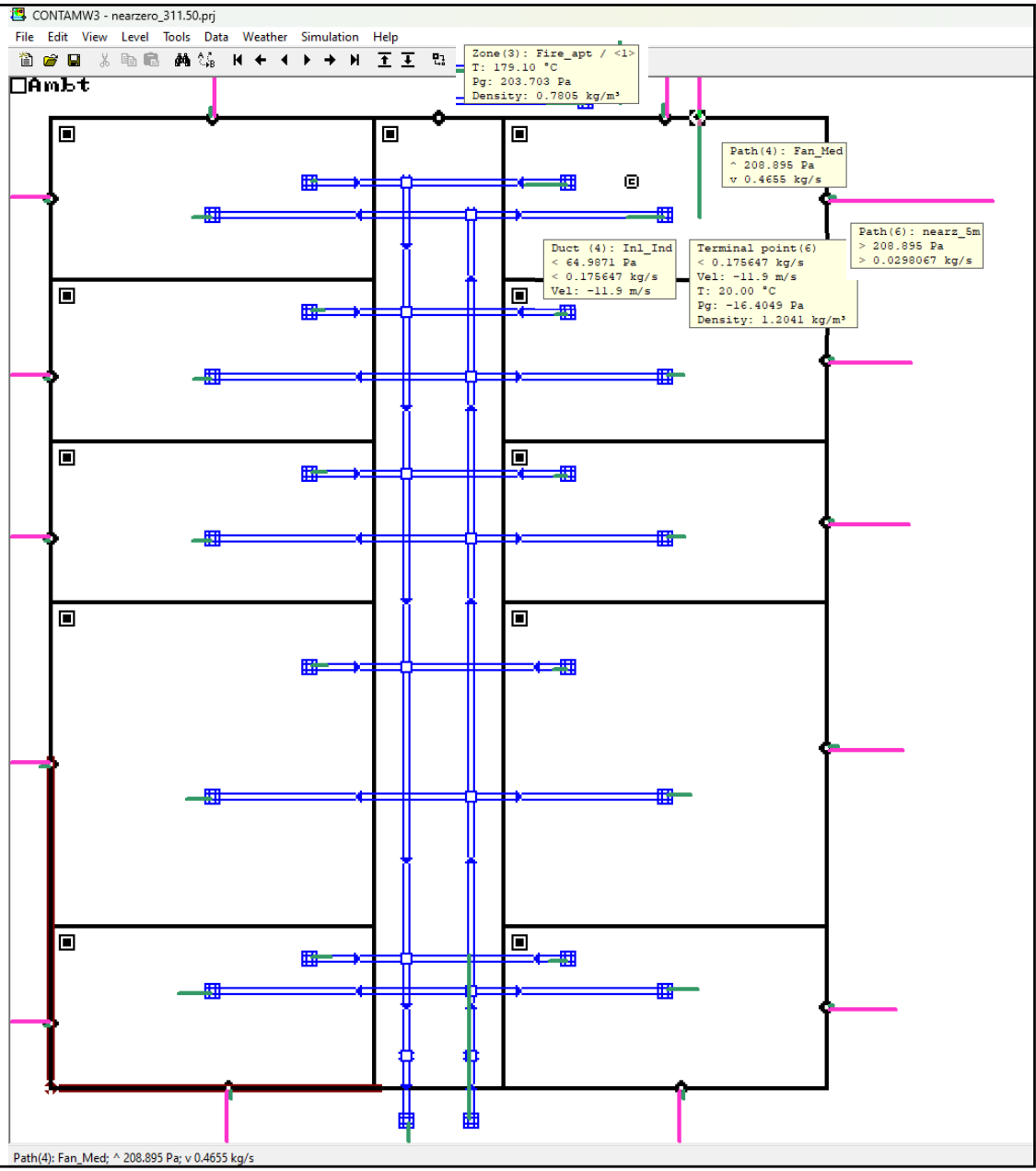

Ambient		
Ambient temperature	20	°C
Absolute pressure	101325	Pa
Relative humidity	0	RH
Humiditity ratio	0	g(w)/kg (dry)
Mass fraction (H2O)	0	kg (w)/kg (air)
Wind speed	0	m/s
Wind direction	0	deg
Day type	1	(1-12)

Zones		m²	m³	Temperature		Initial contaminant	
1	Non-fire1	50	125	20	°C	0	kg/kg
2	Hallway	120	300	20	°C	0	kg/kg
3*	Fire_apt	50	125	Scheduled	°C	0	kg/kg
4	Non-fire2	50	125	20	°C	0	kg/kg
5	Non-fire6	50	125	20	°C	0	kg/kg
6	Non-fire3	50	125	20	°C	0	kg/kg
7	Non-fire7	50	125	20	°C	0	kg/kg
8	Non-fire4	100	250	20	°C	0	kg/kg
9	Non-fire8	100	250	20	°C	0	kg/kg
10	Non-fire5	50	125	20	°C	0	kg/kg
11	Non-fire9	50	125	20	°C	0	kg/kg

* Includes scheduled contaminant source

Species	CELLULOSE	
Molar mass	180	kg/kmol
Duffusion coefficient	2.00E-05	m²/s
Mean diameter	0	m²/s
Effective density	0	kg/m³
Specific heat	1000	J/kgK
Decay rate	0	1/s
UVGI Susceptibility constant	0	m²/J
Default concentration	0	kg/kg
Trace contamintant	Trace	
Use in simulation	Use	

Junction/terminal

	Type	Direction	Shape	Length	Length	Diameter	Maximum	Roughness	Leakage rate	dP	schedule	Other
	-	-	-	m	m	m	L/s	mm	L/s/m²	Pa	-	
1	Ext_Ind	ETA	circle	2.5		0.125	-	0.09	0	1	None	
2	Ext_Ind	ETA	circle	4.5		0.125	-	0.09	0	1	None	
3	Inl_Ind	SUP	circle	4.5		0.125	-	0.09	0	1	None	
4	Inl_Ind	SUP	circle	4.5		0.125	-	0.09	0	1	None	
5	Ext_Col	ETA	circle	3.5	3.5	0.250	-	0.09	0	1	None	
6	Int_Col	SUP	circle	4.5	4.5	0.250	-	0.09	0	1	None	
7	Ext_Ind	ETA	circle	2.5		0.125	-	0.09	0	1	None	
8	Ext_Ind	ETA	circle	4.5		0.125	-	0.09	0	1	None	
9	Inl_Ind	SUP	circle	4.5		0.125	-	0.09	0	1	None	
10	Inl_Ind	SUP	circle	4.5		0.125	-	0.09	0	1	None	
11	Ext_Col	ETA	circle	4.5	3.5	0.250	-	0.09	0	1	None	
12	Int_Col	SUP	circle	4.5	4.5	0.250	-	0.09	0	1	None	
13	Ext_Ind	ETA	circle	2.5		0.125	-	0.09	0	1	None	
14	Ext_Ind	ETA	circle	4.5		0.125	-	0.09	0	1	None	
15	Inl_Ind	SUP	circle	4.5		0.125	-	0.09	0	1	None	
16	Inl_Ind	SUP	circle	4.5		0.125	-	0.09	0	1	None	
17	Ext_Col	ETA	circle	5.5	3.5	0.250	-	0.09	0	1	None	
18	Int_Col	SUP	circle	7.5	4.5	0.250	-	0.09	0	1	None	
19	Ext_Ind	ETA	circle	2.5		0.125	-	0.09	0	1	None	
20	Ext_Ind	ETA	circle	4.5		0.125	-	0.09	0	1	None	
21	Inl_Ind	SUP	circle	4.5		0.125	-	0.09	0	1	None	
22	Inl_Ind	SUP	circle	4.5		0.125	-	0.09	0	1	None	
23	Ext_Col	ETA	circle	8.5	3.5	0.250	-	0.09	0	1	None	
24	Int_Col	SUP	circle	5.5	4.5	0.250	-	0.09	0	1	None	
25	Ext_Ind	ETA	circle	2.5		0.125	-	0.09	0	1	None	
26	Ext_Ind	ETA	circle	4.5		0.125	-	0.09	0	1	None	
27	Inl_Ind	SUP	circle	4.5		0.125	-	0.09	0	1	None	
28	Inl_Ind	SUP	circle	4.5		0.125	-	0.09	0	1	None	
29	Ext_Col	ETA	circle	2.5	3.5	0.250	-	0.09	0	1	None	
30	Int_Col	SUP	circle	1.5	4.5	0.250	-	0.09	0	1	None	
31	Fan and forced flow model | Constant volume flow	EHA	circle	1.5		0.250	650.0	-	0	1	None	
32	Fan and forced flow model | Constant volume flow	ODA	circle	1.5		0.250	650.0	-	0	1	None	

#		Schedule
2	Junction	None
5	Junction	None
8	Junction	None
11	Junction	None
14	Junction	None
17	Junction	None
20	Junction	None
23	Junction	None
26	Junction	None
29	Junction	None
31	Junction	None
32	Junction	None

Flow paths

Traditional facade		Reference parameters			Fan and forced flow	
	Leakage area per item	Pressure drop	Discharge coefficient	Flow exponent	Maximum flow rate	Schedule
	cm²	Pa	-	-	kg/s	
1 trad_10m	180.2	50	0.6 (by default)	0.65 (by default)		
2 trad_5m	88.8	50	0.6 (by default)	0.65 (by default)		
3 trad_10m	180.2	50	0.6 (by default)	0.65 (by default)		
4 FAN	-	-	-	-	0.61	FanSched, dependent on the scenario
5 trad_5m	88.8	50	0.6 (by default)	0.65 (by default)		
6 trad_5m	88.8	50	0.6 (by default)	0.65 (by default)		
7 trad_5m	88.8	50	0.6 (by default)	0.65 (by default)		
8 trad_5m	88.8	50	0.6 (by default)	0.65 (by default)		
9 trad_5m	88.8	50	0.6 (by default)	0.65 (by default)		
10 trad_5m	88.8	50	0.6 (by default)	0.65 (by default)		
11 trad_10m	180.2	50	0.6 (by default)	0.65 (by default)		
12 trad_10m	180.2	50	0.6 (by default)	0.65 (by default)		
13 trad_5m	88.8	50	0.6 (by default)	0.65 (by default)		
14 trad_5m	88.8	50	0.6 (by default)	0.65 (by default)		
15 trad_5m	88.8	50	0.6 (by default)	0.65 (by default)		
16 trad_5m	88.8	50	0.6 (by default)	0.65 (by default)		

Modern facade		Reference parameters			Fan and forced flow	
	Leakage area per item	Pressure drop	Discharge coefficient	Flow exponent	Maximum flow rate	Schedule
	cm²	Pa	-	-	kg/s	
1 mod_10m	90.1	50	0.6 (by default)	0.65 (by default)		
2 mod_5m	44.4	50	0.6 (by default)	0.65 (by default)		
3 mod_10m	90.1	50	0.6 (by default)	0.65 (by default)		
4 FAN	-	-	-	-	0.61	FanSched, dependent on the scenario
5 mod_5m	44.4	50	0.6 (by default)	0.65 (by default)		
6 mod_5m	44.4	50	0.6 (by default)	0.65 (by default)		
7 mod_5m	44.4	50	0.6 (by default)	0.65 (by default)		
8 mod_5m	44.4	50	0.6 (by default)	0.65 (by default)		
9 mod_5m	44.4	50	0.6 (by default)	0.65 (by default)		
10 mod_5m	44.4	50	0.6 (by default)	0.65 (by default)		
11 mod_10m	90.1	50	0.6 (by default)	0.65 (by default)		
12 mod_10m	90.1	50	0.6 (by default)	0.65 (by default)		
13 mod_5m	44.4	50	0.6 (by default)	0.65 (by default)		
14 mod_5m	44.4	50	0.6 (by default)	0.65 (by default)		
15 mod_5m	44.4	50	0.6 (by default)	0.65 (by default)		
16 mod_5m	44.4	50	0.6 (by default)	0.65 (by default)		

Traditional facade		Reference parameters			Fan and forced flow	
	Leakage area per item	Pressure drop	Discharge coefficient	Flow exponent	Maximum flow rate	Schedule
	cm²	Pa	-	-	kg/s	
1 nearz_10m	45.1	50	0.6 (by default)	0.65 (by default)		
2 nearz_5m	22.2	50	0.6 (by default)	0.65 (by default)		
3 nearz_10m	45.1	50	0.6 (by default)	0.65 (by default)		
4 FAN	-	-	-	-	0.61	FanSched, dependent on the scenario
5 nearz_5m	22.2	50	0.6 (by default)	0.65 (by default)		
6 nearz_5m	22.2	50	0.6 (by default)	0.65 (by default)		
7 nearz_5m	22.2	50	0.6 (by default)	0.65 (by default)		
8 nearz_5m	22.2	50	0.6 (by default)	0.65 (by default)		
9 nearz_5m	22.2	50	0.6 (by default)	0.65 (by default)		
10 nearz_5m	22.2	50	0.6 (by default)	0.65 (by default)		
11 nearz_10m	45.1	50	0.6 (by default)	0.65 (by default)		
12 nearz_10m	45.1	50	0.6 (by default)	0.65 (by default)		
13 nearz_5m	22.2	50	0.6 (by default)	0.65 (by default)		
14 nearz_5m	22.2	50	0.6 (by default)	0.65 (by default)		
15 nearz_5m	22.2	50	0.6 (by default)	0.65 (by default)		
16 nearz_5m	22.2	50	0.6 (by default)	0.65 (by default)		

Appendix C – Schedules for CONTAM for the calibration study

Appendix C: All schedules for the calibration study

1.1.1 (Traditional façade, Medium fire growth rate, Damper=Off)

Temperature

1.1.1											
Time	0	30	60	80	105	135	185	195	210	285	400
Time [mm:ss]	00:00	00:30	01:00	01:20	01:45	02:15	03:05	03:15	03:30	04:45	06:40
Temp [°C]	20	21.4	28.7	39.9	64.2	113.1	241.8	220.8	205.2	156.2	102.3

Fan action

1.1.1															
Time	0	15	45	60	95	130	160	180	185	190	200	220	290	295	400
Time [mm:ss]	00:00	00:15	00:45	01:00	01:35	02:10	02:40	03:00	03:05	03:10	03:20	00:03:40	00:04:50	00:04:55	06:40
Mass flow rate [kg/s]	0	0.02	0.11	0.18	0.39	0.6	0.61	0.53	0.39	0.41	0.21	0.17	0.09	0.18	0.11
Fraction [-]	0	0.03	0.17	0.29	0.62	0.95	0.97	0.84	0.62	0.65	0.33	0.27	0.14	0.29	0.17

Contaminant concentration

1.1.1																		
Time	0	30	60	90	120	150	185	190	200	240	265	270	275	340	365	370	375	400
Time [mm:ss]	00:00	00:30	01:00	01:30	02:00	02:30	03:05	03:10	03:20	04:00	04:25	04:30	04:35	05:40	06:05	06:10	06:15	06:40
HRR	0	40	160	360	640	1000	1526.7	481	561.6	336.1	259	350.8	165.1	29.8	14.7	141.6	0.6	0
Fraction	0	0.01	0.04	0.09	0.16	0.25	0.382	0.120	0.140	0.084	0.065	0.088	0.041	0.007	0.004	0.035	0.000	0.000

1.1.2 (Traditional façade, Medium fire growth rate, Damper=Inlet)

Temperature

1.1.2											
Time	0	30	60	80	105	135	185	195	210	285	400
Time [mm:ss]	00:00	00:30	01:00	01:20	01:45	02:15	03:05	03:15	03:30	04:45	06:40
Temp [°C]	20	21.4	28.8	40.1	64.7	113.9	241.2	222.2	208.5	165.7	119.8

Fan action

1.1.2															
Time	0	45	95	130	160	180	185	190	200	220	290	295	305	310	400
Time [mm:ss]	00:00	00:45	01:35	02:10	02:40	03:00	03:05	03:10	03:20	00:03:40	00:04:50	00:04:55	00:05:05	00:05:10	06:40
Mass flow rate [kg/s]	0	0.11	0.41	0.59	0.6	0.53	0.34	0.38	0.2	0.14	0.09	0.07	0.16	0.14	0.09
Fraction [-]	0	0.17	0.65	0.94	0.95	0.84	0.54	0.60	0.32	0.22	0.14	0.11	0.25	0.22	0.14

Contaminant concentration

1.1.2															
Time	0	30	60	90	120	150	185	190	200	270	280	285	330	340	400
Time [mm:ss]	00:00	00:30	01:00	01:30	02:00	02:30	03:05	03:10	03:20	04:30	04:40	04:45	05:30	05:40	06:40
HRR	0	40	160	360	640	1000	1526.7	492.9	593.3	275.9	684.1	187.1	100.3	29.8	14.3
Fraction	0	0.01	0.04	0.09	0.16	0.25	0.382	0.123	0.148	0.069	0.171	0.047	0.025	0.007	0.004

1.1.3 (Traditional façade, Medium fire growth rate, Damper=Both)

Temperature

1.1.3											
Time	0	30	60	80	105	135	185	195	210	285	400
Time [mm:ss]	00:00	00:30	01:00	01:20	01:45	02:15	03:05	03:15	03:30	04:45	06:40
Temp [°C]	20	21.5	28.8	40.2	65	114.1	240.7	220.7	206.5	160.7	108

Fan action

1.1.3																
Time	0	15	45	60	95	130	165	180	185	190	200	220	280	295	300	400
Time [mm:ss]	00:00	00:15	00:45	01:00	01:35	02:10	02:45	03:00	03:05	03:10	03:20	00:03:40	00:04:40	00:04:55	00:05:00	06:40
Mass flow rate [kg/s]	0	0.02	0.11	0.18	0.4	0.59	0.61	0.53	0.34	0.4	0.21	0.14	0.12	0.07	0.17	0.09
Fraction [-]	0	0.03	0.17	0.29	0.63	0.94	0.97	0.84	0.54	0.63	0.33	0.22	0.19	0.11	0.27	0.14

Contaminant concentration

1.1.3																
Time	0	30	60	90	120	150	185	190	200	270	275	330	370	375	385	400
Time [mm:ss]	00:00	00:30	01:00	01:30	02:00	02:30	03:05	03:10	03:20	04:30	04:35	05:30	06:10	06:15	06:25	06:40
HRR	0	40	160	360	640	1000	1526.7	474.5	564.4	284.5	157.1	46.4	14.5	18	0	0
Fraction	0	0.01	0.04	0.09	0.16	0.25	0.382	0.119	0.141	0.071	0.039	0.012	0.004	0.005	0.000	0.000

2.1.1 (Modern façade, Medium fire growth rate, Damper=Off)

Temperature

2.1.1											
Time	0	30	60	80	105	135	185	195	210	285	400
Time [mm:ss]	00:00	00:30	01:00	01:20	01:45	02:15	03:05	03:15	03:30	04:45	06:40
Temp [°C]	20	21.4	28.8	40.1	64.8	114.2	243.2	219.8	203	155.2	100.4

Fan action

2.1.1																	
Time	0	15	45	60	95	130	140	160	180	185	190	200	215	280	290	295	400
Time [mm:ss]	00:00	00:15	00:45	01:00	01:35	02:10	02:20	02:40	03:00	03:05	03:10	00:03:20	00:03:35	00:04:40	00:04:50	00:04:55	06:40
Mass flow rate [kg/s]	0	0.02	0.11	0.18	0.41	0.59	0.61	0.6	0.52	0.46	0.44	0.26	0.16	0.12	0.03	0.18	0.11
Fraction [-]	0	0.03	0.17	0.29	0.65	0.94	0.97	0.95	0.83	0.73	0.70	0.41	0.25	0.19	0.05	0.29	0.17

Contaminant concentration

2.1.1																		
Time	0	30	60	90	120	150	185	190	200	210	260	265	270	330	355	360	365	400
Time [mm:ss]	00:00	00:30	01:00	01:30	02:00	02:30	03:05	03:10	03:20	03:30	04:20	04:25	04:30	05:30	05:55	06:00	06:05	06:15
HRR	0	40	160	360	640	1000	1526.7	442.1	523.1	493.7	252.7	273.4	174.1	28.9	15.5	33.1	0.1	0
Fraction	0	0.01	0.04	0.09	0.16	0.25	0.382	0.111	0.131	0.123	0.063	0.068	0.044	0.007	0.004	0.008	0.000	0.000

2.1.2 (Modern façade, Medium fire growth rate, Damper=Inlet)

Temperature

2.1.2											
Time	0	30	60	80	105	135	185	195	210	285	400
Time [mm:ss]	00:00	00:30	01:00	01:20	01:45	02:15	03:05	03:15	03:30	04:45	06:40
Temp [°C]	20	21.4	28.8	40.3	65.1	114.6	243.6	220.7	206.1	164.1	118.4

Fan action

2.1.2																	
Time	0	15	45	60	95	130	160	180	185	190	215	290	305	310	315	400
Time [mm:ss]	00:00	00:15	00:45	01:00	01:35	02:10	02:40	03:00	03:05	03:10	00:03:35	00:03:35	00:05:05	00:05:10	00:05:15	06:40
Mass flow rate [kg/s]	0	0.02	0.11	0.18	0.41	0.59	0.6	0.52	0.45	0.44	0.14	0.1	0.03	0.13	0.14	0.09
Fraction [-]	0	0.03	0.17	0.29	0.65	0.94	0.95	0.83	0.71	0.70	0.22	0.16	0.05	0.21	0.22	0.14

Contaminant concentration

2.1.2															
Time	0	30	60	90	120	150	185	190	205	270	275	280	285	350	400
Time [mm:ss]	00:00	00:30	01:00	01:30	02:00	02:30	03:05	03:10	03:25	04:35	04:30	04:40	04:45	05:50	06:40
HRR	0	40	160	360	640	1000	1526.7	443.7	555.9	269.4	316	107.2	178.7	44.4	14.3
Fraction	0	0.01	0.04	0.09	0.16	0.25	0.382	0.111	0.139	0.067	0.079	0.027	0.045	0.011	0.000

2.1.3 (Modern façade, Medium fire growth rate, Damper=Both)

Temperature

2.1.3											
Time	0	30	60	80	105	135	185	195	210	285	400
Time [mm:ss]	00:00	00:30	01:00	01:20	01:45	02:15	03:05	03:15	03:30	04:45	06:40
Temp [°C]	20	21.5	29	40.5	65.4	114.8	243.1	219.5	204.7	159.1	106.6

Fan action

2.1.3																
Time	0	15	45	60	95	130	160	180	185	190	200	220	285	295	300	400
Time [mm:ss]	00:00	00:15	00:45	01:00	01:35	02:10	02:40	03:00	03:05	03:10	00:03:20	00:03:40	00:04:45	00:04:55	00:05:00	06:40
Mass flow rate [kg/s]	0	0.02	0.11	0.18	0.41	0.58	0.59	0.52	0.44	0.45	0.23	0.15	0.1	0.02	0.16	0.1
Fraction [-]	0	0.03	0.17	0.29	0.65	0.92	0.94	0.83	0.70	0.71	0.37	0.24	0.16	0.03	0.25	0.16

Contaminant concentration

2.1.3																	
Time	0	30	60	90	120	150	185	190	200	265	270	275	315	360	365	370	400
Time [mm:ss]	00:00	00:30	01:00	01:30	02:00	02:30	03:05	03:10	03:20	04:25	04:30	04:35	05:15	06:00	06:05	06:10	06:40
HRR	0	40	160	360	640	1000	1526.7	481	561.6	259	350.8	165.1	70.9	14.9	129.6	0.5	0
Fraction	0	0.01	0.04	0.09	0.16	0.25	0.382	0.120	0.140	0.065	0.088	0.041	0.018	0.004	0.032	0.000	0.000

3.1.1 (Near-zero façade, Medium fire growth rate, Damper=Off)

Temperature

3.1.1												
Time	0	30	60	80	105	135	185	195	210	280	360	400
Time [mm:ss]	00:00	00:30	01:00	01:20	01:45	02:15	03:05	03:15	03:30	04:40	06:00	06:40
Temp [°C]	20	21.4	29	40.7	66	115.8	242.4	222.2	197.3	154	113	98.1

Fan action

3.1.1														
Time	0	15	45	60	95	130	160	180	185	220	285	290	295	400
Time [mm:ss]	00:00	00:15	00:45	01:00	01:35	02:10	02:40	03:00	03:05	00:03:40	00:04:45	00:04:50	00:04:55	06:40
Mass flow rate [kg/s]	0	0.02	0.11	0.18	0.42	0.58	0.58	0.5	0.48	0.16	0.11	0.26	0.15	0.11
Fraction [-]	0	0.03	0.17	0.29	0.67	0.92	0.92	0.79	0.76	0.25	0.17	0.41	0.24	0.17

Contaminant concentration

3.1.1																			
Time	0	30	60	90	120	150	185	195	200	215	260	265	270	275	280	345	350	355	400
Time [mm:ss]	00:00	00:30	01:00	01:30	02:00	02:30	03:05	03:15	03:20	03:35	04:20	04:25	04:30	04:35	04:40	05:45	05:50	05:55	06:40
HRR	0	40	160	360	640	1000	1526.7	384.1	350.8	418.8	250.7	441.9	144.7	173.7	123.8	14.7	19.2	3.9	0
Fraction	0	0.01	0.04	0.09	0.16	0.25	0.382	0.096	0.088	0.105	0.063	0.110	0.036	0.043	0.031	0.004	0.005	0.001	0.000

3.1.2 (Near-zero façade, Medium fire growth rate, Damper=Inlet)

Temperature

3.1.2											
Time	0	30	60	80	105	135	185	195	210	285	400
Time [mm:ss]	00:00	00:30	01:00	01:20	01:45	02:15	03:05	03:15	03:30	04:45	06:40
Temp [°C]	20	21.4	29	40.8	66.3	116.2	243	222.9	198.7	160.2	115.5

Fan action

3.1.2															
Time	0	15	45	60	95	130	160	180	185	200	290	295	305	310	400
Time [mm:ss]	00:00	00:15	00:45	01:00	01:35	02:10	02:40	03:00	03:05	00:03:20	00:04:50	00:04:55	00:05:05	00:05:10	06:40
Mass flow rate [kg/s]	0	0.02	0.11	0.19	0.42	0.58	0.58	0.5	0.48	0.12	0.09	0.07	0.29	0.12	0.11
Fraction [-]	0	0.03	0.17	0.30	0.67	0.92	0.92	0.79	0.76	0.19	0.14	0.11	0.46	0.19	0.17

Contaminant concentration

3.1.2																			
Time	0	30	60	90	120	150	185	195	200	215	265	275	280	285	375	380	385	400
Time [mm:ss]	00:00	00:30	01:00	01:30	02:00	02:30	03:05	03:15	03:20	03:35	04:25	04:35	04:40	04:45	06:15	06:20	06:25	06:40
HRR	0	40	160	360	640	1000	1526.7	387.7	353.6	448	263.8	354.1	103.5	155.1	14.6	21	2.5	0
Fraction	0	0.01	0.04	0.09	0.16	0.25	0.382	0.097	0.088	0.112	0.066	0.089	0.026	0.039	0.004	0.005	0.001	0.000

3.1.3 (Near-zero façade, Medium fire growth rate, Damper=Both)

Temperature

3.1.3											
Time	0	30	60	80	105	135	185	195	210	285	400
Time [mm:ss]	00:00	00:30	01:00	01:20	01:45	02:15	03:05	03:15	03:30	04:45	06:40
Temp [°C]	20	21.5	29.2	41.2	66.7	116.5	242.5	222.6	196.9	156.1	104.2

Fan action

3.1.3															
Time	0	15	45	60	95	130	160	180	185	215	280	285	295	300	400
Time [mm:ss]	00:00	00:15	00:45	01:00	01:35	02:10	02:40	03:00	03:05	00:03:35	00:04:40	00:04:45	00:04:55	00:05:00	06:40
Mass flow rate [kg/s]	0	0.02	0.12	0.19	0.42	0.58	0.58	0.5	0.47	0.15	0.11	0.08	0.28	0.14	0.11
Fraction [-]	0	0.03	0.19	0.30	0.67	0.92	0.92	0.79	0.75	0.24	0.17	0.13	0.44	0.22	0.17

Contaminant concentration

3.1.3																		
Time	0	30	60	90	120	150	185	195	200	215	260	265	270	275	350	355	360	400
Time [mm:ss]	00:00	00:30	01:00	01:30	02:00	02:30	03:05	03:15	03:20	03:35	04:20	04:25	04:30	04:35	05:50	05:55	06:00	06:40
HRR	0	40	160	360	640	1000	1526.7	377.9	333.8	430.7	250.1	296.5	100.5	149.4	14.7	20.1	3.1	0
Fraction	0	0.01	0.04	0.09	0.16	0.25	0.382	0.094	0.083	0.108	0.063	0.074	0.025	0.037	0.004	0.005	0.001	0.000

1.2.1 (Traditional façade, Fast fire growth rate, Damper=Off)

Temperature

1.2.1													
Time	0	30	45	60	80	100	115	155	200	245	290	330	400
Time [mm:ss]	00:00	00:30	00:45	01:00	01:20	01:40	01:55	02:35	03:20	04:05	04:50	05:30	06:40
Temp [C]	20	24.5	34.6	54.6	103.7	185.6	267.4	200.6	146.3	106.9	80.8	65.1	49.9

Fan action

1.2.1																			
Time	0	30	45	60	80	100	115	120	125	170	180	185	215	220	290	295	300	400
Time [mm:ss]	00:00	00:30	00:45	01:00	01:20	01:40	01:55	02:00	02:05	02:50	03:00	03:05	03:35	03:40	04:50	04:55	05:00	06:40
Mass flow rate [kg/s]	0	0.18	0.4	0.68	0.98	1.05	0.92	0.22	0.34	0.27	0.14	0.32	0.27	0.23	0.16	0.13	0.17	0.06
Fraction [-]	0.00	0.16	0.36	0.62	0.89	0.95	0.84	0.20	0.31	0.25	0.13	0.29	0.25	0.21	0.15	0.12	0.15	0.05

Contaminant concentration

1.2.1																
Time	0	15	45	75	90	115	120	160	170	175	180	220	285	290	300	400
Time [mm:ss]	00:00	00:15	00:45	01:15	01:30	01:55	02:00	02:40	02:50	02:55	03:00	03:40	04:45	04:50	06:00	06:10
HRR	0	40	360	1000	1440	2360	849.9	380.4	331.5	448.5	231.8	121.5	14.5	23.8	0	0
Fraction	0	0.01	0.09	0.25	0.36	0.59	0.21	0.10	0.08	0.11	0.06	0.03	0.00	0.01	0.00	0.00

1.2.2 (Traditional façade, Fast fire growth rate, Damper=Inlet)

Temperature

1.2.2													
Time	0	30	45	60	80	100	115	155	200	245	290	330	400
Time [mm:ss]	00:00	00:30	00:45	01:00	01:20	01:40	01:55	02:35	03:20	04:05	04:50	05:30	06:40
Temp [C]	20	24.4	34.7	54.9	104.1	186.1	268	205.6	156.6	117.3	91.5	75.1	55.3

Fan action

1.2.2																		
Time	0	30	45	60	80	100	115	120	125	180	185	195	245	325	330	335	400
Time [mm:ss]	00:00	00:30	00:45	01:00	01:20	01:40	01:55	02:00	02:05	03:00	03:05	03:15	04:05	05:25	05:30	05:35	06:40
Mass flow rate [kg/s]	0	0.18	0.41	0.68	0.98	1.05	0.91	0.21	0.31	0.22	0.07	0.28	0.19	0.13	0.1	0.14	0.08
Fraction [-]	0.00	0.16	0.37	0.62	0.89	0.95	0.83	0.19	0.28	0.20	0.06	0.25	0.17	0.12	0.09	0.13	0.07

Contaminant concentration

1.2.2																		
Time	0	15	45	75	90	115	120	165	180	185	190	220	270	320	330	335	400
Time [mm:ss]	00:00	00:15	00:45	01:15	01:30	01:55	02:00	02:45	03:00	03:05	03:10	03:40	04:30	05:20	05:30	05:35	06:40
HRR	0	40	360	1000	1440	2360	869.6	387.9	335.5	1165.5	243	140.4	62.5	14.4	19	0	0
Fraction	0	0.01	0.09	0.25	0.36	0.59	0.22	0.10	0.08	0.29	0.06	0.04	0.02	0.00	0.00	0.00	0.00

1.2.3 (Traditional façade, Fast fire growth rate, Damper=Both)

Temperature

1.2.3													
Time	0	30	45	60	80	100	115	155	200	245	290	330	400
Time [mm:ss]	00:00	00:30	00:45	01:00	01:20	01:40	01:55	02:35	03:20	04:05	04:50	05:30	06:40
Temp [C]	20	24.5	34.8	55.1	104.3	186.1	267.8	203	150.4	111	84.4	68.1	51.9

Fan action

1.2.3																			
Time	0	30	45	60	80	100	115	120	125	175	180	185	220	225	295	300	305	400
Time [mm:ss]	00:00	00:30	00:45	01:00	01:20	01:40	01:55	02:00	02:05	02:55	03:00	03:05	03:40	03:45	04:55	05:00	05:05	06:40
Mass flow rate [kg/s]	0	0.18	0.41	0.68	0.98	1.05	0.91	0.24	0.33	0.23	0.06	0.32	0.25	0.22	0.16	0.12	0.17	0.07
Fraction [-]	0.00	0.16	0.37	0.62	0.89	0.95	0.83	0.22	0.30	0.21	0.05	0.29	0.23	0.20	0.15	0.11	0.15	0.06

Contaminant concentration

1.2.3																
Time	0	15	45	75	90	115	120	165	175	180	185	205	290	300	305	400
Time [mm:ss]	00:00	00:15	00:45	01:15	01:30	01:55	02:00	02:45	02:55	03:00	03:05	03:25	04:50	05:00	05:05	06:40
HRR	0	40	360	1000	1440	2360	841.9	356.7	315.2	196.1	222.7	140.4	14.5	13.4	0	0
Fraction	0	0.01	0.09	0.25	0.36	0.59	0.21	0.09	0.08	0.05	0.06	0.04	0.00	0.00	0.00	0.00

2.2.1 (Modern façade, Fast fire growth rate, Damper=Off)

Temperature

2.2.1													
Time	0	30	45	60	80	100	115	155	200	245	290	330	400
Time [mm:ss]	00:00	00:30	00:45	01:00	01:20	01:40	01:55	02:35	03:20	04:05	04:50	05:30	06:40
Temp [C]	20	24.5	34.9	55.5	105.4	186.5	265.6	199.3	144.2	104.8	78.1	63.4	49.1

Fan action

2.2.1																					
Time	0	30	45	60	80	100	115	120	125	130	170	175	180	185	210	215	275	280	285	330	400
Time [mm:ss]	00:00	00:30	00:45	01:00	01:20	01:40	01:55	02:00	02:05	02:10	02:50	02:55	03:00	03:05	03:30	03:35	04:35	04:40	04:45	05:30	06:40
Mass flow rate [kg/s]	0	0.18	0.41	0.69	0.98	1.03	0.89	0.01	0.5	0.34	0.26	0.03	0.39	0.32	0.28	0.24	0.18	0.15	0.16	0.12	0.06
Fraction [-]	0.00	0.16	0.37	0.63	0.89	0.94	0.81	0.01	0.45	0.31	0.24	0.03	0.35	0.29	0.25	0.22	0.16	0.14	0.15	0.11	0.05

Contaminant concentration

2.2.1																		
Time	0	15	45	75	90	115	120	125	160	170	175	210	220	250	275	280	285	400
Time [mm:ss]	00:00	00:15	00:45	01:15	01:30	01:55	02:00	02:05	02:40	02:50	02:55	03:30	03:40	04:10	04:35	04:40	04:45	06:40
HRR	0	40	360	1000	1440	2360	867.9	734.3	369.1	340.5	230.2	118.7	104.8	30.6	14.9	122.4	0.5	0
Fraction	0	0.01	0.09	0.25	0.36	0.59	0.22	0.18	0.09	0.09	0.06	0.03	0.03	0.01	0.00	0.03	0.00	0.00

2.2.2 (Modern façade, Fast fire growth rate, Damper=Inlet)

Temperature

2.2.2													
Time	0	30	45	60	80	100	115	155	200	245	290	330	400
Time [mm:ss]	00:00	00:30	00:45	01:00	01:20	01:40	01:55	02:35	03:20	04:05	04:50	05:30	06:40
Temp [C]	20	24.5	35	55.7	105.7	166.1	266.1	203.6	154.3	115.5	88.9	71.9	53.8

Fan action

2.2.2																				
Time	0	30	45	60	80	100	115	120	125	130	175	180	185	190	245	310	315	320	400
Time [mm:ss]	00:00	00:30	00:45	01:00	01:20	01:40	01:55	02:00	02:05	02:10	02:55	03:00	03:05	03:10	04:05	05:10	05:15	05:20	06:40
Mass flow rate [kg/s]	0	0.18	0.42	0.69	0.98	1.03	0.88	0.01	0.48	0.33	0.24	0.2	0.08	0.29	0.2	0.15	0.11	0.16	0.07
Fraction [-]	0.00	0.16	0.38	0.63	0.89	0.94	0.80	0.01	0.44	0.30	0.22	0.18	0.07	0.26	0.18	0.14	0.10	0.15	0.06

Contaminant concentration

2.2.2																		
Time	0	15	45	75	90	115	120	155	175	180	185	190	215	275	305	310	320	400
Time [mm:ss]	00:00	00:15	00:45	01:15	01:30	01:55	02:00	02:35	02:55	03:00	03:05	03:10	03:35	04:35	05:05	05:10	05:20	06:15
HRR	0	40	360	1000	1440	2360	878.8	453.8	332.5	370.9	143.15	234	141.1	38.1	14.5	16.8	0	0
Fraction	0	0.01	0.09	0.25	0.36	0.59	0.22	0.11	0.08	0.09	0.04	0.06	0.04	0.01	0.00	0.00	0.00	0.00

2.2.3 (Modern façade, Fast fire growth rate, Damper=Both)

Temperature

2.2.3													
Time	0	30	45	60	80	100	115	155	200	245	290	330	400
Time [mm:ss]	00:00	00:30	00:45	01:00	01:20	01:40	01:55	02:35	03:20	04:05	04:50	05:30	06:40
Temp [C]	20	24.6	35.2	56	105.9	187	265.9	201	147.9	108.6	82.3	66	51

Fan action

2.2.3																					
Time	0	30	45	60	80	100	115	120	125	130	170	175	180	185	245	285	290	295	345	400
Time [mm:ss]	00:00	00:30	00:45	01:00	01:20	01:40	01:55	02:00	02:05	02:10	02:50	02:55	03:00	03:05	04:05	04:45	04:50	04:55	05:45	06:40
Mass flow rate [kg/s]	0	0.18	0.42	0.69	0.97	1.02	0.88	0.02	0.51	0.34	0.26	0.17	0.2	0.31	0.22	0.16	0.14	0.18	0.1	0.06
Fraction [-]	0.00	0.16	0.38	0.63	0.88	0.93	0.80	0.02	0.46	0.31	0.24	0.15	0.18	0.28	0.20	0.15	0.13	0.16	0.09	0.05

Contaminant concentration

2.2.3																		
Time	0	15	45	75	90	115	120	160	170	175	180	215	250	280	285	290	400
Time [mm:ss]	00:00	00:15	00:45	01:15	01:30	01:55	02:00	02:40	02:50	02:55	03:00	03:35	04:10	04:40	04:45	04:50	06:40
HRR	0	40	360	1000	1440	2360	853.5	377.4	331.9	556.9	260.9	120.9	39.4	14.7	27.4	1.36	0
Fraction	0	0.01	0.09	0.25	0.36	0.59	0.21	0.09	0.08	0.14	0.07	0.03	0.01	0.00	0.01	0.00	0.00

3.2.1 (Near-zero façade, Fast fire growth rate, Damper=Off)

Temperature

3.2.1													
Time	0	30	45	60	80	100	115	155	200	245	290	330	400
Time [mm:ss]	00:00	00:30	00:45	01:00	01:20	01:40	01:55	02:35	03:20	04:05	04:50	05:30	06:40
Temp [C]	20	24.7	35.5	57.1	108.3	188.7	286.2	196.3	141.1	102.5	76.9	62.6	49.2

Fan action

3.2.1																		
Time	0	30	45	60	80	100	115	150	170	175	180	235	270	275	280	330	400
Time [mm:ss]	00:00	00:30	00:45	01:00	01:20	01:40	01:55	02:30	02:50	02:55	03:00	03:55	04:30	04:35	04:40	05:30	06:40
Mass flow rate [kg/s]	0	0.19	0.43	0.71	0.98	0.99	0.84	0.31	0.22	0.19	0.34	0.23	0.19	0.13	0.2	0.1	0.06
Fraction [-]	0.00	0.17	0.39	0.65	0.89	0.90	0.76	0.28	0.20	0.17	0.31	0.21	0.17	0.12	0.18	0.09	0.05

Contaminant concentration

3.2.1																			
Time	0	15	45	75	90	115	125	135	165	170	175	180	205	210	215	240	275	280	400
Time [mm:ss]	00:00	00:15	00:45	01:15	01:30	01:55	02:05	02:15	02:45	02:50	02:55	03:00	03:15	03:30	03:45	04:00	04:35	04:40	06:40
HRR	0	40	360	1000	1440	2360	836.4	614.7	331.7	430.3	121.9	212	124.4	136.5	111	36.2	16.1	0	0
Fraction	0	0.01	0.09	0.25	0.36	0.59	0.21	0.15	0.08	0.11	0.03	0.053	0.031	0.034	0.028	0.01	0.00	0	0

3.2.2 (Near-zero façade, Fast fire growth rate, Damper=Inlet)

Temperature

3.2.2													
Time	0	30	45	60	80	100	115	155	200	245	290	330	400
Time [mm:ss]	00:00	00:30	00:45	01:00	01:20	01:40	01:55	02:35	03:20	04:05	04:50	05:30	06:40
Temp [C]	20	24.7	35.6	57.3	108.6	189.2	286.8	197.7	149	112.2	85.8	69.4	52.8

Fan action

3.2.2																			
Time	0	30	45	60	80	90	100	115	150	175	180	185	190	300	305	310	340	400
Time [mm:ss]	00:00	00:30	00:45	01:00	01:20	01:30	01:40	01:55	02:30	02:55	03:00	03:05	03:10	05:00	05:05	05:10	05:40	06:40
Mass flow rate [kg/s]	0	0.19	0.44	0.71	0.98	1.02	0.99	0.84	0.3	0.21	0.02	0.4	0.26	0.15	0.11	0.17	0.12	0.07
Fraction [-]	0.00	0.17	0.40	0.65	0.89	0.93	0.90	0.76	0.27	0.19	0.02	0.36	0.24	0.14	0.10	0.15	0.11	0.06

Contaminant concentration

3.2.2																		
Time	0	15	45	75	90	115	125	135	160	175	180	185	210	290	300	305	400
Time [mm:ss]	00:00	00:15	00:45	01:15	01:30	01:55	02:05	02:15	02:40	02:55	03:00	03:05	03:30	04:50	05:00	05:05	06:40
HRR	0	40	360	1000	1440	2360	843.7	615.6	380.6	355.5	140.7	266.5	140.5	15.6	19	4.1	0
Fraction	0	0.01	0.09	0.25	0.36	0.59	0.21	0.15	0.10	0.09	0.04	0.07	0.04	0.00	0.00	0.00	0.00

3.2.3 (Near-zero façade, Fast fire growth rate, Damper=Both)

Temperature

3.2.3													
Time	0	30	45	60	80	100	115	155	200	245	290	330	400
Time [mm:ss]	00:00	00:30	00:45	01:00	01:20	01:40	01:55	02:35	03:20	04:05	04:50	05:30	06:40
Temp [C]	20	24.9	36	57.8	109	189.2	287.6	196.1	143.4	105.4	79.6	64.7	50.6

Fan action

3.2.3																			
Time	0	30	45	60	80	100	115	150	170	175	180	185	245	275	280	285	330	400
Time [mm:ss]	00:00	00:30	00:45	01:00	01:20	01:40	01:55	02:30	02:50	02:55	03:00	03:05	04:05	04:35	04:40	04:45	05:30	06:40
Mass flow rate [kg/s]	0	0.19	0.44	0.71	0.97	0.99	0.84	0.3	0.21	0.16	0.34	0.3	0.22	0.18	0.13	0.19	0.11	0.06
Fraction [-]	0.00	0.17	0.40	0.65	0.88	0.90	0.76	0.27	0.19	0.15	0.31	0.27	0.20	0.16	0.12	0.17	0.10	0.05

Contaminant concentration

3.2.3																	
Time	0	15	45	75	90	115	125	145	165	170	175	180	230	270	275	280	400
Time [mm	00:00	00:15	00:45	01:15	01:30	01:55	02:05	02:25	02:45	02:50	02:55	03:00	03:50	04:35	04:40	04:45	06:40
HRR	0	40	360	1000	1440	2360	825.8	458.9	331.8	413.8	145.1	233.5	68.3	14.8	18	6.1	0
Fraction	0	0.01	0.09	0.25	0.36	0.59	0.21	0.11	0.08	0.10	0.04	0.06	0.02	0.00	0.00	0.00	0.00

Appendix D – Calculation of the mass flow rates for the calibration study (CFAST)

3.1.1

Time	W_1_Outside_1	M_Outside_1_1	M_1_Outside_2	
Simulation Time	Net Inflow	Net Inflow	Net Inflow	
Time	LOCALEAK	Inlet	Outlet	
s	kg/s	kg/s	kg/s	Sum flow out/in
0.00	0.00	0.05	0.05	0.00
5.00	0.01	0.05	0.05	0.01
10.00	0.02	0.05	0.05	0.02
15.00	0.02	0.05	0.05	0.02
20.00	0.03	0.05	0.05	0.03
25.00	0.04	0.05	0.05	0.04
30.00	0.05	0.05	0.05	0.05
35.00	0.06	0.05	0.05	0.06
40.00	0.09	0.05	0.05	0.08
45.00	0.11	0.05	0.05	0.10
50.00	0.13	0.05	0.05	0.12
55.00	0.14	0.03	0.04	0.16
60.00	0.14	0.01	0.04	0.18
65.00	0.16	0.00	0.04	0.20
70.00	0.18	0.00	0.04	0.22
75.00	0.21	0.00	0.04	0.25
80.00	0.23	0.00	0.04	0.28
85.00	0.26	0.00	0.04	0.30
90.00	0.28	0.00	0.04	0.32
95.00	0.31	0.00	0.04	0.35
100.00	0.34	0.00	0.04	0.38
105.00	0.37	0.00	0.04	0.41
110.00	0.39	0.00	0.04	0.43
115.00	0.42	0.00	0.04	0.46
120.00	0.44	0.00	0.04	0.48
125.00	0.46	0.00	0.04	0.50
130.00	0.49	0.00	0.04	0.52
135.00	0.51	0.00	0.04	0.54
140.00	0.53	0.00	0.04	0.56
145.00	0.54	0.00	0.04	0.58
150.00	0.55	0.00	0.03	0.59
155.00	0.56	0.00	0.03	0.60
160.00	0.57	0.00	0.03	0.61
165.00	0.5795	0.00	0.03	0.61
170.00	0.5820	0.00	0.03	0.61
175.00	0.5806	0.00	0.03	0.61
180.00	0.5752	0.00	0.03	0.61
185.00	0.57	0.00	0.03	0.60
190.00	0.54	0.00	0.03	0.57
195.00	0.29	0.00	0.03	0.32
200.00	-0.16	0.05	0.00	-0.21
205.00	-0.22	0.05	0.00	-0.27
210.00	-0.18	0.05	0.00	-0.23
215.00	-0.11	0.05	0.03	-0.13
220.00	-0.06	0.05	0.03	-0.08
225.00	-0.04	0.05	0.03	-0.05
230.00	-0.03	0.05	0.03	-0.05
235.00	-0.03	0.05	0.03	-0.05
240.00	-0.02	0.05	0.03	-0.04
245.00	-0.02	0.05	0.03	-0.03
250.00	-0.01	0.05	0.03	-0.03
255.00	0.00	0.05	0.03	-0.02
260.00	0.02	0.05	0.03	0.00
265.00	0.10	0.05	0.03	0.08
270.00	-0.06	0.05	0.03	-0.07
275.00	-0.05	0.05	0.03	-0.06
280.00	-0.04	0.05	0.03	-0.06
285.00	-0.04	0.05	0.03	-0.05
290.00	-0.02	0.05	0.04	-0.03
295.00	0.01	0.05	0.04	0.00
300.00	0.01	0.05	0.04	0.00
305.00	0.01	0.05	0.04	0.00
310.00	0.01	0.05	0.04	0.00
315.00	0.01	0.05	0.04	0.00
320.00	0.01	0.05	0.04	0.00
325.00	0.02	0.05	0.04	0.01
330.00	0.02	0.05	0.04	0.01
335.00	0.03	0.05	0.04	0.02
340.00	0.04	0.05	0.04	0.03
345.00	0.05	0.05	0.04	0.04
350.00	0.06	0.05	0.04	0.05
355.00	0.08	0.05	0.04	0.07
360.00	0.05	0.05	0.04	0.05
365.00	0.06	0.05	0.04	0.05
370.00	0.07	0.05	0.04	0.06
375.00	0.08	0.05	0.04	0.07
380.00	0.08	0.05	0.04	0.08
385.00	0.09	0.05	0.04	0.09
390.00	0.10	0.05	0.04	0.09
395.00	0.11	0.05	0.04	0.10
400.00	0.11	0.05	0.04	0.11
MAX VALUE	0.58			0.61

3.2.1

Time	W_1_Outside_1	M_Outside_1_1	M_1_Outside_2	
Simulation Time	Net Inflow	Net Inflow	Net Inflow	
Time	LOCALEAK	Inlet	Outlet	
s	kg/s	kg/s	kg/s	Sum flow out/in
0.00	0.00	0.05	0.05	0.00
5.00	0.02	0.05	0.05	0.01
10.00	0.03	0.05	0.05	0.03
15.00	0.05	0.05	0.05	0.04
20.00	0.08	0.05	0.05	0.08
25.00	0.11	0.03	0.05	0.13
30.00	0.13	0.00	0.04	0.17
35.00	0.17	0.00	0.04	0.21
40.00	0.22	0.00	0.04	0.26
45.00	0.27	0.00	0.04	0.31
50.00	0.32	0.00	0.04	0.37
55.00	0.38	0.00	0.04	0.42
60.00	0.44	0.00	0.04	0.48
65.00	0.50	0.00	0.04	0.54
70.00	0.56	0.00	0.04	0.60
75.00	0.62	0.00	0.04	0.65
80.00	0.67	0.00	0.04	0.71
85.00	0.73	0.00	0.04	0.76
90.00	0.77	0.00	0.04	0.81
95.00	0.82	0.00	0.04	0.85
100.00	0.85	0.00	0.03	0.89
105.00	0.88	0.00	0.03	0.92
110.00	0.90	0.00	0.03	0.94
115.00	0.92	0.00	0.03	0.95
120.00	0.90	0.00	0.03	0.93
125.00	0.71	0.00	0.03	0.73
130.00	0.52	0.00	0.03	0.55
135.00	0.35	0.00	0.03	0.38
140.00	0.18	0.00	0.03	0.20
145.00	-0.06	0.05	0.03	-0.08
150.00	-0.05	0.05	0.03	-0.07
155.00	-0.04	0.05	0.03	-0.06
160.00	-0.04	0.05	0.03	-0.06
165.00	-0.02	0.05	0.03	-0.03
170.00	0.06	0.05	0.03	0.04
175.00	-0.09	0.05	0.03	-0.11
180.00	-0.07	0.05	0.03	-0.09
185.00	-0.06	0.05	0.03	-0.08
190.00	-0.05	0.05	0.03	-0.07
195.00	-0.04	0.05	0.03	-0.06
200.00	-0.05	0.05	0.03	-0.06
205.00	-0.03	0.05	0.03	-0.05
210.00	0.02	0.05	0.03	0.01
215.00	0.00	0.05	0.04	-0.01
220.00	0.00	0.05	0.04	-0.01
225.00	0.00	0.05	0.04	-0.01
230.00	0.01	0.05	0.04	-0.01
235.00	0.01	0.05	0.04	0.00
240.00	0.01	0.05	0.04	0.00
245.00	0.01	0.05	0.04	0.00
250.00	0.02	0.05	0.04	0.01
255.00	0.02	0.05	0.04	0.02
260.00	0.03	0.05	0.04	0.02
265.00	0.04	0.05	0.04	0.03
270.00	0.05	0.05	0.04	0.04
275.00	0.09	0.05	0.04	0.09
280.00	0.05	0.05	0.04	0.05
285.00	0.06	0.05	0.04	0.05
290.00	0.06	0.05	0.04	0.06
295.00	0.07	0.05	0.04	0.07
300.00	0.08	0.05	0.04	0.07
305.00	0.09	0.05	0.04	0.08
310.00	0.10	0.05	0.04	0.09
315.00	0.10	0.05	0.04	0.10
320.00	0.10	0.04	0.04	0.11
325.00	0.11	0.03	0.04	0.12
330.00	0.11	0.03	0.04	0.12
335.00	0.11	0.02	0.04	0.13
340.00	0.11	0.02	0.04	0.13
345.00	0.11	0.01	0.04	0.14
350.00	0.11	0.01	0.04	0.14
355.00	0.11	0.01	0.04	0.15
360.00	0.11	0.00	0.04	0.15
365.00	0.11	0.00	0.04	0.15
370.00	0.11	0.00	0.04	0.16
375.00	0.12	0.00	0.04	0.16
380.00	0.12	0.00	0.04	0.16
385.00	0.12	0.00	0.04	0.16
390.00	0.12	0.00	0.04	0.17
395.00	0.12	0.00	0.04	0.17
400.00	0.13	0.00	0.04	0.17
MAX VALUE	0.92			0.95

Appendix E – Calculation of the mass flow rates for the calibration study (CONTAM)

3.1.1

Date/Time	Property	Path #3	Path #6	Duct #2	Duct #4	Total	Leakage only
1-1-2023 00:00	Flow 1 [kg/s]	0.00	0.00	0.05	0.11	0.16	0.00
1-1-2023 00:00	Flow 1 [kg/s]	0.00	0.00	0.05	0.11	0.17	0.00
1-1-2023 00:00	Flow 1 [kg/s]	0.00	0.00	0.05	0.11	0.17	0.01
1-1-2023 00:00	Flow 1 [kg/s]	0.00	0.00	0.06	0.11	0.18	0.01
1-1-2023 00:00	Flow 1 [kg/s]	0.01	0.00	0.06	0.12	0.19	0.01
1-1-2023 00:00	Flow 1 [kg/s]	0.01	0.00	0.06	0.12	0.20	0.01
1-1-2023 00:00	Flow 1 [kg/s]	0.01	0.01	0.07	0.12	0.21	0.02
1-1-2023 00:00	Flow 1 [kg/s]	0.01	0.01	0.07	0.13	0.21	0.02
1-1-2023 00:00	Flow 1 [kg/s]	0.01	0.01	0.07	0.13	0.22	0.02
1-1-2023 00:00	Flow 1 [kg/s]	0.02	0.01	0.08	0.13	0.23	0.02
1-1-2023 00:00	Flow 1 [kg/s]	0.02	0.01	0.08	0.13	0.24	0.03
1-1-2023 00:00	Flow 1 [kg/s]	0.02	0.01	0.08	0.13	0.25	0.03
1-1-2023 00:01	Flow 1 [kg/s]	0.02	0.01	0.09	0.14	0.26	0.03
1-1-2023 00:01	Flow 1 [kg/s]	0.03	0.01	0.10	0.14	0.28	0.04
1-1-2023 00:01	Flow 1 [kg/s]	0.03	0.01	0.10	0.15	0.30	0.04
1-1-2023 00:01	Flow 1 [kg/s]	0.03	0.02	0.11	0.16	0.32	0.05
1-1-2023 00:01	Flow 1 [kg/s]	0.04	0.02	0.12	0.16	0.34	0.06
1-1-2023 00:01	Flow 1 [kg/s]	0.04	0.02	0.13	0.17	0.36	0.06
1-1-2023 00:01	Flow 1 [kg/s]	0.04	0.02	0.14	0.18	0.38	0.07
1-1-2023 00:01	Flow 1 [kg/s]	0.05	0.02	0.15	0.18	0.40	0.07
1-1-2023 00:01	Flow 1 [kg/s]	0.05	0.02	0.16	0.19	0.42	0.08
1-1-2023 00:01	Flow 1 [kg/s]	0.05	0.03	0.16	0.19	0.44	0.08
1-1-2023 00:01	Flow 1 [kg/s]	0.06	0.03	0.17	0.20	0.45	0.08
1-1-2023 00:01	Flow 1 [kg/s]	0.06	0.03	0.18	0.20	0.47	0.09
1-1-2023 00:02	Flow 1 [kg/s]	0.06	0.03	0.18	0.21	0.48	0.09
1-1-2023 00:02	Flow 1 [kg/s]	0.06	0.03	0.19	0.21	0.50	0.09
1-1-2023 00:02	Flow 1 [kg/s]	0.06	0.03	0.20	0.22	0.51	0.10
1-1-2023 00:02	Flow 1 [kg/s]	0.06	0.03	0.20	0.22	0.51	0.09
1-1-2023 00:02	Flow 1 [kg/s]	0.06	0.03	0.20	0.22	0.51	0.09
1-1-2023 00:02	Flow 1 [kg/s]	0.06	0.03	0.20	0.22	0.51	0.09
1-1-2023 00:02	Flow 1 [kg/s]	0.06	0.03	0.20	0.22	0.51	0.09
1-1-2023 00:02	Flow 1 [kg/s]	0.06	0.03	0.20	0.22	0.51	0.09
1-1-2023 00:02	Flow 1 [kg/s]	0.06	0.03	0.20	0.22	0.51	0.09
1-1-2023 00:02	Flow 1 [kg/s]	0.06	0.03	0.19	0.22	0.50	0.09
1-1-2023 00:02	Flow 1 [kg/s]	0.06	0.03	0.19	0.21	0.48	0.08
1-1-2023 00:02	Flow 1 [kg/s]	0.05	0.03	0.18	0.21	0.47	0.08
1-1-2023 00:03	Flow 1 [kg/s]	0.05	0.02	0.18	0.20	0.45	0.07
1-1-2023 00:03	Flow 1 [kg/s]	0.05	0.02	0.17	0.20	0.44	0.07
1-1-2023 00:03	Flow 1 [kg/s]	0.04	0.02	0.16	0.19	0.41	0.07
1-1-2023 00:03	Flow 1 [kg/s]	0.04	0.02	0.14	0.18	0.38	0.06
1-1-2023 00:03	Flow 1 [kg/s]	0.03	0.02	0.13	0.17	0.35	0.05
1-1-2023 00:03	Flow 1 [kg/s]	0.03	0.02	0.12	0.16	0.32	0.05
1-1-2023 00:03	Flow 1 [kg/s]	0.03	0.01	0.10	0.15	0.29	0.04
1-1-2023 00:03	Flow 1 [kg/s]	0.02	0.01	0.09	0.14	0.27	0.03
1-1-2023 00:03	Flow 1 [kg/s]	0.02	0.01	0.08	0.13	0.24	0.03
1-1-2023 00:03	Flow 1 [kg/s]	0.02	0.01	0.08	0.13	0.24	0.03
1-1-2023 00:03	Flow 1 [kg/s]	0.02	0.01	0.08	0.13	0.24	0.03
1-1-2023 00:03	Flow 1 [kg/s]	0.02	0.01	0.08	0.13	0.24	0.03
1-1-2023 00:04	Flow 1 [kg/s]	0.02	0.01	0.08	0.13	0.24	0.03
1-1-2023 00:04	Flow 1 [kg/s]	0.02	0.01	0.08	0.13	0.24	0.03
1-1-2023 00:04	Flow 1 [kg/s]	0.02	0.01	0.08	0.13	0.23	0.02
1-1-2023 00:04	Flow 1 [kg/s]	0.02	0.01	0.08	0.13	0.23	0.02
1-1-2023 00:04	Flow 1 [kg/s]	0.02	0.01	0.08	0.13	0.23	0.02
1-1-2023 00:04	Flow 1 [kg/s]	0.02	0.01	0.08	0.13	0.23	0.02
1-1-2023 00:04	Flow 1 [kg/s]	0.02	0.01	0.08	0.13	0.23	0.02
1-1-2023 00:04	Flow 1 [kg/s]	0.02	0.01	0.08	0.13	0.23	0.02
1-1-2023 00:04	Flow 1 [kg/s]	0.01	0.01	0.08	0.13	0.23	0.02
1-1-2023 00:04	Flow 1 [kg/s]	0.03	0.01	0.11	0.15	0.30	0.04
1-1-2023 00:04	Flow 1 [kg/s]	0.02	0.01	0.08	0.13	0.24	0.03
1-1-2023 00:05	Flow 1 [kg/s]	0.02	0.01	0.08	0.13	0.24	0.03
1-1-2023 00:05	Flow 1 [kg/s]	0.02	0.01	0.08	0.13	0.24	0.03
1-1-2023 00:05	Flow 1 [kg/s]	0.02	0.01	0.08	0.13	0.24	0.03
1-1-2023 00:05	Flow 1 [kg/s]	0.02	0.01	0.08	0.13	0.24	0.03
1-1-2023 00:05	Flow 1 [kg/s]	0.02	0.01	0.08	0.13	0.24	0.03
1-1-2023 00:05	Flow 1 [kg/s]	0.02	0.01	0.08	0.13	0.24	0.03
1-1-2023 00:05	Flow 1 [kg/s]	0.02	0.01	0.08	0.13	0.24	0.03
1-1-2023 00:05	Flow 1 [kg/s]	0.02	0.01	0.08	0.13	0.24	0.03
1-1-2023 00:05	Flow 1 [kg/s]	0.02	0.01	0.08	0.13	0.24	0.03
1-1-2023 00:05	Flow 1 [kg/s]	0.02	0.01	0.08	0.13	0.24	0.03
1-1-2023 00:05	Flow 1 [kg/s]	0.02	0.01	0.08	0.13	0.23	0.02
1-1-2023 00:05	Flow 1 [kg/s]	0.02	0.01	0.08	0.13	0.23	0.02
1-1-2023 00:05	Flow 1 [kg/s]	0.02	0.01	0.08	0.13	0.23	0.02
1-1-2023 00:05	Flow 1 [kg/s]	0.02	0.01	0.08	0.13	0.23	0.02
1-1-2023 00:06	Flow 1 [kg/s]	0.02	0.01	0.08	0.13	0.23	0.02
1-1-2023 00:06	Flow 1 [kg/s]	0.02	0.01	0.08	0.13	0.23	0.02
1-1-2023 00:06	Flow 1 [kg/s]	0.02	0.01	0.08	0.13	0.23	0.02
1-1-2023 00:06	Flow 1 [kg/s]	0.02	0.01	0.08	0.13	0.23	0.02
1-1-2023 00:06	Flow 1 [kg/s]	0.02	0.01	0.08	0.13	0.23	0.02
1-1-2023 00:06	Flow 1 [kg/s]	0.02	0.01	0.08	0.13	0.23	0.02
1-1-2023 00:06	Flow 1 [kg/s]	0.02	0.01	0.08	0.13	0.23	0.02
1-1-2023 00:06	Flow 1 [kg/s]	0.02	0.01	0.08	0.13	0.23	0.02
Max all flows				0.20	0.22	0.51	0.10

3.2.1

Date/Time	Property	Path #3	Path #6	Duct #2	Duct #4	Total	Leakage on
1-1-2023 00:00	Flow 1 [kg/s]	0.00	0.00	0.05	0.11	0.16	0.00
1-1-2023 00:00	Flow 1 [kg/s]	0.01	0.00	0.06	0.12	0.19	0.01
1-1-2023 00:00	Flow 1 [kg/s]	0.01	0.01	0.07	0.13	0.21	0.02
1-1-2023 00:00	Flow 1 [kg/s]	0.02	0.01	0.08	0.13	0.23	0.02
1-1-2023 00:00	Flow 1 [kg/s]	0.02	0.01	0.08	0.13	0.25	0.03
1-1-2023 00:00	Flow 1 [kg/s]	0.02	0.01	0.09	0.14	0.27	0.04
1-1-2023 00:00	Flow 1 [kg/s]	0.03	0.01	0.10	0.15	0.29	0.04
1-1-2023 00:00	Flow 1 [kg/s]	0.04	0.02	0.12	0.17	0.35	0.06
1-1-2023 00:00	Flow 1 [kg/s]	0.05	0.03	0.15	0.19	0.41	0.08
1-1-2023 00:00	Flow 1 [kg/s]	0.06	0.03	0.18	0.21	0.48	0.09
1-1-2023 00:00	Flow 1 [kg/s]	0.08	0.04	0.22	0.23	0.56	0.12
1-1-2023 00:00	Flow 1 [kg/s]	0.09	0.04	0.25	0.26	0.65	0.14
1-1-2023 00:01	Flow 1 [kg/s]	0.11	0.05	0.29	0.28	0.73	0.16
1-1-2023 00:01	Flow 1 [kg/s]	0.11	0.06	0.31	0.30	0.79	0.17
1-1-2023 00:01	Flow 1 [kg/s]	0.12	0.06	0.34	0.32	0.84	0.18
1-1-2023 00:01	Flow 1 [kg/s]	0.13	0.07	0.37	0.34	0.90	0.20
1-1-2023 00:01	Flow 1 [kg/s]	0.14	0.07	0.39	0.36	0.96	0.21
1-1-2023 00:01	Flow 1 [kg/s]	0.14	0.07	0.39	0.36	0.96	0.21
1-1-2023 00:01	Flow 1 [kg/s]	0.14	0.07	0.40	0.36	0.96	0.21
1-1-2023 00:01	Flow 1 [kg/s]	0.14	0.07	0.40	0.36	0.97	0.20
1-1-2023 00:01	Flow 1 [kg/s]	0.13	0.07	0.40	0.37	0.97	0.20
1-1-2023 00:01	Flow 1 [kg/s]	0.12	0.06	0.38	0.35	0.92	0.19
1-1-2023 00:01	Flow 1 [kg/s]	0.11	0.06	0.37	0.34	0.88	0.17
1-1-2023 00:01	Flow 1 [kg/s]	0.11	0.05	0.35	0.32	0.83	0.16
1-1-2023 00:02	Flow 1 [kg/s]	0.10	0.05	0.32	0.30	0.76	0.14
1-1-2023 00:02	Flow 1 [kg/s]	0.09	0.04	0.29	0.28	0.70	0.13
1-1-2023 00:02	Flow 1 [kg/s]	0.08	0.04	0.26	0.26	0.63	0.11
1-1-2023 00:02	Flow 1 [kg/s]	0.07	0.03	0.23	0.24	0.57	0.10
1-1-2023 00:02	Flow 1 [kg/s]	0.06	0.03	0.20	0.22	0.50	0.09
1-1-2023 00:02	Flow 1 [kg/s]	0.05	0.02	0.17	0.20	0.44	0.07
1-1-2023 00:02	Flow 1 [kg/s]	0.04	0.02	0.14	0.18	0.38	0.06
1-1-2023 00:02	Flow 1 [kg/s]	0.04	0.02	0.13	0.17	0.36	0.05
1-1-2023 00:02	Flow 1 [kg/s]	0.03	0.02	0.12	0.17	0.34	0.05
1-1-2023 00:02	Flow 1 [kg/s]	0.03	0.02	0.12	0.16	0.32	0.05
1-1-2023 00:02	Flow 1 [kg/s]	0.03	0.01	0.11	0.15	0.31	0.04
1-1-2023 00:02	Flow 1 [kg/s]	0.03	0.01	0.10	0.15	0.28	0.04
1-1-2023 00:03	Flow 1 [kg/s]	0.04	0.02	0.15	0.19	0.40	0.07
1-1-2023 00:03	Flow 1 [kg/s]	0.04	0.02	0.15	0.18	0.40	0.06
1-1-2023 00:03	Flow 1 [kg/s]	0.04	0.02	0.14	0.18	0.39	0.06
1-1-2023 00:03	Flow 1 [kg/s]	0.04	0.02	0.14	0.18	0.38	0.06
1-1-2023 00:03	Flow 1 [kg/s]	0.04	0.02	0.14	0.17	0.37	0.06
1-1-2023 00:03	Flow 1 [kg/s]	0.04	0.02	0.13	0.17	0.36	0.06
1-1-2023 00:03	Flow 1 [kg/s]	0.04	0.02	0.13	0.17	0.36	0.06
1-1-2023 00:03	Flow 1 [kg/s]	0.04	0.02	0.13	0.17	0.35	0.05
1-1-2023 00:03	Flow 1 [kg/s]	0.04	0.02	0.12	0.16	0.34	0.05
1-1-2023 00:03	Flow 1 [kg/s]	0.03	0.02	0.12	0.16	0.33	0.05
1-1-2023 00:03	Flow 1 [kg/s]	0.03	0.02	0.12	0.16	0.32	0.05
1-1-2023 00:03	Flow 1 [kg/s]	0.03	0.02	0.11	0.16	0.32	0.05
1-1-2023 00:04	Flow 1 [kg/s]	0.03	0.02	0.11	0.16	0.31	0.05
1-1-2023 00:04	Flow 1 [kg/s]	0.03	0.01	0.11	0.15	0.31	0.05
1-1-2023 00:04	Flow 1 [kg/s]	0.03	0.01	0.11	0.15	0.30	0.04
1-1-2023 00:04	Flow 1 [kg/s]	0.03	0.01	0.10	0.15	0.30	0.04
1-1-2023 00:04	Flow 1 [kg/s]	0.03	0.01	0.10	0.15	0.29	0.04
1-1-2023 00:04	Flow 1 [kg/s]	0.03	0.01	0.10	0.15	0.29	0.04
1-1-2023 00:04	Flow 1 [kg/s]	0.03	0.01	0.10	0.15	0.29	0.04
1-1-2023 00:04	Flow 1 [kg/s]	0.02	0.01	0.08	0.14	0.25	0.03
1-1-2023 00:04	Flow 1 [kg/s]	0.03	0.01	0.10	0.15	0.29	0.04
1-1-2023 00:04	Flow 1 [kg/s]	0.03	0.01	0.10	0.15	0.29	0.04
1-1-2023 00:04	Flow 1 [kg/s]	0.03	0.01	0.10	0.14	0.28	0.04
1-1-2023 00:04	Flow 1 [kg/s]	0.02	0.01	0.09	0.14	0.27	0.04
1-1-2023 00:05	Flow 1 [kg/s]	0.02	0.01	0.09	0.14	0.27	0.03
1-1-2023 00:05	Flow 1 [kg/s]	0.02	0.01	0.09	0.14	0.26	0.03
1-1-2023 00:05	Flow 1 [kg/s]	0.02	0.01	0.09	0.14	0.25	0.03
1-1-2023 00:05	Flow 1 [kg/s]	0.02	0.01	0.08	0.13	0.25	0.03
1-1-2023 00:05	Flow 1 [kg/s]	0.02	0.01	0.08	0.13	0.24	0.03
1-1-2023 00:05	Flow 1 [kg/s]	0.02	0.01	0.08	0.13	0.24	0.03
1-1-2023 00:05	Flow 1 [kg/s]	0.02	0.01	0.08	0.13	0.23	0.02
1-1-2023 00:05	Flow 1 [kg/s]	0.02	0.01	0.08	0.13	0.23	0.02
1-1-2023 00:05	Flow 1 [kg/s]	0.02	0.01	0.08	0.13	0.23	0.02
1-1-2023 00:05	Flow 1 [kg/s]	0.02	0.01	0.08	0.13	0.23	0.02
1-1-2023 00:05	Flow 1 [kg/s]	0.01	0.01	0.08	0.13	0.23	0.02
1-1-2023 00:06	Flow 1 [kg/s]	0.01	0.01	0.07	0.13	0.22	0.02
1-1-2023 00:06	Flow 1 [kg/s]	0.01	0.01	0.07	0.13	0.22	0.02
1-1-2023 00:06	Flow 1 [kg/s]	0.01	0.01	0.07	0.13	0.22	0.02
1-1-2023 00:06	Flow 1 [kg/s]	0.01	0.01	0.07	0.13	0.22	0.02
1-1-2023 00:06	Flow 1 [kg/s]	0.01	0.01	0.07	0.13	0.22	0.02
1-1-2023 00:06	Flow 1 [kg/s]	0.01	0.01	0.07	0.13	0.22	0.02
1-1-2023 00:06	Flow 1 [kg/s]	0.01	0.01	0.07	0.12	0.21	0.02
1-1-2023 00:06	Flow 1 [kg/s]	0.01	0.01	0.07	0.12	0.21	0.02
1-1-2023 00:06	Flow 1 [kg/s]	0.01	0.01	0.07	0.12	0.21	0.02
Max all flows				0.40	0.37	0.97	0.21

Appendix F – Floor plans of De Cavaliere

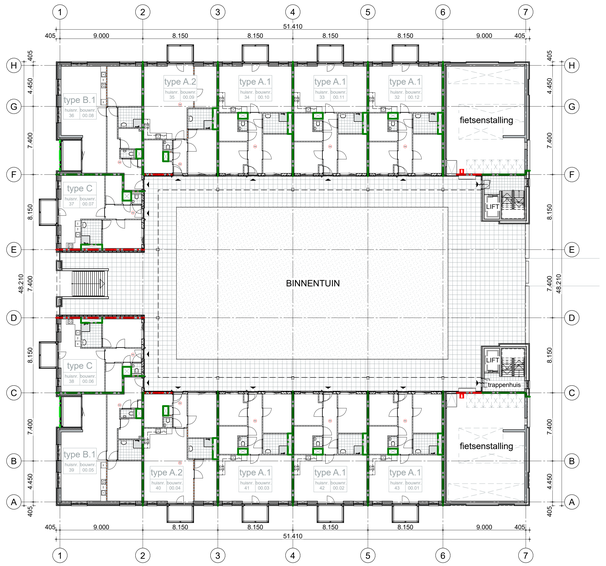

00 BEGANE GROND
3.100mm+ PEIL
+20,90m NAP

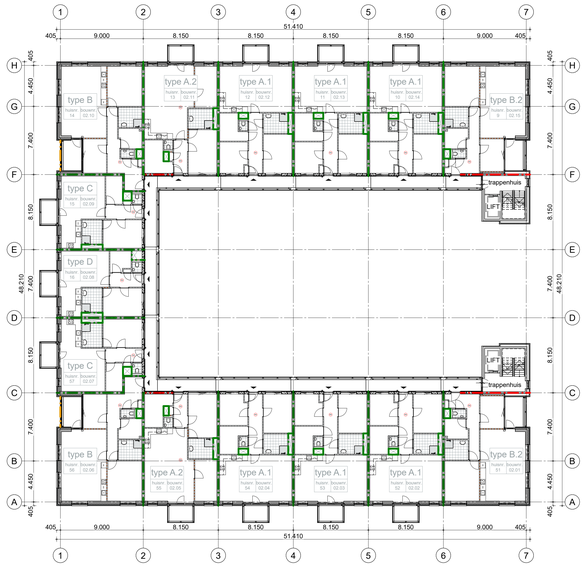

02 TWEEDE VERDIEPING
9.100+ PEIL
+26,90 NAP

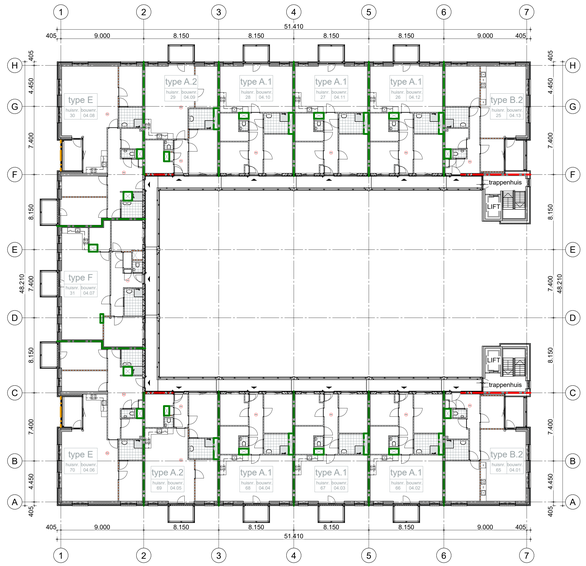

04 VIERDE VERDIEPING
15.100+ PEIL
+32,90 NAP

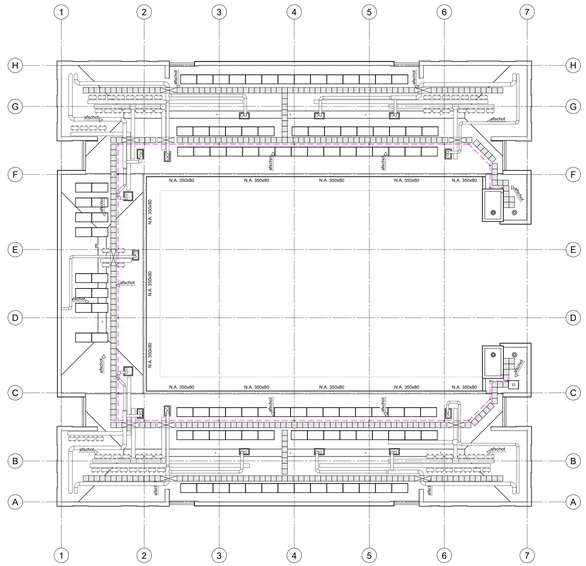

05 DAKOVERZICHT
18.000+ PEIL
+35,80 NAP

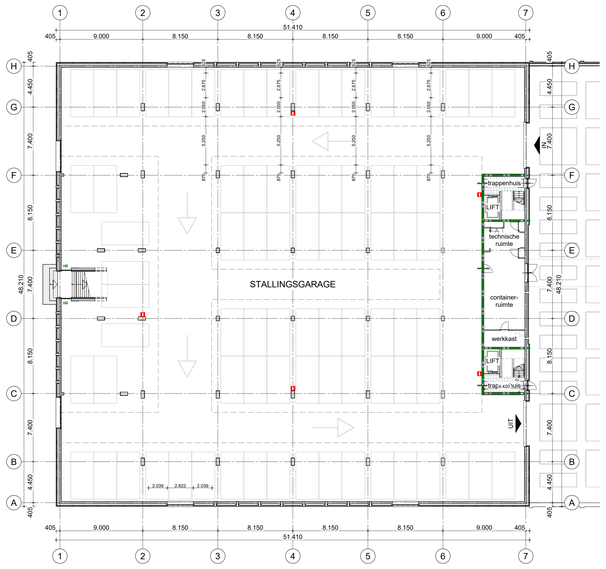

-1 STALLINGSGARAGE
PEIL = 0
+17,80m NAP

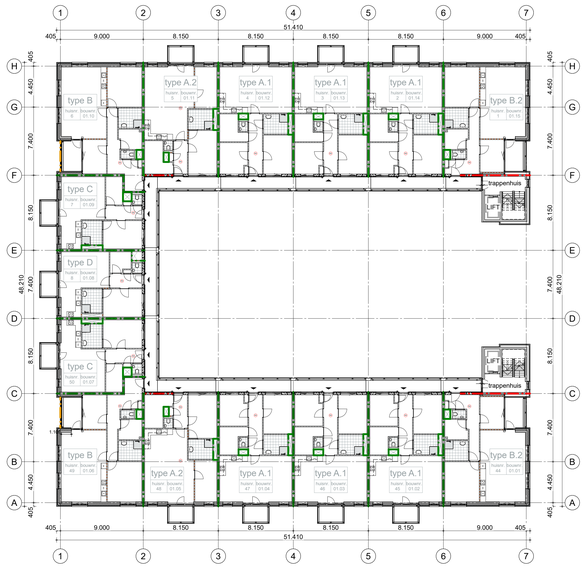

01 EERSTE VERDIEPING
6.100+ PEIL
+23,90m NAP

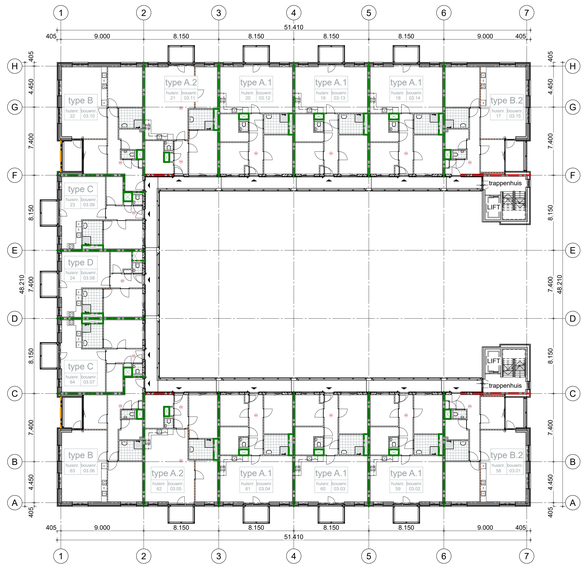

03 DERDE VERDIEPING
12.100+ PEIL
+29,90 NAP

RENVOOI

algemeen
PEIL = 0 = 16.250+NAP
bakstenen
bakstenen
kalkzandsteen
isolatie
cellenbeton G4/600
cellenbeton G5/600
h.w. gewiert beton
prefab beton
wandhegels, afm. vlgs. TO
vloerhegels, afm. vlgs. TO
HSB-wand vlgs. opgave leverancier, t.v. gevelbepleiting

brandveiligheid
zelfsluitende deur
zelfsluitende deur 30 min. WBDBO
zelfsluitende deur 60 min. WBDBO rookklasse S200
brandscheiding 30 min. WBDBO
brandscheiding 60 min. WBDBO
30 min. WBDBO
onderste 90cm: 30 min. brandwerende voorziening
60 min. WBDBO
onderste 90cm: 60 min. brandwerende voorziening
120 min. WBDBO
brandblusser
Specificatie vlgs. rapport brandveiligheid GBB
Alle schachtwt 60 min. brandwerend uitvoeren.

annotaties en symbolen
MK meterkast
KT kookkoeiwtel (opstelplaats)
KK koelkast (opstelplaats)
VW vaatwasser (opstelplaats)
WM wasmachine (opstelplaats)
WD wasdroger (opstelplaats)
vlt. vlaktedekking
h.w. hanwtelverdiover
rookmelder op schriftwt volgens NEN2555
bellentrekkwu
deur o.v. parkeeluitlcing. Deur is te openen wanneer de vluchtrichting zonder sleutel
pedtraat op steenniveau tw plaatse (vloerpeil is 0.k. afgewerkte vloer)
+33,615 pedtraat op gewelv / doorsneden
dh. 930 deurbreedte
dm. 910 dagmaat van kozijn
100-185-250 opbouw wand ddiles
loopdeur
WTW ventilatie unit
warmtepomp
NA nooddiafoon, positie volgens architect en afhwting volgens constructeur
aanlijnbeveiliging dak
afhwmepunt droge bluiledcing
vulpunt droge bluiledcing
kraan

annotaties en symbolen
type
Hoofdstr. Bouwstr.
appartement type, nummer en huisnummer
12 appartementnummer / bouwnummer
08 ruimtenummer
XXX ruimte omschrijving
0.00 vloeroppervlak in m²

Ditdatlies volgens nader advies, op te vragen door aannemer en ter goedkeuring architect.

Alle deuren min. vrije doorgang 850x2300, m.u.v. meterkasten of anders aangegeven.

Toegepast ventilatiesystem op basis van mechanische aan- en afvoer.

hoofdtrap: aantrede: 220 mm
optrede: 185,31 mm

vluchttrap: aantrede: 188 mm (looplijn)
optrede: 197,87 mm

balustrade: hoofdtrap vloer: 1000+mlwr
vluchttrap hoogte: 1000+mlwr
gelelrij: 1050+mlwr

WIJZIGINGEN	
A	- positie wastafel in badkamers type B, B1, B2 & E - indeling en installaties op het dak
B	
C	
D	

MAATVOERING VOORAF IN HET WERK TE CONTROLEREN
CONSTRUCTIEVE ONDERDELEN CONFORM OPGAVE CONSTRUCTEUR
KLEUREN VOLGENS KLEURENSCHEMA
ALLE INSTALLATIES CONFORM INSTALLATEUR
BRANDVEILIGHEIDSVOORZIENGEN CONFORM OPGAVE BRANDVEILIGHEIDSADVISEUR

N

DEFINITIEF

algemeen
Maatvoering in millimeters
Maatvoering voorraf in het werk te controleren. Niet meten vanaf tekening.

Constructieve onderdelen conform tekeningen en berekeningen contructeur.
Installaties conform tekeningen en berekeningen installateur.
Leidingverloop is indicatief, definitieve leidingverloop conform tekeningen en berekeningen E- en W- installateur(s)

Brandveiligheidsvoorzieningen conform opgave brandveiligheidsadviseur

Uitvoering van leveranciers gebonden onderdelen conform leveranciers, t.o.m. opdrachtgever / aannemer en architect

Afwijkende / overige zaken conform opdrachtgever / aannemer en ter goedkeuring architect.

metselwerk
- isgemaat metselwerk 62.50mm
- gemiddelde metselwerkdikte Muren: en materiaalstaat architect
- gevelparamelen = 100/2mm uitzetten op kozijnmaat
- dilitaties in het metselwerk conform adviseur/leverancier, op te vragen door aannemer en ter goedkeuring architect

LXARCHITECTEN

project :	**Waterburcht W7**	project nr.	**19.627**
tekening :	**Uitvoeringsgereed ontwerp**	fase - tekening nr.	**UO - 101**
onderdeel :	**Overzichtsplattegronden**	datum - inicialeur :	11-10-2021 MR
formaat :	**A0+ (1399 x 841)**	a:	22-10-2021 MR
schaal :	**1:200**	b:	10-11-2021 MR
		c:	
		d:	
		e:	
opdrachtgever :	**Van Wijnen Projectontwikkeling Zuid BV, Rosmalen**	f:	

Cacookade 3 - 5705 LA - Helmond - Tel +31 (0)492 52 44 27 **Postbus 66 - 5700 AB - Helmond**
internet : www.lxcprchitecten.nl e-mail : info@lxcprchitecten.nl

© 2021 LXarchitecten BV Alle rechten op deze tekening en/of gebruik van deze tekening zijn uitsluitend toegestaan aan de opdrachtgever volgens de overeenkomst van uitvoering van de opdracht. Elk ander gebruik is ook voor de opdrachtgever niet toegestaan zonder voorafgaande schriftelijke toestemming van de ontwerper / auteur.

A0+

Appendix G – Reports on the (de)pressurization tests by K+ Adviesgroep

Metingen Waterburcht W7 Helmond
Luchtdichtheid

Rapportnummer: Rm230112aaA0

K+ ADVIESGROEP

Opdrachtgever:	Van Wijnen Rosmalen B.V.	
	Heikampweg 6	5249 JX ROSMALEN
	Heikampweg 6	5240 AA ROSMALEN
	Tel.: 0735219014	
	Contactpersoon:	de heer R. Antoinissen

Adviseur:	K+ Adviesgroep	
	Jodenstraat 6	6101 AS ECHT
	Postbus 224	6100 AE ECHT
	Tel: 0475-470470	
	E-mail: info@k-plus.nl	
	Behandeld door:	Dhr. J. Hanssen

Datum	:	19-04-2023
Referentie	:	Rm230112aaA0.joha_01

Inhoud

1	Inleiding	4
2	Eisen en definities	5
3	Meetmethode en meerapparatuur	6
4	Meetresultaten	8
5	Conclusies en luchtlekkages	9

Bijlagen:

Bijlage I: Meetresultaten bouwkavel 3.04

Bijlage II: Meetresultaten bouwkavel 3.06

Bijlage III: Meetresultaten bouwkavel 4.05

1 INLEIDING

In opdracht van Van Wijnen Rosmalen B.V. is op 31 maart 2023 bij drie appartementen van het project Waterburcht W7 te Helmond een luchtdichtheidsmeting uitgevoerd. Doel van deze meting is inzicht te verkrijgen in de mate van luchtdoorlatendheid van de betreffende woningen. Hiertoe is de luchtvolumestroom door de gebouwschil bij een drukverschil van 10 Pa ($q_{v;10}$) bepaald.

De gemeten waarde zal gebruikt worden om te controleren of de geteste woning voldoet aan de gestelde waarde voor infiltratie conform de EPC-berekeningen wordt behaald.

De metingen zijn verricht bij bouwkavel 3.04, 3.06 en 4.05.

2 EISEN EN DEFINITIES

De luchtdoorlatendheid is de eigenschap van een gebouwschil om lucht door te laten, indien hierover een luchtdrukverschil aanwezig is. Deze luchtdoorlatendheid wordt uitgedrukt in een luchtvolumestroom bij een bepaald drukverschil $q_{v;10}$ in dm³/s. Door middel van een meting wordt de druk/volumestroom-karakteristiek van de gebouwschil bepaald, waaruit de $q_{v;10}$ waarde kan worden afgeleid.

Voor het onderhavige project geldt een $q_{v;10} \leq 0{,}400$ $dm^3/s.m^2$.

3 MEETMETHODE EN MEERAPPARATUUR

De metingen zijn uitgevoerd volgens de voorschriften van de Europese NEN-EN 13829 (Meetmethode A), NEN 2686, NEN-EN-ISO 9972:2015 en de SKH-beoordelingsgrondslag 13-01 LUCHTDICHTHEIDSMETINGEN, en verwerkt volgens de voorschriften van deze documenten.

Bij de meting is gebruik gemaakt van een Retrotec 6000 PH600423 Automated Blower Door Systeem. Dit systeem is ter plaatse van de voordeuren geïnstalleerd.

Blowerdoorsysteem Retrotec 6000

Voorafgaand aan de metingen zijn de lekverliezen via de installatietechnische componenten zoveel mogelijk geëlimineerd door de ventilatiecomponenten af te dichten met ballonnen of plaktape. Sifons en andere waterafvoeren zijn afgeplakt gezien de woningen nog niet beschikte over water. Binnendeuren binnen de te meten zone waren nog niet geplaatst tijdens de meting. Op deze wijze zijn enkel de luchtlekkages via de bouwkundige uitwendige schil gemeten.

In tabel 1 is de tijdens de meting heersende omstandigheden weergegeven:

Atmosferische temperatuur	+/- 13,0°C
Ruimtetemperatuur woningen	+/- 13,0°C
Relatieve luchtvochtigheid buiten	+/- 87%
Relatieve luchtvochtigheid binnen	+/- 50%
Windkracht	2 Bft

Tabel 1: Omstandigheden tijdens de luchtdichtheidsmeting bij benadering

4 MEETRESULTATEN

Het drukverschil over de gevel van het gebouw voor aanvang en na afloop van de meting was niet groter dan 5 Pascal.

Met behulp van de gebruiksoppervlakte is de waarde ten behoeve van de EPC ($q_{v;10;kar}$ [dm³/s.m²]) bepaald. In tabel 2 is deze waarde vermeld.

Meetconfiguratie	$q_{v;10}$ eis [dm³/s·m²]	$q_{v;10}$ gemeten [dm³/s·m²]
Bouwkavel 3.04	0,400	0,215
Bouwkavel 3.06	0,400	0,295
Bouwkavel 4.05	0,400	0,371

Tabel 2: Meetresultaten luchtdichtheidsmetingen

5 CONCLUSIES EN LUCHTLEKKAGES

Op basis van de meetresultaten kan worden geconcludeerd dat de uitwendige scheidingsconstructie van alle tien de bouwkavels voldoet aan de in de EPC berekening gehanteerde $q_{v;10}$ waarde van 0,400 $dm^3/s.m^2$.

Bijlage I

Meetresultaten bouwnummer 3.04

Luchtdoorlaatbaarheidstest

Opgesteld volgens de Europese Norm EN13829, de NEN 2686 en de BeoordelingsGrondSlag van SKH

Adres gebouw:	Type 3.04
Client:	Van Wijnen
Test-technicus:	J.Hanssen
Test-datum:	2023-03-31
Computerbestand:	LDH type 3.04 - onderdruk

Overzicht

retrotec **FanTestic**	version: **5.14.30**	Test-bedrijf: **K+ Adviesgroep bv**
Test-datum: **2023-03-31**	Test-technicus: **J.Hanssen**	
Opdrachtgever:	**Van Wijnen**	
Adres gebouw: **Type 3.04**		

Bouwdetails	
Kenmerk:	**LDH type 3.04 - onderdruk**
Vloeroppervlak – G.O. [m²]:	**96**
Nauwkeurigheid van de gebouwafmetingen	**0%**

Resultaten	
Luchtdebiet bij 10 Pa, Q_{10} [L/s]	**20,670**
Luchtdebiet bij 10 Pa, Qv_{10} [L/s]	**20,670**
Luchtdoorlaatbaarheid bij 10 Pa, $Qv_{10}kar$ [L/s/m²]	**0,2153**
Effective leakage area at 10 Pa, A_L [cm²]	**50,72**
Equivalent leakage area at 10 Pa, A_L [cm²]	**83,15**

Test omschrijving en Qv_{10} waarde

Tijdens deze test is de blower opgesteld in de en zijn de doorvoeringen van de naar buiten toe afgeplakt. De meetmethode is een type A meting waarbij de woning bouwkundig gereed is voor oplevering en volledig is afgewerkt en er geen doorvoeringen door de luchtdichte- schil zullen worden aangebracht.

De apparatuur voor deze luchtdichtheidsmetingen zal haar waardes weergeven in M³ per uur en indien deze moet worden omgerekend naar dm³/s of L/s zal deze gedeeld moeten worden met het getal 3.6.
Voor de zuiverheid van deze meting is een test uitgevoerd op onder en overdruk en is hiervan een gemiddelde waarde genomen .
Het werkelijke lekverlies =(Qv_{10}) van deze woning bedraagt **20,670 L/s**, $Qv_{10}kar$ = **0,2153 L/s/m²** en zou hiermee aan de gestelde eis uit de EP berekening van L/s.

Bespreking van de resultaten

	Resultaten	95% betrouwbaarheidsinterval		Onzekerheid
Luchtdebiet bij 10 Pa, Q_{10} [L/s]	20,670	19,585	21,821	+/-5,4%
Luchtdebiet bij 10 Pa, Qv_{10} [L/s]	20,670	19,585	21,821	+/-5,4%
Luchtdoorlaatbaarheid 10 Pa, Qv_{10} kar [L/s/m²]	0,2153	0,204	0,227	+/-5,4%
Effective leakage area at 10 Pa, A_L [cm²]	50,72	48,05	53,54	+/-5,6%
Equivalent leakage area at 10 Pa, A_L [cm²]	83,15	78,77	87,77	+/-5,4%

Appendix– Testgegevens

Milieu-omstandigheden		
Windsnelheid:	2. lichte wind	voor
Operator Location:	Binnen	
Initiële Bias Pressure:	0,50 Pa	
Finale Bias Pressure:	-0,30 Pa	
Average Bias Pressure	0,1 Pa	
Initiële temperatuur:	binnen: 12 C	buiten: 18 C
Finale temperatuur:	binnen: 12 C	buiten: 18 C
Barometrische druk	101,325 kPa	voor Directe meting

Onderdruk (1) testresultaten				
Correlatie, r [%]:	99,885			
	resultaten	95% betrouwbaarheid		Onzekerheid
		Lower	Upper	
Slope, n:	0,756	0,72347	0,78826	
Doorlaatbaarheid gebouwschil, C_{env} [L/s/Pa^n]:	3,6207	3,189	4,110	
Doorlaatbaarheid gebouwschil, C_L [L/s/Pa^n]:	3,6267	3,195	4,117	
Luchtdebiet bij 10 Pa, Q_{10} [L/s]	20,672	19,58	21,82	+/-5,4%
Luchtdoorlaatbaarheid 10 Pa, [L/s/m²]	0,21533	0,2037	0,2270	+/-5,4%
Effective leakage area at 10 Pa, A_L [cm²]	50,72	48,05	53,54	+/-5,6%
Equivalent leakage area at 10 Pa, A_L [cm²]	83,15	78,77	87,77	+/-5,4%

Inbegr druk [Pa]		-15,4	-25,5	-35,6	-44,6	-54,5	-65,4	-74,8	-85,7	-95,3
Induced Pressure [Pa]		-15,5	-25,6	-35,7	-44,7	-54,6	-65,5	-74,9	-85,8	-95,4
#1, Range B74	Ventilator druk [Pa]	77,9	154,0	229,0	360,5					
	Stroom [L/s]	28,32	42,08	52,51	66,82					
#1, Range B1	Ventilator druk [Pa]					149,5	192,0	223,5	276,0	338,5
	Stroom [L/s]					74,35	85,08	92,05	102,8	114,2
Stroom, V_r [L/s]		28,3228	42,0797	52,5089	66,8211	74,3494	85,0817	92,0497	102,763	114,159
Gecorrigeerd stroom, V_{env} [L/s]		28,460	42,284	52,763	67,145	74,710	85,494	92,496	103,26	114,71
Fout [%]		-1,0%	0,7%	-2,3%	4,9%	0,3%	0,1%	-2,2%	-1,4%	1,1%

12 meetpunten gedurende 0 s. (of the required 10 seconds).

3 natuurlijk drukverschil gedurende 0 s. (of required 10 seconds).

Average Baseline, ΔP: 0,1 Pa

Bias gemiddelde druk:			
Average Baseline [Pa]	ΔP 0,1		
initiële [Pa]	ΔP01 0,50	ΔP01- 0,00	ΔP01+ 0,50
finale [Pa]	ΔP02 -0,30	ΔP02- -0,30	ΔP02+ 0,00

Bias, de initiële [Pa]	0,50	0,50	0,50	0,50	0,50	0,50	0,50	0,50	0,50
Bias, finale [Pa]	-0,30	-0,30	-0,30	-0,30	-0,30	-0,30	-0,30	-0,30	-0,30

Gebouw Stroom Onderdruk (1) gegevens

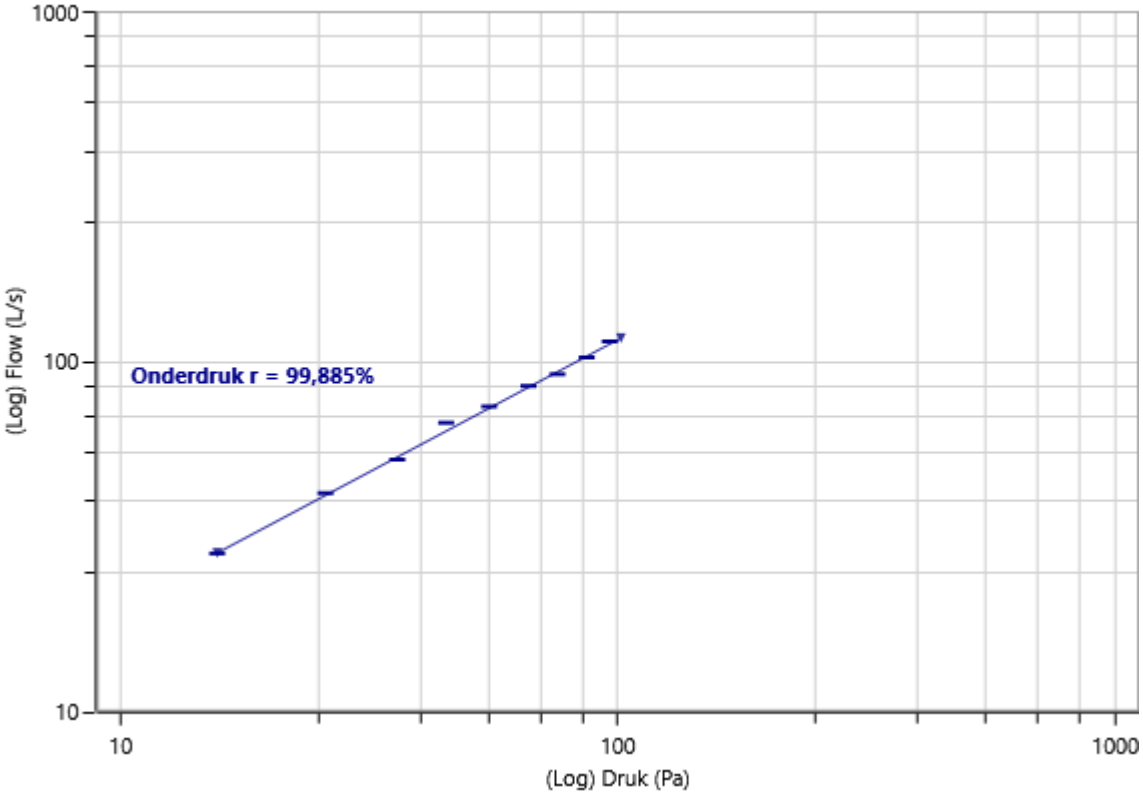

Gebouw Druk (Onderdruk (1) gegevens)

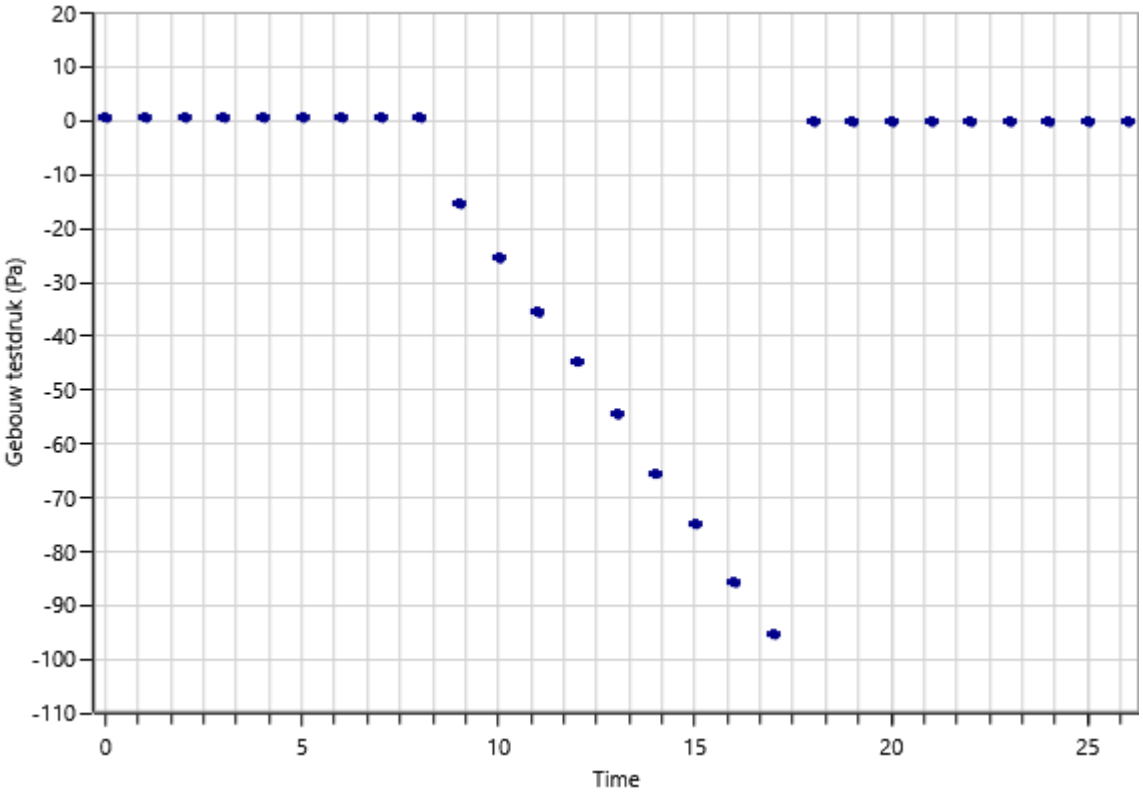

Gebruikte apparatuur

	Ventilatie	Ventilatie Serie #	Ventilatie location	Meter	Meter Serie #	Meter Calibration
#1	Retrotec 6000	PH600423		DM32		

kalibratiecertificaat Retrotec 6000:

Retrotec 6000 PH600423 Fan last calibrated: 2023-04-18 (ventilator kalibratie - PH600423B1) . Published Flow Equation Parameters, Round B1. CFM

Range	**n**	**K**	**K1**	**K2**	**K3**	**K4**	**MF**
Open	0,498	548	0	0,5	0	1	25
A	0,502	287	0	0,5	0	1	25
B8	0,54	113,25	0	0,8	0	1	40

Polynomial Range	**g**	**f**	**a**	**b**	**c**	**d**	**K2**	**MF**
B4	0	0,7	0,00000662	-0,0078	4,75	205	0,8	40
B2	40	0,85	0,000003	-0,0037	2,2	49	1	50
B1	65	0,2	0,00000106	-0,001382	0,96511	38,5	1	60
B74	25	0,15	0,000000796	-0,00095	0,59	18	0,8	35
B47	25	0,09	0,000000269	-0,0003591	0,2435	12,05	1	50
B29	25	-0,02	0,000000111	-0,000149	0,092	4,4	0,6	50

Fan Pressure (FP) is the measured fan pressure when using a self-referenced fan or when Room Pressure (RP) is negative. If using a fan which is not self-referenced, and Room Pressure is positive, Fan Pressure is calculated by subtracting the measured Room Pressure from the Absolute Value of the Fan Pressure.

If PrA>0 and fan is not self-referencing: FP = |PrB|-PrA
If PrA<0 or fan is self-referencing: FP = PrB

Flow calculations are not valid if Fan Pressure is less than either MF or (K2 x |RP|).

Flow in CFM using the above coefficients is calculated as follows for standard Ranges:

$$flow = (FP - (|RP| \times K1))^N \times (K + (K3 \times FP))$$

Flow in CFM using the above polynomial coefficients is calculated as follows:

$$flow = (a \times FP^3) + (b \times FP^2) + (c \times FP) + d + \big((g - |RP|) \times f\big)$$

Bijlage II

Meetresultaten bouwnummer 3.06

Luchtdoorlaatbaarheidstest

Opgesteld volgens de Europese Norm EN13829, de NEN 2686 en de BeoordelingsGrondSlag van SKH

Adres gebouw:	Type 3.06
Client:	Van Wijnen
Test-technicus:	J.Hanssen
Test-datum:	2023-03-31
Computerbestand:	LDH type 3.06 - onderdruk

Overzicht

retrotec **FanTestic**	version: **5.14.30**	Test-bedrijf: **K+ Adviesgroep bv**
Test-datum: **2023-03-31**	Test-technicus: **J.Hanssen**	
Opdrachtgever:	**Van Wijnen**	
Adres gebouw: **Type 3.06**		

Bouwdetails	
Kenmerk:	**LDH type 3.06 - onderdruk**
Vloeroppervlak – G.O. [m²]:	**102**
Nauwkeurigheid van de gebouwafmetingen	**0%**

Resultaten	
Luchtdebiet bij 10 Pa, Q_{10} [L/s]	**30,080**
Luchtdebiet bij 10 Pa, Qv_{10} [L/s]	**30,080**
Luchtdoorlaatbaarheid bij 10 Pa, $Qv_{10}kar$ [L/s/m²]	**0,2949**
Effective leakage area at 10 Pa, A_L [cm²]	**73,80**
Equivalent leakage area at 10 Pa, A_L [cm²]	**121,0**

Test omschrijving en Qv_{10} waarde

Tijdens deze test is de blower opgesteld in de en zijn de doorvoeringen van de naar buiten toe afgeplakt. De meetmethode is een type A meting waarbij de woning bouwkundig gereed is voor oplevering en volledig is afgewerkt en er geen doorvoeringen door de luchtdichte- schil zullen worden aangebracht.

De apparatuur voor deze luchtdichtheidsmetingen zal haar waardes weergeven in M³ per uur en indien deze moet worden omgerekend naar dm³/s of L/s zal deze gedeeld moeten worden met het getal 3.6.
Voor de zuiverheid van deze meting is een test uitgevoerd op onder en overdruk en is hiervan een gemiddelde waarde genomen .
Het werkelijke lekverlies =(Qv_{10}) van deze woning bedraagt **30,080 L/s**, $Qv_{10}kar$ = **0,2949 L/s/m²** en zou hiermee aan de gestelde eis uit de EP berekening van L/s.

Bespreking van de resultaten

	Resultaten	95% betrouwbaarheidsinterval		Onzekerheid
Luchtdebiet bij 10 Pa, Q_{10} [L/s]	30,080	28,325	31,940	+/-6,0%
Luchtdebiet bij 10 Pa, Qv_{10} [L/s]	30,080	28,325	31,940	+/-6,0%
Luchtdoorlaatbaarheid 10 Pa, Qv_{10} kar [L/s/m²]	0,2949	0,277	0,313	+/-6,0%
Effective leakage area at 10 Pa, A_L [cm²]	73,80	69,50	78,37	+/-6,2%
Equivalent leakage area at 10 Pa, A_L [cm²]	121,0	113,9	128,5	+/-6,0%

Appendix– Testgegevens

Milieu-omstandigheden		
Windsnelheid:	2. lichte wind	voor
Operator Location:	Binnen	
Initiële Bias Pressure:	1,30 Pa	
Finale Bias Pressure:	0,20 Pa	
Average Bias Pressure	0,75 Pa	
Initiële temperatuur:	binnen: 12 C	buiten: 18 C
Finale temperatuur:	binnen: 12 C	buiten: 18 C
Barometrische druk	101,325 kPa	voor Directe meting

Onderdruk (1) testresultaten				
Correlatie, r [%]:	99,770			
	resultaten	95% betrouwbaarheid		Onzekerheid
		Lower	Upper	
Slope, n:	0,622	0,58435	0,65990	
Doorlaatbaarheid gebouwschil, C_{env} [L/s/Pa^n]:	7,1617	6,202	8,270	
Doorlaatbaarheid gebouwschil, C_L [L/s/Pa^n]:	7,1803	6,218	8,292	
Luchtdebiet bij 10 Pa, Q_{10} [L/s]	30,079	28,33	31,94	+/-6,0%
Luchtdoorlaatbaarheid 10 Pa, [L/s/m²]	0,29489	0,2772	0,3126	+/-6,0%
Effective leakage area at 10 Pa, A_L [cm²]	73,80	69,50	78,37	+/-6,2%
Equivalent leakage area at 10 Pa, A_L [cm²]	121,0	113,9	128,5	+/-6,0%

Inbegr druk [Pa]		-10,5	-20,2	-29,6	-40,1	-49,7	-60,5	-70,9	-79,9	-89,7
Induced Pressure [Pa]		-11,3	-21,0	-30,4	-40,9	-50,5	-61,3	-71,7	-80,7	-90,5
#1, Range B74	Ventilator druk [Pa]	87,2	200,5	294,5						
	Stroom [L/s]	30,64	49,67	60,88						
#1, Range B1	Ventilator druk [Pa]				141,0	174,0	212,5	250,0	305,0	356,5
	Stroom [L/s]				73,18	81,76	90,73	98,54	109,2	118,0
Stroom, V_r [L/s]		30,6422	49,6681	60,8825	73,1783	81,7564	90,7325	98,5356	109,205	117,990
Gecorrigeerd stroom, V_{env} [L/s]		30,791	49,909	61,177	73,533	82,152	91,172	99,013	109,73	118,56
Fout [%]		-4,6%	5,0%	2,2%	2,1%	0,0%	-1,6%	-3,1%	-0,2%	0,4%

Bias gemiddelde druk:			
Average Baseline [Pa]	ΔP 0,75		
initiële [Pa]	ΔP01 1,30	ΔP01- 0,00	ΔP01+ 1,30
finale [Pa]	ΔP02 0,20	ΔP02- 0,00	ΔP02+ 0,20

Bias, de initiële [Pa]	1,30	1,30	1,30	1,30	1,30	1,30	1,30	1,30	1,30
Bias, finale [Pa]	0,20	0,20	0,20	0,20	0,20	0,20	0,20	0,20	0,20

Gebouw Stroom Onderdruk (1) gegevens

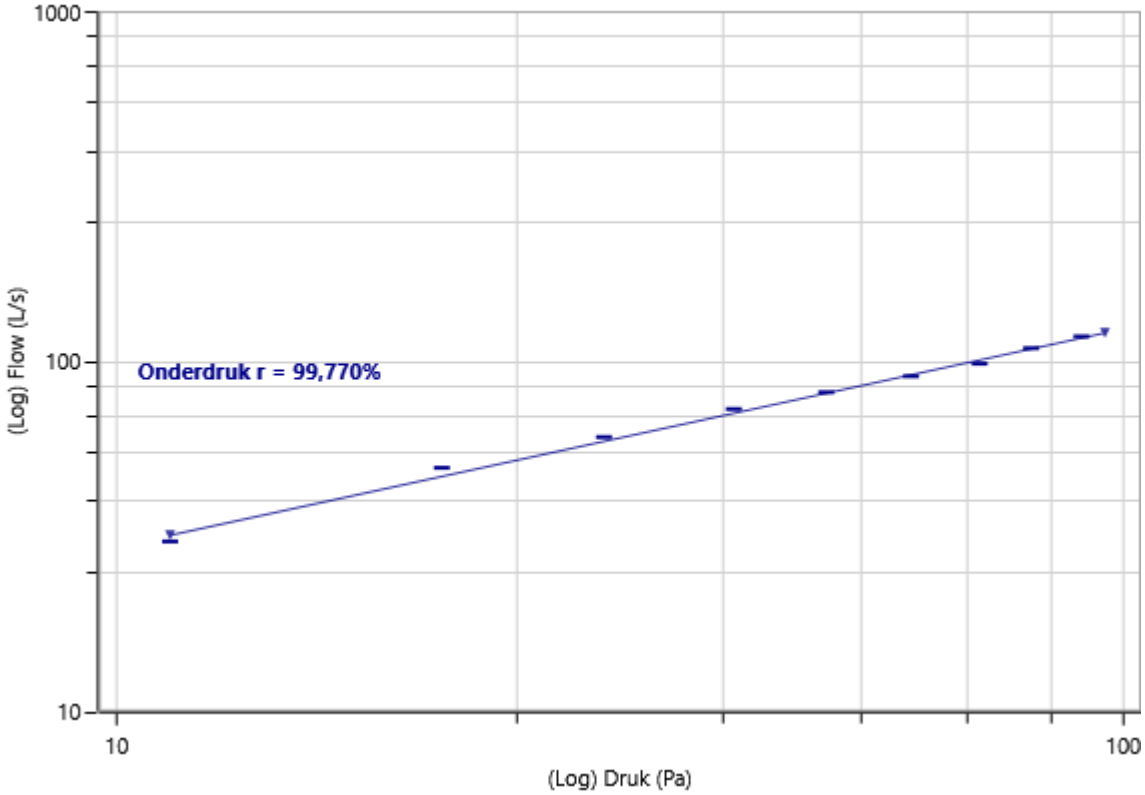

Gebouw Druk (Onderdruk (1) gegevens)

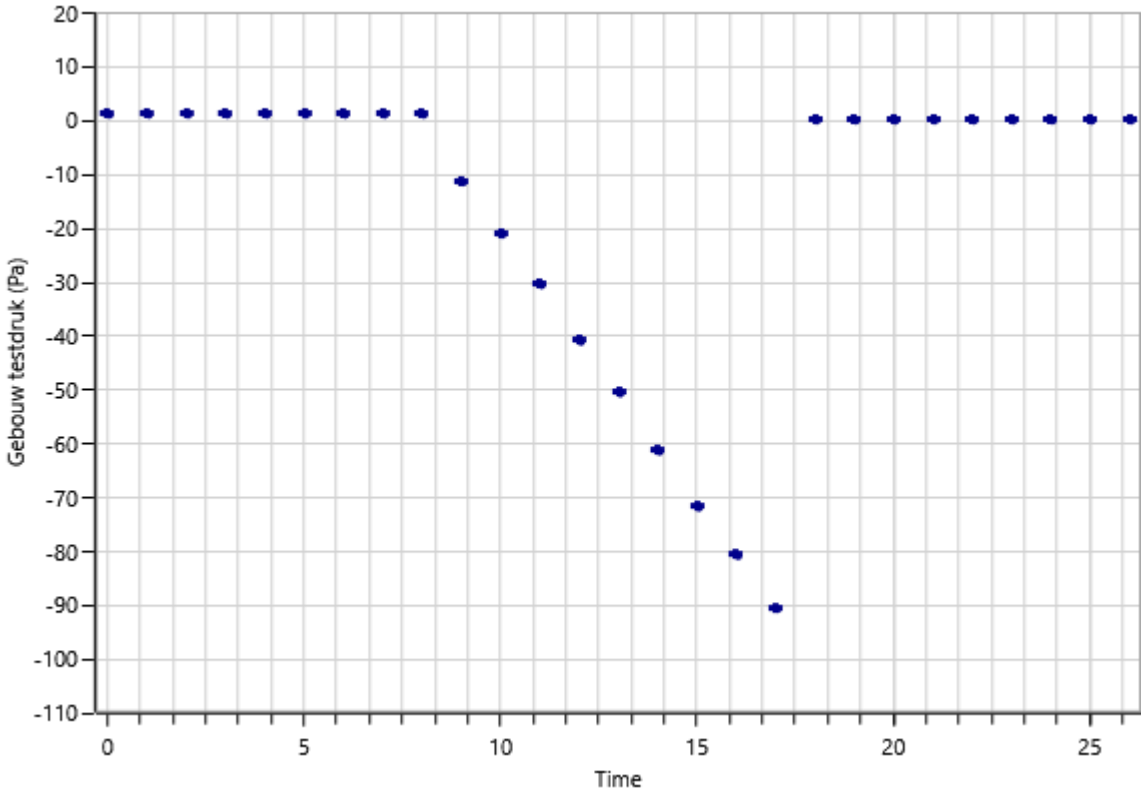

Gebruikte apparatuur

	Ventilatie	Ventilatie Serie #	Ventilatie location	Meter	Meter Serie #	Meter Calibration
#1	Retrotec 6000	PH600423		DM32		

kalibratiecertificaat Retrotec 6000:

Retrotec 6000 PH600423 Fan last calibrated: 2023-04-18 (ventilator kalibratie - PH600423B1) . Published Flow Equation Parameters. Round B1. CFM

Range	**n**	**K**	**K1**	**K2**	**K3**	**K4**	**MF**
Open	0,498	548	0	0,5	0	1	25
A	0,502	287	0	0,5	0	1	25
B8	0,54	113,25	0	0,8	0	1	40

Polynomial Range	**g**	**f**	**a**	**b**	**c**	**d**	**K2**	**MF**
B4	0	0,7	0,00000662	-0,0078	4,75	205	0,8	40
B2	40	0,85	0,000003	-0,0037	2,2	49	1	50
B1	65	0,2	0,00000106	-0,001382	0,96511	38,5	1	60
B74	25	0,15	0,000000796	-0,00095	0,59	18	0,8	35
B47	25	0,09	0,000000269	-0,0003591	0,2435	12,05	1	50
B29	25	-0,02	0,000000111	-0,000149	0,092	4,4	0,6	50

Fan Pressure (FP) is the measured fan pressure when using a self-referenced fan or when Room Pressure (RP) is negative. If using a fan which is not self-referenced, and Room Pressure is positive, Fan Pressure is calculated by subtracting the measured Room Pressure from the Absolute Value of the Fan Pressure.

If PrA>0 and fan is not self-referencing: FP = |PrB|-PrA
If PrA<0 or fan is self-referencing: FP = PrB

Flow calculations are not valid if Fan Pressure is less than either MF or (K2 x |RP|).

Flow in CFM using the above coefficients is calculated as follows for standard Ranges:

$$flow = (FP - (|RP| \times K1))^N \times (K + (K3 \times FP))$$

Flow in CFM using the above polynomial coefficients is calculated as follows:

$$flow = (a \times FP^3) + (b \times FP^2) + (c \times FP) + d + \big((g - |RP|) \times f\big)$$

Bijlage III

Meetresultaten bouwnummer 4.05

Luchtdoorlaatbaarheidstest

Opgesteld volgens de Europese Norm EN13829, de NEN 2686 en de BeoordelingsGrondSlag van SKH

Adres gebouw:	Type 4.05
Client:	Van Wijnen
Test-technicus:	J.Hanssen
Test-datum:	2023-03-31
Computerbestand:	LDH type 4.05 - onderdruk

Overzicht

retrotec **FanTestic**	version: **5.14.30**	Test-bedrijf: **K+ Adviesgroep bv**
Test-datum: **2023-03-31**	Test-technicus: **J.Hanssen**	
Opdrachtgever:	**Van Wijnen**	
Adres gebouw: **Type 4.05**		

Bouwdetails	
Kenmerk:	**LDH type 4.05 - onderdruk**
Vloeroppervlak – G.O. [m²]:	**96**
Nauwkeurigheid van de gebouwafmetingen	**0%**

Resultaten	
Luchtdebiet bij 10 Pa, Q_{10} [L/s]	**35,610**
Luchtdebiet bij 10 Pa, Qv_{10} [L/s]	**35,610**
Luchtdoorlaatbaarheid bij 10 Pa, $Qv_{10}kar$ [L/s/m²]	**0,3709**
Effective leakage area at 10 Pa, A_L [cm²]	**87,37**
Equivalent leakage area at 10 Pa, A_L [cm²]	**143,2**

Test omschrijving en Qv_{10} waarde

Tijdens deze test is de blower opgesteld in de en zijn de doorvoeringen van de naar buiten toe afgeplakt. De meetmethode is een type A meting waarbij de woning bouwkundig gereed is voor oplevering en volledig is afgewerkt en er geen doorvoeringen door de luchtdichte- schil zullen worden aangebracht.

De apparatuur voor deze luchtdichtheidsmetingen zal haar waardes weergeven in M³ per uur en indien deze moet worden omgerekend naar dm³/s of L/s zal deze gedeeld moeten worden met het getal 3.6.
Voor de zuiverheid van deze meting is een test uitgevoerd op onder en overdruk en is hiervan een gemiddelde waarde genomen .
Het werkelijke lekverlies =(Qv_{10}) van deze woning bedraagt **35,610 L/s**, $Qv_{10}kar$ = **0,3709 L/s/m²** en zou hiermee aan de gestelde eis uit de EP berekening van L/s.

Bespreking van de resultaten

	Resultaten	95% betrouwbaarheidsinterval		Onzekerheid
Luchtdebiet bij 10 Pa, Q_{10} [L/s]	35,610	34,215	37,055	+/-4,0%
Luchtdebiet bij 10 Pa, Qv_{10} [L/s]	35,610	34,215	37,055	+/-4,0%
Luchtdoorlaatbaarheid 10 Pa, Qv_{10} kar [L/s/m²]	0,3709	0,356	0,386	+/-4,0%
Effective leakage area at 10 Pa, A_L [cm²]	87,37	83,96	90,93	+/-4,1%
Equivalent leakage area at 10 Pa, A_L [cm²]	143,2	137,6	149,1	+/-4,0%

Appendix– Testgegevens

Milieu-omstandigheden		
Windsnelheid:	2. lichte wind	voor
Operator Location:	Binnen	
Initiële Bias Pressure:	-0,30 Pa	
Finale Bias Pressure:	-0,20 Pa	
Average Bias Pressure	-0,25 Pa	
Initiële temperatuur:	binnen: 12 C	buiten: 18 C
Finale temperatuur:	binnen: 12 C	buiten: 18 C
Barometrische druk	101,325 kPa	voor Directe meting

Onderdruk (1) testresultaten				
Correlatie, r [%]:	99,931			
	resultaten	95% betrouwbaarheid		Onzekerheid
		Lower	Upper	
Slope, n:	0,614	0,59102	0,63651	
Doorlaatbaarheid gebouwschil, C_{env} [L/s/Pa^n]:	8,6426	7,886	9,471	
Doorlaatbaarheid gebouwschil, C_L [L/s/Pa^n]:	8,6654	7,907	9,496	
Luchtdebiet bij 10 Pa, Q_{10} [L/s]	35,609	34,22	37,06	+/-4,0%
Luchtdoorlaatbaarheid 10 Pa, [L/s/m²]	0,37092	0,3561	0,3857	+/-4,0%
Effective leakage area at 10 Pa, A_L [cm²]	87,37	83,96	90,93	+/-4,1%
Equivalent leakage area at 10 Pa, A_L [cm²]	143,2	137,6	149,1	+/-4,0%

Inbegr druk [Pa]		-25,2	-34,5	-44,8	-55,1	-65,0	-75,1	-84,8	-93,7
Induced Pressure [Pa]		-25,0	-34,3	-44,6	-54,9	-64,8	-74,9	-84,6	-93,5
#1, Range B1	Ventilator druk [Pa]	99,2	151,5	194,5	254,5	309,0			
	Stroom [L/s]	61,18	76,82	87,67	101,0	111,4			
#1, Range B2	Ventilator druk [Pa]						134,5	158,0	178,5
	Stroom [L/s]						120,5	131,2	139,3
Stroom, V_r [L/s]		61,1803	76,8236	87,6747	101,026	111,398	120,550	131,195	139,332
Gecorrigeerd stroom, V_{env} [L/s]		61,477	77,196	88,099	101,52	111,94	121,13	131,83	140,01
Fout [%]		-1,2%	2,1%	-0,8%	0,6%	0,2%	-0,8%	0,1%	0,0%

Bias gemiddelde druk:			
Average Baseline [Pa]	ΔP -0,25		
initiële [Pa]	ΔP01 -0,30	ΔP01- -0,30	ΔP01+ 0,00
finale [Pa]	ΔP02 -0,20	ΔP02- -0,20	ΔP02+ 0,00

Bias, de initiële [Pa]	-0,30	-0,30	-0,30	-0,30	-0,30	-0,30	-0,30	-0,30
Bias, finale [Pa]	-0,20	-0,20	-0,20	-0,20	-0,20	-0,20	-0,20	-0,20

Gebouw Stroom Onderdruk (1) gegevens

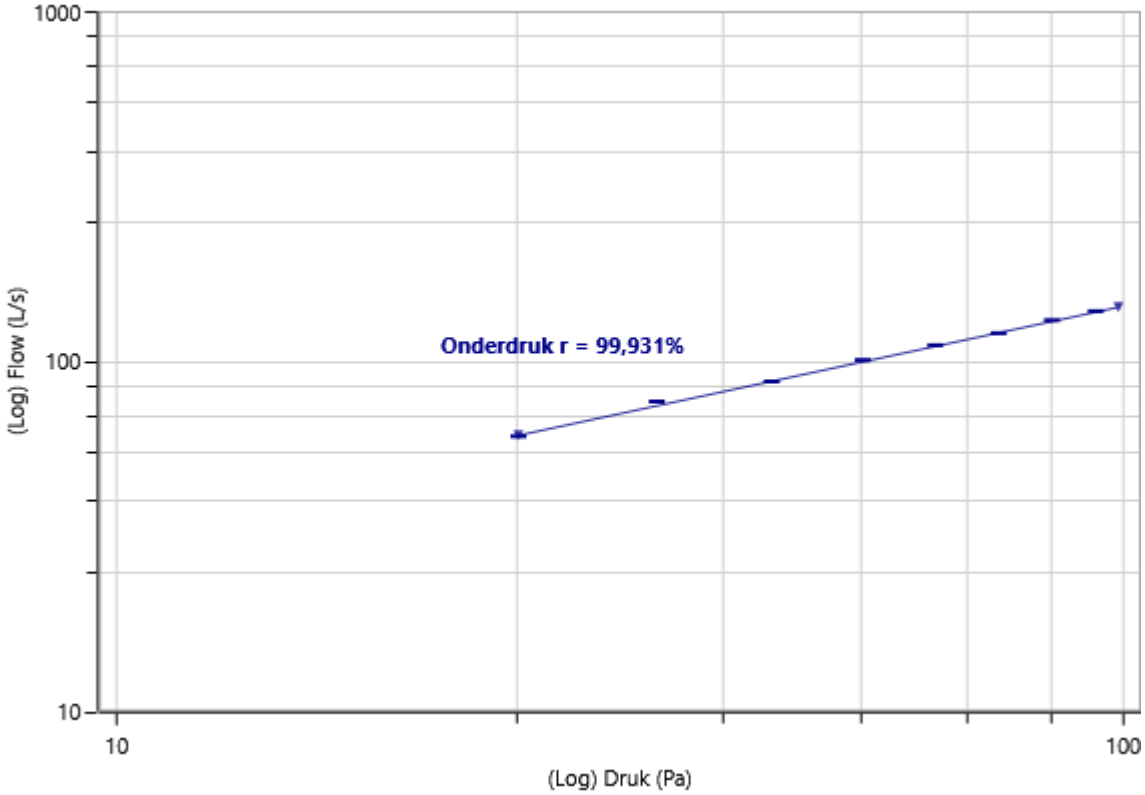

Gebouw Druk (Onderdruk (1) gegevens)

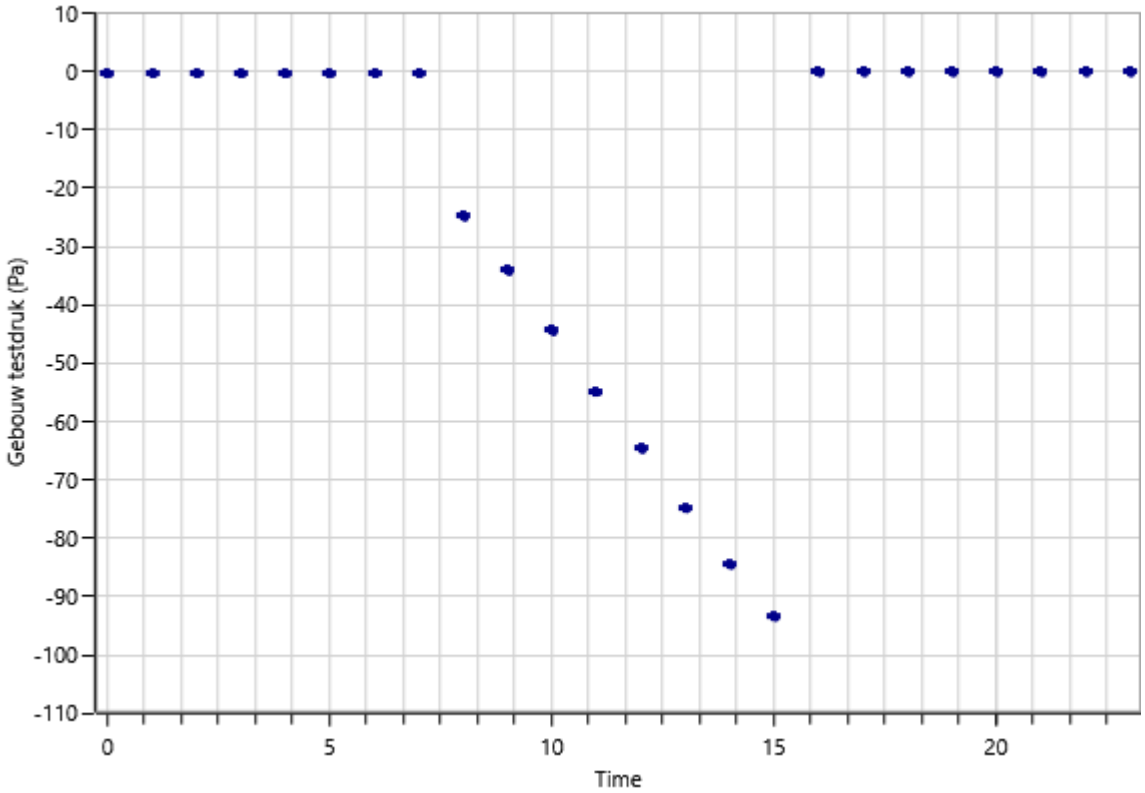

Gebruikte apparatuur

	Ventilatie	Ventilatie Serie #	Ventilatie location	Meter	Meter Serie #	Meter Calibration
#1	Retrotec 6000	PH600423		DM32		

kalibratiecertificaat Retrotec 6000:

Retrotec 6000 PH600423 Fan last calibrated: 2023-04-18 (ventilator kalibratie - PH600423B1) . Published Flow Equation Parameters. Round B1. CFM

Range	**n**	**K**	**K1**	**K2**	**K3**	**K4**	**MF**
Open	0,498	548	0	0,5	0	1	25
A	0,502	287	0	0,5	0	1	25
B8	0,54	113,25	0	0,8	0	1	40

Polynomial Range	**g**	**f**	**a**	**b**	**c**	**d**	**K2**	**MF**
B4	0	0,7	0,00000662	-0,0078	4,75	205	0,8	40
B2	40	0,85	0,000003	-0,0037	2,2	49	1	50
B1	65	0,2	0,00000106	-0,001382	0,96511	38,5	1	60
B74	25	0,15	0,000000796	-0,00095	0,59	18	0,8	35
B47	25	0,09	0,000000269	-0,0003591	0,2435	12,05	1	50
B29	25	-0,02	0,000000111	-0,000149	0,092	4,4	0,6	50

Fan Pressure (FP) is the measured fan pressure when using a self-referenced fan or when Room Pressure (RP) is negative. If using a fan which is not self-referenced, and Room Pressure is positive, Fan Pressure is calculated by subtracting the measured Room Pressure from the Absolute Value of the Fan Pressure.

If PrA>0 and fan is not self-referencing: FP = |PrB|-PrA
If PrA<0 or fan is self-referencing: FP = PrB

Flow calculations are not valid if Fan Pressure is less than either MF or (K2 x |RP|).

Flow in CFM using the above coefficients is calculated as follows for standard Ranges:

$$flow = (FP - (|RP| \times K1))^N \times (K + (K3 \times FP))$$

Flow in CFM using the above polynomial coefficients is calculated as follows:

$$flow = (a \times FP^3) + (b \times FP^2) + (c \times FP) + d + \big((g - |RP|) \times f\big)$$

Appendix H – Input CFAST for a fire scenario in apartment 3.04 (medium fire growth rate) and 4.05 (fast fire growth rate)

CFAST

Release Version : CFAST 7.7.3
Revision   : CFAST7.7.3-4-g0c33733b
Revision Date   : Thu May 12 10:19:24 2022 -0400
Compilation Date : Fri 05/13/2022 01:48 PM

Data file: C:\Users\n.kuiper\OneDrive - Peutz B.V\0. Afstudeerproject Nora\Casus\CFAST\CFAST_model_3.04.in
Title: CFAST Simulation

OVERVIEW

Compartments	Doors, ...	Ceil. Vents, ...	MV Connects
1	1	0	2

Simulation Time (s)	Output Interval (s)	Smokeview Interval (s)	Spreadsheet Interval (s)
400.00	10.00	5.00	5.00

AMBIENT CONDITIONS

Interior Temperature (C)	Interior Pressure (Pa)	Exterior Temperature (C)	Exterior Pressure (Pa)
20.	101325.	20.	101325.

THERMAL PROPERTIES

Name	Conductivity (kW/(m °C))	Specific Heat (kJ/(m °C))	Density (kg/m^3)	Thickness (m)	Emissivity
CONCRETE	2.00	840.	2.400E+03	0.150	0.940
DEFAULT	0.120	900.	800.	1.200E-02	0.900

COMPARTMENTS

Compartment	Name	Width (m)	Depth (m)	Height (m)	Floor Height (m)	Ceiling Height (m)	Shaft	Hall	Wall Leakage (m^2)	Floor Leakage (m^2)
1	Fire_apt	8.15	11.85	2.60	0.00	2.60			0.0	0.0

COMPARTMENT MATERIALS

Compartment	Name	Surface	Layer	Conductivity (kW/(m °C))	Specific Heat (kJ/(m °C))	Density (kg/m^3)	Thickness (m)	Emissivity	Material
1	Fire_apt	Ceiling	1	2.00	840.	2.400E+03	0.150	0.940	CONCRETE
		Walls	1	2.00	840.	2.400E+03	0.150	0.940	CONCRETE

VENT CONNECTIONS

Wall Vents (Doors, Windows, ...)

From Initial Compartment	To Initial Compartment	Vent Number	Width (m)	Sill Height (m)	Soffit Height (m)	Open/Close Type	Trigger Value (C/W/m^2)	Target	Final Time (s)	Final Fraction
Fire_apt	Outside	1	0.00	0.00	2.60	Time			0.00	1.00

There are no vertical natural flow connections

Mechanical Vents (Fans)

From Initial Compartment	To Initial Compartment	Fan Number	Area (m^2)	Flowrate (m^3/s)	Open/Close Type	Trigger Value (C/W/m^2)	Target	Initial Time (s)	Final Time (s)	Final Fraction
Outside	Fire_apt	1	0.01	0.02	Time			0.00	1.00	0.00
Fire_apt	Outside	2	0.01	0.02	Time			0.00	1.00	0.00

VENT RAMPS

There are no vent opening ramp specifications

FIRES

Name: New Fire 1 Referenced as object # 1 Normal fire

Compartment	Fire Type	Time to Flaming	Position (x,y,z)			Relative Humidity	Lower O2 Limit	Radiative Fraction
Fire_apt	Constrained	0.0	2.50	5.00	0.00	50.0	15.00	0.35

Chemical formula of the fuel

Carbon	Hydrogen	Oxygen	Nitrogen	Chlorine
4.000	6.000	3.000	0.000	0.000

Time (s)	Mdot (kg/s)	Hcomb (J/kg)	Qdot (W)	Zoffset (m)	Soot (kg/kg)	CO (kg/kg)	HCN (kg/kg)	HCl (kg/kg)	TS (kg/kg)
0.	0.0	1.75E+07	0.0	0.0	1.00E-02	4.00E-02	0.0	0.0	0.0
30.	2.29E-03	1.75E+07	4.00E+04	0.0	1.00E-02	4.00E-02	0.0	0.0	0.0
60.	9.14E-03	1.75E+07	1.60E+05	0.0	1.00E-02	4.00E-02	0.0	0.0	0.0
90.	2.06E-02	1.75E+07	3.60E+05	0.0	1.00E-02	4.00E-02	0.0	0.0	0.0
120.	3.66E-02	1.75E+07	6.40E+05	0.0	1.00E-02	4.00E-02	0.0	0.0	0.0
150.	5.71E-02	1.75E+07	1.00E+06	0.0	1.00E-02	4.00E-02	0.0	0.0	0.0
180.	8.23E-02	1.75E+07	1.44E+06	0.0	1.00E-02	4.00E-02	0.0	0.0	0.0
210.	0.11	1.75E+07	1.96E+06	0.0	1.00E-02	4.00E-02	0.0	0.0	0.0
240.	0.15	1.75E+07	2.56E+06	0.0	1.00E-02	4.00E-02	0.0	0.0	0.0
270.	0.19	1.75E+07	3.24E+06	0.0	1.00E-02	4.00E-02	0.0	0.0	0.0
300.	0.23	1.75E+07	4.00E+06	0.0	1.00E-02	4.00E-02	0.0	0.0	0.0
900.	0.23	1.75E+07	4.00E+06	0.0	1.00E-02	4.00E-02	0.0	0.0	0.0
930.	0.19	1.75E+07	3.24E+06	0.0	1.00E-02	4.00E-02	0.0	0.0	0.0
960.	0.15	1.75E+07	2.56E+06	0.0	1.00E-02	4.00E-02	0.0	0.0	0.0
990.	0.11	1.75E+07	1.96E+06	0.0	1.00E-02	4.00E-02	0.0	0.0	0.0
1020.	8.23E-02	1.75E+07	1.44E+06	0.0	1.00E-02	4.00E-02	0.0	0.0	0.0
1050.	5.71E-02	1.75E+07	1.00E+06	0.0	1.00E-02	4.00E-02	0.0	0.0	0.0
1080.	3.66E-02	1.75E+07	6.40E+05	0.0	1.00E-02	4.00E-02	0.0	0.0	0.0

1110.	2.06E-02	1.75E+07	3.60E+05	0.0	1.00E-02	4.00E-02	0.0	0.0	0.0
1140.	9.14E-03	1.75E+07	1.60E+05	0.0	1.00E-02	4.00E-02	0.0	0.0	0.0
1170.	2.29E-03	1.75E+07	4.00E+04	0.0	1.00E-02	4.00E-02	0.0	0.0	0.0
1200.	0.0	1.75E+07	0.0	0.0	1.00E-02	4.00E-02	0.0	0.0	0.0
1210.	0.0	1.75E+07	0.0	0.0	1.00E-02	1.00E-02	0.0	0.0	0.0

```
****************************
* Time =      0.0 seconds. *
****************************
```

Compartment	Upper Temp. (C)	Lower Temp (C)	Inter. Height (m)	Upper Vol (m^3)	Upper Absor (1/m)	Lower Absorb (1/m)	Pressure (Pa)
Fire_apt	20.00	20.00	2.600	2.51E-02(0%)	69.2	6.075E-02	0.00

FIRES

Compartment	Fire	Ign	Plume Flow (kg/s)	Pyrol Rate (kg/s)	Fire Size (W)	Flame Height (m)	Fire in Upper (W)	Fire in Lower (W)	Vent Fire (W)	Convec. (W)	Radiat. (kg)	Pyrolysate (kg)	Trace
	New Fire 1	Y	0.00	0.00	0.00	0.00	0.00	0.00	0.00	0.00	0.00	0.00	0.00

UPPER LAYER SPECIES

Compartment	N2 (%)	O2 (%)	CO2 (%)	CO (%)	HCN (%)	HCL (%)	TUHC (%)	H2O (%)	OD (1/m)	OD_F (1/m)	OD_S (1/m)	TS kg
Fire_apt	78.4	20.5	0.00	0.00	0.00	0.00	0.00	1.15	0.00	0.00	0.00	0.00

LOWER LAYER SPECIES

Compartment	N2 (%)	O2 (%)	CO2 (%)	CO (%)	HCN (%)	HCL (%)	TUHC (%)	H2O (%)	OD (1/m)	OD_F (1/m)	OD_S (1/m)	TS kg
Fire_apt	78.4	20.5	0.00	0.00	0.00	0.00	0.00	1.15	0.00	0.00	0.00	0.00

FLOW THROUGH VENTS (kg/s)

Vent	From/Bottom	To/Top	Opening Fraction	Flow relative to 'From' Upper Layer Inflow	Upper Layer Outflow	Lower Layer Inflow	Lower Layer Outflow	Flow Relative to 'To' Upper Layer Inflow	Upper Layer Outflow	Lower Layer Inflow	Lower Layer Outflow
H 1	Fire_apt	Outside	1.000								
M 1	Outside	Fire_apt	1.000					2.690E-02	2.690E-02		
M 2	Fire_apt	Outside	1.000					2.690E-02	2.690E-02		

TOTAL MASS FLOW THROUGH MECHANICAL VENTS (kg)

CFAST

Release Version : CFAST 7.7.3
Revision   : CFAST7.7.3-4-g0c33733b
Revision Date   : Thu May 12 10:19:24 2022 -0400
Compilation Date : Fri 05/13/2022 01:48 PM

Data file: C:\Users\n.kuiper\OneDrive - Peutz B.V\0. Afstudeerproject Nora\Casus\CFAST\CFAST_model_4.05_fast_v2ceilingleak.in
Title: CFAST Simulation

OVERVIEW

Compartments	Doors, ...	Ceil. Vents, ...	MV Connects
1	1	1	2

Simulation Time (s)	Output Interval (s)	Smokeview Interval (s)	Spreadsheet Interval (s)
400.00	10.00	5.00	5.00

AMBIENT CONDITIONS

Interior Temperature (C)	Interior Pressure (Pa)	Exterior Temperature (C)	Exterior Pressure (Pa)
20.	101325.	20.	101325.

THERMAL PROPERTIES

Name	Conductivity (kW/(m °C))	Specific Heat (kJ/(m °C))	Density (kg/m^3)	Thickness (m)	Emissivity
CONCRETE	2.00	840.	2.400E+03	0.150	0.940
DEFAULT	0.120	900.	800.	1.200E-02	0.900

COMPARTMENTS

Compartment	Name	Width (m)	Depth (m)	Height (m)	Floor Height (m)	Ceiling Height (m)	Shaft	Hall	Wall Leakage (m^2)	Floor Leakage (m^2)
1	Fire_apt	8.15	11.85	2.60	0.00	2.60			0.0	0.0

COMPARTMENT MATERIALS

Compartment	Name	Surface	Layer	Conductivity (kW/(m °C))	Specific Heat (kJ/(m °C))	Density (kg/m^3)	Thickness (m)	Emissivity	Material
1	Fire_apt	Ceiling	1	2.00	840.	2.400E+03	0.150	0.940	CONCRETE
		Walls	1	2.00	840.	2.400E+03	0.150	0.940	CONCRETE

VENT CONNECTIONS

Wall Vents (Doors, Windows, ...)

From Compartment	To Compartment	Vent Number	Width (m)	Sill Height (m)	Soffit Height (m)	Open/Close Type (m)	Trigger Value (C/W/m^2)	Target	Initial Time (s)	Initial Fraction	Final Time (s)	Final Fraction
Fire_apt	Outside	1	0.00	0.00	2.60	Time			0.00	1.00		

Ceiling and Floor Vents

Top Compartment	Bottom Compartment	Vent Number	Shape	Area (m^2)	Open/Close Type	Trigger Value (C/W/m^2)	Target	Initial Time (s)	Initial Fraction	Final Time (s)	Final Fraction
Outside	Fire_apt	1	Square	0.01	Time			0.00	1.00	0.00	1.00

Mechanical Vents (Fans)

From Compartment	To Compartment	Fan Number	Area (m^2)	Flowrate (m^3/s)	Open/Close Type	Trigger Value (C/W/m^2)	Target	Initial Time (s)	Initial Fraction	Final Time (s)	Final Fraction
Outside	Fire_apt	1	0.01	0.02	Time			0.00	1.00	0.00	1.00
Fire_apt	Outside	2	0.01	0.02	Time			0.00	1.00	0.00	1.00

VENT RAMPS

There are no vent opening ramp specifications

FIRES

Name: New Fire 2 Referenced as object # 1 Normal fire

Compartment	Fire Type	Time to Flaming	Position (x,y,z)			Relative Humidity	Lower O2 Limit	Radiative Fraction
Fire_apt	Constrained	0.0	4.08	5.92	0.00	50.0	15.00	0.35

Chemical formula of the fuel

Carbon	Hydrogen	Oxygen	Nitrogen	Chlorine
4.000	6.000	3.000	0.000	0.000

Time (s)	Mdot (kg/s)	Hcomb (J/kg)	Qdot (W)	Zoffset (m)	Soot (kg/kg)	CO (kg/kg)	HCN (kg/kg)	HCl (kg/kg)	TS (kg/kg)
0.	0.0	1.75E+07	0.0	0.0	1.00E-02	4.00E-02	0.0	0.0	0.0
15.	2.29E-03	1.75E+07	4.00E+04	0.0	1.00E-02	4.00E-02	0.0	0.0	0.0
30.	9.14E-03	1.75E+07	1.60E+05	0.0	1.00E-02	4.00E-02	0.0	0.0	0.0
45.	2.06E-02	1.75E+07	3.60E+05	0.0	1.00E-02	4.00E-02	0.0	0.0	0.0
60.	3.66E-02	1.75E+07	6.40E+05	0.0	1.00E-02	4.00E-02	0.0	0.0	0.0

75.	5.71E-02	1.75E+07	1.00E+06	0.0	1.00E-02	4.00E-02	0.0	0.0	0.0
90.	8.23E-02	1.75E+07	1.44E+06	0.0	1.00E-02	4.00E-02	0.0	0.0	0.0
105.	0.11	1.75E+07	1.96E+06	0.0	1.00E-02	4.00E-02	0.0	0.0	0.0
120.	0.15	1.75E+07	2.56E+06	0.0	1.00E-02	4.00E-02	0.0	0.0	0.0
135.	0.19	1.75E+07	3.24E+06	0.0	1.00E-02	4.00E-02	0.0	0.0	0.0
150.	0.23	1.75E+07	4.00E+06	0.0	1.00E-02	4.00E-02	0.0	0.0	0.0
450.	0.23	1.75E+07	4.00E+06	0.0	1.00E-02	4.00E-02	0.0	0.0	0.0
465.	0.19	1.75E+07	3.24E+06	0.0	1.00E-02	4.00E-02	0.0	0.0	0.0
480.	0.15	1.75E+07	2.56E+06	0.0	1.00E-02	4.00E-02	0.0	0.0	0.0
495.	0.11	1.75E+07	1.96E+06	0.0	1.00E-02	4.00E-02	0.0	0.0	0.0
510.	8.23E-02	1.75E+07	1.44E+06	0.0	1.00E-02	4.00E-02	0.0	0.0	0.0
525.	5.71E-02	1.75E+07	1.00E+06	0.0	1.00E-02	4.00E-02	0.0	0.0	0.0
540.	3.66E-02	1.75E+07	6.40E+05	0.0	1.00E-02	4.00E-02	0.0	0.0	0.0
555.	2.06E-02	1.75E+07	3.60E+05	0.0	1.00E-02	4.00E-02	0.0	0.0	0.0
570.	9.14E-03	1.75E+07	1.60E+05	0.0	1.00E-02	4.00E-02	0.0	0.0	0.0
585.	2.29E-03	1.75E+07	4.00E+04	0.0	1.00E-02	4.00E-02	0.0	0.0	0.0
600.	0.0	1.75E+07	0.0	0.0	1.00E-02	4.00E-02	0.0	0.0	0.0
610.	0.0	1.75E+07	0.0	0.0	1.00E-02	4.00E-02	0.0	0.0	0.0

```
****************************
* Time =      0.0 seconds. *
****************************
```

Compartment	Upper Temp. (C)	Lower Temp (C)	Inter. Height (m)	Upper Vol (m^3)	Upper Absor (1/m)	Lower Absorb (1/m)	Pressure (Pa)
Fire_apt	20.00	20.00	2.600	2.51E-02(0%)	69.2	6.075E-02	0.00

FIRES

Compartment	Fire	Ign	Plume Flow (kg/s)	Pyrol Rate (kg/s)	Fire Size (W)	Flame Height (m)	Fire in Upper (W)	Fire in Lower (W)	Vent Fire (W)	Convec. (W)	Radiat. (W)	Pyrolysate (kg)	Trace (kg)
	New Fire 2	Y	0.00	0.00	0.00	0.00				0.00	0.00	0.00	0.00

Appendix I – List of elements in CONTAM for the case study

Ambient			Species	CELLULOSE	
Ambient temperature	20	°C	Molar mass	180	kg/kmol
Absolute pressure	101325	Pa	Duffusion coefficient	2.00E-05	m²/s
Relative humidity	0	RH	Mean diameter	0	m²/s
Humiditity ratio	0	g(w)/kg (dry)	Effective density	0	kg/m³
Mass fraction (H2O)	0	kg (w)/kg (air)	Specific heat	1000	J/kgK
Wind speed	0	m/s	Decay rate	0	1/s
Wind direction	0	deg	UVGI Susceptibility constatnt	0	m²/J
Day type	1	(1-12)	Default concentration	0	kg/kg
			Trace contamintant	Trace	
			Use in simulation	Use	

Duct segments

	Level	Type		Shape	Length	Diameter	Maximum	Roughness	Leakage rate	dP static	schedule	Other
	#	-		-	m	m	m³/h	mm	L/s/m²	Pa	-	
1	Roof	Duct355mm ([	ODA	circle	0.2	0.355		0.09	0	1	None	
2	Downward	Duct355mm ("	ODA	circle	2.6	0.355		0.09	0	1	None	
3	Roof	Duct355mm	EHA	circle	0.2	0.355		0.09	0	1	None	
4	Downward	Duct355mm	EHA	circle	2.6	0.355		0.09	0	1	None	
5	Level 5	Duct125mm	SUP	circle	2.6	0.125		0.09	0	1	None	
6	Level 5	Duct125mm	SUP	circle	3.0	0.125		0.09	0	1	None	
7	Level 5	Duct125mm	SUP	circle	4.6	0.125		0.09	0	1	None	
8	Level 5	Duct125mm	ETA	circle	3.8	0.125		0.09	0	1	None	
9	Level 5	Duct125mm	SUP	circle	2.2	0.125		0.09	0	1	None	
10	Level 5	Duct125mm	ETA	circle	0.2	0.125		0.09	0	1	None	
11	Level 5	Duct125mm	ETA	circle	2.2	0.125		0.09	0	1	None	
12	Level 5	Duct125mm	SUP	circle	1.8	0.125		0.09	0	1	None	
13	Level 5	Duct160mm	SUP	circle	1.0	0.160		0.09	0	1	None	
14	Level 5	FanLaagstand (	SUP	circle	0.6	0.160	62.5	-	0	1	None	
15	Downward	Duct355mm	ODA	circle	2.6	0.355		0.09	0	1	None	
16	Level 5	Duct125mm	ETA	circle	1.8	0.125		0.09	0	1	None	
17	Level 5	Duct160mm	ETA	circle	1.4	0.160		0.09	0	1	None	
18	Level 5	FanLaagstand (	EHA	circle	0.6	0.160	62.5	-	0	1	None	
19	Downward	Duct355mm	EHA	circle	2.6	0.355		0.09	0	1	None	
20	Level 5	Duct125mm	ETA	circle	0.2	0.125		0.09	0	1	None	
21	Level 5	Duct125mm	ETA	circle	1.4	0.125		0.09	0	1	None	
22	Level 5	Duct125mm	SUP	circle	4.6	0.125		0.09	0	1	None	
23	Level 5	Duct125mm	SUP	circle	0.2	0.125		0.09	0	1	None	
24	Level 5	Duct125mm	SUP	circle	3.8	0.125		0.09	0	1	None	
25	Level 5	Duct125mm	SUP	circle	0.6	0.125		0.09	0	1	None	
26	Level 5	Duct125mm	SUP	circle	3.6	0.125		0.09	0	1	None	
27	Level 4	Duct125mm	SUP	circle	2.6	0.125		0.09	0	1	None	
28	Level 4	Duct125mm	SUP	circle	3.0	0.125		0.09	0	1	None	
29	Level 4	Duct125mm	SUP	circle	4.6	0.125		0.09	0	1	None	
30	Level 4	Duct125mm	ETA	circle	2.2	0.125		0.09	0	1	None	
31	Level 4	Duct125mm	ETA	circle	3.6	0.125		0.09	0	1	None	
32	Level 4	Duct125mm	SUP	circle	2.2	0.125		0.09	0	1	None	
33	Level 4	Duct125mm	ETA	circle	0.2	0.125		0.09	0	1	None	
34	Level 4	Duct160mm	ETA	circle	0.2	0.160		0.09	0	1	None	
35	Level 4	Duct160mm	SUP	circle	0.2	0.160		0.09	0	1	None	
36	Level 4	Duct125mm	SUP	circle	1.8	0.125		0.09	0	1	None	
37	Level 4	WTW-nobypas	WTW	circle	0.2	0.227		0.09	0	1	None	C = 19.796;
38	Level 4	Duct160mm	ODA	circle	0.2	0.160		0.09	0	1	None	
39	Level 4	Duct160mm	ODA	circle	0.6	0.160		0.09	0	1	None	
40	Downward	Duct355mm	ODA	circle	2.6	0.355		0.09	0	1	None	
41	Level 4	Duct160mm	EHA	circle	0.2	0.160		0.09	0	1	None	
42	Level 4	Duct160mm	EHA	circle	0.6	0.160		0.09	0	1	None	
43	Downward	Duct355mm	EHA	circle	2.6	0.355		0.09	0	1	None	
44	Level 4	Duct125mm	ETA	circle	1.8	0.125		0.09	0	1	None	
45	Level 4	Duct125mm	ETA	circle	0.2	0.125		0.09	0	1	None	
46	Level 4	Duct125mm	ETA	circle	1.4	0.125		0.09	0	1	None	
47	Level 4	Duct125mm	SUP	circle	4.6	0.125		0.09	0	1	None	
48	Level 4	Duct125mm	SUP	circle	0.2	0.125		0.09	0	1	None	
49	Level 4	Duct125mm	SUP	circle	3.6	0.125		0.09	0	1	None	
50	Level 4	Duct125mm	SUP	circle	3.8	0.125		0.09	0	1	None	
51	Level 4	Duct125mm	SUP	circle	0.6	0.125		0.09	0	1	None	
52	Level 3	Duct125mm	SUP	circle	2.6	0.125		0.09	0	1	None	
53	Level 3	Duct125mm	SUP	circle	3.0	0.125		0.09	0	1	None	
54	Level 3	Duct125mm	SUP	circle	4.6	0.125		0.09	0	1	None	
55	Level 3	Duct125mm	ETA	circle	2.2	0.125		0.09	0	1	None	
56	Level 3	Duct125mm	ETA	circle	3.8	0.125		0.09	0	1	None	
57	Level 3	Duct125mm	ETA	circle	0.2	0.125		0.09	0	1	None	
58	Level 3	Duct125mm	SUP	circle	2.2	0.125		0.09	0	1	None	
59	Level 3	Duct125mm	SUP	circle	1.8	0.125		0.09	0	1	None	
60	Level 3	Duct160mm	SUP	circle	1.0	0.160		0.09	0	1	None	
61	Level 3	Duct160mm	EHA	circle	1.4	0.160		0.09	0	1	None	
62	Level 3	FanLaagstand (	ODA	circle	0.6	0.160	62.5	-	0	1	None	
63	Downward	Duct355mm	ODA	circle	2.6	0.355		0.09	0	1	None	
64	Level 3	FanLaagstand (	EHA	circle	0.6	0.160	62.5	-	0	1	None	
65	Downward	Duct355mm	EHA	circle	2.6	0.355		0.09	0	1	None	
66	Level 3	Duct125mm	ETA	circle	1.8	0.125		0.09	0	1	None	
67	Level 3	Duct125mm	ETA	circle	0.2	0.125		0.09	0	1	None	
68	Level 3	Duct125mm	ETA	circle	1.4	0.125		0.09	0	1	None	
69	Level 3	Duct125mm	SUP	circle	4.6	0.125		0.09	0	1	None	
70	Level 3	Duct125mm	SUP	circle	0.2	0.125		0.09	0	1	None	
71	Level 3	Duct125mm	SUP	circle	3.6	0.125		0.09	0	1	None	
72	Level 3	Duct125mm	SUP	circle	3.8	0.125		0.09	0	1	None	
73	Level 3	Duct125mm	SUP	circle	0.6	0.125		0.09	0	1	None	
74	Level 2	Duct125mm	SUP	circle	2.6	0.125		0.09	0	1	None	
75	Level 2	Duct125mm	SUP	circle	3.0	0.125		0.09	0	1	None	
76	Level 2	Duct125mm	SUP	circle	4.6	0.125		0.09	0	1	None	
77	Level 2	Duct125mm	ETA	circle	2.2	0.125		0.09	0	1	None	
78	Level 2	Duct125mm	ETA	circle	3.8	0.125		0.09	0	1	None	
79	Level 2	Duct125mm	ETA	circle	0.2	0.125		0.09	0	1	None	
80	Level 2	Duct125mm	SUP	circle	2.2	0.125		0.09	0	1	None	
81	Level 2	Duct125mm	SUP	circle	1.8	0.125		0.09	0	1	None	
82	Level 2	Duct160mm	SUP	circle	1.0	0.160		0.09	0	1	None	
83	Level 2	Duct160mm	EHA	circle	1.4	0.160		0.09	0	1	None	
84	Level 2	FanLaagstand (	ODA	circle	0.6	0.160	62.5	-	0	1	None	
85	Downward	Duct355mm	ODA	circle	2.6	0.355		0.09	0	1	None	
86	Level 2	Duct125mm	ETA	circle	1.8	0.125		0.09	0	1	None	
87	Level 2	FanLaagstand (	EHA	circle	0.6	0.160	62.5	-	0	1	None	
88	Downward	Duct355mm	EHA	circle	2.6	0.355		0.09	0	1	None	
89	Level 2	Duct125mm	ETA	circle	0.2	0.125		0.09	0	1	None	
90	Level 2	Duct125mm	ETA	circle	1.4	0.125		0.09	0	1	None	
91	Level 2	Duct125mm	SUP	circle	4.6	0.125		0.09	0	1	None	
92	Level 2	Duct125mm	SUP	circle	0.2	0.125		0.09	0	1	None	
93	Level 2	Duct125mm	SUP	circle	3.6	0.125		0.09	0	1	None	
94	Level 2	Duct125mm	SUP	circle	3.8	0.125		0.09	0	1	None	
95	Level 2	Duct125mm	SUP	circle	0.6	0.125		0.09	0	1	None	
96	BG/level 1	Duct125mm	SUP	circle	2.6	0.125		0.09	0	1	None	
97	BG/level 1	Duct125mm	SUP	circle	3.0	0.125		0.09	0	1	None	
98	BG/level 1	Duct125mm	SUP	circle	4.6	0.125		0.09	0	1	None	
99	BG/level 1	Duct125mm	SUP	circle	3.8	0.125		0.09	0	1	None	
100	BG/level 1	Duct125mm	ETA	circle	2.2	0.125		0.09	0	1	None	
101	BG/level 1	Duct125mm	ETA	circle	0.2	0.125		0.09	0	1	None	
102	BG/level 1	Duct125mm	ETA	circle	2.2	0.125		0.09	0	1	None	
103	BG/level 1	Duct125mm	ETA	circle	3.8	0.125		0.09	0	1	None	
104	BG/level 1	Duct160mm	SUP	circle	1.0	0.160		0.09	0	1	None	
105	BG/level 1	FanLaagstand (	ODA	circle	0.6	0.160	62.5	-	0	1	None	
106	BG/level 1	Duct125mm	ETA	circle	1.8	0.125		0.09	0	1	None	
107	BG/level 1	Duct160mm	ETA	circle	1.4	0.160		0.09	0	1	None	
108	BG/level 1	FanLaagstand (	EHA	circle	0.6	0.160	62.5	-	0	1	None	
109	BG/level 1	Duct125mm	ETA	circle	0.2	0.125		0.09	0	1	None	
110	BG/level 1	Duct125mm	ETA	circle	1.4	0.125		0.09	0	1	None	
111	BG/level 1	Duct125mm	SUP	circle	4.6	0.125		0.09	0	1	None	
112	BG/level 1	Duct125mm	SUP	circle	0.2	0.125		0.09	0	1	None	
113	BG/level 1	Duct125mm	SUP	circle	3.8	0.125		0.09	0	1	None	
114	BG/level 1	Duct125mm	SUP	circle	0.6	0.125		0.09	0	1	None	
115	BG/level 1	Duct125mm	SUP	circle	3.6	0.125		0.09	0	1	None	

Junction/terminal

		Level		Terminal loss coefficient	Free face area	Design flow rate	Max balance coefficient	Balance loss coefficient	Schedule
		#		-	m²	m³/h			-
1	Terminal	Roof		0.125 (by default)	0.14	1500	0.8 (by default)	0 (by default)	None
3	Terminal	Roof		0.125 (by default)	0.14	1500	0.8 (by default)	0 (by default)	None
5	Terminal	5	SUP	0.125 (by default)	0.0035	0	0.8 (by default)	0 (by default)	None
7	Terminal	5	SUP	0.125 (by default)	0.0035	0	0.8 (by default)	0 (by default)	None
8	Terminal	5	SUP	0.125 (by default)	0.0069	0	0.8 (by default)	0 (by default)	None
10	Terminal	5	ETA	0.125 (by default)	0.0104	0	0.8 (by default)	0 (by default)	None
11	Terminal	5	ETA	0.125 (by default)	0.0104	0	0.8 (by default)	0 (by default)	None
20	Terminal	5	ETA	0.125 (by default)	0.0104	0	0.8 (by default)	0 (by default)	None
21	Terminal	5	ETA	0.125 (by default)	0.0104	0	0.8 (by default)	0 (by default)	None
24	Terminal	5	SUP	0.125 (by default)	0.0069	0	0.8 (by default)	0 (by default)	None
25	Terminal	5	SUP	0.125 (by default)	0.0069	0	0.8 (by default)	0 (by default)	None
26	Terminal	5	SUP	0.125 (by default)	0.0069	0	0.8 (by default)	0 (by default)	None
27	Terminal	4	SUP	0.125 (by default)	0.0035	0	0.8 (by default)	0 (by default)	None
29	Terminal	4	SUP	0.125 (by default)	0.0035	0	0.8 (by default)	0 (by default)	None
30	Terminal	4	SUP	0.125 (by default)	0.0069	0	0.8 (by default)	0 (by default)	None
32	Terminal	4	ETA	0.125 (by default)	0.0104	0	0.8 (by default)	0 (by default)	None
33	Terminal	4	ETA	0.125 (by default)	0.0104	0	0.8 (by default)	0 (by default)	None
44	Terminal	4	SUP	0.125 (by default)	0.0104	0	0.8 (by default)	0 (by default)	None
45	Terminal	4	SUP	0.125 (by default)	0.0104	0	0.8 (by default)	0 (by default)	None
48	Terminal	4	SUP	0.125 (by default)	0.0069	0	0.8 (by default)	0 (by default)	None
49	Terminal	4	SUP	0.125 (by default)	0.0069	0	0.8 (by default)	0 (by default)	None
50	Terminal	4	SUP	0.125 (by default)	0.0069	0	0.8 (by default)	0 (by default)	None
51	Terminal	3	SUP	0.125 (by default)	0.0035	0	0.8 (by default)	0 (by default)	None
53	Terminal	3	SUP	0.125 (by default)	0.0035	0	0.8 (by default)	0 (by default)	None
54	Terminal	3	SUP	0.125 (by default)	0.0069	0	0.8 (by default)	0 (by default)	None
56	Terminal	3	ETA	0.125 (by default)	0.0104	0	0.8 (by default)	0 (by default)	None
57	Terminal	3	ETA	0.125 (by default)	0.0104	0	0.8 (by default)	0 (by default)	None
66	Terminal	3	SUP	0.125 (by default)	0.0104	0	0.8 (by default)	0 (by default)	None
67	Terminal	3	SUP	0.125 (by default)	0.0104	0	0.8 (by default)	0 (by default)	None
70	Terminal	3	SUP	0.125 (by default)	0.0069	0	0.8 (by default)	0 (by default)	None
71	Terminal	3	SUP	0.125 (by default)	0.0069	0	0.8 (by default)	0 (by default)	None
72	Terminal	3	SUP	0.125 (by default)	0.0069	0	0.8 (by default)	0 (by default)	None
73	Terminal	2	SUP	0.125 (by default)	0.0035	0	0.8 (by default)	0 (by default)	None
75	Terminal	2	SUP	0.125 (by default)	0.0035	0	0.8 (by default)	0 (by default)	None
76	Terminal	2	SUP	0.125 (by default)	0.0069	0	0.8 (by default)	0 (by default)	None
78	Terminal	2	ETA	0.125 (by default)	0.0104	0	0.8 (by default)	0 (by default)	None
79	Terminal	2	ETA	0.125 (by default)	0.0104	0	0.8 (by default)	0 (by default)	None
88	Terminal	2	SUP	0.125 (by default)	0.0104	0	0.8 (by default)	0 (by default)	None
89	Terminal	2	SUP	0.125 (by default)	0.0104	0	0.8 (by default)	0 (by default)	None
92	Terminal	2	SUP	0.125 (by default)	0.0069	0	0.8 (by default)	0 (by default)	None
93	Terminal	2	SUP	0.125 (by default)	0.0069	0	0.8 (by default)	0 (by default)	None
94	Terminal	2	SUP	0.125 (by default)	0.0069	0	0.8 (by default)	0 (by default)	None
95	Terminal	BG/1	SUP	0.125 (by default)	0.0035	0	0.8 (by default)	0 (by default)	None
97	Terminal	BG/1	SUP	0.125 (by default)	0.0035	0	0.8 (by default)	0 (by default)	None
98	Terminal	BG/1	SUP	0.125 (by default)	0.0069	0	0.8 (by default)	0 (by default)	None
100	Terminal	BG/1	ETA	0.125 (by default)	0.0104	0	0.8 (by default)	0 (by default)	None
101	Terminal	BG/1	ETA	0.125 (by default)	0.0104	0	0.8 (by default)	0 (by default)	None
110	Terminal	BG/1	SUP	0.125 (by default)	0.0104	0	0.8 (by default)	0 (by default)	None
111	Terminal	BG/1	SUP	0.125 (by default)	0.0104	0	0.8 (by default)	0 (by default)	None
114	Terminal	BG/1	SUP	0.125 (by default)	0.0069	0	0.8 (by default)	0 (by default)	None
115	Terminal	BG/1	SUP	0.125 (by default)	0.0069	0	0.8 (by default)	0 (by default)	None
116	Terminal	BG/1	SUP	0.125 (by default)	0.0069	0	0.8 (by default)	0 (by default)	None

				Connection	Schedule
2	Junction	Roof		Downward	None
4	Junction	Roof		Downward	None
6	Junction		5	Horizontal	None
9	Junction		5	Horizontal	None
12	Junction		5	Horizontal	None
13	Junction		5	Horizontal	None
14	Junction		5	Horizontal	None
15	Junction		5	Horizontal	None
16	Junction		5	Up- and downward	None
17	Junction		5	Horizontal	None
18	Junction		5	Up- and downward	None
19	Junction		5	Horizontal	None
22	Junction		5	Horizontal	None
23	Junction		5	Horizontal	None
28	Junction		4	Horizontal	None
31	Junction		4	Horizontal	None
34	Junction		4	Horizontal	None
35	Junction		4	Horizontal	None
36	Junction		4	Horizontal	None
37	Junction		4	Horizontal	None
38	Junction		4	Horizontal	None
39	Junction		4	Horizontal	None
40	Junction		4	Up- and downward	None
41	Junction		4	Horizontal	None
42	Junction		4	Up- and downward	None
43	Junction		4	Horizontal	None
46	Junction		4	Horizontal	None
47	Junction		4	Horizontal	None
52	Junction		3	Horizontal	None
55	Junction		3	Horizontal	None
58	Junction		3	Horizontal	None
59	Junction		3	Horizontal	None
60	Junction		3	Horizontal	None
61	Junction		3	Horizontal	None
62	Terminal		3	Up- and downward	None
63	Junction		3	Horizontal	None
64	Terminal		3	Up- and downward	None
65	Junction		3	Horizontal	None
68	Junction		3	Horizontal	None
69	Junction		3	Horizontal	None
74	Junction		2	Horizontal	None
77	Junction		2	Horizontal	None
80	Junction		2	Horizontal	None
81	Junction		2	Horizontal	None
82	Junction		2	Horizontal	None
83	Junction		2	Horizontal	None
84	Junction		2	Up- and downward	None
85	Junction		2	Horizontal	None
86	Junction		2	Up- and downward	None

87	Junction		2	Horizontal	None
90	Junction		2	Horizontal	None
91	Junction		2	Horizontal	None
96	Junction	BG/1		Horizontal	None
99	Junction	BG/1		Horizontal	None
102	Junction	BG/1		Horizontal	None
103	Junction	BG/1		Horizontal	None
104	Junction	BG/1		Horizontal	None
105	Junction	BG/1		Horizontal	None
106	Junction	BG/1		Upwards	None
107	Junction	BG/1		Horizontal	None
108	Junction	BG/1		Upwards	None
109	Junction	BG/1		Horizontal	None
112	Junction	BG/1		Horizontal	None
113	Junction	BG/1		Horizontal	None

Scenario II: Bypass HRV
Adaptations

Segment		Type	Direction	Shape	Length	Diameter	Maximum flow rate	Roughness	Leakage rate	dP static	schedule	Other
#		-		-	m	m	m³/h	mm	L/s/m²	Pa	-	
37	Level 4	WTW-bypass (Backdraft damper - Volume flow)		circle	0.2	0.227		0.09	0	1	None	C = 19.7

Scenario III: Bypass Extra
Adaptations

Segment		Type	Direction	Shape	Length	Diameter	Maximum flow rate	Roughness	Leakage rate	dP static	schedule	Other
#		-		-	m	m	m³/h	mm	L/s/m²	Pa	-	
34	Level 4	Duct160mm	ETA	circle	0.2	0.160	-	0.09	0	1	None	
35	Level 4	Duct160mm	SUP	circle	0.2	0.160	-	0.09	0	1	None	
36	Level 4	Duct125mm	SUP	circle	1.8	0.125	-	0.09	0	1	None	
37	Level 4	WTW-bypassclosed (Backdraft damper - Volume flow)	WTW	circle	0.2	0.227	-	-	0	1	None	C = 19.796;
38	Level 4	Bypass ETA - EHA | Duct160mm	Bypass	circle	1.0	0.160	-	0.09	0	1	None	
39	Level 4	Duct160mm	ODA	circle	0.2	0.160	-	0.09	0	1	None	
40	Level 4	Duct160mm	ODA	circle	0.6	0.160	-	0.09	0	1	None	
41	Downward	Duct355mm	ODA	circle	2.6	0.355	-	0.09	0	1	None	
42	Level 4	Duct125mm	ETA	circle	1.8	0.125	-	0.09	0	1	None	
43	Level 4	Duct160mm	EHA	circle	0.2	0.160	-	0.09	0	1	None	
44	Level 4	Duct160mm	EHA	circle	0.2	0.160	-	0.09	0	1	None	
45	Level 4	Duct160mm	EHA	circle	0.6	0.160	-	0.09	0	1	None	
46	Downward	Duct355mm	EHA	circle	2.6	0.355	-	0.09	0	1	None	

All ducts after 46, +1

All junctions before 34 stay the same

34	4	Junction	Horizontal	None
35	4	Junction	Horizontal	None
36	4	Junction	Horizontal	None
37	4	Junction	Horizontal	None
38	4	Junction	Horizontal	None
39	4	Junction	Horizontal	None
40	4	Junction	Up- and downward	None
41	4	Junction	Horizontal	None
42	4	Junction	Horizontal	None
43	4	Junction	Up- and downward	None
44	4	Junction	Horizontal	None
46	4	Junction	Horizontal	None
47	4	Junction	Horizontal	None

All other junctions after 47, +1

Scenario IV: Bypass Scheduled
Adaptations

Segment		Type	Direction	Shape	Length	Diameter	Maximum flow rate	Roughness	Leakage rate	dP static	schedule	Other
#		-		-	m	m	m³/h	mm	L/s/m²	Pa	-	
34	Level 4	Damper (Fan - Constant mass flow)	ETA	circle	0.2	0.160	2989.8	-	0	1	bypassclosed; fraction of mass flow rate, closed at t=1	
35	Level 4	Duct160mm	SUP	circle	0.2	0.160	-	0.09	0	1	None	
36	Level 4	Duct125mm	SUP	circle	1.8	0.125	-	0.09	0	1	None	
37	Level 4	WTW-bypassclosed (Backdraft damper - Volume flow)	WTW	circle	0.2	0.227	-	-	0	1	None	C = 19.796;
38	Level 4	Bypass ETA - EHA | Powerlaw model - Volume flow	Bypass	circle	1.0	0.160	-	-	0	1	BYPASSOPEN; open at t=111s or t=186s	C = 0.14; n
39	Level 4	Duct160mm	ODA	circle	0.2	0.160	-	0.09	0	1	None	
40	Level 4	Duct160mm	ODA	circle	0.6	0.160	-	0.09	0	1	None	
41	Downward	Duct355mm	ODA	circle	2.6	0.355	-	0.09	0	1	None	
42	Level 4	Duct125mm	ETA	circle	1.8	0.125	-	0.09	0	1	None	
43	Level 4	Duct160mm	EHA	circle	0.2	0.160	-	0.09	0	1	None	
44	Level 4	Duct160mm	EHA	circle	0.2	0.160	-	0.09	0	1	None	
45	Level 4	Duct160mm	EHA	circle	0.6	0.160	-	0.09	0	1	None	
46	Downward	Duct355mm	EHA	circle	2.6	0.355	-	0.09	0	1	None	

All ducts after 46, +1

All junctions before 34 stay the same

34	4	Junction	Horizontal	None
35	4	Junction	Horizontal	None
36	4	Junction	Horizontal	None
37	4	Junction	Horizontal	None
38	4	Junction	Horizontal	None
39	4	Junction	Horizontal	None
40	4	Junction	Up- and downward	None
41	4	Junction	Horizontal	None
42	4	Junction	Horizontal	None
43	4	Junction	Up- and downward	None
44	4	Junction	Horizontal	None
46	4	Junction	Horizontal	None
47	4	Junction	Horizontal	None

All other junctions after 47, +1

Scenario V: Fire damper inlet (I)
Adaptations

Segment		Type	Direction	Shape	Length	Diameter	Maximum flow rate	Roughness	Leakage rate	dP static	schedule	Other
#		-		-	m	m	kg/s	mm	L/s/m²	Pa	-	
39	Level 4	firedamper (Constant mass flow fan)		circle	0.6	0.160	1.0	-	0	1	fraction of max mass flow rate; closes at t=90 s / t=15	

Scenario VI: Fire damper both (I)
Adaptations

Segment		Type	Direction	Shape	Length	Diameter	Maximum flow rate	Roughness	Leakage rate	dP static	schedule	Other
#		-		-	m	m	kg/s	mm	L/s/m²	Pa	-	
39	Level 4	firedamper (Constant mass flow fan)	ODA	circle	0.6	0.160	1.0	-	0	1	fraction of max mass flow rate; closes at t=90 s / t=15	
42	Level 4	firedamper (Constant mass flow fan)	EHA		0.6	0.160	1.0	-	0	1	fraction of max mass flow rate; closes at t=90 s / t=15	

Scenario VII: Fire damper inlet (II)
Adaptations

Segment		Type	Direction	Shape	Length	Diameter	Maximum flow rate	Roughness	Leakage rate	dP static	schedule	Other
#		-		-	m	m	m³/h	mm	L/s/m²	Pa	-	
39	Level 4	firedamper (Constant mass flow fan)	ODA	circle	0.6	0.160	1.0	-	0	1	fraction of max mass flow rate; closes at t=120 s / t=2	

Scenario VIII: Fire damper both (II)
Adaptations

Segment		Type	Direction	Shape	Length	Diameter	Maximum flow rate	Roughness	Leakage rate	dP static	schedule	Other
#		-		-	m	m	m³/h	mm	L/s/m²	Pa	-	
39	Level 4	firedamper (Constant mass flow fan)	ODA	circle	0.6	0.160	1.0	-	0	1	fraction of max mass flow rate; closes at t=120 s / t=2	
42	Level 4	firedamper (Constant mass flow fan)	EHA	circle	0.6	0.160	1.0	-	0	1	fraction of max mass flow rate; closes at t=120 s / t=2	

Appendix J – Schedules for CONTAM for the case study

Appendix schedules case study

Apartment 3.04

Medium fire growth rate

Weighted averaged day temperature																				
Time	0	60	120	150	180	240	245	270	290	345	350	355	400							
Time [mm:ss]	00:00:00	00:01:00	00:02:00	00:02:30	00:03:00	00:04:00	00:04:05	00:04:30	00:04:50	00:05:45	00:05:50	00:05:55	00:06:40							
Temp [°C]	20	23.8	49.1	76.4	115.9	225	229.9	185.1	164.4	134.2	135.3	130.8	107.9							
Fan operation (0.91 kg/s)																				
Time	0	30	60	135	150	190	210	240	245	250	255	290	305	340	350	355	360	365	375	400
Time [mm:ss]	00:00:00	00:00:30	00:01:00	00:02:15	00:02:30	00:03:10	00:03:30	00:04:00	00:04:05	00:04:10	00:04:15	00:04:50	00:05:05	00:05:40	00:05:50	00:05:55	00:06:00	00:06:05	00:06:15	00:06:40
Mass flow rate [kg/s]	0	0.04	0.16	0.71	0.79	0.89	0.85	0.72	0.35	0.77	0.76	0.38	0.3	0.23	0.11	0.49	0.42	0.26	0.29	0.27
Fraction [-]	0.00	0.04	0.18	0.78	0.87	0.98	0.93	0.79	0.38	0.85	0.84	0.42	0.33	0.25	0.12	0.54	0.46	0.29	0.32	0.30
Contaminant generation rate																				
Time	0.00	30.00	60.00	90.00	120.00	150.00	180.00	240.00	245.00	250.00	290.00	340.00	345.00	350.00	360.00	365.00	370.00	400.00		
Time [mm:ss]	00:00:00	00:00:30	00:01:00	00:01:30	00:02:00	00:02:30	00:03:00	00:04:00	00:04:05	00:04:10	00:04:50	00:05:40	00:05:45	00:05:50	00:06:00	00:06:05	00:06:10	00:06:40		
HRR	0.00	40.00	160.00	360.00	640.00	1000.00	1440.00	2560.00	1182.98	835.74	454.91	345.46	469.29	176.62	165.02	238.00	178.84	118.65		
Fraction	0.00	0.01	0.04	0.09	0.16	0.25	0.36	0.64	0.30	0.21	0.11	0.09	0.12	0.04	0.04	0.06	0.04	0.03		

Fast fire growth rate

Weighted averaged day temperature																				
Time	0	30	60	90	120	150	155	200	220	270	275	280	340	400						
Time [mm:ss]	00:00:00	00:00:30	00:01:00	00:01:30	00:02:00	00:02:30	00:02:35	00:03:20	00:03:40	00:04:30	00:04:35	00:04:40	00:05:40	00:06:40						
Temp [°C]	20	22	35.7	73.7	146.3	252.1	262.3	189.7	166.9	136.3	138.2	134	103.6	83.4						
Fan operation (1.56 kg/s)																				
Time	0.00	15.00	30.00	45.00	85.00	100.00	115.00	130.00	150.00	155.00	160.00	165.00	190.00	270.00	275.00	280.00	285.00	290.00	345.00	400.00
Time [mm:ss]	00:00:00	00:00:15	00:00:30	00:00:45	00:01:25	00:01:40	00:01:55	00:02:10	00:02:30	00:02:35	00:02:40	00:02:45	00:03:10	00:04:30	00:04:35	00:04:40	00:04:45	00:04:50	00:05:45	00:06:40
Mass flow rate [kg/s]	0.00	0.04	0.16	0.38	1.21	1.43	1.53	1.50	1.28	0.65	0.51	0.57	0.59	0.19	0.19	0.44	0.45	0.30	0.22	0.21
Fraction [-]	0.00	0.02	0.10	0.25	0.78	0.92	0.98	0.96	0.82	0.42	0.33	0.36	0.38	0.12	0.12	0.28	0.29	0.19	0.14	0.13
Contaminant generation rate																				
Time	0.00	15.00	45.00	75.00	90.00	115.00	150.00	155.00	180.00	220.00	265.00	270.00	275.00	280.00	285.00	290.00	295.00	400.00		
Time [mm:ss]	00:00:00	00:00:15	00:00:45	00:01:15	00:01:30	00:01:55	00:02:30	00:02:35	00:03:00	00:03:40	00:04:25	00:04:30	00:04:35	00:04:40	00:04:45	00:04:50	00:04:55	00:06:40		
HRR	0.00	40.00	360.00	1000.00	1440.00	2360.00	4000.00	2070.25	1020.73	433.10	335.97	390.05	780.45	142.16	125.91	257.54	186.83	33.81		
Fraction	0.00	0.01	0.09	0.25	0.36	0.59	1.00	0.52	0.26	0.11	0.08	0.10	0.20	0.04	0.03	0.06	0.05	0.01		

Appendix K – Inventory on the ventilation rate

A1	Supply	Return	Amount of valves					
			Supply	Extraction	Volume flow rate per valve in [m³/h]	Volume flow rate per valve in [m³/s]	Velocity	Free face area [m²]
Living	150 m³/h		3		50	0.0139	2	0.006944444
Open kitchen		150 m³/h		2	75	0.0208	2	0.010416667
Bedroom 1	25 m³/h		1		25	0.0069	2	0.003472222
Bedroom 2	25 m³/h		1		25	0.0069	2	0.003472222
Bathroom		75 m³/h		1	75	0.0208	2	0.010416667
Toilet		25 m³/h		1	25	0.0069	2	0.003472222
Tech space	50 m³/h	m³/h	1		50	0.0139	2	0.006944444
Total	250 m³/h	250 m³/h						
A2 and A3 - A3 modeled as simple system								
Living	150 m³/h		3		50	0.0139	2	0.006944444
Open kitchen		150 m³/h		2	75	0.0208	2	0.010416667
Bedroom 1	25 m³/h		1		25	0.0069	2	0.003472222
Bedroom 2	25 m³/h		1		25	0.0069	2	0.003472222
Bathroom		75 m³/h		1	75	0.0208	2	0.010416667
Toilet		25 m³/h		1	25	0.0069	2	0.003472222
Tech space	50 m³/h	m³/h	1		50	0.0139	2	0.006944444
Total	250 m³/h	250 m³/h						
B								
Living	150 m³/h		3		50	0.0139	2	0.006944444
Open kitchen		150 m³/h		2	75	0.0208	2	0.010416667
Bedroom 1	25 m³/h		1		25	0.0069	2	0.003472222
Bedroom 2	25 m³/h		1		25	0.0069	2	0.003472222
Bathroom		75 m³/h		1	75	0.0208	2	0.010416667
Toilet		25 m³/h		1	25	0.0069	2	0.003472222
Tech space	50 m³/h	m³/h	1		50	0.0139	2	0.006944444
Total	250 m³/h	250 m³/h						
C - modeled as simple system								
Living	150 m³/h		3		50	0.0139	2	0.006944444
Open kitchen		150 m³/h		2	75	0.0208	2	0.010416667
Bedroom 1	50 m³/h		1		50	0.0139	2	0.006944444
Bathroom		75 m³/h		1	75	0.0208	2	0.010416667
Toilet		25 m³/h		1	25	0.0069	2	0.003472222
Tech space	50 m³/h	m³/h	1		50	0.0139	2	0.006944444
Total	250 m³/h	250 m³/h						
E								
Living	200 m³/h		4		50	0.0139	2	0.006944444
Open kitchen		150 m³/h		2	75	0.0208	2	0.010416667
Bedroom 1	25 m³/h		1		25	0.0069	2	0.003472222
Bedroom 2	25 m³/h		1		25	0.0069	2	0.003472222
Bedroom 3	25 m³/h		1		25	0.0069	2	0.003472222
Bathroom 1		75 m³/h		1	75	0.0208	2	0.010416667
Bathroom 2		75 m³/h		1	75	0.0208	2	0.010416667
Toilet		25 m³/h		1	25	0.0069	2	0.003472222
Tech space	50 m³/h	m³/h	1		50	0.0139	2	0.006944444
Total	325 m³/h	325 m³/h						

Appendix L – Regression analysis on the measurement results of an HRV unit

Appendix regression analyses

1. **HRV-unit off; bypass closed; EHA & ODA open**
   a. *Original*

Measurement results

ΔP_{st} [Pa]	9.9	38.8	62.3	79.1	102.0	127.5	131.5
q [m³/h]	127.6	202.0	246.8	269.7	277.6	315.4	336.2
q [dm³/s]	35.44	56.11	68.56	74.92	77.11	87.61	93.39

REGRESSIERESULTATEN

q = C * (dP)^(1/n) [dm3/s]

regressie-coefficient :	r2 =	0.991		toetswaarden :	q(1) =	15.35	[dm3/s]
vermenigvuldigingsfaktor:	C =	15.355			q(10) =	35.19	[dm3/s]
stromings-coefficient :	n =	2.777					
	1/n =	0.360					
equivalent oppervlak :	Aeq =	0.0131	[m2]	DICHT			

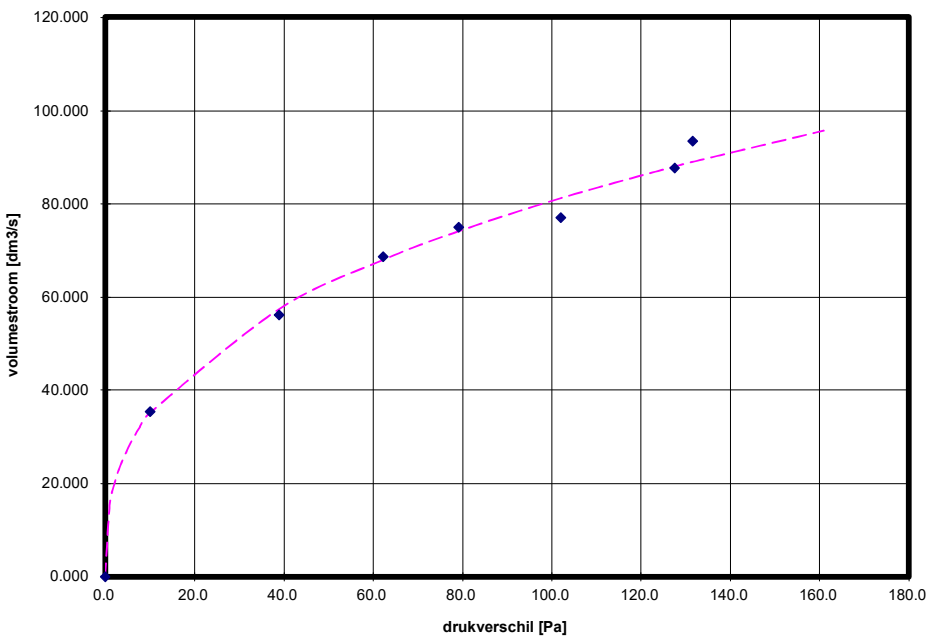

   b. *Excluding leakage of the HRV-unit*

Calculation results

$$q = (15.355 * (\Delta P_{st})^{0.360}) - (0.029 * (\Delta P_{st})^{0.774})$$

ΔP_{st} [Pa]	5	10	50	100	200
q [m³/h]	98.306	126.01	223.88	286.42	366.02
q [dm³/s]	27.307	35.004	62.189	79.560	101.67

REGRESSIERESULTATEN

q = C * (dP)^(1/n) [dm3/s]

regressie-coefficient :	r2	=	1.000		toetswaarden :	q(1) =	15.40	[dm3/s]
vermenigvuldigingsfaktor:	C	=	15.399			q(10) =	34.99	[dm3/s]
stromings-coefficient :	n	=	2.805					
	1/n	=	0.356					
equivalent oppervlak :	Aeq	=	0.0132	[m2]	DICHT			

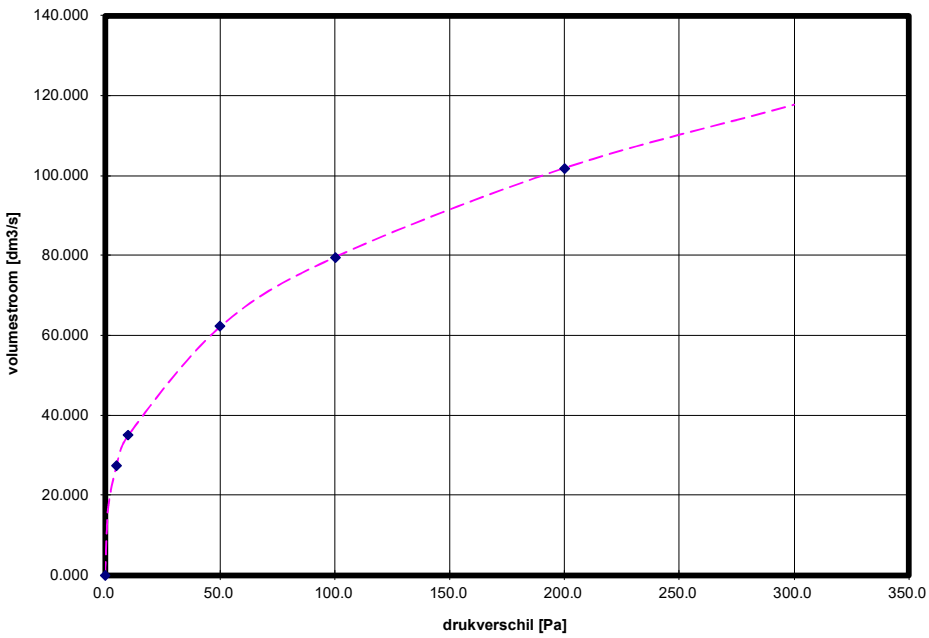

2. HRV-unit off; bypass open; EHA & ODA open

a. Original

Measurement results

ΔP_{st} [Pa]	9.9	28.9	47.1	73.0	87.4	109.5	138.5
q [m³/h]	124.2	180.0	224.8	260.3	267.9	287.0	310.2
q [dm³/s]	34.50	50.00	62.44	72.31	74.42	79.72	86.17

REGRESSIERESULTATEN

q = C * (dP)^(1/n) [dm3/s]

regressie-coefficient :	r2	=	0.995		toetswaarden :	q(1) =	15.62	[dm3/s]
vermenigvuldigingsfaktor:	C	=	15.622			q(10) =	35.00	[dm3/s]
stromings-coefficient :	n	=	2.855					
	1/n	=	0.350					
equivalent oppervlak :	Aeq	=	0.0134	[m2]	DICHT			

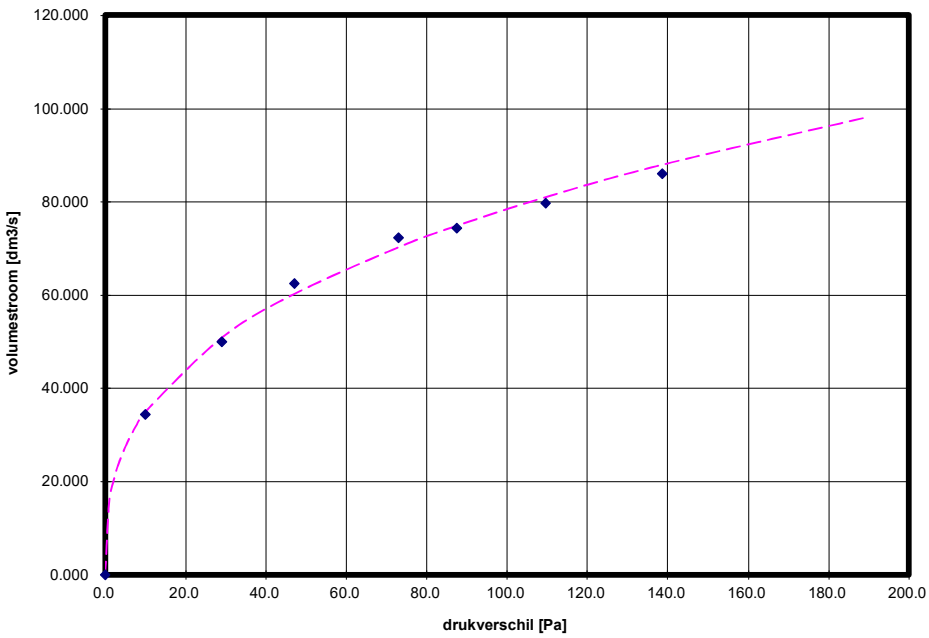

b. Excluding leakage towards the apartment by the HRV-unit

Calculation results

$$q = (15.622 * (\Delta P_{st})^{0.350}) - (0.029 * (\Delta P_{st})^{0.774})$$

ΔP_{st} [Pa]	5	10	50	100	200
q [m³/h]	98.419	125.28	218.99	278.18	352.95
q [dm³/s]	27.339	34.801	60.830	77.271	98.041

REGRESSIERESULTATEN

q = C * (dP)^(1/n) [dm3/s]

regressie-coefficient :	r2	=	1.000		toetswaarden :	q(1) =	15.67	[dm3/s]
vermenigvuldigingsfaktor:	C	=	15.671			q(10) =	34.79	[dm3/s]
stromings-coefficient :	n	=	2.887					
	1/n	=	0.346					
equivalent oppervlak :	Aeq	=	0.0135	[m2]	DICHT			

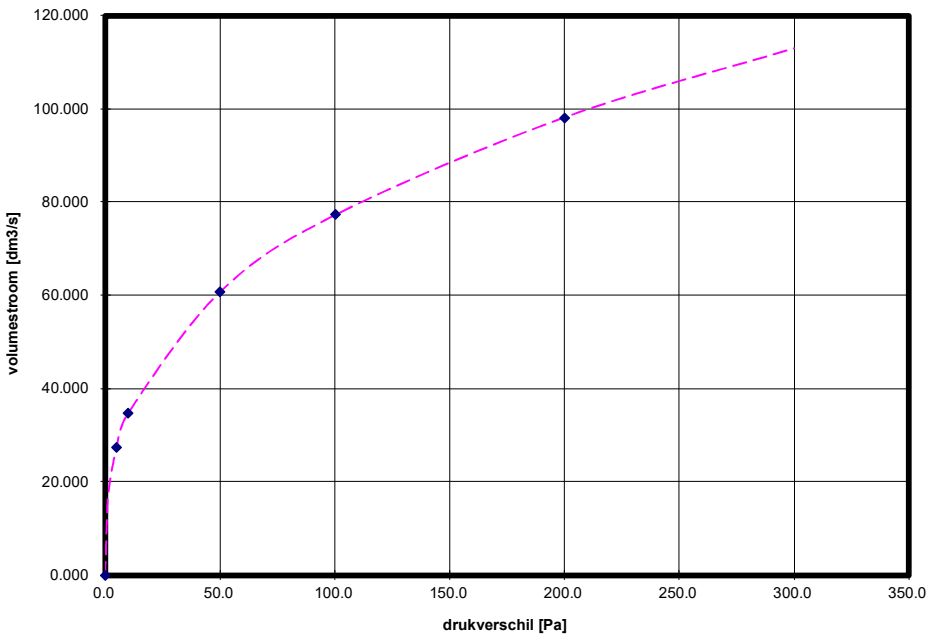

3. HRV-unit on; bypass closed; EHA & ODA open

a. Original

Measurement results

ΔP_{st} [Pa]	21.3	53.2	79.1	98.1	110.0	141.5
q [m³/h]	181.2	262.3	268.5	295.6	303.0	338.5
q [dm³/s]	50.33	72.86	74.58	82.11	84.17	94.03

REGRESSIERESULTATEN

q = C * (dP)^(1/n) [dm3/s]

regressie-coefficient :	r2	=	0.972		toetswaarden :	q(1) =	19.72	[dm3/s]
vermenigvuldigingsfaktor:	C	=	19.722			q(10) =	40.50	[dm3/s]
stromings-coefficient :	n	=	3.200					
	1/n	=	0.313					
equivalent oppervlak :	Aeq	=	0.0174	[m2]	DICHT			

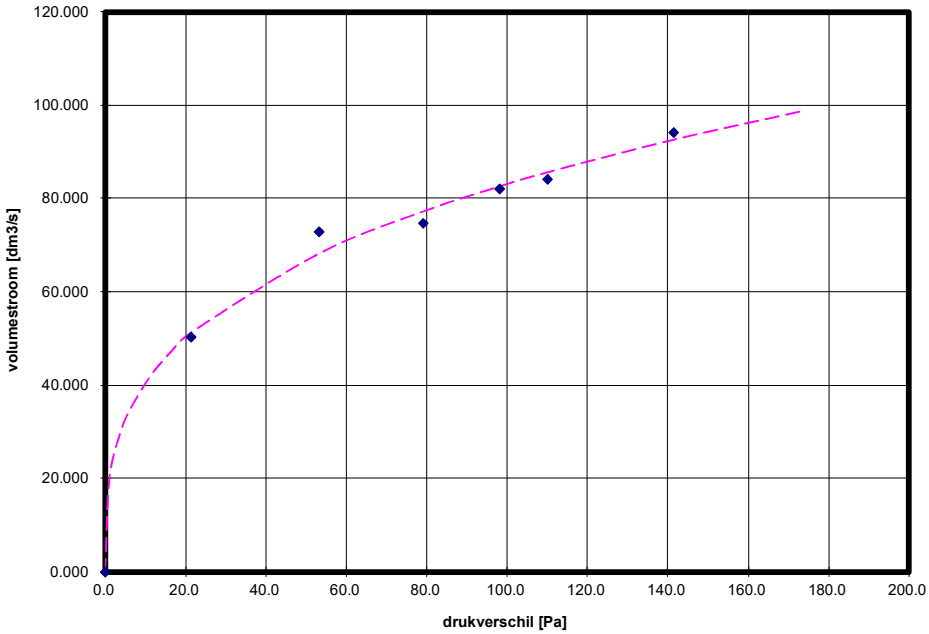

c. Excluding leakage towards the apartment by the HRV-unit

Calculation results

$$q = (19.722 * (\Delta P_{st})^{0.313}) - (0.029 * (\Delta P_{st})^{0.774})$$

ΔP_{st} [Pa]	5	10	50	100	200
q [m³/h]	117.14	145.35	239.41	296.40	366.49
q [dm³/s]	32.538	40.374	66.502	82.334	101.80

REGRESSIERESULTATEN

q = C * (dP)^(1/n) [dm3/s]

regressie-coefficient :	r2	=	1.000		toetswaarden :	q(1) =	19.80	[dm3/s]
vermenigvuldigingsfaktor:	C	=	19.796			q(10) =	40.36	[dm3/s]
stromings-coefficient :	n	=	3.232					
	1/n	=	0.309		eis :			
equivalent oppervlak :	Aeq	=	0.0175	[m2]	DICHT			

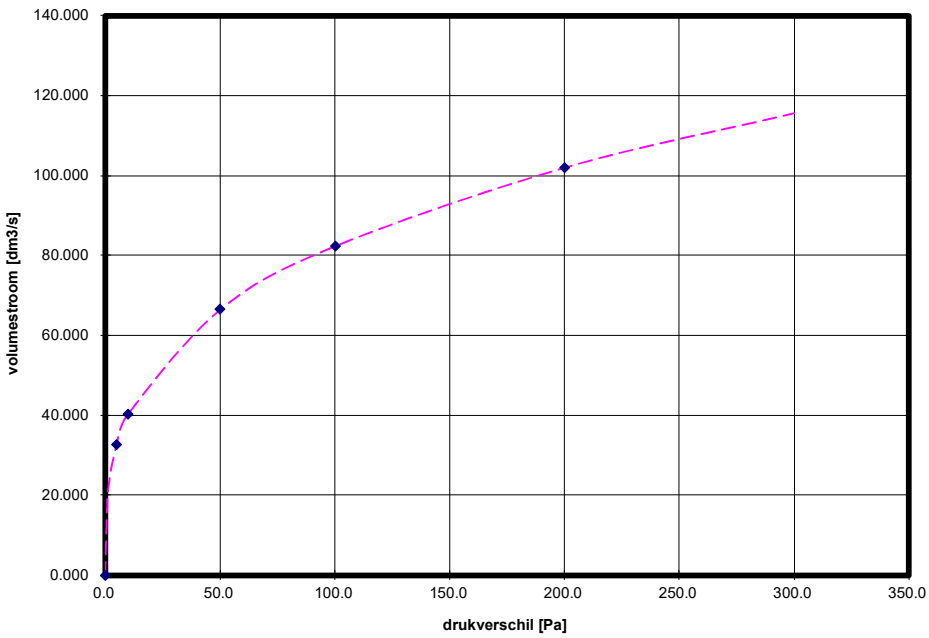

4. HRV-unit on; bypass open; EHA & ODA open

a. Original

Measurement results

ΔP_{st} [Pa]	9.9	30.4	49.4	73.0	98.8	134.5
q [m³/h]	87.61	133.7	170.9	200.1	232.2	258.2
q [dm³/s]	24.34	37.14	47.47	55.58	64.50	71.72

REGRESSIERESULTATEN

q = C * (dP)^(1/n) [dm3/s]

regressie-coefficient :	r2	=	0.998		toetswaarden :	q(1) =	9.10 [dm3/s]
vermenigvuldigingsfaktor:	C	=	9.102			q(10) =	24.06 [dm3/s]
stromings-coefficient :	n	=	2.369				
	1/n	=	0.422				
equivalent oppervlak :	Aeq	=	0.0075	[m2]	DICHT		

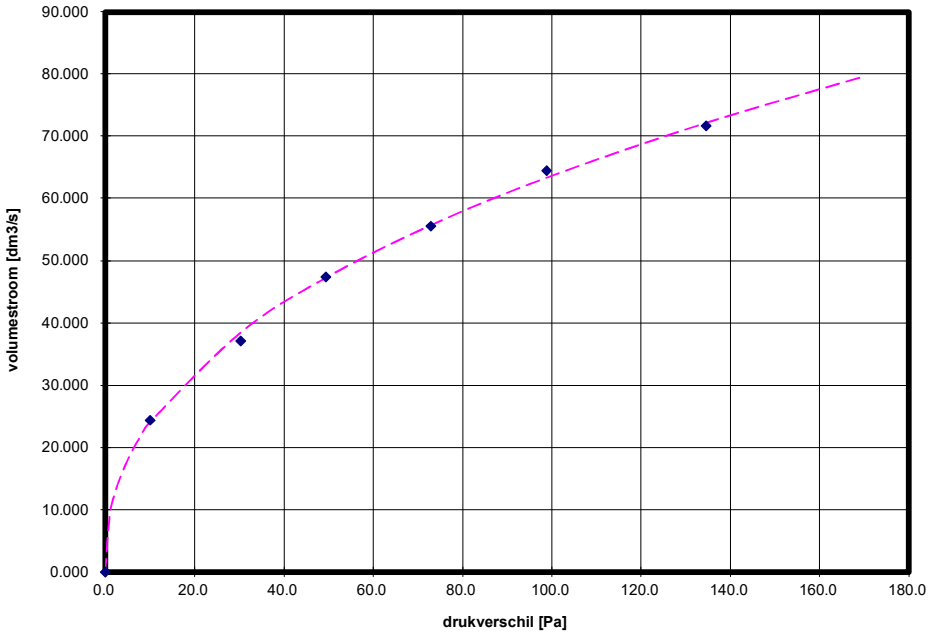

b. Excluding leakage towards the apartment by the HRV-unit

Calculation results

$$q = (9.102 * (\Delta P_{st})^{0.422}) - (0.029 * (\Delta P_{st})^{0.774})$$

ΔP_{st} [Pa]	5	10	50	100	200
q [m³/h]	64.263	85.964	168.61	225.10	300.23
q [dm³/s]	17.851	23.879	46.836	62.529	83.396

REGRESSIERESULTATEN

q = C * (dP)^(1/n) [dm3/s]

regressie-coefficient :	r2	=	1.000		toetswaarden :	q(1) =	9.12 [dm3/s]
vermenigvuldigingsfaktor:	C	=	9.117			q(10) =	23.87 [dm3/s]
stromings-coefficient :	n	=	2.392				
	1/n	=	0.418				
equivalent oppervlak :	Aeq	=	0.0075	[m2]	DICHT		

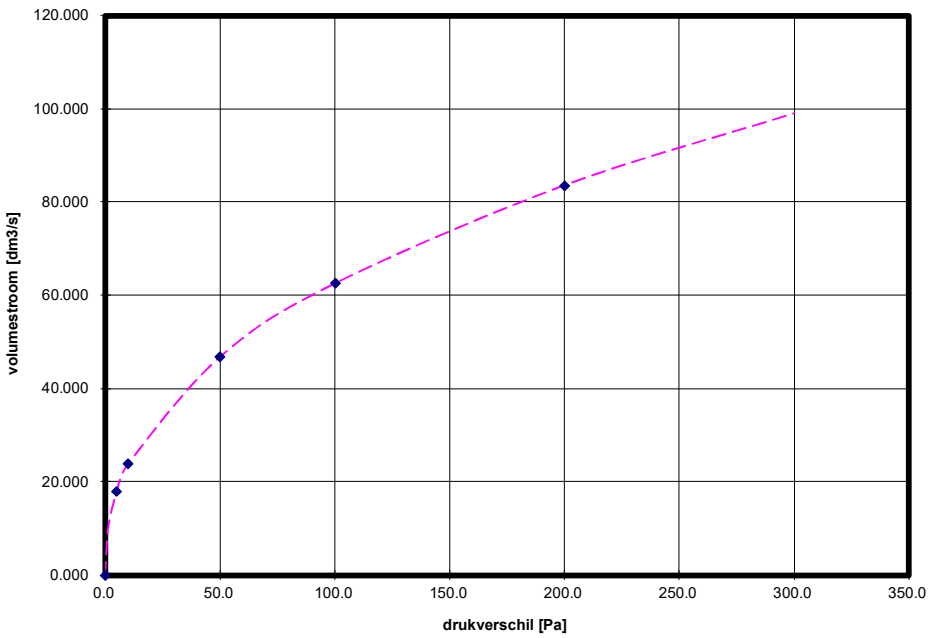

5. Leakage of the HRV-unit

Measurement results: HRV-unit off; bypass closed

ΔP_{st} [Pa]	23.6	52.5	74.5	105.0	133.0	151.5
q [m³/h]	1.298	2.373	3.090	4.044	4.645	5.124
q [dm³/s]	0.361	0.659	0.858	1.123	1.290	1.423

Measurement results: HRV-unit off; bypass open

ΔP_{st} [Pa]	22.0	47.9	70.7	98.8	130.5	150.0
q [m³/h]	1.199	2.117	2.778	3.580	4.578	5.089
q [dm³/s]	0.333	0.588	0.772	0.994	1.272	1.414

Measurement results: HRV-unit on; bypass closed

ΔP_{st} [Pa]	22.8	50.2	72.2	101.0	131.5	157.5
q [m³/h]	1.037	2.049	2.832	3.709	4.480	5.203
q [dm³/s]	0.288	0.569	0.787	1.030	1.244	1.445

Measurement results: HRV-unit on; bypass open

ΔP_{st} [Pa]	20.5	49.4	73.7	103.5	127.0	152.0
q [m³/h]	1.053	2.140	2.938	3.672	4.301	4.951

q [dm³/s]	0.293	0.594	0.816	1.020	1.195	1.375

Regression analysis based on the 4 aforementioned measurement data:

REGRESSIERESULTATEN

q = C * (dP)^(1/n) [dm3/s]

regressie-coefficient :	r2	=	0.993	toetswaarden :	q(1) =	0.03	[dm3/s]
vermenigvuldigingsfaktor:	C	=	0.029		q(10) =	0.17	[dm3/s]
stromings-coefficient :	n	=	1.291				
	1/n	=	0.774				
equivalent oppervlak :	Aeq	=	0.0000 [m2]	DICHT			

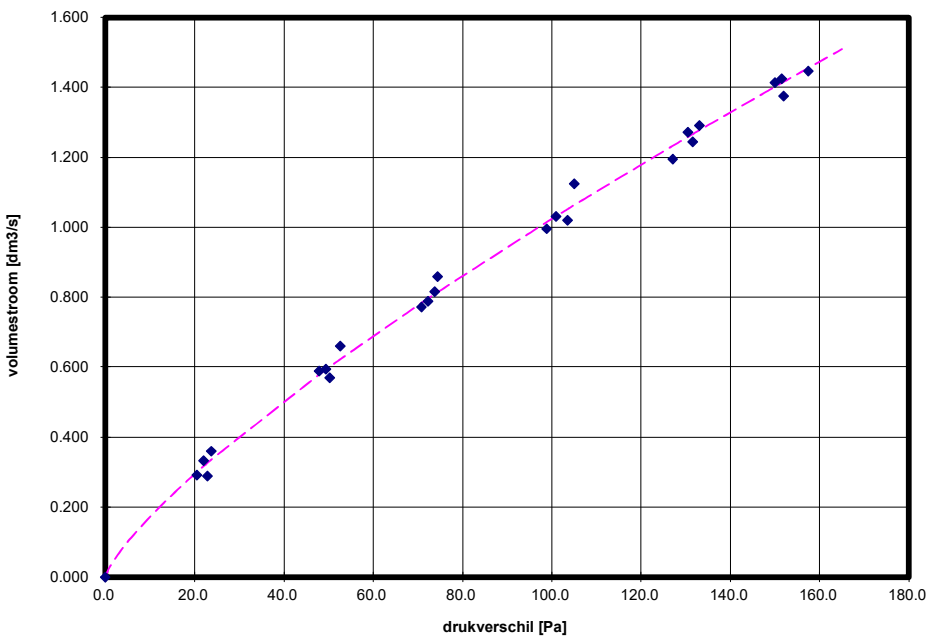

Appendix M – Mass flow rates for ducts 34, 39 and 42

Contaminant concentrations Medium fire growth rate

Date/Time	Contaminant	Junction #34	Junction #39	Junction #41
1-1-2023 00:00	CELLULOSE [kg/kg]	0.00	0.00	0.00
1-1-2023 00:00	CELLULOSE [kg/kg]	0.00	0.00	0.00
1-1-2023 00:00	CELLULOSE [kg/kg]	0.00	0.00	0.00
1-1-2023 00:00	CELLULOSE [kg/kg]	0.00	0.00	0.00
1-1-2023 00:00	CELLULOSE [kg/kg]	0.00	0.00	0.00
1-1-2023 00:00	CELLULOSE [kg/kg]	0.00	0.00	0.00
1-1-2023 00:00	CELLULOSE [kg/kg]	0.00	0.00	0.00
1-1-2023 00:00	CELLULOSE [kg/kg]	0.00	0.00	0.00
1-1-2023 00:00	CELLULOSE [kg/kg]	0.00	0.00	0.00
1-1-2023 00:00	CELLULOSE [kg/kg]	0.00	0.00	0.00
1-1-2023 00:00	CELLULOSE [kg/kg]	0.00	0.00	0.00
1-1-2023 00:01	CELLULOSE [kg/kg]	0.00	0.00	0.00
1-1-2023 00:01	CELLULOSE [kg/kg]	0.00	0.00	0.00
1-1-2023 00:01	CELLULOSE [kg/kg]	0.00	0.00	0.00
1-1-2023 00:01	CELLULOSE [kg/kg]	0.00	0.00	0.00
1-1-2023 00:01	CELLULOSE [kg/kg]	0.00	0.00	0.00
1-1-2023 00:01	CELLULOSE [kg/kg]	0.00	0.00	0.00
1-1-2023 00:01	CELLULOSE [kg/kg]	0.00	0.00	0.00
1-1-2023 00:01	CELLULOSE [kg/kg]	0.00	0.00	0.00
1-1-2023 00:01	CELLULOSE [kg/kg]	0.00	0.00	0.00
1-1-2023 00:01	CELLULOSE [kg/kg]	0.00	0.00	0.00
1-1-2023 00:01	CELLULOSE [kg/kg]	0.00	0.00	0.00
1-1-2023 00:01	CELLULOSE [kg/kg]	0.00	0.00	0.00
1-1-2023 00:01	CELLULOSE [kg/kg]	0.01	0.00	0.00
1-1-2023 00:02	CELLULOSE [kg/kg]	0.01	0.00	0.00
1-1-2023 00:02	CELLULOSE [kg/kg]	0.01	0.01	0.01
1-1-2023 00:02	CELLULOSE [kg/kg]	0.01	0.01	0.01
1-1-2023 00:02	CELLULOSE [kg/kg]	0.01	0.01	0.01
1-1-2023 00:02	CELLULOSE [kg/kg]	0.01	0.01	0.01
1-1-2023 00:02	CELLULOSE [kg/kg]	0.01	0.01	0.01
1-1-2023 00:02	CELLULOSE [kg/kg]	0.01	0.01	0.01
1-1-2023 00:02	CELLULOSE [kg/kg]	0.01	0.01	0.01
1-1-2023 00:02	CELLULOSE [kg/kg]	0.01	0.01	0.01
1-1-2023 00:02	CELLULOSE [kg/kg]	0.02	0.01	0.01
1-1-2023 00:02	CELLULOSE [kg/kg]	0.02	0.01	0.01
1-1-2023 00:02	CELLULOSE [kg/kg]	0.02	0.01	0.01
1-1-2023 00:03	CELLULOSE [kg/kg]	0.02	0.01	0.01
1-1-2023 00:03	CELLULOSE [kg/kg]	0.02	0.02	0.02
1-1-2023 00:03	CELLULOSE [kg/kg]	0.02	0.02	0.02
1-1-2023 00:03	CELLULOSE [kg/kg]	0.02	0.02	0.02
1-1-2023 00:03	CELLULOSE [kg/kg]	0.03	0.02	0.02
1-1-2023 00:03	CELLULOSE [kg/kg]	0.03	0.02	0.02
1-1-2023 00:03	CELLULOSE [kg/kg]	0.03	0.02	0.02
1-1-2023 00:03	CELLULOSE [kg/kg]	0.03	0.02	0.02
1-1-2023 00:03	CELLULOSE [kg/kg]	0.03	0.03	0.03
1-1-2023 00:03	CELLULOSE [kg/kg]	0.04	0.03	0.03
1-1-2023 00:03	CELLULOSE [kg/kg]	0.04	0.03	0.03
1-1-2023 00:03	CELLULOSE [kg/kg]	0.04	0.03	0.03
1-1-2023 00:04	CELLULOSE [kg/kg]	0.04	0.03	0.03
1-1-2023 00:04	CELLULOSE [kg/kg]	0.05	0.03	0.03
1-1-2023 00:04	CELLULOSE [kg/kg]	0.05	0.04	0.04
1-1-2023 00:04	CELLULOSE [kg/kg]	0.05	0.04	0.04
1-1-2023 00:04	CELLULOSE [kg/kg]	0.05	0.04	0.04
1-1-2023 00:04	CELLULOSE [kg/kg]	0.05	0.04	0.04
1-1-2023 00:04	CELLULOSE [kg/kg]	0.05	0.04	0.04
1-1-2023 00:04	CELLULOSE [kg/kg]	0.05	0.04	0.04
1-1-2023 00:04	CELLULOSE [kg/kg]	0.05	0.04	0.04
1-1-2023 00:04	CELLULOSE [kg/kg]	0.05	0.04	0.04
1-1-2023 00:04	CELLULOSE [kg/kg]	0.05	0.04	0.04
1-1-2023 00:05	CELLULOSE [kg/kg]	0.05	0.04	0.04
1-1-2023 00:05	CELLULOSE [kg/kg]	0.05	0.04	0.04
1-1-2023 00:05	CELLULOSE [kg/kg]	0.05	0.04	0.04
1-1-2023 00:05	CELLULOSE [kg/kg]	0.05	0.04	0.04
1-1-2023 00:05	CELLULOSE [kg/kg]	0.05	0.04	0.04
1-1-2023 00:05	CELLULOSE [kg/kg]	0.05	0.04	0.04
1-1-2023 00:05	CELLULOSE [kg/kg]	0.05	0.04	0.04
1-1-2023 00:05	CELLULOSE [kg/kg]	0.05	0.04	0.04
1-1-2023 00:05	CELLULOSE [kg/kg]	0.05	0.04	0.04
1-1-2023 00:05	CELLULOSE [kg/kg]	0.05	0.04	0.04
1-1-2023 00:05	CELLULOSE [kg/kg]	0.05	0.04	0.04
1-1-2023 00:06	CELLULOSE [kg/kg]	0.05	0.04	0.04
1-1-2023 00:06	CELLULOSE [kg/kg]	0.05	0.04	0.04
1-1-2023 00:06	CELLULOSE [kg/kg]	0.05	0.04	0.04
1-1-2023 00:06	CELLULOSE [kg/kg]	0.05	0.04	0.04
1-1-2023 00:06	CELLULOSE [kg/kg]	0.05	0.04	0.04
1-1-2023 00:06	CELLULOSE [kg/kg]	0.05	0.04	0.04
1-1-2023 00:06	CELLULOSE [kg/kg]	0.05	0.04	0.04
1-1-2023 00:06	CELLULOSE [kg/kg]	0.05	0.04	0.04
1-1-2023 00:06	CELLULOSE [kg/kg]	0.05	0.04	0.04

Mass air flow rates Medium fire growth rate

Date/Time	Property	Duct #34	Duct #39	Duct #42
1-1-2023 00:00	Flow 1 [kg/s]	0.00	-0.02	-0.02
1-1-2023 00:00	Flow 1 [kg/s]	0.00	-0.02	-0.02
1-1-2023 00:00	Flow 1 [kg/s]	0.01	-0.03	-0.01
1-1-2023 00:00	Flow 1 [kg/s]	0.01	-0.03	-0.01
1-1-2023 00:00	Flow 1 [kg/s]	0.01	-0.03	-0.01
1-1-2023 00:00	Flow 1 [kg/s]	0.02	-0.03	0.00
1-1-2023 00:00	Flow 1 [kg/s]	0.02	-0.04	0.00
1-1-2023 00:00	Flow 1 [kg/s]	0.03	-0.04	0.01
1-1-2023 00:00	Flow 1 [kg/s]	0.04	-0.05	0.02
1-1-2023 00:00	Flow 1 [kg/s]	0.05	-0.06	0.03
1-1-2023 00:00	Flow 1 [kg/s]	0.06	-0.07	0.04
1-1-2023 00:00	Flow 1 [kg/s]	0.07	-0.08	0.05
1-1-2023 00:01	Flow 1 [kg/s]	0.08	-0.10	0.06
1-1-2023 00:01	Flow 1 [kg/s]	0.10	-0.11	0.08
1-1-2023 00:01	Flow 1 [kg/s]	0.12	-0.13	0.09
1-1-2023 00:01	Flow 1 [kg/s]	0.14	-0.15	0.11
1-1-2023 00:01	Flow 1 [kg/s]	0.16	-0.17	0.12
1-1-2023 00:01	Flow 1 [kg/s]	0.18	-0.19	0.14
1-1-2023 00:01	Flow 1 [kg/s]	0.19	-0.21	0.15
1-1-2023 00:01	Flow 1 [kg/s]	0.21	-0.23	0.17
1-1-2023 00:01	Flow 1 [kg/s]	0.23	-0.25	0.19
1-1-2023 00:01	Flow 1 [kg/s]	0.25	-0.26	0.20
1-1-2023 00:01	Flow 1 [kg/s]	0.27	-0.28	0.22
1-1-2023 00:01	Flow 1 [kg/s]	0.28	-0.30	0.23
1-1-2023 00:02	Flow 1 [kg/s]	0.30	-0.32	0.25
1-1-2023 00:02	Flow 1 [kg/s]	0.32	-0.34	0.26
1-1-2023 00:02	Flow 1 [kg/s]	0.34	-0.36	0.28
1-1-2023 00:02	Flow 1 [kg/s]	0.36	-0.38	0.29
1-1-2023 00:02	Flow 1 [kg/s]	0.37	-0.39	0.31
1-1-2023 00:02	Flow 1 [kg/s]	0.38	-0.40	0.32
1-1-2023 00:02	Flow 1 [kg/s]	0.40	-0.42	0.33
1-1-2023 00:02	Flow 1 [kg/s]	0.40	-0.43	0.34
1-1-2023 00:02	Flow 1 [kg/s]	0.41	-0.43	0.34
1-1-2023 00:02	Flow 1 [kg/s]	0.42	-0.44	0.35
1-1-2023 00:02	Flow 1 [kg/s]	0.42	-0.44	0.35
1-1-2023 00:02	Flow 1 [kg/s]	0.43	-0.45	0.36
1-1-2023 00:03	Flow 1 [kg/s]	0.44	-0.46	0.36
1-1-2023 00:03	Flow 1 [kg/s]	0.44	-0.46	0.37
1-1-2023 00:03	Flow 1 [kg/s]	0.45	-0.47	0.37
1-1-2023 00:03	Flow 1 [kg/s]	0.44	-0.47	0.37
1-1-2023 00:03	Flow 1 [kg/s]	0.44	-0.46	0.36
1-1-2023 00:03	Flow 1 [kg/s]	0.43	-0.45	0.36
1-1-2023 00:03	Flow 1 [kg/s]	0.43	-0.45	0.35
1-1-2023 00:03	Flow 1 [kg/s]	0.42	-0.44	0.35
1-1-2023 00:03	Flow 1 [kg/s]	0.41	-0.43	0.34
1-1-2023 00:03	Flow 1 [kg/s]	0.40	-0.42	0.33
1-1-2023 00:03	Flow 1 [kg/s]	0.39	-0.41	0.32
1-1-2023 00:03	Flow 1 [kg/s]	0.38	-0.39	0.31
1-1-2023 00:04	Flow 1 [kg/s]	0.37	-0.38	0.30
1-1-2023 00:04	Flow 1 [kg/s]	0.18	-0.19	0.14
1-1-2023 00:04	Flow 1 [kg/s]	0.39	-0.41	0.32
1-1-2023 00:04	Flow 1 [kg/s]	0.39	-0.41	0.32
1-1-2023 00:04	Flow 1 [kg/s]	0.36	-0.38	0.30
1-1-2023 00:04	Flow 1 [kg/s]	0.33	-0.35	0.27
1-1-2023 00:04	Flow 1 [kg/s]	0.31	-0.32	0.25
1-1-2023 00:04	Flow 1 [kg/s]	0.28	-0.29	0.23
1-1-2023 00:04	Flow 1 [kg/s]	0.25	-0.27	0.20
1-1-2023 00:04	Flow 1 [kg/s]	0.22	-0.24	0.18
1-1-2023 00:04	Flow 1 [kg/s]	0.19	-0.21	0.15
1-1-2023 00:04	Flow 1 [kg/s]	0.18	-0.19	0.14
1-1-2023 00:05	Flow 1 [kg/s]	0.17	-0.18	0.13
1-1-2023 00:05	Flow 1 [kg/s]	0.15	-0.17	0.12
1-1-2023 00:05	Flow 1 [kg/s]	0.15	-0.16	0.11
1-1-2023 00:05	Flow 1 [kg/s]	0.14	-0.16	0.11
1-1-2023 00:05	Flow 1 [kg/s]	0.14	-0.15	0.11
1-1-2023 00:05	Flow 1 [kg/s]	0.13	-0.14	0.10
1-1-2023 00:05	Flow 1 [kg/s]	0.13	-0.14	0.10
1-1-2023 00:05	Flow 1 [kg/s]	0.12	-0.13	0.09
1-1-2023 00:05	Flow 1 [kg/s]	0.12	-0.13	0.09
1-1-2023 00:05	Flow 1 [kg/s]	0.08	-0.10	0.06
1-1-2023 00:05	Flow 1 [kg/s]	0.05	-0.07	0.04
1-1-2023 00:05	Flow 1 [kg/s]	0.25	-0.27	0.20
1-1-2023 00:06	Flow 1 [kg/s]	0.21	-0.23	0.17
1-1-2023 00:06	Flow 1 [kg/s]	0.13	-0.15	0.10
1-1-2023 00:06	Flow 1 [kg/s]	0.14	-0.15	0.11
1-1-2023 00:06	Flow 1 [kg/s]	0.15	-0.16	0.12
1-1-2023 00:06	Flow 1 [kg/s]	0.15	-0.16	0.11
1-1-2023 00:06	Flow 1 [kg/s]	0.14	-0.16	0.11
1-1-2023 00:06	Flow 1 [kg/s]	0.14	-0.16	0.11
1-1-2023 00:06	Flow 1 [kg/s]	0.14	-0.15	0.11
1-1-2023 00:06	Flow 1 [kg/s]	0.14	-0.15	0.11

Contaminant concentration Fast fire growth rate

Date/Time	Contaminant	Junction #34	Junction #39	Junction #41
1-1-2023 00:00	CELLULOSE [kg/kg]	0.00	0.00	0.00
1-1-2023 00:00	CELLULOSE [kg/kg]	0.00	0.00	0.00
1-1-2023 00:00	CELLULOSE [kg/kg]	0.00	0.00	0.00
1-1-2023 00:00	CELLULOSE [kg/kg]	0.00	0.00	0.00
1-1-2023 00:00	CELLULOSE [kg/kg]	0.00	0.00	0.00
1-1-2023 00:00	CELLULOSE [kg/kg]	0.00	0.00	0.00
1-1-2023 00:00	CELLULOSE [kg/kg]	0.00	0.00	0.00
1-1-2023 00:00	CELLULOSE [kg/kg]	0.00	0.00	0.00
1-1-2023 00:00	CELLULOSE [kg/kg]	0.00	0.00	0.00
1-1-2023 00:00	CELLULOSE [kg/kg]	0.00	0.00	0.00
1-1-2023 00:00	CELLULOSE [kg/kg]	0.00	0.00	0.00
1-1-2023 00:00	CELLULOSE [kg/kg]	0.00	0.00	0.00
1-1-2023 00:01	CELLULOSE [kg/kg]	0.00	0.00	0.00
1-1-2023 00:01	CELLULOSE [kg/kg]	0.00	0.00	0.00
1-1-2023 00:01	CELLULOSE [kg/kg]	0.01	0.00	0.00
1-1-2023 00:01	CELLULOSE [kg/kg]	0.01	0.00	0.00
1-1-2023 00:01	CELLULOSE [kg/kg]	0.01	0.01	0.01
1-1-2023 00:01	CELLULOSE [kg/kg]	0.01	0.01	0.01
1-1-2023 00:01	CELLULOSE [kg/kg]	0.01	0.01	0.01
1-1-2023 00:01	CELLULOSE [kg/kg]	0.02	0.01	0.01
1-1-2023 00:01	CELLULOSE [kg/kg]	0.02	0.01	0.01
1-1-2023 00:01	CELLULOSE [kg/kg]	0.02	0.02	0.02
1-1-2023 00:01	CELLULOSE [kg/kg]	0.02	0.02	0.02
1-1-2023 00:01	CELLULOSE [kg/kg]	0.03	0.02	0.02
1-1-2023 00:02	CELLULOSE [kg/kg]	0.03	0.02	0.02
1-1-2023 00:02	CELLULOSE [kg/kg]	0.03	0.03	0.03
1-1-2023 00:02	CELLULOSE [kg/kg]	0.04	0.03	0.03
1-1-2023 00:02	CELLULOSE [kg/kg]	0.04	0.03	0.03
1-1-2023 00:02	CELLULOSE [kg/kg]	0.04	0.03	0.03
1-1-2023 00:02	CELLULOSE [kg/kg]	0.05	0.04	0.04
1-1-2023 00:02	CELLULOSE [kg/kg]	0.05	0.04	0.04
1-1-2023 00:02	CELLULOSE [kg/kg]	0.05	0.04	0.04
1-1-2023 00:02	CELLULOSE [kg/kg]	0.05	0.04	0.04
1-1-2023 00:02	CELLULOSE [kg/kg]	0.06	0.04	0.04
1-1-2023 00:02	CELLULOSE [kg/kg]	0.06	0.05	0.05
1-1-2023 00:02	CELLULOSE [kg/kg]	0.06	0.05	0.05
1-1-2023 00:03	CELLULOSE [kg/kg]	0.06	0.05	0.05
1-1-2023 00:03	CELLULOSE [kg/kg]	0.06	0.05	0.05
1-1-2023 00:03	CELLULOSE [kg/kg]	0.06	0.05	0.05
1-1-2023 00:03	CELLULOSE [kg/kg]	0.06	0.05	0.05
1-1-2023 00:03	CELLULOSE [kg/kg]	0.06	0.05	0.05
1-1-2023 00:03	CELLULOSE [kg/kg]	0.06	0.05	0.05
1-1-2023 00:03	CELLULOSE [kg/kg]	0.06	0.05	0.05
1-1-2023 00:03	CELLULOSE [kg/kg]	0.06	0.05	0.05
1-1-2023 00:03	CELLULOSE [kg/kg]	0.06	0.05	0.05
1-1-2023 00:03	CELLULOSE [kg/kg]	0.06	0.05	0.05
1-1-2023 00:03	CELLULOSE [kg/kg]	0.06	0.05	0.05
1-1-2023 00:03	CELLULOSE [kg/kg]	0.06	0.05	0.05
1-1-2023 00:04	CELLULOSE [kg/kg]	0.06	0.05	0.05
1-1-2023 00:04	CELLULOSE [kg/kg]	0.06	0.05	0.05
1-1-2023 00:04	CELLULOSE [kg/kg]	0.06	0.05	0.05
1-1-2023 00:04	CELLULOSE [kg/kg]	0.06	0.05	0.05
1-1-2023 00:04	CELLULOSE [kg/kg]	0.06	0.05	0.05
1-1-2023 00:04	CELLULOSE [kg/kg]	0.06	0.05	0.05
1-1-2023 00:04	CELLULOSE [kg/kg]	0.06	0.05	0.05
1-1-2023 00:04	CELLULOSE [kg/kg]	0.07	0.05	0.05
1-1-2023 00:04	CELLULOSE [kg/kg]	0.07	0.05	0.05
1-1-2023 00:04	CELLULOSE [kg/kg]	0.06	0.05	0.05
1-1-2023 00:04	CELLULOSE [kg/kg]	0.06	0.05	0.05
1-1-2023 00:04	CELLULOSE [kg/kg]	0.06	0.05	0.05
1-1-2023 00:05	CELLULOSE [kg/kg]	0.06	0.05	0.05
1-1-2023 00:05	CELLULOSE [kg/kg]	0.06	0.05	0.05
1-1-2023 00:05	CELLULOSE [kg/kg]	0.06	0.05	0.05
1-1-2023 00:05	CELLULOSE [kg/kg]	0.06	0.05	0.05
1-1-2023 00:05	CELLULOSE [kg/kg]	0.06	0.05	0.05
1-1-2023 00:05	CELLULOSE [kg/kg]	0.06	0.05	0.05
1-1-2023 00:05	CELLULOSE [kg/kg]	0.06	0.05	0.05
1-1-2023 00:05	CELLULOSE [kg/kg]	0.06	0.05	0.05
1-1-2023 00:05	CELLULOSE [kg/kg]	0.06	0.05	0.05
1-1-2023 00:05	CELLULOSE [kg/kg]	0.06	0.05	0.05
1-1-2023 00:05	CELLULOSE [kg/kg]	0.06	0.05	0.05
1-1-2023 00:05	CELLULOSE [kg/kg]	0.06	0.05	0.05
1-1-2023 00:06	CELLULOSE [kg/kg]	0.06	0.05	0.05
1-1-2023 00:06	CELLULOSE [kg/kg]	0.06	0.05	0.05
1-1-2023 00:06	CELLULOSE [kg/kg]	0.06	0.05	0.05
1-1-2023 00:06	CELLULOSE [kg/kg]	0.06	0.05	0.05
1-1-2023 00:06	CELLULOSE [kg/kg]	0.06	0.05	0.05
1-1-2023 00:06	CELLULOSE [kg/kg]	0.06	0.05	0.05
1-1-2023 00:06	CELLULOSE [kg/kg]	0.06	0.05	0.05
1-1-2023 00:06	CELLULOSE [kg/kg]	0.06	0.05	0.05
1-1-2023 00:06	CELLULOSE [kg/kg]	0.06	0.05	0.05

Mass air flow rate Fast fire growth rate

Date/Time	Property	Duct #34	Duct #39	Duct #42
1-1-2023 00:00	Flow 1 [kg/s]	0.00	-0.02	-0.02
1-1-2023 00:00	Flow 1 [kg/s]	0.01	-0.02	-0.02
1-1-2023 00:00	Flow 1 [kg/s]	0.01	-0.03	-0.01
1-1-2023 00:00	Flow 1 [kg/s]	0.02	-0.03	0.00
1-1-2023 00:00	Flow 1 [kg/s]	0.04	-0.05	0.02
1-1-2023 00:00	Flow 1 [kg/s]	0.06	-0.07	0.04
1-1-2023 00:00	Flow 1 [kg/s]	0.08	-0.09	0.06
1-1-2023 00:00	Flow 1 [kg/s]	0.12	-0.13	0.09
1-1-2023 00:00	Flow 1 [kg/s]	0.16	-0.17	0.12
1-1-2023 00:00	Flow 1 [kg/s]	0.20	-0.21	0.16
1-1-2023 00:00	Flow 1 [kg/s]	0.25	-0.27	0.20
1-1-2023 00:00	Flow 1 [kg/s]	0.30	-0.32	0.25
1-1-2023 00:01	Flow 1 [kg/s]	0.35	-0.37	0.29
1-1-2023 00:01	Flow 1 [kg/s]	0.40	-0.42	0.33
1-1-2023 00:01	Flow 1 [kg/s]	0.45	-0.48	0.38
1-1-2023 00:01	Flow 1 [kg/s]	0.51	-0.53	0.42
1-1-2023 00:01	Flow 1 [kg/s]	0.56	-0.58	0.47
1-1-2023 00:01	Flow 1 [kg/s]	0.61	-0.63	0.51
1-1-2023 00:01	Flow 1 [kg/s]	0.64	-0.67	0.54
1-1-2023 00:01	Flow 1 [kg/s]	0.68	-0.71	0.57
1-1-2023 00:01	Flow 1 [kg/s]	0.72	-0.75	0.60
1-1-2023 00:01	Flow 1 [kg/s]	0.73	-0.76	0.62
1-1-2023 00:01	Flow 1 [kg/s]	0.75	-0.78	0.63
1-1-2023 00:01	Flow 1 [kg/s]	0.76	-0.79	0.64
1-1-2023 00:02	Flow 1 [kg/s]	0.76	-0.79	0.64
1-1-2023 00:02	Flow 1 [kg/s]	0.76	-0.78	0.64
1-1-2023 00:02	Flow 1 [kg/s]	0.75	-0.78	0.63
1-1-2023 00:02	Flow 1 [kg/s]	0.73	-0.75	0.61
1-1-2023 00:02	Flow 1 [kg/s]	0.70	-0.73	0.59
1-1-2023 00:02	Flow 1 [kg/s]	0.67	-0.70	0.56
1-1-2023 00:02	Flow 1 [kg/s]	0.65	-0.67	0.54
1-1-2023 00:02	Flow 1 [kg/s]	0.33	-0.35	0.27
1-1-2023 00:02	Flow 1 [kg/s]	0.26	-0.28	0.21
1-1-2023 00:02	Flow 1 [kg/s]	0.29	-0.30	0.23
1-1-2023 00:02	Flow 1 [kg/s]	0.29	-0.31	0.24
1-1-2023 00:02	Flow 1 [kg/s]	0.29	-0.31	0.24
1-1-2023 00:03	Flow 1 [kg/s]	0.30	-0.31	0.24
1-1-2023 00:03	Flow 1 [kg/s]	0.30	-0.32	0.24
1-1-2023 00:03	Flow 1 [kg/s]	0.30	-0.32	0.25
1-1-2023 00:03	Flow 1 [kg/s]	0.29	-0.31	0.23
1-1-2023 00:03	Flow 1 [kg/s]	0.28	-0.29	0.22
1-1-2023 00:03	Flow 1 [kg/s]	0.26	-0.28	0.21
1-1-2023 00:03	Flow 1 [kg/s]	0.25	-0.27	0.20
1-1-2023 00:03	Flow 1 [kg/s]	0.24	-0.25	0.19
1-1-2023 00:03	Flow 1 [kg/s]	0.22	-0.24	0.18
1-1-2023 00:03	Flow 1 [kg/s]	0.21	-0.23	0.17
1-1-2023 00:03	Flow 1 [kg/s]	0.20	-0.21	0.16
1-1-2023 00:03	Flow 1 [kg/s]	0.19	-0.20	0.15
1-1-2023 00:04	Flow 1 [kg/s]	0.17	-0.19	0.14
1-1-2023 00:04	Flow 1 [kg/s]	0.16	-0.17	0.12
1-1-2023 00:04	Flow 1 [kg/s]	0.15	-0.16	0.11
1-1-2023 00:04	Flow 1 [kg/s]	0.13	-0.15	0.10
1-1-2023 00:04	Flow 1 [kg/s]	0.12	-0.13	0.09
1-1-2023 00:04	Flow 1 [kg/s]	0.11	-0.12	0.08
1-1-2023 00:04	Flow 1 [kg/s]	0.09	-0.11	0.07
1-1-2023 00:04	Flow 1 [kg/s]	0.09	-0.11	0.07
1-1-2023 00:04	Flow 1 [kg/s]	0.22	-0.24	0.18
1-1-2023 00:04	Flow 1 [kg/s]	0.23	-0.25	0.18
1-1-2023 00:04	Flow 1 [kg/s]	0.15	-0.16	0.12
1-1-2023 00:04	Flow 1 [kg/s]	0.15	-0.16	0.11
1-1-2023 00:05	Flow 1 [kg/s]	0.14	-0.16	0.11
1-1-2023 00:05	Flow 1 [kg/s]	0.14	-0.15	0.11
1-1-2023 00:05	Flow 1 [kg/s]	0.14	-0.15	0.10
1-1-2023 00:05	Flow 1 [kg/s]	0.13	-0.15	0.10
1-1-2023 00:05	Flow 1 [kg/s]	0.13	-0.14	0.10
1-1-2023 00:05	Flow 1 [kg/s]	0.12	-0.14	0.10
1-1-2023 00:05	Flow 1 [kg/s]	0.12	-0.13	0.09
1-1-2023 00:05	Flow 1 [kg/s]	0.12	-0.13	0.09
1-1-2023 00:05	Flow 1 [kg/s]	0.11	-0.13	0.09
1-1-2023 00:05	Flow 1 [kg/s]	0.11	-0.12	0.08
1-1-2023 00:05	Flow 1 [kg/s]	0.11	-0.12	0.08
1-1-2023 00:05	Flow 1 [kg/s]	0.11	-0.12	0.08
1-1-2023 00:06	Flow 1 [kg/s]	0.11	-0.12	0.08
1-1-2023 00:06	Flow 1 [kg/s]	0.11	-0.12	0.08
1-1-2023 00:06	Flow 1 [kg/s]	0.11	-0.12	0.08
1-1-2023 00:06	Flow 1 [kg/s]	0.11	-0.12	0.08
1-1-2023 00:06	Flow 1 [kg/s]	0.11	-0.12	0.08
1-1-2023 00:06	Flow 1 [kg/s]	0.10	-0.12	0.08
1-1-2023 00:06	Flow 1 [kg/s]	0.10	-0.12	0.08
1-1-2023 00:06	Flow 1 [kg/s]	0.10	-0.12	0.08
1-1-2023 00:06	Flow 1 [kg/s]	0.10	-0.12	0.08